University of Strathclyde
Department of Civil Engineering

THE INTEGRATION OF TOPOLOGY AND ENTROPY-BASED RELIABILITY INTO THE OPTIMAL DESIGN OF WATER DISTRIBUTION SYSTEMS

This thesis was submitted to and in accordance with the requirements of the **University of Strathclyde** for the degree of

Doctor of Philosophy

by

SALAH H. A. SALEH

DECEMBER 2013

Signed:

Date:

THE INTEGRATION OF TOPOLOGY AND ENTROPY-BASED RELIABILITY INTO THE OPTIMAL DESIGN OF WATER DISTRIBUTION SYSTEMS

Salah H. A. Saleh

ABSTRACT

Establishing a new water distribution system (WDS) essentially involves proper planning of system components to minimize cost, sizing of such components to operate under normal operating conditions and assessing system performance under abnormal operating conditions to minimize effects of components failure. This thesis investigates combining these optimization aspects while specifically focusing on optimal planning of system components amongst all possible topologies, optimal design over all possible combinations of components sizes, and improving system performance over all possible levels of hydraulic reliability. In order to address these issues in full, a novel many-objective genetic algorithm approach to the simultaneous optimization of topology, design and reliability of the WDS has been developed in this research.

The novelty and originality carried out in this research are presented next.

A new multi-objective approach for coupled topology and pipe size optimization of WDS is developed. The approach is the first to exploit in full both feasible and infeasible parts of the entire solution space of topology and design within the search procedure. A new algorithm for topology confirmation is developed to identify and quantify infeasible topologies containing nodes and pipes isolated from supplying sources. The algorithm is coupled with the penalty-free strategy to enable both infeasible topologies and designs with insufficient pressures to contribute to achieving the least cost design of the WDS. Previously, solutions belonging to either infeasible topologies or having insufficient pressure were being discarded from the search process. The approach is computationally efficient and outperforms previous methods of coupled topology and design optimization of WDS.

A new multi-objective approach for design and entropy-based reliability optimization of WDS is developed. The statistical entropy highly dependent on flow directions was used as a measure of the WDS reliability within the approach. The approach is the first to globally maximize entropy of the WDS. Previously, the search procedure was locally restricted to predefined sets of flow directions. To address this issue, a new algorithm that eliminates the need to specify limited sets of flow directions in advance of the search process is developed. The algorithm is integrated with the

penalty-free strategy in order to fully exploit the entire solution space of entropy and design. The approach simultaneously combines local and global maximization of entropy with cost minimization over the entire solution space of pipe sizing. To reduce difficulties encountered in searching into the solution space of this many-objective problem, a new concept that computationally combines objectives of hydraulic infeasibility with global and local maximization of entropy into one objective is developed. The approach is applied to two benchmark networks yielding superior results in terms of global maximization of entropy and good balance between cost and entropy.

The coupled topology and entropy-based design optimization of WDS are integrated into a penalty-free many-objective framework. It is the first to combine topology, pipe size and entropy-based reliability optimization of the WDS in a simultaneous way. The maximization of entropy in this combination is tackled in an entirely novel way by simultaneously exploring entropy belonging to multiple topologies and multiple entropies belonging to the same topology. To address exploring entropy of new topologies, a network complexity measure that accounts for number of pipes contained in a topology is introduced as an objective. The concept of handling this many-objective problem is extended to account for topologic infeasibility, hydraulic infeasibility and global and local maximization of entropy. Excellent results have been efficiently achieved regarding the provision of a variety of maximum entropy designs distributed to different topologies and having good compromise between entropy and cost.

ACKNOWLEGEMENT

I am deeply grateful and thankful to the Almighty Allah, God, for establishing and helping me complete my PhD research.

I would like to express the deepest appreciation to my supervisor, Dr. Tiku Tanyimboh, who has the attitude of a genius to methodically and patiently guide me throughout this study. He has continually and convincingly conveyed a spirit of adventure to motivate me for excellence in my work. Without his valuable guidance and persistent help, this thesis would not have come to light.

Additionally, I would like to thank the Libyan government for fully funding my PhD program.

I express my deep and sincere gratitude to my beloved father, Hussain Awaidat and mother, Khadija Assadeq who faithfully prayed for me during tough times; and my beloved wife, Majda Amer who has strongly supported me, never ceased to provide me with invaluable advice and relaxed atmosphere during hard times. I also want to thank my sons, Muhab and Muaad who has added a spirit of enjoyment and excitement to my life; and my brothers and sisters who has continually encouraged me to complete my study.

Finally, I would like to thank my friends, Calvin Siew, Alemtsehay Seyoum, Anna Czajkowska, Upaka Rathnayake and Euan Barlow for creating a relaxed working and sometimes a social environment by which I could enhance carrying out my research with great enjoyment.

DEDICATION

This thesis is dedicated to my father, Hussain Awaidat, mother, Khadija Assadeq, wife, Majda Amer, sons, Muhab and Muaad, and brothers and sisters.

TABLE OF CONTENTS

3.0 CHAPTER THREE DESIGN OPTIMIZATION OF WATER DISTRIBUTION SYSTEMS

LIST OF FIGURES

Chapter Three

Chapter Four

Chapter Five

Chapter Six

Appendix A

Appendix C

LIST OF TABLES

Chapter Three

Chapter Four

Chapter Five

Chapter Six

Appendix A

Appendix B

Appendix D

Appendix E

Appendix F

NOTATION

$\underline{\Delta H}$	vector of nodal head corrections
ΔQ	loop-flow correction
ΔQ_l^k	loop-flow correction at iteration *k* to be applied for all pipes belonging to loop *l*
α_i	parameter to be calibrated in Logit function
β_i	parameter to be calibrated in Logit function
γ	specific weight of water
η	dimensionless conversion factor of the Hazen-Williams head loss equation
a_m	probability that link *m* is in service
b_i	coefficient to be calibrated for node *i* in Germanopoulos's outflow equation
C_{ij}	Hazen-Williams roughness coefficient of pipe *ij*
c_i	coefficient to be calibrated for node *i* in Germanopoulos's outflow equation
CV	coefficient of variance
C_i	uniformity of pipe diameter for node *i*
DDA	demand driven analysis
DDL	dynamic link library
D_m	diameter of pipe *m*
DP	dynamic programming
D_{ij}	diameter of pipe *ij*
DSR	demand satisfaction ratio
EA	evolutionary algorithm
EPS	extended period simulation
f	objective function
f_{ij}	friction coefficient of pipe *ij*.

f_i^m	value of objective m for solution i
fn_i^m	normalized value of objective m for solution i
$f_{\min}^m$	minimum value of objective m
$f_{\max}^m$	maximum value of objective m
$\underline{F}$	vector containing function values
F'	derivative of function F
FE	number of function evaluations
FT	failure tolerance
$F(x^k)$	value of function F at value of x and iteration k
GA	genetic algorithm
GGM	global gradient method
GME	global maximum entropy
GMEMC	global maximum entropy minimum cost
h_{ij}	head loss in pipe ij
$\underline{H}$	vector of nodal heads
H_j	available head at node j
H_j^{req}	required head at node j
$H_j^{\min}$	minimum head at node j
H_k	head at reservoir k
HIM	hydraulic infeasibility measure
$in(N_j)$	all pipe flows to node j
I	number of source nodes in a network
I_j	set of all source nodes supplying node j
IJ_l	number of pipes in loop l
J_j	set of nodes connected to node j
J_x	Jacobian matrix that contains first partial derivatives of each function with each variable
J_H	Jacobian matrix for the unknown nodal heads

J	number of demand nodes in a network
K_{ij}	pipe resistance coefficient of pipe *ij*
l	set of pipes in the closed circuit of pipes that form a loop
L_{ij}	length of pipe *ij*
LIM	layout infeasibility measure
LP	linear programming
M	number of links in a network
ME	maximum entropy
MMEMC	minimum maximum entropy minimum cost
MO	many objective
MOEA	multi-objective evolutionary algorithm
MOGA	multi-objective genetic algorithm
MRI	modified resilience index
n	number of outcomes for a random variable
n	population size
n_f	flow exponent
n_g	chromosome length
n_{ij}	Manning roughness coefficient of pipe *ij*
n_n	number of demand nodes in a network
np	number of candidate pipes from which a layout can be built
n_{pu}	number of pumps in a network
n_r	number of reservoirs in a network
N	number of nodes in a network
Nl	number of loops in a network
NCM_{ij}	measure of topologic complexity for pipe *ij*
NLP	non-linear programming
NP	non-deterministic polynomial-time
N_p	number of pipes in a network
NP_{ij}	number of paths from source node *i* to demand node *j*
n_s	domination count

NS	number of sources in a network
$out(N_j)$	all pipe flows from node j
p_c	crossover probability
p_{ij}	path flow probability of pipe ij
p_m	mutation probability
$p(m)$	probability that only link m is not in service
$p(m,n)$	probability that only links m and n are not in service
$p(x)$	probability of a random variable
$p(0)$	probability that all links are in service
P_i	fraction of the total flow through a network that reaches node i
P_j	power introduced to a network by pump j
Pr_i	available pressure at node i
$\mathrm{Pr}_i^{'}$	sufficient pressure supplies a proportion of the required demand at node i
PEM	path entropy method
PDA	pressure dependent analysis
POF	pareto optimal front
Q_i	available outflow at node i
Q_{ij}	flow rate in pipe ij
Q_{in}	inflow of a pipe
Q_{ij}^k	corrected flow rate of pipe ij at iteration k
Q_i^{req}	required demand at node i
Q_{i0}	demand at node i
Q_j	demand or supply at node j
Q_k	outflow at reservoir k
Q_{max}	flow that provides the maximum hydraulic power at the outlet of a pipe
Q_{0i}	inflow rate at source node i
R	hydraulic reliability
R_i	available number of independent supply flow paths

R_i^{req}	required number of independent supply flow paths
RI	resilience index
RWGA	random weight genetic algorithm
s	surplus power factor
S	network entropy
S_i	entropy of node i
S_0	entropy of source supplies
SD	standard deviation
SPEM	simplified path entropy method
S_s	set of solutions that the solution s dominates
SSS	steady state simulation
T	sum of nodal demands
T_i	total flow reaching node i
$T(m)$	total flows supplied with only link m out of service
$T(m,n)$	total flows supplied with only links m and n out of service
TD	total pressure deficit
$T(0)$	total flows supplied with all links in service
u_m	probability that link m is unavailable
VEGA	vector evaluated genetic algorithm
WDS	water distribution system
$\underline{x}$	vector containing x variables
x^k	value of variable x at iteration k

CHAPTER ONE

INTRODUCTION

1.1 BACKGROUND

Water Distribution Systems (WDS) form an important part of the world's infrastructure. As such, a great amount of cost is annually spent to construct and operate newly established systems. Basically, the establishment of a new WDS undergoes three main design stages: planning of system components layout; sizing of system components to operate under normal operating conditions; and assessing system performance under abnormal operating conditions. In normal operating conditions, all system components are considered available, while not all of them are available in abnormal operating conditions due to the uncertain failure conditions that are likely to occur during the operation period of the WDS. Pipe breakage, burst and erosion are typical examples of failure conditions that could occur during the operation of the WDS. Besides the uncertain failure conditions, the abnormal operating conditions include uncertain spatial and temporal increases in water demands a WDS is likely to undergo throughout the operation period.

The planning stage involves optimally determining number and locations of the various components forming the WDS. This includes determining the optimal number and configuration of pipe topology to be identified from a large set of different topologies each represent a possible planning to the WDS. To reduce the complexity of the planning stage, the layout or topology of the WDS is assumed to be predefined in advance of the design stage. In reality, this is not always the case

because there are many situations in which the topology of the WDS is not fixed to some configuration. In developing countries, for example, there are a large number of societies lacking infrastructure facilities and so having no access to drinking water. Establishing new large systems in such situations means it is extremely hard to determine the topology to which the optimal design belongs. Accordingly, system topology represents an essential element that should be incorporated into the determination of the optimal design of the WDS.

Even though the planning stage involves identifying the optimal number and locations of other components such as storage tanks and pumping stations, the capital cost of the WDS mainly comes from pipes forming transmission mains and distribution networks (Swamee and Sharma, 2008). Accordingly, the determination of optimal pipe topology is a key factor towards saving a significant amount of the capital cost of the WDS. Since the planning stage alone is not sufficient to determine the optimal cost of the WDS unless system components are sized, the determination of the optimal topology of the WDS should be carried out in conjunction with the design stage in which all system components are sized.

Besides the assumption that the system topology is dealt with as being known, the WDS is conventionally designed under the consideration that the system operates under normal conditions in which all system components are always considered in service. In reality, there are some circumstances that make some system components unavailable during the operation period. Deterioration of components with time, scheduled maintenance of the system, pipe breakage and pump failure conditions are some of the abnormal conditions a system could experience while being in operation. Accordingly, rehabilitation and upgrading become essential to restore the system to its original capacity. These two processes add a significant amount of capital to the construction and operation cost. To reduce effects of failure conditions on system performance, further assessment component that is potentially able to evaluate the hydraulic performance under abnormal operating conditions becomes a crucial element to be included in the determination of the optimal design of the WDS.

Hydraulic reliability is commonly used to assess the WDS performance under abnormal operating conditions.

Since it is computationally impractical to assess hydraulic reliability based on simulating all failure conditions that could occur within a proposed design of the WDS, a number of surrogate measures of reliability able to assess reliability without the need of a full failure simulation was developed in literature. The disagreement on a universal definition of reliability of the WDS was another reason behind developing such measures. Statistical entropy (Tanyimboh and Templeman, 1993), resilience index (Todini, 2000), network resilience (Prasad and Park 2004) and surplus power factor (Vaabel et al. 2006) are common examples of such measures. Among the aforementioned measures, statistical entropy has been found to have a good relationship with hydraulic reliability. For this reason, network entropy has been employed as a measure of reliability within the current research.

The fact that either considering topology alone is not sufficient to determine cost and reliability or considering pipe sizing alone is not sufficient to determine design and reliability indicates that the relationship between topology, design and reliability is very strong. This high dependency strongly suggests that the determination of the optimal design of a WDS should be based on carrying out the trade-off between topology, design and reliability in a simultaneous way. Such a simultaneous combination enables both design and reliability of the WDS to be determined once topology is defined, which is advantageous to striking the balance between cost saving and improving the long-term hydraulic performance of the WDS. The application of such a concept requires simultaneously searching into the entire solution space of topology, design and reliability of the WDS.

In literature, this highly complex task has not been yet achieved. The only notable work attempted to address the joint effect between topology, design and reliability optimization dealt with this issue as a sequence of multiple optimization stages (Tanyimboh and Setiadi, 2008). Dealing with this problem as separated stages was

imposed by the concept that it would be extremely and computationally expensive if the three optimization aspects were handled together. Therefore, the development of a robust and efficient methodology able to simultaneously handle topology, design and reliability optimization of the WDS has become a pressing problem. This thesis smashes this idea by developing a very robust and efficient approach for the joint optimization of topology, design and reliability of the WDS. The concept of the approach is based on carrying out the decision-making process of the search procedure once three entities of the system are determined: pipe sizes; topology to which the system belongs; and reliability of the system. The idea is to maintain the joint effect between topology, pipe sizing and reliability inter-dependent throughout the search procedure.

1.2 SCOPE OF CURRENT RESEARCH

The objective of this research is to develop a rational and efficient optimization approach able to identify the optimal combinations of planning, design and hydraulic reliability for a WDS in one integrated process. The aim of the current study aims to demonstrate the possibility of simultaneously handling the optimization of topology, pipe sizing and reliability of the WDS in an efficient and robust way. The present research encompasses two active, highly complex and challenging research areas related to the WDS optimization: 1) addressing the inter-connecting strong effect of topology, design and reliability on identifying the optimal design of the WDS; and 2) the potential of efficiently searching into the entire solution space of topology, design and reliability of the WDS.

During the achievement of the extremely complex objective of the present research, a number of difficult issues have been robustly addressed. To solve the issue of flow directions associated with calculating network entropy, an algorithm for automatic detection of flow directions has been developed and incorporated. This algorithm has been extensively tested and demonstrated high robustness and efficiency in handling

any set of flow directions that change from one design to another. The issue of searching into the infeasible part of topology solution space has been tackled with developing an algorithm for topology confirmation. The algorithm quantifies infeasible topologies and essentially replaces the misleading results, i.e. extremely large negative pressures, obtained by the DDA hydraulic simulator with realistic results suitably depicting the situation of isolated parts in a WDS.

1.3 OBJECTIVES OF THE RESEARCH

1) To develop an efficient and robust EA based model able to simultaneously optimize topology, design and reliability of the WDS by searching into feasible and infeasible parts of the entire solution space of topology, pipe sizing and reliability.

2) To develop a highly reliable algorithm for handling infeasible topologies. The motivation for developing such an algorithm is to enhance the topology optimization with generating a large number of topologies within the optimization process.

3) To develop a robust algorithm capable of handling any set of flow directions without the need of being specified in advance of the optimization process. The motivation for developing such an algorithm is to enable the EA to assess the hydraulic performance using informational entropy, which is highly dependent on flow directions, for any feasible set of flow directions belonging to the design space.

4) To assess the robustness, efficiency and practicality of the developed optimization model by testing it on both benchmark hypothetical networks and real systems.

1.4 DESCRIPTION OF THE RESEARCH METHODOLOGY

This thesis introduces a novel penalty-free multi-objective evolutionary approach for the simultaneous optimization of topology, design and reliability of the WDS. The approach completely eradicates the necessity of dividing the optimization of planning, design and long-term hydraulic performance assessment into a sequence of multiple separate processes. It also eliminates the need of constraining the search process to the feasible part of the solution space. The approach is mainly composed of four integrated interactive modules, which are a flow-direction handling model, topology handling model, hydraulic simulator and multi-objective genetic algorithm (MOGA). Both of the flow directions handling and topology handling models are developed as part of the present research, while the hydraulic simulator and the GA are employed from literature. The four models are fully integrated in such a way that the interaction of data is so smooth that it takes place automatically and without any manual involvement once the approach is launched. The integration of such models is sufficient to efficiently direct the approach search, through both infeasible and feasible regions, towards the unified feasibility region of topology and reliable designs in a penalty-free way.

The MOGA is used to generate and sort solutions to obtain the set of optimal solutions based on the trade-off between topology, design and reliability. The MOGA has been significantly modified in such a way that it sorts solutions for non-domination and diversity within a unified domain. Additionally, a new technique for handling the issue of redundant codes associated with binary coded genetic algorithms has been developed and incorporated. In terms of topologic optimization, a new model for handling infeasible topologies has been developed and incorporated. Most importantly, a new strategy for coping with such a many-objective problem has been developed based on involving all problem objectives and incorporated to reduce the computational complexity of the optimization problem.

1.5 THE THESIS OUTLINES

This thesis has seven chapters in total. Apart from the introduction given here, the thesis is organized as follows:

Chapter 2 covers the basics of hydraulic analysis and methods of assessing the long-term hydraulic performance of the WDS. This includes a description of the governing equations involved in modelling the WDS, the two types of hydraulic analysis and reliability assessment of the WDS.

Chapter 3 introduces the tools and methods applied in the optimization of the WDS. A special focus on EA, particularly GA, as an optimization tool was provided. The most important part of this chapter is the discussion of conventional and EA based optimization methods used in the literature.

Chapter 4 introduces a novel method for coupled topology and design optimization of the WDS. The methodology is presented in detail and applied to benchmark hypothetical and real networks to demonstrate it robustness, efficiency and performance. Comparison of results with the previous best designs in the literature is provided.

Chapter 5 presents a novel search strategy that simultaneously combines a global and local search towards maximum entropy solutions of the WDS. The formulation and description of the new method is explained in detail. The new approach is tested by designing a benchmark hypothetical network and a real system to demonstrate its robustness, efficiency and performance in comparison with previous and new developed methods.

Chapter 6 introduces a novel approach that is the first in literature to address the joint effect problem of topology, design and reliability optimization of the WDS. The approach strikes this goal by simultaneously combining the optimization of topology,

design and reliability of the WDS into one integrated process. The methodology is presented and explained in detail. The robustness, performance and efficiency of the method are demonstrated by designing a benchmark hypothetical network and a real system in the literature.

Chapter 7 brings the present research to an end through summarizing the present research in general and providing suggestions for future research.

CHAPTER TWO

HYDRAULIC MODELING AND PERFORMANCE ASSESSMENT OF WATER DISTRIBUTION SYSTEMS

2.1 INTRODUCTION

Real water distribution systems involve a large number of different components such as pipes, valves, pumps, tanks and reservoirs. Each component of which a system is made up forms a vital part of the system without which water can not be provided from the supplying sources to the tapping points of the consumers. Basically, each real system is unique in terms of the supplying sources, layout of system components, topography of the service zone, distribution of consumer points, material of pipes and types of valves. For example, the layout of a WDS is dependent on the existing planning of streets and roads that is unique to the system, the property of right-of-way, potential locations for ground and elevated service reservoirs, and locations and types of land users. Additionally, in a service area with topography of hilly terrains, booster pumps may be required to deliver water to high areas while, to reduce pressure, pressure-reducing valves may be necessary for lower areas. In contrast, a service area with flat topology may require just an elevated reservoir to deliver water to the whole service area.

Since it is extremely difficult to include all system components starting from the supplying sources to the tapping points of consumers, the WDS is primarily

skeletonised to a network made up of nodes and links in which nodes represent sources and consumption points, while links represent pipes, valves and pumps.

Within the skeletonised system, water demands occur along pipes but for an ease of analysis conservative assumptions are required. For example, large water consumptions are considered individually while small consumptions are lumped together and assumed to take place at demand nodes. One way of lumping demands is to allocate half of the total demand occurring along a pipe at each end of the pipe (Swamee and Sharma, 2008). To depict the behaviour of the real WDS within acceptable limits, the skeletonised model should include important elements of the detailed system.

The assessment of hydraulic performance of the WDS is carried out by applying hydraulic simulation models to the corresponding skeletonised network. These models utilize the formulation of mathematical equations to replicate the process of operating a real WDS. Hydraulic simulation models are able to predict how a system responses and behaves under different operating conditions such as peak demands, fire flows, pump failures and pipe bursts. As a result, the feasibility of the existing system or a proposed solution to it can be evaluated before putting such a solution into operation. The information provided by hydraulic models is extremely valuable to assist engineers in making important decisions about the investment of a WDS project. With the aid of the technological advancement in computational tools, hydraulic simulation models has become so sophisticated that they have the ability to deal with real WDS in more realistic way than ever before.

The modelling of WDS can be of two types: either steady-state simulation (SSS) or extended period simulation (EPS). Basically, an SSS analysis simulates the WDS under fixed operating conditions of node demands and water levels of storage reservoirs. In practice, it is common to deal with the worst operating condition (i.e. hourly peak demands and fire conditions) to design the WDS using SSS modelling. However, this assumption is not realistic as the operation of WDS varies with time

(e.g. node demands vary over the day). EPS analysis is able to model the changes in operating conditions over a defined period of time (i.e. the filling and emptying of tanks, operation of regulating valves, operation of pumps with variable speeds, and variations in nodal pressures and pipe flow rates due to changes in demands). As a result, EPS analysis is more realistic in evaluating the performance of the WDS over a defined period of time.

There are two methods for analysing the WDS depending on whether the analysis is based on nodal flows or nodal heads. The conventional method uses the assumption that all nodal demands are satisfied in full. This method of analysis is denoted by demand driven analysis (DDA). In reality, the nodal flow can not be fully satisfied unless the WDS has sufficient pressure. As a result, this method of analysis is not capable of analyzing the WDS under pressure deficiency due to failure condition scenarios such as pipe bursts and pump failure. To evaluate nodal flows under failure conditions, the second method of analysis uses a relationship between nodal heads and nodal demands. As such, this method referred to as pressure dependent analysis (PDA) is more accurate than DDA method in analysing the WDS under pressure deficiency conditions.

To assess the performance of the WDS in fulfilling the design requirements for which it is aimed to meet, it is essential to evaluate the system ability to deal with unforeseen abnormal operating conditions. As a result, important performance assessment measures were developed to accurately assess the hydraulic performance of the WDS. These include hydraulic reliability and failure tolerance (Tanyimboh and Templeman, 1998). The hydraulic reliability and failure tolerance are classified as being accurate measures because they evaluate the hydraulic performance based on multiple simulations of failure conditions using pressure dependent analysis (PDA). Since it is impractical to simulate all failure conditions for the WDS, surrogate performance measures that use DDA analysis were proposed. These include informational entropy (Tanyimboh and Templeman 1993), resilience index (Todini 2000), network resilience (Prasad and Park, 2004), modified resilience index

(Jayaram and Srinivasan 2008) and surplus power factor (Vaabel *et al.* 2006).

This chapter provides a detailed description of the basic equations incorporated in the hydraulic modelling of the WDS. Section 2.2 presents the main hydraulic equations controlling the hydraulic analysis of the WDS. In section 2.3, the accurate and surrogate performance measures widely used in the literature are presented. Due to using entropy as a measure of WDS performance in the present research, a special emphasis is placed on the description of statistical entropy and the corresponding framework developed to enable applying the principle of maximizing entropy for the WDS performance. This covers the methods developed for calculating maximum entropy values in both single and multiple source WDSs.

2.2 MAIN EQUATIONS OF HYDRAULIC MODELLING

The hydraulic modelling of the WDS is mainly governed by the equations of conservation of mass and energy. The principle of the conservation of mass gives rise to the continuity equation, while the principle of conservation of energy results in the head loss equation. Therefore, the hydraulic analysis of the WDS can be formulated to be controlled by the following system of nonlinear equations.

$$\sum_{ij \in in(N_j)} Q_{ij} - \sum_{ij \in out(N_j)} Q_{ij} = Q_j \qquad j = 1,.....,N-1 \qquad (2.1)$$

$$\sum_{ij \in l} h_{ij} = 0 \qquad \forall l \qquad (2.2)$$

where N is number of nodes; l represents a loop of closed circuit of pipes; Q_j is demand or supply at node j; $in(N_j)$ and $out(N_j)$ are all pipe flows to and from node j, respectively. In the analysis, the calculation of head loss (h_{ij}) in pipe ij arising from the friction between water and internal pipe walls is dependent on the formula used.

Eq. 2.1 represents the continuity equation, while Eq. 2.2 represents the head loss equation. In practice, there are three main empirical formulae widely used to calculate the head loss in Eq. 2.2 (Bhave and Gupta, 2006). These are Hazen-Williams formula, Chezy-Manning formula and Darcy-Weisbach formula given by Eq. 2.3, Eq. 2.4 and Eq. 2.5 respectively as follows

$$h_{ij} = \eta\, L_{ij} \left(Q_{ij} / C_{ij}\right)^{1.852}\, D_{ij}^{-4.871} \qquad \forall ij \qquad (2.3)$$

$$h_{ij} = 10.29 n_{ij}^2 L_{ij} Q_{ij}^2 D_{ij}^{16/3} \qquad \forall ij \qquad (2.4)$$

$$h_{ij} = \frac{8 f_{ij} L_{ij} Q_{ij}^2}{\pi^2 g D_{ij}} \qquad \forall ij \qquad (2.5)$$

where η is a dimensionless conversion factor (10.67 in SI units); D_{ij}, h_{ij}, L_{ij} and Q_{ij} are respectively diameter in metres, head loss in metres, length in metres and flow rate in cubic metres per second for pipe ij; C_{ij} and n_{ij} are Hazen-Williams roughness coefficient and Manning roughness coefficient respectively; f_{ij} is the coefficient of friction in pipe ij.

The relationship between head loss (h_{ij}) and flow (Q_{ij}) for pipe ij is often expressed in terms of the pipe resistance coefficient (K_{ij}) as follows:

$$h_{ij} = K_{ij} Q_{ij}^{n_f} \qquad \forall ij \qquad (2.6)$$

where n_f represents the flow exponent that is equal to 1.852 for Hazen-Williams formula, while it equals 2 for the formulae of Chezy-Manning and Darcy-Weisbach. The resistance coefficients of Hazen-Williams formula, Chezy-Manning formula and Darcy-Weisbach formula can be respectively expressed as:

$$K_{ij} = \frac{\eta L_{ij}}{C_{ij}^{1.852} D_{ij}^{4.871}} \qquad \forall ij \qquad (2.7)$$

$$K_{ij} = \frac{10.29 n_{ij}^2 L_{ij}}{D_{ij}^{16/3}} \qquad \forall ij \qquad (2.8)$$

$$K_{ij} = \frac{8 f_{ij} L_{ij}}{\pi^2 g D_{ij}^5} \qquad \forall ij \qquad (2.9)$$

To assess the capability of the WDS in satisfying nodal demands in full, minimum required heads are normally set at each demand node. This constraint can be expressed as

$$H_j \geq H_j^{req} \qquad j = 1,....., N \qquad (2.10)$$

where H_j and H_j^{req} are available and the required head respectively at node *j*. H_j is obtained from the hydraulic simulation, while the required head is the head at a node above which demands are satisfied in full. The introduction of Eq. 2.10 as one of the governing equations in evaluating the hydraulic performance of the WDS was to ensure there is sufficient pressure at each demand node. In the UK, for example, H_j^{req} is often taken as a minimum residual pressure of 15 m (OFWAT, 2004).

2.2.1 Formulation of hydraulic modelling equations

Based on the main hydraulic equations governing the WDS modelling, the analysis of WDS involves formulating a system of hydraulic equations that can be iteratively solved using numerical methods for two unknowns: nodal heads and pipe flows. There are several ways to formulate such a system of equations according to the type

of unknown variable used in the formulation. For example, the formulation of q-equations (Bhave and Gupta, 2006) refers to a system of equations in which pipe flows are used as the unknown variables in Eqs. 2.1 and 2.2. Expressing pipe flows in terms of nodal heads in Eqs. 2.1 and 2.2 results in the formulation known as H-equations (Bhave and Gupta, 2006). For example, rewriting the continuity equation (Eq. 2.1) in terms of nodal heads at node *j* gives

$$\sum_{i:H_i>H_j}\left(\frac{H_i-H_j}{K_{ij}}\right)^{1/n_f}-\sum_{i:H_i<H_j}\left(\frac{H_j-H_i}{K_{ij}}\right)^{1/n_f}-Q_j=0 \qquad \forall i\in J_j \qquad (2.11)$$

where J_j represents the set of nodes connected to node *j*. Eq. 2.11 produces a set of H-equations that contain a number of nodal head unknowns of *N*. To solve this system of equations, the number of unknown nodal heads must be equal to number of continuity equations (Eq. 2.11) and one nodal head needs to be known, which is normally taken as the fixed head at source node.

The ΔQ-equations refers to the formulation in which loop-flow corrections are used as the unknown variables in Eqs. 2.1 and 2.2. The application of this formulation starts by assuming initial pipe flows that satisfy the continuity equation (Eq. 2.1). Then, pipe flows are iteratively adapted by correcting the loop-flow at each loop as follows:

$$Q_{ij}^{k}=Q_{ij}^{k-1}+\sum_{l\in l_{ij}}\Delta Q_l^k \qquad \forall ij\in l \qquad (2.12)$$

where Q_{ij}^{k} is the corrected flow rate of pipe *ij* at iteration *k*; Q_{ij}^{k-1} is the flow rate of pipe *ij* at iteration *k*-1; ΔQ_l^k is the loop-flow correction to be applied for all pipes belonging to loop *l*; and $\sum_{l\in l_{ij}}\Delta Q_l^k$ is the overall correction of all loops to which pipe *ij* belongs; and l_{ij} is the number of loops to which pipe *ij* belongs.

By applying the head loss equation (Eq. 2.2), the unknown loop-flow correction (ΔQ_l^k) can be formulated as:

$$\sum_{ij \in IJ_l} K_{ij} \left(Q_{ij}^{k-1} + \sum \Delta Q_l^k \right)^{n_f} = 0 \qquad \forall ij \in IJ_l ; \quad l \in Nl \tag{2.13}$$

where Nl is number of all loops in the WDS and IJ_l is the set of pipes in loop l; Eq. 2.13 produces a system of ΔQ-equations that can be simultaneously solved using an iterative method.

2.3 TYPES OF HYDRAULIC SIMULATIONS

2.3.1 Steady State Simulation

In steady state analysis, the hydraulic simulation model is conducted at a particular point of time in which all node demands and reservoir water levels are dealt with as being constant. This assumption of constant node demands and reservoir water levels can be valid for a short period (Bhave and Gupta, 2006). Therefore, steady state analysis can be only used to analyse the WDS at a single or short period of time and can not be used to determine the continued behaviour of the system over a certain period of time where both nodal demands and water level in storage reservoirs vary over the considered time interval.

In practice, it is common to design the WDS using steady state analysis under the worst operating condition such as peak hour demand and fire events. Nevertheless, there are some operation aspects that can not be simulated by steady state analysis. In reality, the operation of the WDS varies with time such as tank filling and emptying. For example, node demands fluctuate over the day depending on the demand type. Additionally, water levels in tanks would change depending whether water is

withdrawn from a tank or supplied to it from an external source. This makes using steady state simulation limited to a short period of time and the simulation of the WDS with time becomes essential.

2.3.2 Extended Period Simulation

Extended period simulation (EPS) is carried out over a longer period of time (i.e. 1 day, 2 days) where the total period of analysis is divided into a number of small time intervals (e.g. 24 or 48 hours). Within these time intervals, it is assumed that nodal demands remain constant while water levels of the reservoir could change or remain constant. For each time interval, repetitive steady state analysis is carried out to update the dynamics of tank filling and emptying, pump scheduling and valve setup, for example. EPS is more realistic than SSS in the sense that the fluctuations in node demands and water levels in tanks can be modelled. This indicates that the performance of the WDS during peak and low hour demands can be evaluated. In addition, the WDS operated with pumps of varying speed can be modelled and valve setting at each time step can be tracked. EPS analysis is important to ensure providing an adequate level of service to the consumers that operates under a pattern of varying demands. Most importantly, EPS is essential to optimize pump scheduling, sizing and location of storage tanks.

2.4 METHODS OF HYDRAULIC SIMULATIONS

2.4.1 Demand Dependent Analysis

Demand driven analysis (DDA) conventionally considers all nodal demands as being constant and satisfied in full and irrespective of nodal pressures. This assumption neglects the fact that nodal outflows are dependent on nodal pressures. Satisfying nodal demands at all times using DDA analysis has the effect of producing inaccurate and misleading results of nodal heads in case the system has no sufficient

pressure even under normal operating conditions. For example, satisfying nodal demands in full via pipes of small diameters could produce large negative nodal pressures in DDA analysis. Accordingly, it is practically more accurate to evaluate the system performance based on considering nodal demands to be dependent on nodal pressures. Due to the simplicity in using DDA models, they are still widely used in industry and research as a tool of assessing performance of the WDS. The DDA analysis is commonly carried out using four methods: 1) the Hardy-Cross method; 2) the Newton-Rasphon method; 3) the Linear Theory method; and 4) the Global Gradient method.

2.4.1.1 Hardy-Cross Method

This analysis method presented by Hardy Cross in 1936 uses the loop-flow correction equation (i.e. Eq. 2.13) to determine pipe flows that satisfy Eq. 2.1 and Eq. 2.2. First, initial pipe flow rates satisfying the flow continuity within a loop are assumed as follows:

$$\sum_{ij \in IJ_l} K_{ij} \left(Q_{ij}^{k-1} + \sum \Delta Q_l^k \right)^{n_f} = 0 \qquad \forall ij \in IJ_l ; \quad l \in Nl \tag{2.14}$$

where Nl is number of all loops in the WDS and n_f is the flow exponent. Expanding Eq. 2.14 according to Taylor's series and neglecting second order of ΔQ_l^k gives:

$$\sum_{ij \in IJ_l} K_{ij} \left(Q_{ij}^{k-1} \right)^{n_f} + \Delta Q_l^k \sum_{ij \in IJ_l} \left| n_f K_{ij} \left(Q_{ij}^{k} \right)^{n_f - 1} \right| = 0 \qquad \forall ij \in l \tag{2.15}$$

The value of the loop-flow correction (ΔQ_l^k) can be obtained by rearranging Eq.2.15 as follows:

$$\Delta Q_l^k = -\frac{\sum_{ij \in IJ_l} K_{ij} \left(Q_{ij}^{k-1}\right)^{n_f}}{\sum_{ij \in IJ_l} \left| n_f K_{ij} \left(Q_{ij}^{k}\right)^{n_f - 1} \right|} \qquad \forall ij \in l \qquad (2.16)$$

Assuming that the loop-flow correction for loop l (i.e. ΔQ_l^k) is not affected by adjacent loops to loop l (i.e. each loop is corrected separately) shows that Eq. 2.16 has one unknown, which is ΔQ_l^k. Knowing ΔQ_l^k for all loops, the corrections are then applied as follows

$$Q_{ij}^k = Q_{ij}^{k-1} + \Delta Q_l^k \qquad \forall ij \in IJ_l \,;\, l \in Nl \qquad (2.17)$$

Eq. 2.17 represents the end of one iteration. The following iteration uses the corrected flows as the updated values for pipe flow rates in Eqs. 2.14 to 2.16. The process is continued until the values of loop-flow corrections are insignificant or relatively very small.

2.4.1.2 Newton-Raphson Method

The Newton-Raphson method analyzes the entire WDS altogether and not loop by loop as in the Hardy-Cross method,. The Newton-Raphson method first introduced by Martin and Peters (1963) is a powerful numerical method for solving systems of non-linear equations. To solve a non-linear equation of a single variable $F(x) = 0$, the method assumes an initial solution that is iteratively adapted as follows:

$$x^{k+1} = x^k - \frac{F\left(x^k\right)}{F'\left(x^k\right)} \qquad (2.18)$$

in which $dF\left(x^k\right)/dx$ is the value of the derivative of $F(x)$ at x^k. Applying Eq. 2.18

to a system of non-linear equations yields

$$\underline{x}^{k+1} = \underline{x}^{k} - \left(J_x^k\right)^{-1} \underline{F}\left(\underline{x}^{k}\right) \tag{2.19}$$

where $\underline{x}$ is the vector of the variables; $\underline{F}$ is the vector containing function values; and J_x is the Jacobian matrix of F. To apply the Newton-Raphson method to the WDS, the continuity equations are expressed in terms of the vector of nodal continuity equations ($\underline{F}$) and the vector of nodal heads ($\underline{H}$) as follows

$$\underline{F}(\underline{H}) = 0 \tag{2.20}$$

Assuming initial values for nodal heads, the vector of nodal heads ($\underline{H}$) in Eq. 2.20 can be iteratively adapted according to Eq. 2.19 as follows

$$\underline{H}^{k+1} = \underline{H}^{k} - \left(J_H^k\right)^{-1} \underline{F}\left(\underline{H}^{k}\right) \tag{2.21}$$

where J_H represents the Jacobian matrix for the unknown nodal heads. Eq. 2.21 can be expressed in terms of the vector of the nodal head corrections ($\underline{\Delta H}^{k} = \underline{H}^{k+1} - \underline{H}^{k}$) as follows

$$J_H^k \underline{\Delta H}^{k} = -\underline{F}\left(\underline{H}^{k}\right) \tag{2.22}$$

The system of equations in Eq. 2.22 is solved simultaneously for $\underline{\Delta H}^{k}$ to obtain $\underline{H}^{k+1}$. The iterative process continues until reaching a pre-specified value for $\underline{\Delta H}^{k}$ or $\underline{F}\left(\underline{H}^{k}\right)$.

2.4.1.3 Linear Theory Method

The linear theory method presented by Wood and Charles (1972) is another analysis method in which the entire WDS is analyzed altogether. Obviously, the continuity equation is linear but the head loss equations are non-linear. In this method, the head loss equations are linearized by merging the non-linear term with the pipe resistance coefficient as follows

$$h_{ij}^{k} = \left\lfloor K_{ij}\left(Q_{ij}^{k-1}\right)^{n_f} \right\rfloor Q_{ij}^{k} \qquad \forall ij; \quad k = 1,2 \tag{2.23}$$

$$h_{ij}^{k} = \left[K_{ij}\left(\frac{Q_{ij}^{k-1} + Q_{ij}^{k-2}}{2} \right)^{n_f} \right] Q_{ij}^{k} \qquad \forall ij; \quad k = 3,4,5,... \tag{2.24}$$

Eq. 2.23, Eq. 2.24 and the continuity equation form a system of linear equations that can be simultaneously solved for pipe flow rates using an iterative method. Eq. 2.23 is applied to the first and second iterations where the initial pipe flow rate is set to unity, while Eq. 2.24 is applied to the next iterations in which pipe flow rates Q_{ij}^{k} are determined by averaging flow rates obtained from previous iterations (i.e. Q_{ij}^{k-1} and Q_{ij}^{k-2}). The iterative process is repeated until the difference between pipe flow rates in two consecutive iterations (i.e. Q_{ij}^{k-1} and Q_{ij}^{k-2}) are insignificant or negligible.

2.4.1.4 Global Gradient Method

Todini and Pilati (1988) proposed the application of the Newton-Raphson method to simultaneously obtain both values of pipe flow rates and nodal heads. The Newton-Raphson method solves for the corrections of either pipe flow rates or nodal heads. This method known as the Global Gradient Method (GGM) applies the Newton-Raphson method by replacing the corrections of pipe flow rates and nodal heads with

the corrected values of pipe flow rates and nodal heads in the head loss equation, i.e. $H_i^{k+1} = H_i^k + \Delta H_i^k$ and $Q_{ij}^{k+1} = Q_{ij}^k + \Delta Q_{ij}^k$ respectively. Accordingly, the GGM method directly obtains the corrected values of pipe flow rates and nodal heads in the head loss equation, instead of obtaining corrections to them (i.e. Newton Raphson method), in an iterative procedure that continues until no improvement occurs. Additionally, the GGM is similar to the linear theory method in that it does not require satisfying the continuity equations at all nodes to start the solution procedure.

The GGM takes pipe flow rates and nodal heads as the basic unknowns to formulate the Q-H equations. The non-linear equations of head loss are linearized using the expansion of Taylor's series and neglecting all terms after the second term. Accordingly, the non-linear head loss equations for k^{th} iteration can be written as

$$\left(H_i^k + \Delta H_i^k\right) - \left(H_j^k + \Delta H_j^k\right) = K_{ij}\left(Q_{ij}^k\right)^{n_f} + n_f K_{ij}\left|Q_{ij}^k\right|^{n_f - 1}\Delta Q_{ij}^k \qquad \forall ij \tag{2.25}$$

Rearranging and rewriting Eq. 2.25 in terms of corrected nodal heads H_i^{k+1} and H_j^{k+1} yields

$$H_i^{k+1} - H_j^{k+1} - n_f K_{ij}\left|Q_{ij}^k\right|^{n_f - 1}\Delta Q_{ij}^k = K_{ij}\left(Q_{ij}^k\right)^{n_f} \qquad \forall ij \tag{2.26}$$

where $H_i^{k+1} = H_i^k + \Delta H_i^k$ and $H_j^{k+1} = H_j^k + \Delta H_j^k$. Now, replacing $Q_{ij}^k + \Delta Q_{ij}^k$ with corrected pipe flow rate Q_{ij}^{k+1} in Eq. 2.26 gives

$$H_i^{k+1} - H_j^{k+1} - n_f K_{ij}\left|Q_{ij}^k\right|^{n_f - 1} Q_{ij}^{k+1} = \left(1 - n_f\right)K_{ij}\left(Q_{ij}^k\right)^{n_f} \qquad \forall ij \tag{2.27}$$

Eq. 2.27 provides a system of linear equations that combine the corrected values of pipe flow rates and nodal heads. The continuity equation is linear and can be expressed in terms of corrected pipe flow rates as

$$\sum_{ij \in j} Q_{ij}^{k+1} + Q_j = 0 \qquad j = 1,....., N-1 \qquad (2.28)$$

Eqs. 2.27 and 2.28 can be simultaneously solved to provide the corrected values of pipe flow rates and nodal heads. For the first iteration, pipe flow rates Q_{ij}^{k} can be set to unity or alternatively to some arbitrarily chosen value. As the iteration procedure continues, the changes in the values of pipe flow rates and nodal heads become insignificant.

The widely used EPANET 2 (Rossman, 2000) is a DDA hydraulic simulator that employs the GGM as its network solver. EPANET 2 provides a comprehensive tool that can carry out both types of the hydraulic analysis (i.e. SSA and ESP); handle any size of pipe networks; compute friction head loss using the three common formula (i.e. Hazen-Williams, the Chezy-Manning formula and the Darcy Weisbach); compute minor losses (e.g. for bends and fittings); compute pumping energy and cost; model different types of valves (e.g. pressure regulating valves and flow control valves); handle any shape of storage tanks; handle demand variation at nodes; model pressure-dependent flow at sprinkles and operate the system based on simple tank level, timer controls and complex rule-based controls.

In addition, EPANET 2 is equipped with water quality simulator that can model, over a period of time, the movement of a non-reactive tracer material through the network; the movement and fate of a reactive material as it grows (e.g., a disinfection by-product) or decays (e.g., chlorine residual); the age of water throughout a network; reactions both in the bulk flow and at the pipe wall; and storage tanks as being complete mix, plug flow, or two-compartment reactors. The water quality analyzer can also track the percent of flow from a given node reaching all other nodes, allow growth or decay reactions to proceed up to a limiting concentration, employ global reaction rate coefficients that can be modified on a pipe-by-pipe basis and allow for time-varying concentration or mass inputs at any location in the

network. Recently, an extended version of EPANET 2 called EPANET-MSX (Multi-Species eXtension) was developed to enable modelling complex reaction schemes between multiple chemical and biological species in both the bulk flow and at the pipe wall.

In terms of practicality, EPANET 2 is equipped with a useful tool known as EPANET' Programmers Toolkit to enable researchers to develop special applications that require running several hydraulic simulations such as optimization. The toolkit is a dynamic link library (DLL) composed of over 50 functions that can: open a network description file; read and modify various network design and operating parameters; run multiple extended-period simulations accessing results as they are generated or saving them to file; and write selected results to a file in a user-specified format.

2.4.2 Pressure Dependent Analysis

Instead of assuming that all nodal demands are satisfied in full at all times, pressure dependent analysis (PDA) addresses this assumption by explicitly considering that nodal demands are dependent on nodal pressures. The formulation of PDA methodology expresses nodal demands as a relationship between nodal outflows and nodal heads. The main advantage of PDA models over DDA models is in the ability to model pressure deficient conditions in which nodal demands are not satisfied in full. Furthermore, they alleviate the issue of yielding misleading results of nodal heads associated with the application of DDA models. In practice, the development of PDA models could enable the decision makers in water companies to evaluate the performance of the WDS operating under pressure deficiency conditions.

In literature, there are a number of relationships proposed to depict the behaviour of nodal outflows under variations in pressure. All these relationships are based on the concept of satisfying nodal demands when nodal heads are above or equal to required heads (H_i^{req}), while producing zero flows when nodal heads are below minimum

heads ($H_i^{\min}$). In practice, $H_i^{\min}$ is normally taken as the node elevation. In between, nodal outflows are dependent on how the proposed relationship depicts the behaviour of such outflows with nodal heads.

Germanopoulos (1985) suggested an exponential relationship between nodal outflow and nodal pressure according to the following equation

$$Q_i = Q_i^{req}\left(1 - b_i\, e^{-c_i\left(\frac{\mathrm{Pr}_i}{\mathrm{Pr}_i'}\right)}\right) \tag{2.29}$$

where Q_i and Q_i^{req} are the available outflow and the required demand at node i respectively; b_i and c_i are coefficients that need calibration for node i; Pr_i is the available pressure at node i, while Pr_i' is the pressure sufficiently supply a proportion of the required demand at node i. The suggested values for b_i and c_i are, if no field data are available, 10 and 5 respectively, while Pr_i' takes a value satisfying 93.2% of the required nodal demand (Q_i^{req}). Eq. 2.29 does not satisfy the condition that $Q_i = 0$ when $H_i = H_i^{\min}$ and $Q_i = Q_i^{req}$ when $H_i = H_i^{req}$.

Gupta and Bhave (1996) suggested an improved formulation for Eq. 2.29 that satisfies the aforementioned conditions as follows

$$Q_i = Q_i^{req}\left(1 - b_i\, e^{-c_i\left(\frac{H_i - H_i^{\min}}{H_i^{req} - H_i^{\min}}\right)}\right) \tag{2.30}$$

Wagner et al. (1988) and Chandapillai (1991) suggested that nodal outflow and pressure follow a parabolic relationship using the following equation

$$H_i^{des} = H_i^{\min} + R_i\left(Q_i^{req}\right)^{n_e} \tag{2.31}$$

where R_i is the resistance coefficient and n_e is a constant that can take a value between 1.5 and 2 (Gupta and Bhave, 1996). Accordingly,

$$Q_i = Q_i^{req} \qquad H_i \geq H_i^{req} \tag{2.32}$$

$$Q_i = Q_i^{req}\left(\frac{H_i - H_i^{\min}}{H_i^{req} - H_i^{\min}}\right)^{\frac{1}{n_e}} \qquad H_i^{\min} \leq H_i \leq H_i^{req} \tag{2.33}$$

$$Q_i = 0 \qquad H_i \leq H_i^{\min} \tag{2.34}$$

Fujiwara and Ganesharajah (1993) proposed a differentiable function for the relationship between nodal outflow and pressure according to the following equation

$$Q_i = Q_i^{req}\frac{\int_{H_i^{\min}}^{H_i}\left(H - H_i^{\min}\right)\left(H_i^{req} - H\right)dH}{\int_{H_i^{\min}}^{H_i^{req}}\left(H - H_i^{\min}\right)\left(H_i^{req} - H\right)dH} \qquad H_i^{\min} \leq H_i \leq H_i^{req} \tag{2.35}$$

Based on the logit function, which is a mathematical function with an S-shape that grows exponentially in the initial stage of growth then the growth becomes slow until reaching saturation where growth stops, Tanyimboh and Templeman (2004, 2010) proposed a nodal flow relationship that has the following form

$$O_i = Q_i^{req}\frac{e^{(\alpha_i + \beta_i H_i)}}{1 + e^{(\alpha_i + \beta_i H_i)}} \tag{2.36}$$

where α_i and β_i are parameters that need calibration from field data. These two parameters essentially determine the shape of the function curve. Rearranging Eq.

2.36 gives

$$\frac{O_i}{Q_i^{req}} = \frac{e^{(\alpha_i+\beta_i H_i)}}{1+e^{(\alpha_i+\beta_i H_i)}} \tag{2.37}$$

The ratio of Q_i / Q_i^{req} in Eq. 2.37 is known as the nodal demand satisfaction ratio (*DSR*). The nodal *DSR* takes a value of 1.0 when H_i is larger than or equal to H_i^{req}, while it takes a value of zero when H_i is less than or equal to $H_i^{\min}$. When H_i is between $H_i^{\min}$ and H_i^{req}, the nodal *DSR* takes values between 0 and 1. Accordingly, the nodal demand is considered fully satisfied when the nodal *DSR* = 1, partially satisfied when the nodal *DSR* is between 0 and 1, and no nodal outflow when the nodal *DSR* = 0.

In case of no field data are available; Tanyimboh and Templeman (2010) suggested obtaining values for α_i and β_i by substituting Eq. 2.37 with 0.001 and 0.999 for the values of *DSR* and then simultaneously solving the resulting equations.

Unlike most of the proposed nodal outflow relationships, Eq. 2.36 is unique in that it has no discontinuities in its functions and/or derivative and produces restricted values of nodal outflow ranging between zero and fully satisfied demands. This function has the advantage of enabling a smooth transition between zero and partial outflow and between partial outflow and full outflow.

PRAAWDS (Program for the realistic analysis of the availability of the water distribution systems) is a PDA hydraulic model developed by Tanyimboh and Templeman (2010). The prototype computer model of PRAAWDS written in FORTRAN provides two options to carry out a hydraulic analysis. The first one contains four choices of pressure flow relationships by which a PDA analysis can be carried out. These include functions of Wagner et al. (1988), Germanopoulos-Gupta-Bhave (Gupta and Bhave, 1996), Fujiwara and Ganeshrajah (1993) and Tayimboh

and Templeman (2004). The second one uses DDA analysis to enable comparison of results with PDA analysis. In addition, it offers a built-in feasibility procedure to evaluate the accuracy of results obtained from PDA analysis. PRAAWDS has been used to evaluate performance measures that require PDA analysis (e.g. hydraulic reliability and failure tolerance) in several studies, e.g. Setiadi et al. (2005), and demonstrated high robustness and accuracy.

2.5 PERFORMANCE ASSESSMENT OF WATER DISTRIBUTION SYSTEMS

Water distribution system (WDS) design problems are conventionally dealt with as the determination of the cheapest design that is marginally able to supply consumers with sufficient amounts of water at the required pressures. The resulting designs are supposed to have the cheapest set of pipe sizes that are capable of satisfying both required nodal demands and pressures in normal operating conditions (i.e. all system components are considered available in service). This has the restriction that such a design is conditioned on the uninterrupted availability of all the components making up the whole system.

In reality, the WDS is very likely to be subject to abnormal operating conditions such as component failures and components deterioration with time. For example, pipe breakage could happen due to suddenly increased pressures or pipe diameters could become smaller because of accumulated sediments on the internal walls of pipes. The occurrence of abnormal operating conditions give rise to pressure deficiency within the system and accordingly node demands could not be satisfied in full in these conditions. These circumstances significantly affect the WDS capacity especially those having the cheapest set of pipe diameters. As a result, the WDS should be well designed to have some spare capacity above the minimum prescribed that can be used to partially or fully compensate for any reduction in capacity during failure conditions.

In addition to cost saving, the performance assessment of the WDS under both normal and abnormal operating conditions has become an essential element in the design process of the WDS optimization. As a result, obtaining a design with a balance between cost and reliability is crucial in saving a significant amount of cost throughout the whole life of the WDS. In literature, network reliability is widely used as a performance measure of the WDS. This measure focuses on the hydraulic aspects rather than the network connectivity in terms of components layout. Based on the method of assessing reliability, the performance measures are classified into two types: accurate measures and surrogate measures.

2.6 ACCURATE PERFORMANCE MEASURES

The formulation of these measures is based on assessing reliability by considering the effect of each possible combination of components failure on the hydraulic performance of the WDS. Since DDA models are not able to simulate failure conditions, the calculation of accurate measures requires employing PDA models such as PRAAWDS (Tanyimboh and Templeman, 2010) and EPANET-PDX (Siew and Tanyimboh, 2011). In the following sections 2.6.1 and 2.6.2, the accurate measures of hydraulic reliability and failure tolerance widely used in literature are presented.

2.6.1 Hydraulic Reliability

In practice, there is no universally agreed definition of reliability. The definition of reliability herein is adopted from Tanyimboh and Templeman (2000). They define the reliability as the ability of the system on average to satisfy nodal demands and considered as the average value of the ratio of the flow delivered to the flow required whilst considering both normal and abnormal operating conditions (Tanyimboh and Templeman, 2000). Taking a peak demand as a constant value for more conservative

assessment of reliability, the hydraulic reliability can be computed as in Tanyimboh and Templeman (2000), i.e.

$$R = \frac{1}{T}\left(p(0)T(0) + \sum_{m=1}^{M} p(m)T(m) + \sum_{m=1}^{M-1}\sum_{n=m+1}^{M} p(m,n)T(m,n) + ... \right)$$

$$+ \frac{1}{2}\left(1 - p(0) - \sum_{m=1}^{M} p(m) - \sum_{m=1}^{M-1}\sum_{n=m+1}^{M} p(m,n) - .... \right) \qquad (2.38)$$

where R is hydraulic reliability; M is number of links; $p(0)$ is $a_1a_2a_3.....a_M$ = probability that all links are in service; a_m is probability that link m is in service at any given moment; $p(m) = p(0)(u_m/ a_m)$ is probability that only link m is not in service; $u_m = 1- a_m$ is probability that link m is unavailable, $p(m,n) = p(0)(u_m/ a_m)(u_n/a_n)$ is probability that only links m and n are not in service; $T(0)$, $T(m)$ and $T(m,n)$ are, respectively, the total flows supplied with all links in service, only link m out of service, and only links m and n out of service; and T is the sum of the nodal demands.

Apparently, Eq. 2.38 is composed of two main parts, i.e. the two pairs of large parentheses. The first part accounts for the fraction of the total demand satisfied by the system on average. Since it is impractical to model all the combinations of components failure of the WDS, the first part of Eq. 2.38 generally results in underestimating the reliability in practice. The second part is introduced to estimate the quantity by which the first part underestimates the reliability.

The pipe availability (a_m) values can be calculated using the factor of mechanical reliability, which is usually given by the probability that the component m encounters no failure within a defined period of time (Mays, 2002). In literature, there are several formulae for calculating pipe availability such as the formula developed by Cullinane *et al.* (1992) defined as

$$a_m = \frac{0.21218 D_m^{1.462131}}{0.00074 D_m^{0.285} + 0.21218 D_m^{1.462131}} \qquad \forall m \in M \qquad (2.39)$$

where D_m is diameter of pipe m in inches.

2.6.2 Failure Tolerance

Another equally important performance measure is the network redundancy. Network redundancy evaluates the network robustness Redundancy arises from the existence of alternative paths from the source to demand nodes or from the existence of spare capacity within the network during normal operating conditions that can be used to balance any energy loss during failure operating conditions. Like reliability, quantifying the redundancy is difficult. Tanyimboh and Templeman (1998) were likely the only researchers who developed a rigorous mathematical model for the redundancy measure. They showed that calculating how much demands are satisfied while some components are out of service provides a realistic measure of hydraulic redundancy. Tanyimboh et al (2011) pointed out that failure tolerance may provide a better measure of supply disruption for a network in case of failure than the hydraulic reliability gives for similar reliable systems, i.e. designs with similar reliabilities may have behave differently when considering failure alone.

The hydraulic redundancy or failure tolerance (*FT*) is another performance indicator that incorporates only pipe-failure effects in order to measure the amount of satisfied demands while some components are unavailable. The equation for failure tolerance is given by

$$FT = \frac{R - p(0)T(0)/T}{1 - p(0)} \qquad (2.40)$$

Clearly, Eq. 2.40 excludes periods in which all links are unavailable. The hydraulic redundancy provides a quantification of any spare capacity available in the system in terms of surplus nodal heads. In general, the value of *FT* is less than *R* where *FT* becomes closer to *R* as the redundancy or spare capacity increases. Given that R and $p(0)$ were already calculated in Eq. 2.38, the calculation of *FT* is straightforward.

2.7 SURROGATE PERFORMANCE MEASURES

Due to the high computational effort required to accurately evaluate reliability of the WDS along with no universally agreed definition of reliability is available in literature, a number of surrogate measures of reliability were proposed. These measures have the advantages of being simple to calculate, do not require simulations of failure conditions and able to be incorporated in the optimization of the WDS. Additionally, these measures use the hydraulic results of pipe flows or/and nodal heads obtained from modelling the WDS under normal operating conditions to approximate the hydraulic performance under abnormal operating conditions. As such, DDA models are still suitable to evaluate such measures.

2.7.1 Informational Entropy

Shannon (1948) introduced the informational entropy as a measure of the amount of uncertainty associated with a probability distribution. For a random variable having a set of possible values $\{x_1, x_2, x_3, \ldots, x_n\}$ with corresponding probabilities such that $p(x_1) + p(x_2) + p(x_3) + \ldots + p(x_n) = 1$, where n = number of outcomes, the Shannon entropy function can be written as

$$S = -\sum_{i=1}^{n} p(x_i) \ln p(x_i) \tag{2.41}$$

where S is the entropy and $p(x_i)$ is the probability of the ith outcome.

Awumah *et al.* (1990, 1991) and Tanyimboh and Templeman (1993a,b) developed a framework for applying informational entropy to WDSs. Knowing the pipe flow rates, the entropy function can be expressed as in Tanyimboh and Templeman (1993a) as

$$S = S_0 + \sum_{i=1}^{N} P_i S_i \tag{2.42}$$

in which S is WDS entropy; S_0 is entropy of source supplies; S_i is entropy of node i; $P_i = T_i/T$ is fraction of the total flow through the WDS that reaches node i; T_i is total flow reaching node i; T is total demand; N is number of nodes in the network.

$$S_0 = -\sum_{i \in I} \frac{Q_{0i}}{T} \ln\left(\frac{Q_{0i}}{T}\right) \tag{2.43}$$

where Q_{0i} is inflow rate at source node i and I is set of the source nodes. In a similar way, the entropy of the nodes can be written as

$$S_i = -\frac{Q_{i0}}{T_i} \ln\left(\frac{Q_{i0}}{T_i}\right) - \sum_{ij \in out(N_i)} \frac{Q_{ij}}{T_i} \ln\left(\frac{Q_{ij}}{T_i}\right) \qquad i = 1,....., N \tag{2.44}$$

where Q_{i0} is demand at node i; Q_{ij} is flow rate in pipe ij; $out(N_i)$ is the set of all pipe flows from node i. A comparison of the Awumah *et al.* (1990, 1991) and Tanyimboh and Templeman (1993a,b) models is available in Tanyimboh (1993).

2.7.1.1 Maximum Entropy for Water Distribution Systems

The relationship between informational entropy and reliability of the WDS owes to the principle of maximizing informational entropy, which corresponds to Laplace's

principle of insufficient reason. This principle suggests that probability mass functions should be dealt with as uniform if there is no information on the appropriate random variables. In WDS, demand nodes are either supplied with only one path or more from the source(s). For those supplied with more than one path, there is no reason for preferring any path over any other path to supply the demand node. According to Laplace's principle, all of the paths supplying a demand node should deliver the same amount of water, and so the same probability, to the demand node. This means that the flow supplied by a source to a demand node should be evenly distributed to all of the paths delivering that demand from that source. For such a distribution, the effect of cutting off a supplying path on satisfying the demand node could be less than if the demand is unequally distributed. For example, removing a path being allocated a large proportion of the demand will definitely have a significant effect on satisfying the supply to that node.

In single-source networks, all flow paths supplying demand nodes originate from the source. Based on this fact, Tanyimboh and Templeman (1993a,b,c) developed a non-iterative method to calculate maximum-entropy flows for single-source networks. Once maximum-entropy flows are determined using this method, these ME flows are substituted for Q_{ij} in Eq. 2.44. Ang and Jowitt (2005a) developed a simple method named the Path Entropy Method (PEM) that determines ME for single-source networks based on the number of flow paths supplying each demand node. In the same study, the PEM was further extended to SPEM (Simplified SPEM) that uses only demands and number of flow paths to determine ME for single-source networks. In this study, the SPEM method was used to eases calculating ME for single-source networks.

However, the situation is different in multiple-source networks as most of demand nodes are supplied with more than one source and so the proportion received from each source is unknown. Yassin-Kassab *et al* (1999) developed a non-iterative algorithm for calculating maximum-entropy flow distribution for multiple-source

networks. The solution method of this algorithm is based on establishing the hypothesis of Principle A that states:

"The maximum entropy flows in multiple source networks are such that the ratio of the probabilities of the path flows from any pair of sources to a demand node reachable from those sources is the same for every demand node supplied by those sources in the network"

At first, the above principle was numerically proved by Yassin-Kassab *et al* (1999). Then, a formal proof of this hypothesis was provided by Ang and Jowitt (2005b) based on extending the application of the PEM method to multiple source networks. Principle A can be expressed by the following general equation:

$$\frac{p_{ij}}{p_{kj}} = \frac{\alpha_i}{\alpha_k} \qquad \forall i,k \in I_j ; \forall j \in J \tag{2.45}$$

Where i and k denote any pair of sources supplying demand node j in the network; I_j is the set of all source nodes supplying node j; J is the set of all demand nodes in the network. The general formula for path flow probabilities expressed in terms of unknown αs can be written as follows:

$$p_{ij} = \frac{Q_{j0}\alpha_i}{\sum_{i \in I_i} NP_{ij} Q_{0i} \alpha_i} \qquad \forall i \in I_j ; \forall j \in J \tag{2.46}$$

where NP_{ij} is the number of paths from source node i to demand node j. Obviously, the number of αs in Eq. 2.45 is equal to number of sources (NS) in the network. Since number of unknown αs required in a network is equal to NS-1, one of the αs in Eq. 2.45 has to be set to unity. Accordingly, Eq. 2.45 contains (NS-1) unknown αs because $\alpha_i = 1$ for $i = 1$. However, there are NS normality condition equations that can be written from a network as follows:

$$\sum_{j \in J_i} NP_{ij}\, p_{ij} = 1 \qquad \forall i \in I \tag{2.47}$$

Substituting path flow probabilities of Eq. 2.46 into (NS-1) of the normality condition equations of Eq. 2.47 will give (NS-1) equations with (NS-1) unknown αs, which can be solved to determine all the values of the unknown αs. Back-substituting the resulting values of αs into Eq. 2.46 yields all the path flow probabilities in the network. Finally, the *maximum entropy* can be appropriately calculated using the conditional entropy function of Khinchin (1953) as follows:

$$S = -\sum_{i \in I} \frac{Q_{0i}}{T} \ln\left(\frac{Q_{0i}}{T}\right) + \sum_{i \in I} \left(\frac{Q_{0i}}{T}\right) S_i \qquad \forall i \in I \tag{2.48}$$

S_i in Eq. 2.48 is the entropy of all paths supplied by source node i and given by:

$$S_i = -\sum_{j \in J_i} NP_{ij}\, p_{ij} \ln p_{ij} \qquad \forall i \in I \tag{2.49}$$

2.7.2 Resilience Index

The concept of resilience index was introduced by Todini (2000) as a measure of the available surplus power that can be dissipated internally in the event of a failure in the WDS. Since the total power in the network is composed of the power dissipated in the pipes and the power delivered to the nodes, Todini (2000) defined the resilience index as

$$RI = \frac{\sum_{i=1}^{n_n} Q_i^{req}\left(H_i - H_i^{req}\right)}{\sum_{k=1}^{n_r} Q_k H_k + \sum_{j=1}^{n_{pu}} P_j / \gamma - \sum_{i=1}^{n_n} Q_i^{req} H_i^{req}} \tag{2.50}$$

Where RI is resilience index; H_i is available head at node i as obtained from hydraulic simulation; H_i^{req} is the required head of node i at which the demand is satisfied in full; Q_i^{req} is demand at node i; γ is specific weight of water; Q_k and H_k are respectively outflow and head at reservoir k; P_j is power introduced to the network by pump j; n_{pu} is number of pumps in the network; n_n is number of demand nodes in the network; and n_r is number of reservoirs in the network.

2.7.3 Modified Resilience Index

Jayaram and Srinivasan (2008) questioned the suitability of using the resilience index in multiple source networks. They showed that networks with high surplus power can have also high power input. Since the denominator in Eq. 2.50 represents the power input term, a low resilience index could be obtained even with networks having a large amount of surplus power. As a result, they suggested an alternative indicator referred to as modified resilience index (MRI) that measures the surplus power in terms of a percentage of the power required at the nodes as follows

$$MRI = \frac{\sum_{i=1}^{n_n} Q_i^{req}\left(H_i - H_i^{req}\right)}{\sum_{j=1}^{n_n} Q_j^{req} H_j^{req}} \times 100 \tag{2.51}$$

in which MRI is modified resilience index.

2.7.4 Network Resilience

Prasad and Park (2004) extended the concept of resilience index by combining the effects of both surplus power and reliable loops to form a reliability measure known as network resilience (*NR*). They stated that reliable loops can be ensured if the variation in pipe diameters connected to a node is not wide. They introduced the uniformity of pipe diameters at each node as the ratio of the average of the diameters of the pipes incident at a node to the maximum diameter at that node. Thus, the network resilience is defined as

$$NR = \frac{\sum_{i=1}^{n_n} C_i Q_i^{req} \left(H_i - H_i^{req} \right)}{\sum_{k=1}^{n_r} Q_k H_k + \sum_{j=1}^{n_{pu}} P_j / \gamma - \sum_{i=1}^{n_n} Q_i^{req} H_i^{req}} \tag{2.52}$$

in which C_i is the uniformity of pipe diameter for node *i*.

2.7.5 Surplus Power Factor

Vaabel et al. (2006) introduced the surplus power factor (*s*) to evaluate the capacity of hydraulic power of the WDS based on both flow within pipes and pressure head at the inlets of pipes. The surplus power factor can be also used as an indicator of the network resilience of the WDS, i.e. as the value of *s* increases, the resilience of the system to failure conditions increases. The surplus power factor is defined as

$$s = 1 - \frac{n_f + 1}{n_f} \left[1 - \frac{1}{n_f + 1} \frac{Q_{in}^{n_f}}{Q_{\max}^{n_f}} \right] \frac{Q_{in}}{Q_{\max}} \tag{2.53}$$

in which n_f is the flow exponent dependent on the head loss formula used in the analysis; Q_{in} is the inflow of the pipe; and Q_{max} is the flow that provides the

maximum hydraulic power at the outlet of the pipe. The range of values s can take is from 0 to 1. A value of $s = 1$ indicates that the system works at its maximum hydraulic capacity.

2.8 CONCLUSIONS

The hydraulic modelling is a valuable tool for assisting engineers in understanding and evaluating the hydraulic performance during the design process of the WDS. The modelling of the WDS enables simulating the operation of the system under different operating conditions and thus allows evaluating any proposed design and anticipates unforeseen problems that could occur before investing a capital in a real WDS project.

This chapter has presented the basics of modelling the WDS including the formulation of a system of non-linear hydraulic equations. In addition, a review of types of hydraulic simulations and approaches used to model the WDS was carried out. The limitation of steady-state simulation was highlighted in comparison with the extended period simulation. The conventional method of modelling the WDS using DDA analysis, which is restricted to simulations under normal operating conditions, was also outlined in reference with the method of PDA analysis, which is able to simulate systems under abnormal operating conditions.

The WDS is most likely to be subjected to abnormal operating conditions in which some system components could be fully or partly unavailable. Pipe bursts, pump failures and scheduled maintenance of system components can result in a deficiency in pressure within the system. Further assessment of the system performance becomes essential to measure the ability of the WDS to meet design requirements under these situations. Two important performance measures that accurately assess performance have been explained in detail, namely hydraulic reliability and failure tolerance. The hydraulic reliability evaluates the performance of the system under

both normal and abnormal operating conditions, while the failure tolerance quantifies the amount of redundancy available in the system. The calculation of these accurate measures requires high computational effort that makes it impractical to incorporate them in the process of WDS design.

Several surrogate performance measures that are easy to calculate and approximate hydraulic reliability and redundancy has been presented. Due to employing the statistical entropy as measure of reliability in the present research, it has been explained in detail.

The following chapter presents the key concept of and along with the application of evolutionary algorithms in the optimization of the WDS design.

CHAPTER THREE

DESIGN OPTIMIZATION OF WATER DISTRIBUTION SYSTEMS

3.1 INTRODUCTION

Water and air represent essential ingredients for human life. Water distribution systems (WDS) are constructed to deliver clean drinking water to the society and represent a vital part of the infra-structure in urban areas. In general, water distribution systems are composed of four main components: water supply sources, treatment plants and storage, transmission mains and distribution networks. The supplying sources of raw or untreated water are commonly surface water sources (e.g. rivers, lakes and reservoirs) and groundwater sources such as holes and wells. The extraction of water from these sources is carried out by constructing pumping stations. Transmission mains are used to transport the raw water over long distances for processing at treatment plants. After the treatment, the clean water is stored in storage reservoirs. The level of treatment is dependent on the quality of raw water and the required level of water quality. A distribution network supplies water to consumers through service connections.

The construction, operation and maintenance of the WDS incorporate investing a huge amount of capital. Thus, water companies are faced with the challenge of achieving the best compromise between design, management and cost of the system that should be operated under the present standards regulating the supply of water to consumers in terms of quantity, quality and pressure. This reflects that the WDS

optimization is a complex problem that incorporates conflicting objectives in which it is practically impossible to solely use engineering experience and practice to recognize the most economical design of the system that satisfies some level of hydraulic reliability. Thus, it is totally essential and significant to employ suitable optimization methods as a supporting tool to help the decision makers to handle this highly complex multi-criteria problem.

Conventional optimization methods that use mathematical programming were first used to optimize the WDS. These methods have the advantage of being very efficient because they use deterministic rules in the search procedures. However, the fact that these classical methods depends on searching from a single point make them unsuitable for problems having objective functions with multiple peaks in which the search process could end up with a local optimal solution. Furthermore, the dependence of these methods on using derivatives, for example, in the search process makes them inappropriate for problems involving discontinuous or noisy objective functions. Therefore, the application of conventional optimization methods to the WDS optimization becomes highly complex because the formulation essentially involves handling non-linear constraints that can be of large number in case of dealing with real systems.

Evolutionary Algorithms (EA) are one of the optimization techniques developed to deal with many real-world problems that are very complex and extremely hard to solve using conventional methods. These algorithms are stochastic optimization techniques that mimic natural selection and natural genetics in order to survive. Their search concepts are entirely different from the conventional methods in that they widely explore the search space based on stochastic evolution instead of gradient information. As such, they use objective functions instead of derivative, for example, and start the search from a set of points instead of a single point (Goldberg, 1989). Additionally, they deal with a coding of decision variables instead of the variables themselves and use probabilistic transition rules instead of deterministic rules in the search process (Goldberg, 1989). These features make EAs suitable to solve multi-

objective optimization problems. These algorithms are efficient and powerful in the sense that their search procedures use a small fraction of the entire search space of the problem in order to converge at or near the optimal solution. The main classes of EAs are genetic algorithms (Holland, 1975), evolutionary programming (Fogel et al., 1966), evolution strategy (Rechenberg, 1973), genetic programming (Koza, 1992), learning classifier systems (Holland, 1976), swarm intelligence (Dorigo, 1992) and particle swarm optimization (Kennedy and Eberhart, 1995).

The aim of designing the WDS is to supply costumers with required amounts of water demands with both sufficient pressure and sufficient quality. As the system ages with time, the system capacity is prone to decrease due to the effects of environmental degradation on the capacity of system components such as reducing pipe diameters caused by pipe corrosion and encrustation. This has the impact of creating pipe leakages and lowering water supply pressures in addition to water quality problems within the system. As a result, such systems will not be able to deliver the required demands to users at sufficient levels of pressure and quality in such situations. In addition to system degradation, future water demands are hard to determine due to the existence of considerable amount of uncertainty about predicting population growth in some urban areas. The inclusion of some amount of spare capacity in terms of reliability is essential to make the WDS compensate any reduction in capacity and cope with any increase in future demands.

This chapter presents a literature review of both the conventional and evolutionary optimization approaches used to solve WDS problems. The classical methods and both the limitations and drawbacks associated with their applications to WDS problems were first emphasized. As mentioned previously, there are different classes of evolutionary algorithms in literature. Among them, genetic algorithms (GAs) have received particular interest in solving real-world optimization problems. As these algorithms are used as an optimization tool in the present study, they will be discussed in depth herein. An overview of the general structure of the basic GA and the various processes involved in their implementation are outlined. Several GA

techniques for handling constraints and their weaknesses are discussed. Lastly, the application of multi-objective GA to solve WDS problems is presented.

3.2 REVIEW OF METHODS USED IN THE OPTIMIZATION OF WATER DISTRIBUTION SYSTEMS

In general, an algorithm for solving optimization problems is composed of a sequence of procedures that aims to converge to optimal solution. Conventional optimization methods use the gradient or higher order derivatives of objective functions to implement a deterministic set of sequential computational processes that start the optimization from a single point in the search space. The single point is then iteratively improved by gradually following the steepest descending trajectory, which hopefully ends up at optimal solution. The single-point search concept would be applicable in single-peak objective functions. However, applying this concept to multiple peak objective functions, for example, would put conventional methods in the danger of falling into local optima rather than global optima.

Evolutionary algorithms have been developed to avoid this danger by starting the optimization from a set of points called population. As such, the EA performs the search process in multiple directions that use the population as a starting point. The search directions are determined by the fitness of solutions and not by the gradient of the objective function, for example. Then, the starting population is iteratively improved by an evolutionary process to replace relatively bad solutions with relatively good solutions. The population-to-population concept aims to avoid falling into local optima by not seriously limiting the search to a single direction. The EA has attracted several researchers as a potential optimization technique because of their efficiency and robustness in solving complex optimization problems.

3.2.1 Conventional Optimization Methods

The optimization problem of the WDS is conventionally formulated as the determination of the cheapest pipe diameters selected from a set of commercially available pipe sizes while satisfying some hydraulic constraints. The resulting formulation is known to be non-deterministic polynomial-time (NP) hard problem to be solved by considering different optimization aspects like planning of system components, reducing capital and operating costs and improving hydraulic performance in the long-term operation of the WDS. Nevertheless, much research has conventionally applied deterministic optimization techniques such as complete enumeration, linear programming (LP), non-linear programming (NLP) and dynamic programming (DP) to handle such a complex problem.

Complete enumeration is one of the methods that can be used to optimize the WDS. The method is based on analysing each possible combination of discrete pipe sizes in order to determine the least-cost set of pipe sizes satisfying the hydraulic constraints. The main disadvantage of complete enumeration technique is in the amount of computational time required to simulate all possible combinations of pipe sizes. Gessler (1985) suggested using selective enumeration by severely pruning search space based on experience. However, the pruning process may create the danger of eliminating the global optimum from the search space.

Loubser and Gessler (1990) applied heuristics to propose three guidelines for performing the process of pruning the search space. These include: 1) grouping pipe sizes into sets each is assumed to be used by a single size; 2) progressively retain the cheapest solution satisfying the constraints and eliminate all other solutions with higher cost; and 3) investigate combinations of pipe sizes violating the constraints. Nevertheless, the method still requires a significant amount of computational time to solve large networks in addition to that the pruning process does not guarantee retaining the optimum solution in the pruned search space.

Another method that can be applied to solve the WDS optimization problem is the use of nonlinear programming techniques. In these methods, problem constraints can be explicitly included in the formulation. Additionally, the cost of the WDS can take a form of nonlinear function of pipe diameters and lengths. Su et al. (1987) used a nonlinear programming approach that incorporates reliability constraints to optimize looped pipe networks. The optimization model was based on using a constrained generalized reduced gradient technique in which constraints can include continuity equation, head loss equation, minimum and maximum bounds of pressures, and minimum and maximum bounds of pipe diameters. The approach included using a steady state simulation model to evaluate nodal pressures and a separate model for calculating reliability. The reliability was defined as the probability of maintaining pressures at sufficient levels in the network. However, the approach was not able to simulate other components like pumps, valves and storage tanks.

Lansey et al (1989) suggested determining the optimal design of pipe networks under uncertainty in nodal demands, Hazen-Williams coefficients and minimum nodal pressures. To convert the probabilistic constraints of the ability to satisfy the specified nodal heads and pressures into deterministic ones, a chance-constrained technique was used. However, the method was found to have a tendency to yield branched pipe networks.

Lansey and Mays (1989) used nonlinear programming to determine the optimum design and layout of pipe networks. The method is capable of including pumps, tanks and multiple operating conditions. A hydraulic simulator model was incorporated to handle the constraints of continuity and head loss. The generalized reduced gradient technique was used to determine the optimum solution, while the augmented Lagrangian method was used to satisfy minimum head and other constraints. However, the resulting optimum design was often found to have a branched layout.

Duan et al. (1990) extended the work of Lansey and Mays (1989) to develop a general optimization model able to handle pumps and tanks in addition to multiple

loading cases. The model divided the problem into three levels on a hierarchical basis: master problem level, sub-problem level and an inner level. In the master problem level, implicit enumeration is used to optimize location and numbers of pumps and tanks. In the sub-problem level, the generalized reduced gradient technique is used to size pipes for the layout of pumps and tanks determined in the master problem level. In the inner level of the problem, a hydraulic simulator is used to satisfy the constraints of continuity and head loss, while a separate model is used to calculate different measures of reliability.

The linear programming technique was used by Alperovits and Shamir (1977) to develop a solution method for the highly complex optimization problem of the WDS. The approach called linear programming gradient method divides each pipe into segments of constant diameters. This allowed expressing the total head loss in each link as a linear equation in terms of the lengths of constant diameter segments. The solution procedure of the model decomposes the optimization problem into two stages. For a set of candidate diameters in each link, the model uses the lengths of constant diameter segments within each pipe as the decision variables in the first stage. Then, the network is optimized based on the assumption that the distribution of flow is known. In the second stage, the flow distribution is added to the actual decision variables obtained in the first stage to improve the cost of the design resulted from the first stage. The method was applied to optimize a real network containing multiple pumps and storage reservoirs operated under multiple operating conditions. The weakness of this optimization model is represented in yielding a design composed of links each has more than one diameter. In practice, such a type of solutions is not desired as the pipe diameters should be consistent over the total pipe length.

In general, conventional optimization methods use a sequence of deterministic procedures to hopefully converge at the optimal solution. Such methods are advantageous to developing computationally efficient optimization models. However, the high dependence of these methods on initiating the optimization from a

single solution creates a serious limitation to the global optimality of the resulting solution. Accordingly, it is most likely that such point-to-point methods fall into local optimal solutions especially in multi-peak objective functions. Furthermore, the high dependence on the gradient of objective functions in the search makes conventional methods not efficient in solving problems with discontinuous or discrete search spaces. Most importantly, in highly constraint problems where the feasible part of the solution space is divided into a number of disjointed spaces, using gradient of objective functions in the search makes it extremely hard to converge at the optimal solution. The aforementioned frequently encountered difficulties put restrictions to the network size to be effectively solved using conventional methods. Real world systems represent large size highly constrained problems with discrete search spaces that are extremely difficult to be solved by conventional methods.

3.2.2 Evolutionary Algorithms

Evolutionary algorithms (EAs) represent a wide range of heuristic optimization techniques that simulate evolution (Back et al., 2000). These algorithms have frequently demonstrated the ability to solve non-linear, non-convex, multi-criteria and discrete problems in which conventional methods encounter difficulty or even result in a complete failure to solve such complex problems. The increasing complexity in the scope of water resources planning and management has made researchers widely apply evolutionary algorithms to the design optimization of water distribution systems. The fact that these stochastic methods depend on objective functions instead of derivative and continuity, for example, in the search process makes them mathematically non-complex and easy to implement. Furthermore, the fact that they work on a sequence of populations of potential solutions that are exploited to explore a huge solution space considerably increases the potential of reaching the global optimum solution.

The optimization of real-world WDSs incorporates solving a multi-criteria complex problem composed of multiple objectives that are naturally in conflict. For instance,

the determination of a reliable and economical design of the WDS requires simultaneously solving for the objectives of minimizing cost and maximizing reliability. The least-cost design of the WDS is made up of the least-cost set of pipe diameters, for example, normally belonging to a branched layout, which is not desired from the viewpoint of redundancy. In contrast, a highly reliable WDS design is mostly expensive due to the large pipe sizes required for a design with a large capacity and usually has a looped layout. As such, the idea of desiring the least-cost WDS design as the optimal solution is gradually disappearing due to the increased trend among engineers towards expanding the hydraulic capacity (e.g. in terms of reliability and redundancy) of the optimal solution beyond the minimum required under the constraint of the available budget of the WDS project.

EAs have been identified to suitably solve multi-objective optimization problems. Due to the dependence on a population of solutions instead of a single solution, EAs are capable of simultaneously exploring a search space into different directions to search for a variety of solutions in complex problems being non-linear, non-convex, discontinuous and multi-modal. In multi-objective optimization, there is no absolute superiority of one solution to another because a solution may be best in one objective but worst in other objectives. Instead of yielding one absolutely superior solution, the multi-objective optimization is very different from single-objective optimization in that it produces a set of non-dominated solutions, known as pareto-optimal front, each solution is better than the others in at least one objective. Considering cost and reliability as the main objectives of the WDS optimization problem, such an important feature provides more flexibility for engineers in assessing non-dominated solutions with respect to the required level of performance and available budget of the WDS project.

The literature is replete with different EAs applied to the optimization of water distribution systems. Genetic algorithms were one of the earliest EAs applied to the optimal design of WDSs by Murphy and Simpson (1992), Murphy et al. (1993), Simpson et al. (1994), Savic and Walters (1997) and Montesinos et al. (1999).

Murphy and Simpson (1992) applied a simple genetic algorithm technique (i.e. using single-point crossover, bit-wise mutation, binary coding and actual fitness function) to search for the least-cost pipe design of the WDS. Simpson et al. (1994) developed an improved genetic algorithm for the least-cost problem of the WDS. The improved GA uses fitness function with variable power scaling, creeping mutation operator and Gray coding. Savic and Walters (1997) developed a computer model that links a genetic algorithm with a hydraulic simulator to the least-cost design of the WDS. The model used uniform crossover and Gray coding to implement the GA. Montesinos et al. (1999) developed a modified simple genetic algorithm to the least-cost design of the WDS. The modification included introducing several changes to selection and mutation operators in order to improve the convergence of the GA. In each generation, the selection operator eliminates a constant number of solutions, while only a maximum of one mutation is allowed for the remaining solutions.

Vasan and Simonovic (2010) and Suribabu (2010) applied an improved technique known as differential evolution that is linked with a hydraulic model to the optimal design of the WDS. To increase design reliability, a measure of the resilience of looped networks was introduced in the determination of the optimal design. Cunha and Sousa (2001) employed simulated annealing, which is a heuristic method derived from physical annealing of crystals to low energy states, to develop a model for the least-cost design of a gravitational looped water distribution network. The design cost was used as the energy state and temperature as a parameter that is decreased as the model converges at the optimal solution. A hydraulic simulator was linked with the model to solve for hydraulic constraints. Geem et al. (2002) developed a heuristic algorithm known as harmony search that mimics the improvisation of music players to find the optimal design of pipe networks. Practicing sounds on several instruments to improve the sound for better aesthetic estimation was mimicked to improve the values of objective functions by iteration. Eusuff and Lansey (2003) proposed a shuffled frog leaping algorithm, which is a meta-heuristic method used to solve discrete optimization problems, to determine optimal design for new pipe networks and network expansions. The algorithm uses particle swarm optimization as a local

search tool, while the idea of mixing information from parallel local searches is used to proceed towards a global optimum.

Maier et al. (2003) applied ant colony optimization approach, which is an evolutionary method based on the foraging behaviour of ant colonies, to find the optimal design of water distribution networks. The approach constructs a graph composed of links each represents a decision point that in turn contains a number of options equivalent to available pipe diameters. The approach iteratively generates a number of ants or trial solutions and selects a set of options to size each link. The cost associated with each solution is then calculated, while a hydraulic model is used to solve for hydraulic equations. Suribabu and Neelakantan (2006) applied particle swarm optimization to design water distribution networks. The application used the swarm intelligence based on the cognition of individuals and social behaviour as the optimization tool, while a hydraulic simulator to analyse hydraulic equations for each solution. Cunha and Ribeiro (2004) proposed a tabu search algorithm, which is a heuristic optimization method that uses the human memory process as a search basis, to find the least-cost design of looped water distribution networks. The algorithm implements the tabu method by exploring the entire neighbourhood solution or part of it using a mechanism for generating neighbourhood solutions.

Genetic algorithms (GAs) have been the most widely used application of EAs in the literature of water resources planning and management. They show robustness and fast convergence in solving for the problem of optimal design of the WDS. The application of a basic GA to the optimal design of WDSs started in the early 1990s (Murphy and Simpson, 1992). In this study, the basic GA was applied to a small two-source and fourteen-pipe looped WDS to find the least cost combination of pipe diameters and rehabilitation actions. The basic GA was found to outperform a complete enumeration and other optimization methods to solve this small problem (Simpson et al., 1994). Simpson and Goldberg (1994) carried out an investigation on factors affecting the performance of the basic GA in determining the optimal design of this small two-source looped network. They found that the basic GA was sensitive

to the operation of tournament selection and the use of a sufficient population size. Dandy et al. (1996) made an improvement to the basic GA by scaling fitness, creeping mutation and using Gray coding instead of binary coding. The main difficulty accompanied with this improved GA was in the amount of considerable effort required to adapt the GA parameters (e.g. population size, crossover probability and mutation rate) to obtain a set of low cost solutions. Savic and Walters (1997) linked a basic GA to the EPANET 2 hydraulic simulator (Rossman, 2000) and found that the identification of optimal solution is dependent on the conversion factor of Hazen-William formula used in the hydraulic analysis.

Basically, the design space in a simple GA uses tidy representation in which all solutions have identical string lengths. Goldberg et al. (1989) suggested a competent or messy GA in which solutions have variable string lengths. They demonstrated that the messy GA is capable to identify optimal solutions that were difficult to find using a basic GA. It was also found that the optimization of the WDS using messy representation is more effective than tidy representation (Wu and Simpson, 1996 and 1997; Simpson and Wu, 1997; Wu et al., 2000). Halhal et al. (1997) proposed a similar method known as the structured messy GA that retains some features of the messy GA developed by Goldberg et al. (1989). The structured messy GA was applied to maximize the benefit of WDS rehabilitation constrained with a fixed amount of available budget. The present research employs the concept of GA optimization technique and thus the thesis will explain in detail the basic processes involved in the implementation of a basic GA. Further details on other EA techniques can be found in the mentioned publications in this review.

3.3 GENETIC ALGORITHMS

Genetic algorithms (GA) are stochastic search algorithms that use the mechanism of natural selection and natural genetics in order to survive (Goldberg, 1989). The GA technique is different from conventional search methods in that they are population-

based search algorithms. It has been shown that most conventional methods are based on determining a prior set of sequenced procedures that use the gradient and higher order derivatives of objective functions to converge at a solution. These methods are applied to searching from a single point in the search space. The improvement of such a point is dependent on gradually following the deepest descending direction using a sequence of alterations. This point-to-point method puts the search in the danger of falling into local optimal solution. GA avoid this potential danger by maintaining a set of solutions to search in multiple directions instead of one. The population-to-population method aims to make the search avoid falling into local optima.

The implementation of GA starts with creating an initial set of random solutions known as population that should be located within the problem boundaries. Each solution in the population is called a chromosome or an individual that represents a possible solution to the problem under consideration. Each chromosome is represented with a string of symbols normally in the form of a string of binary bits. The chromosomes are evaluated with a measure of fitness called objective function. Selection schemes normally the roulette wheel selection or the tournament selection is used to select chromosomes on the basis of fitness. Chromosomes with high fitness have higher probabilities of being selected than low fitness chromosomes. The selected chromosomes called parents are used to create new chromosomes called offspring by either merging two parents using the operation of crossover or modifying a parent using the operation of mutation. The process of evolving chromosomes is called generation. In each generation, an offspring population is created using the operations of selection, crossover and mutation. Finally, the algorithm converges to a set of best chromosomes that should be optimal or suboptimal solutions to the problem.

Basically, the implementation of a GA requires considering five essential components (Michalewicz, 1994): first, a process of genetic representation of possible solutions to the problem under consideration called encoding; second, a

method to create an initial population; third, a formulation of fitness function to evaluate solutions using a process of decoding; fourth, a design of genetic operators that adjust the genetic structure of solutions such as selection, crossover and mutation; and last, parameter values to be used by the GA such as population size and probabilities of carrying out genetic operators. In addition, another essential component for implementing GA to a constrained problem represented in a method for handling constraints is required.

The GA uses a global search method to solve problems in which determining in advance a sequence of procedures guiding to a solution is not possible. The search strategies can be of two types: blind search or heuristic search (Bolc and Cytowski, 1992). Blind search strategies explore the problem solution space without using any information about the problem domain. Random search represents an example of blind strategy in which the search process does not consider regions of search space showing promise. In contrast, heuristic search strategies exploit the available information about the problem domain as guidance to the best search directions. Hill-climbing represents an example of a search strategy that exploits best solutions for making potential improvement and without exploring the search space. The GA combines the two strategies of exploration and exploitation in a remarkably balanced way.

Basically, simple genetic operators are designed in such a way that they essentially perform a blind search. This general purpose search approach could make genetic operators not able to guarantee producing an improved offspring. In other words, the amount of exploration and exploitation performed by the crossover operator is dependent on how diverse solutions are and not on the operator itself. In the early generations of genetic search, the existence of a random and wide diversity of solutions makes crossover operator widely spread the search as an attempt to explore all solution space. Once solutions with high fitness start to evolve, the crossover operator tends to explore regions near these high fitness solutions. The operation of implementing a simple GA is described in Figure 3.1.

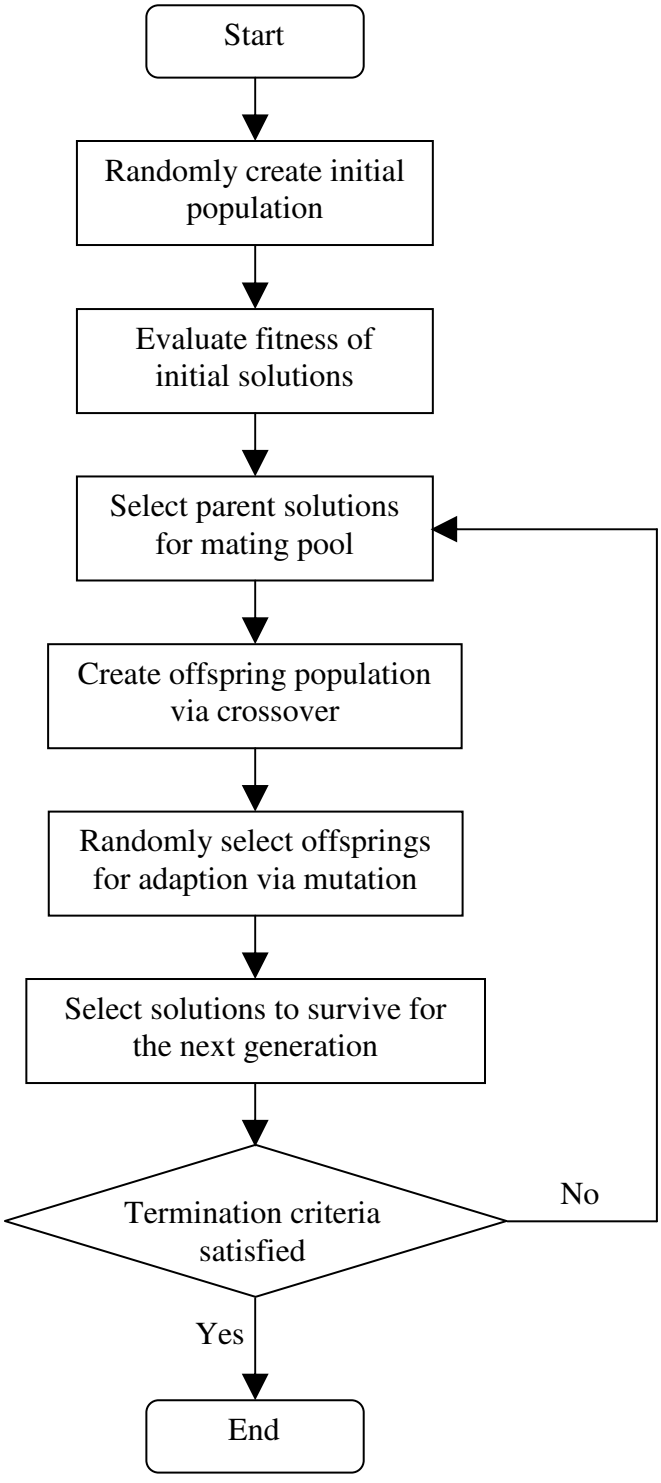

Figure 3-1: Flow chart of simple GA

3.3.1 Main advantages of GA

GAs have attracted many researchers to pay considerable attention to apply such a novel optimization technique in solving real-world problems. The application of GA to problem optimization has provided three major advantages. First, they are simple to adapt to the optimization problem and without the need to a mathematical complexity in their formulation. This is because GA use the nature of evolution to search for solutions and irrespective of the inner structure of the problem. This indicates that the GA can deal with any type of objective functions and constraints whether they are linear or non-linear, have discrete or continuous or even mixed solution spaces. Second, the dependence of GA on evolutionary operators that are probabilistic operators effectively enabled performing a global search rather than a local search normally performed by most conventional heuristic methods. Many studies showed that the GA is very efficient and robust by reducing the computational effort required to converge at optimal solution in comparison with other conventional heuristics. Finally, GAs are very flexible in the sense that they can be implemented by hybridizing different heuristics to efficiently solve a specific problem.

3.3.2 GA terminology

Since GA is originated from both the genetics of nature and computer science, the terms used in the context of GA are a combination between the natural vocabulary and the artificial vocabulary. In biological science, the construction of an organism is defined by an encoded structure known as chromosome. To complete building a specific organism, more than one chromosome may be required. The full set of chromosomes making up the organism is called a genotype, while the produced organism is called a phenotype. Each chromosome is composed of set of sub-structures called genes. Each gene holds a coding of specific feature of the chromosome. The specific characteristic represented by each gene is determined by

the location of the gene within the structure of the chromosome called locus. A particular gene representing a specific characteristic at one location may represent a different characteristic at another location. The different characteristics represented by one gene are called alleles.

3.3.3 GA encoding

The process of encoding a solution of a particular problem in the form of a chromosome structure is a key issue towards the implementation of GA. This issue has been under consideration from different aspects such as the mapping properties associated with converting a genotype into phenotype during the process of decoding a chromosome into a solution. Accordingly, a number of encoding methods have been developed to effectively apply the GA to a particular problem. In Gen et al. (2008), the encoding methods are categorized into four groups according to the type of symbols used to define the alleles of a particular gene. These are binary encoding, real number encoding, integer permutation encoding and a general data structure encoding.

The binary encoding represents each gene by means of the binary alphabet: 0 and 1. Then, a chromosome is expressed in the form of a binary string. This type of encoding is appropriate for representing problems with discrete or discontinuous search spaces. The most important feature of binary encoding is the ability to exploit the similarities, which rely on schemata theory, in a discrete search space. However, two main issues are often experienced with binary encoding systems: 1) existence of redundant binary codes for problems with finite decision variables being not a power of two; 2) difficulties in dealing with continuous search spaces. As such, it is practically almost impossible to use the binary encoding to represent certain types of optimization problems. Since binary encoding is selected to code the GA used in the present research, further explanation of schemata theory follows.

Holland (1975) used binary strings to encode a solution. The main advantage of BCGA (Binary Coded GA) comes from the development of schema theory (Holland, 1975) that provides results able to describe the good behaviour of the GA. A schema is defined as a similarity in patterns of a binary sub-string will have similar characteristics in some locations. Consider a population of five individuals and their associated fitness values is represented with 4-bit binary strings as shown in Table 3.1. The schema **01 appears to be associated with a high fitness, while the schema 10** appears to be associated with a low fitness. The most important result presented by the schema theory is the building block theory (Goldberg, 1989). This theory states that short, low-order, above-average schemata, known as building blocks receive exponentially increasing trials in subsequent generations. For instance, if the optimum arrangement of 3-bit binary string is 111, then high fitness solutions are composed of the building block of 111.

Table 3-1: Similarities between 4-bit binary strings

Binary string	Fitness value
0001	23
1000	2
0101	16
1101	12
1010	5

The real number encoding represents the genes directly as real numbers each have a unique real value. Accordingly, a real coded chromosome is a vector of floating point numbers. This type of encoding addresses the issue of redundancy associated with binary encoding. The main advantage of real number coding is that both genotype space and phenotype space have identical topological structures (Gen et al., 2008). The real number encoding is suitable for problems with continuous search spaces. The most important feature of real number encoding is the capability to exploit the continuity in continuous search spaces. It has been widely proven that real

number encoding more powerful than binary encoding for function optimizations and constrained optimizations (McCormick et al. (1972); Eshelman and Schaffer (1993); and Michalewicz (1996)). Given that combinatorial optimization problems aim to search for a best permutation or combination of certain components to be obtained under some constraints, the integer or literal permutation encoding may suit such types of problems. The general data structure encoding represent a gene in the form of an array or other complex data structure. This type of encoding is appropriate for complex real-world problems in which the problem nature may require a data structure to represent the allele of a gene (Gen et al., 2008). Explanation of representing the network shown in Figure 3.2 using binary and real encoding follows (Table 3.2).

Table 3-2: Binary and real number encoding of eight pipe diameters

Pipe diameter (mm)	Binary coding	Real number coding
100	000	100
200	001	200
300	010	300
400	011	400
500	100	500
600	101	600
700	110	700
800	111	800

To illustrate how to encode a WDS using binary encoding and real number encoding, consider the 5-pipe network shown in Figure 3.2. Typically, the design of the WDS involves selecting a set of pipe sizes subject to hydraulic and cost constraints. Herein, the decision variables are eight discrete pipe sizes to be selected for the five pipes denoted by P1, P2, P3, P4 and P5. Accordingly, a 3-bit binary string that produces 2^3 or 8 possible bit arrangements is suitable to fully represent all pipe sizes. Herein, no

redundancy issue has arisen because each pipe size has a unique binary string as shown in Table 3.1. It is worth highlighting that this case could not be met in practice as the decision variables are normally a set of commercially available pipe sizes. The real number encoding was accomplished by a real number equal to the pipe size itself (Table 3.2).

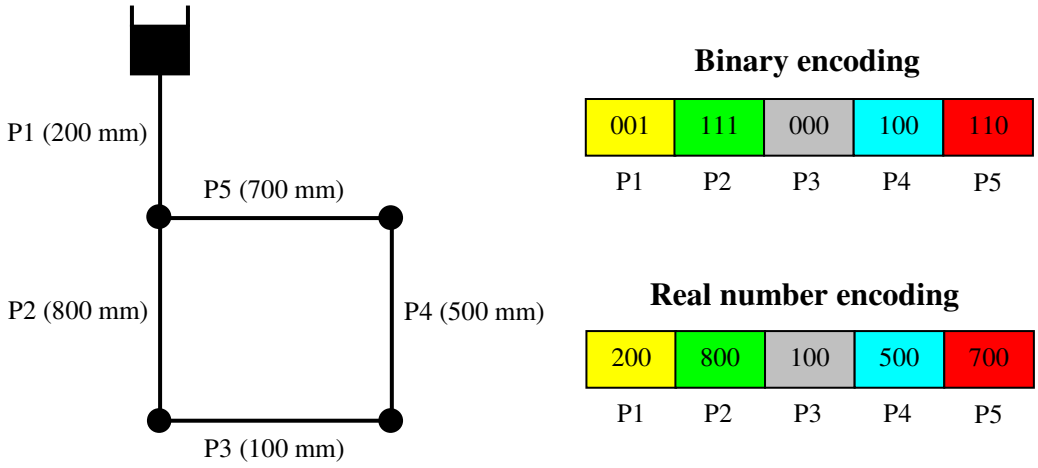

Figure 3-2: Illustration of binary and real number representation of a WDS
(P denotes pipes while numbers in brackets refer to pipe diameters)

3.3.4 Infeasibility and illegality of solutions

It has been shown that the GA deals with two different types of spaces: the genotype space and the phenotype space. All genetic operations are carried out on the genotype space, while the processes of evaluating and selecting solutions take place on the phenotype space. The mapping between solutions in the genotype space (i.e. encoded solutions or chromosomes) and solutions in the phenotype space (i.e. decoded solutions) is carried out by natural selection. The performance of the GA is highly dependent on this mapping process. Two main phenomena may arise when mapping a solution from the genotype space to the phenotype space.

First, some chromosomes could correspond to infeasible solutions to the problem under consideration. The infeasibility of chromosomes naturally comes from the existence of constraints to a given problem. Such constraints divide the solution space of the given problem into two regions: feasible and infeasible. So, the infeasibility of a chromosome or an individual occurs when the decoded solution is situated outside the feasible region of a given problem. Typically, the optimum solution is located at the boundary between feasible and feasible regions. In constrained optimization problems and combinatorial optimization problems, the infeasibility of solutions may have severe effect on the performance of the GA. One way to handle infeasible solutions is the penalty method (Gen and Cheng, 1997). This approach works on discarding infeasible solutions to restrict the search to the feasibility region.

The second phenomenon is illegality of individuals in which a chromosome does not represent a solution to a considered problem. The illegality of a chromosome naturally comes from the technique used in the encoding process. For instance, a simple one-cut-point crossover may result in producing an illegal offspring in some problem-specific encodings (Gen et al., 2008). The travelling salesman problem provides a typical example in which an illegal chromosome could be generated by genetic operators. Consider the problem has five points where the first point represents the starting point from which a salesman has to start the journey to reach the fifth point, which is the final destination. Throughout evolution, the crossover and mutation operations could produce the route {1, 1, 4, 4, 5} in which the first and fourth routes appear twice and therefore represents an illegal solution to such a problem. Repairing techniques are required in such a situation in order to either discard or convert an illegal chromosome to a legal one (Gen et al., 2008). The main techniques developed to deal with the issues of infeasibility and illegality will be presented after explaining the initialization and genetic operators.

3.3.5 Initialization of GA

Typically, the GA is initialized by generating an initial population using a random number generator while satisfying the problem boundary. The random number generator creates pseudo-random numbers using a recurrence known as a linear congruential generator (Murphy and Simpson, 1992). Two entities are to be specified within this generator: the maximum positive integer the computational environment can take and the seeding number. The maximum positive integer allows the recurrence to contain all the integers between 0 and this maximum value in some random sequence. The seeding number represents the starting point within the sequence of random numbers. The same seed results in the same sequence of random numbers and consequently the same seed will create the same initial population. This important feature allows the genetic algorithm to start the optimization from different initial populations using different seeding numbers. The random initialization from different starting points is a useful tool for evaluating convergence properties of the GA.

3.3.6 Evaluation of solution fitness

Typically, the objective function for a given problem represents the mechanism by which each individual is evaluated. Fitness evaluation of a solution is then the solution value obtained from the objective function for a given problem and subject to some constraints. In multi-objective optimization problems, the difference of range of values of objective functions may be significantly large. To maintain consistency in the solution space, all involved objective functions should be normalized to a range of 0 to 1. The selection process is then used to evaluate the individuals of the population based on the normalized value of the objective function.

The objective function plays a crucial role in the GA search. This is because the evolution of chromosomes is dependent on the fitness, which is evaluated using the

objective function. As the GA progresses from one generation to another, relatively high fitness solutions are selected to produce new and relatively higher fitness solutions. At the same time, relatively low fitness solutions are not selected to yield a population of offspring composed of good solutions. To evaluate the fitness of each individual, a decoding procedure dependent on the chromosome structure is normally constructed.

3.3.7 Crossover

Crossover represents the main genetic operator that plays an important role in exploring the solution space. Thus, the performance of the GA is highly dependent on the performance of the crossover operator. The crossover operator works on two chromosomes called parents at a time to produce two offsprings that contain some features of both parent chromosomes. The crossover operation can be simply achieved by randomly choosing a single point to cut at each parent into two segments. The first offspring is generated by combining the segment left to the cut-point in one parent with the segment right to the cut-point in the other parent (Figure 3.3). Similarly, the second offspring is generated by combining the segment right to the cut-point in one parent with the segment left to the cut-point in the other parent (Figure 3.3). The single cut-point method is suitable for binary coded chromosomes.

The number of chromosomes to undergo the crossover operation is controlled by crossover probability (p_c). The crossover probability is defined as the ratio of the number of offspring produced in each generation to the population size. Clearly, the amount of exploration of the solution space is dependent on the crossover probability used. A higher crossover probability enables exploring more of the solution space and thus reducing the chances of falling into a local optimal solution. At the same time, too high crossover probability may result in consuming part of the computational effort in exploring unpromising areas of the solution space.

In Gen et al. (2008), four main types of crossover operators have been proposed for real number encoding: conventional crossover, arithmetical crossover, direction-based crossover, and stochastic crossover. The conventional operators are based on extending the operators developed for binary representation to real number coding. The resulting operators are mainly classified into simple conventional crossover operators (e.g. one-cut point, two-cut point and multi-cut point) and random crossover operators (e.g. flat and blend). The arithmetical crossover operators are designed based on applying the concept of linear combination of vectors that belongs to the theory of convex set. They work on the genetic representation of floating numbers. The direction-based operators use the values of objective functions as an approximated gradient to determine the direction of genetic search. The stochastic operators generate offsprings by modifying parents using random numbers following some distribution.

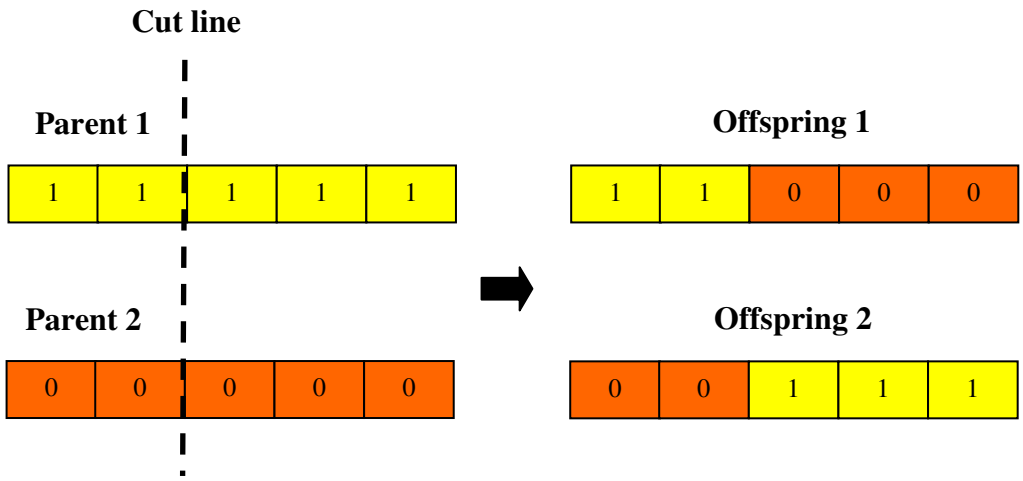

Figure 3-3: Operation of the single-point crossover

3.3.8 Mutation

Mutation is another genetic operator that plays a key role in the GA search process in two main aspects. First, it increases the chances of returning the genes lost by the

selection process and so trying them out in a further selection process. Second, it increases the chances of introducing the genes that were not included in the initial population. The mutation process can be simply achieved by randomly altering one or more genes in the offspring population. The number of genes to undergo mutation is dependent on the mutation probability (p_m). The mutation probability is defined as the ratio of the number of mutated genes to the total number of genes comprising the population. The mutation probability governs the number of new genes to be included in the population for trial. Using too low mutation probability would lead to not trying several useful genes at all. At the same time, high mutation probability will lead to losing the resemblance between the offspring and the parent and so losing the capability to obtain genetic information from the search history. The methods of implementing mutation operation can be of conventional or non-conventional types.

Random mutation operators belong to the conventional methods normally used to perform mutation operation. These include uniform mutation, boundary mutation and plain mutation. They simply generate a random real number within a specified range (e.g. between 0 and 1) for each gene in the offspring population. If this number is less than or equal to the specified mutation probability, the gene undergoes mutation. In binary encoding, the selected gene is converted to its binary complement from 0 to 1 or 1 to 0. For real number encoding, the random mutation directly replaces the selected gene with a randomly selected real number belonging to a particular range.

The non-conventional mutation operators proposed for real number encoding include dynamic mutation or non-uniform mutation classified under the arithmetical mutation operators. Directional mutation is another type of these methods that uses the gradient of objective functions to direct the search in either a random way or using some guiding criteria. Inversion mutation is an operator that works on inverting genes over a substring selected randomly between two points. Insertion mutation selects a gene in a random way and introduces it to the offspring population randomly. Displacement mutation also works on a substring of genes but in a

different way from inversion mutation. The randomly selected substring is displaced at a random position in the offspring population. Reciprocal exchange mutation randomly selects two genes at different positions and swaps them.

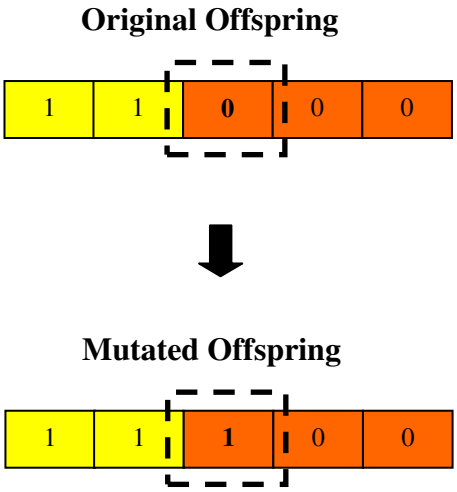

Figure 3-4: Operation of the simple random mutation

3.3.9 Selection

Selection represents the driving engine of the GA that guides the genetic search to regions of the search space showing promise (i.e. region of good solutions). The selection operation is dependent on the selection pressure, which refers to the degree to which good individuals are favoured in the selection. In general, a lower selection pressure is preferred at the beginning of a genetic search in order to widely explore the search space, while a higher selection pressure is preferred at the end to make the search space narrower. A number of selection methods have been proposed to perform the selection process. These include roulette wheel selection (Holland, 1975), tournament selection, truncation selection, elitist selection, ranking and scaling selection and sharing selection.

Roulette wheel selection was proposed by Holland (1975). The implementation of this selection operator starts by determining a selection probability for each individual that is proportional to the fitness value. These probabilities are used to construct a weighted roulette wheel composed of segments equal to number of individuals in the population. The size of segments on the weighted roulette wheel is proportional to the selection probabilities. This representation makes high fitness individuals have larger segments and thus larger selection probability. To select an individual to undergo a genetic operation (e.g. crossover), the wheel is spun a number of times equal to population size. The weighted roulette wheel in Figure 3.5 is used to represent a population of 8 individuals. Individual 1 has a very high fitness and therefore allocated large segment, while individual 8 has a very low fitness and therefore assigned small segment. Accordingly, each time the weighted wheel is spun in the selection process; it is likely that the ball eventually tends to fall into large segments. This selection mechanism makes the selection pressure most likely in favour of high fitness individuals. Goldberg and Deb (1991) pointed out that roulette wheel selection has the disadvantages of lacking diversity and directed search that make the GA converges prematurely.

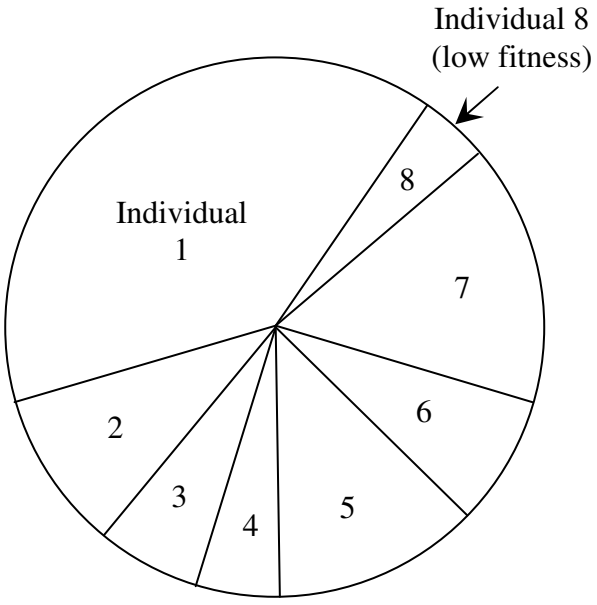

Figure 3-5: Illustration of the weighted roulette wheel

The tournament selection proposed by Goldberg and Deb (1991) runs a "tournament" among a set of individuals selected randomly from the population and selects the one with the best fitness. The tournament process continues until the number of offspring individuals specified by crossover probability is reached. Unlike the roulette wheel selection, the tournament selection has the advantage of being easy to adjust the selection pressure by changing the tournament size, which is the number of individuals to compete in each tournament process. A larger tournament size makes low fitness individuals have less chance to be selected, while a smaller tournament size increases the chance of selecting low fitness individuals. The common tournament size is 2.

3.3.10 Methods of handling constraints in GA

The application of the GA to constraint optimization problems has shown that the genetic operators do not guarantee that all generated solutions are feasible. As such, a component for handling violations with constraints becomes an essential requirement in constraint problems. In GA literature, Michalewicz (1995) summarized the existing techniques proposed to handle constraints in the GA. They are classified into four strategies: 1) rejecting strategy; 2) repairing strategy; 3) modifying strategy; and 4) penalizing strategy.

The rejecting strategy works on excluding all infeasible solutions generated during an evolutionary process. This method may fairly work in problems of which feasible solutions belong to a convex solution space and comprise a significant part of the whole solution space. However, the dependence of such a method on the existence of feasible solutions puts severe limitations on its application. For example, genetic operators can not guarantee that the initial populations contain even a feasible solution. This situation essentially requires introducing procedures to improve the initial population.

The repairing strategy works on converting an infeasible solution to a feasible one. The application of this strategy depends on designing a deterministic repair procedure, which is problem specific. Repairing a solution can be implemented using two different methods: the never replacing approach and the always replacing approach. The never replacing approach uses the repaired solution for evaluation only and never returns it to the population, while the always replacing approach replaces the illegal solution with the repaired one. The weakness of the repairing strategy comes from being problem dependent. Such a strategy could be suitable for combinatorial optimization problems in which it is relatively simple to construct a repairing procedure. However, the process of repairing infeasible solutions might be so complex that it requires similar computational effort to that required for solving the problem itself.

In order to maintain the feasibility of solutions, the modifying strategy works on inventing special genetic operators that are specific to the problem. The serious limitation of using problem-specific representation is in confining the genetic search in a feasible region.

All the above techniques were developed to cope with the issue of feasibility associated with genetic operators. They have the disadvantage of never generating infeasible solutions by not considering any solution located outside the feasibility region. This concept has a serious limitation because, for highly constrained problems, infeasible solutions may represent a relatively large part of the population and so it may be difficult to find solutions if the genetic search is confined within the feasibility region.

Glover and Greenberg (1989) pointed out that searching through infeasible regions improves the GA efficiency in finding better solutions than do strategies restricting search to feasible regions only. The penalizing strategy is a method proposed to search through infeasibility regions to some extent. Even though infeasible solutions may exist in the initial population, they can not survive further due to being

penalized for their infeasibility. Additionally, such a method requires designing problem-specific penalty functions.

3.3.11 Non-dominated solutions and Pareto Optimality

Basically, multi-objective optimization problems are very different from single objective optimization problems. In single objective problems, there is only one best solution that is completely superior to all other alternatives in the solution space of the problem considered. In multi-objective problems, such a solution superior with respect to all objectives is not essentially available because of the conflict among objectives. For example, a solution could be best in objective and at the same time worst in other objectives. Thus, there normally exists a set of solutions for the case of multi-objective problems that can not be directly compared with each other. Such types of solutions are known as non-dominated solutions or Pareto Optimal solutions. These solutions are characterized with the impossibility of making an improvement in one objective without sacrificing at least one of the other objective functions. The non-dominated solutions are also called Pareto Optimal Front (POF).

3.4 REVIEW OF METHODS DEVELOPED TO IMPLEMENT MULTI-OBJECTIVE GENETIC ALGORITHMS

The GA is characterized with multi-directional and global search strategy that employs a population-to-population search approach to explore the solution space. This inherent feature makes the GA potentially suitable for solving multi-objective optimization problems. Since constrained and combinatorial optimization problems can be naturally formulated as multi-objective optimization problems, several MOGA (Multi-Objective GA) methods have been developed in the last two decades (Gen et al., 2008). The major components essentially required to apply the GA for solving a given problem are methods for implementing encoding, genetic operators, fitness assignment and constraint handling. Among these components, a mechanism

for implementing the fitness assignment represents a particular issue associated with the application of the GA to multi-objective optimization problems. In Gen et al. (2008), the development of MOGA can be classified into three main stages according to the method proposed for fitness assignment as follows: 1) vector evaluated GA; 2) Pareto ranking and diversity GA; and 3) weighted sum and elitist preserve GA. However, it could be more convenient to classify the mechanisms of weighted sum and elitist preserve as separate approaches.

3.4.1 Vector evaluated GA

The vector evaluated GA (VEGA) represents the first remarkable GA based work for solving multi-objective optimization problems (Schaffer, 1985). Schaffer's works are considered as the first attempt to apply the GA to multi-objective optimization problems. As the name suggests, the VEGA uses a vector fitness measure instead of a scalar fitness one to create the next generation. In each generation, the entire population is divided into subpopulations of appropriate size and each solution is selected based on the objective value. Then, the mating between subpopulations is carried out by applying operators of crossover and mutation. The non-dominated solutions in each generation are identified by maintaining the best solutions in one of the objectives while providing a set of solutions for multiple selections that are better than the average of more than one objective.

However, the VEGA is found to split the population into different solutions each of them strong in one of the objectives in case of concave problems. This phenomenon of speciation, as called by Schaffer (1985), is not desirable in multi-objective optimization problems due to contradicting the aim of obtaining a compromise solution. Even though speciation makes the VEGA unable to provide a satisfactory solution to the multi-objective optimization problem, the VEGA suggested developing new concepts of implementing MOGA.

3.4.2 Pareto ranking and diversity GA

Goldberg (1989) was the first to propose assigning fitness based on Pareto ranking. The process of ranking starts by assigning rank 1 to the non-dominated solutions within the entire population. Then, solutions of rank 1 are removed to identify the non-dominated solutions of rank 2. The procedure continues until the whole population is ranked. Fonseca and Fleming (1993) proposed a MOGA that represents the rank of each solution by the number of solutions dominating it in the current population. Accordingly, all the non-dominated solutions are assigned rank 1 and the next non-dominated solutions are assigned rank 2 and so on. Srinivas and Deb (1995) proposed a Pareto ranking-based mechanism for fitness assignment to develop NSGA (Non-dominated Sorting GA). In this method, all solutions making up a non-dominated front are assigned the same dummy fitness value. The specified value of dummy fitness of these solutions is used as a sharing parameter that is not accounted for in further classification. Then, the dummy fitness is reduced to a value less than the smallest shared fitness value in the current non-dominated front. The next front is identified after removing the first front from the current population. The procedure continues until all solutions are classified. However, the Pareto ranking and diversity GA are criticized mainly because of not incorporating elitism in the ranking process.

3.4.3 Weighted sum GA

Ishibuchi and Murata (1998) proposed a weighted-sum mechanism for fitness assignment to develop random-weight GA called RWGA characterized with a variable search direction. The weighted-sum approach works on assigning weights to each objective functions and combines these weighted objectives into a single objective function. There are two methods of search according to the method used for assigning weights: fixed direction search and multi-direction search. The fixed

direction search is achieved by fixing weights to direct the GA search towards a fixed point in the search space. The multi-direction search assigns weights in a random way to make the GA search into multiple and variable directions. To gradually direct the search towards a positive ideal point, Gen and Cheng (2000) proposed an adaptive weight mechanism that adjusts weights based on the minimum and maximum extreme points in the current population. As the extreme points are updated at each generation, the weights are also updated accordingly.

3.4.4 Elitist preserve GA

Deb et al. (2002) proposed a non-dominated sorting genetic algorithm called NSGA II that alleviates the difficulties experienced with NSGA, namely, computational complexity, non-elitism approach and the need for specifying a sharing parameter. The NSGA II represents an advancement of its original NSGA described previously. The computational complexity was handled with a fast non-dominated approach. The incorporation of elitism is achieved by developing a selection operator that combines parents and offspring populations into a mating pool and selects the best solutions. In NSGA II, a Pareto rank is assigned for each solution in the mating pool using a non-dominated sorting approach, while a measure of density called crowding distance is estimated for each solution in the mating pool. For two solutions, NSGA II prefers the solution with lower rank value or the solution located in a region of low density if both points belong to the same front. Accordingly, NSGA II combines a fast non-dominated sorting approach, an elitism scheme and a non-parameter sharing method applied in the original NSGA. Based on several difficult test problems, NSGA II demonstrated robustness and efficiency in finding better solutions and better distribution of solutions in comparison with other elitist MOEAs. Since NSGA II has been used as the optimization technique in this research, a detailed description is presented in chapter four.

3.5 REVIEW OF TOPOLOGY-BASED OPTIMIZATION APPROACHES OF WATER DISTRIBUTION SYSTEMS

Typically, the establishment of the WDS has two main design phases: planning of system components and sizing of such components to meet the functional requirements according to the standard used. In reality, it is extremely hard to determine the optimal configuration or topology of system components that belong to the least-cost design of the WDS. This is attributed to the existence of large system configurations that can provide a planning solution to the system. Additionally, it is impossible to determine the system cost without sizing the WDS. In other words, it is essential to couple cost determination with planning of system components if the least-cost design is desired. Even though the capital cost is shared among different components making up the system (e.g. pipes, valves, tanks and pumps), the capital cost mainly comes from the pipeline provision and construction (Djebedjian *et al*., 2008). In general, the cost of transmission mains and the distribution network account for approximately 80% to 85% of the total cost of the WDS (Swamee and Sharma, 2008). Accordingly, a good planning of the system components (i.e. topology optimization) will bring a great saving of the capital cost.

Planning the WDS starts with: 1) identifying any possible locations of supplying sources that should be located at the highest points among the planned zone; and 2) a preliminary planning of pipe locations that should consider many factors such as the right-of-way property of streets and accessibility between supplying sources and all consumption points. At this point, demands occur along pipes in this preliminary detailed plan. Since it is extremely difficult to include all consumption points in this detailed plan, the preliminary detailed plan is skeletonized and demands are lumped at pipe ends as explained in section 1 of Chapter 2. Then, a feasibility analysis of the system is carried out where a choice between gravity and pumped systems can be made. A gravity system could be feasible if the source node is at a higher elevation than all demand nodes. Otherwise, a pumping system could be the alternative solution. Also, the pumping system could provide better solution than gravity one if

the difference in elevation between demand nodes is small where large pipes could be required in the case of gravity systems.

The planning of the WDS components can be categorized into three main groups: branched or tree-like configuration, fully looped configuration, and partially looped configuration. Branched systems are suitable for small and low-density rural areas, while fully or partially looped systems are proper for urban areas (Swamee and Sharma, 2008). Branched configurations have a structure similar to a tree and branch structure (Figure 3.5a) in which the tree trunk represents the supply main while branches stand for pipes connecting consumption points or demand nodes to the supply main. In branched systems, each demand node has a unique supply path from the supplying source. This configuration is not desired because of cutting off the water supply to the consumers downstream of any section of pipe that is not in service, e.g. due to a mains break. The main advantages of branched systems are that the capital cost is relatively low; they are easy to operate; and are suitable for sparsely populated areas (Swamee and Sharma, 2008).

To reduce the effect of such situations, looped systems characterized with the existence of multiple supply paths from the source to the demand points are preferred. The reliability and cost of looped systems is highly dependent on the number of loops (Tanyimboh and Sheahan, 2002; Tanyimboh and Setiadi, 2008). In fully looped systems, pipes are constructed in such a way that each demand node can be supplied from the source(s) through at least two independent paths as shown in Figure 3.5b. Two supply paths are said to be independent if they do not have a pipe in common. From the viewpoint of system reliability, this looping condition has the advantage of providing an alternative flow path in case the other paths are out of service.

Partially looped systems lie between branched and fully looped configurations where each demand node has at least two flow paths but not all of them are independent. For example, nodes 1 to 6 in Figure 3.6c satisfy looping condition, while nodes 7 to 9

do not because they are supplied through pipe 5-8 only. Cutting off the water supply in pipe 5-8 has the effect of putting nodes 7 to 9 out of service.

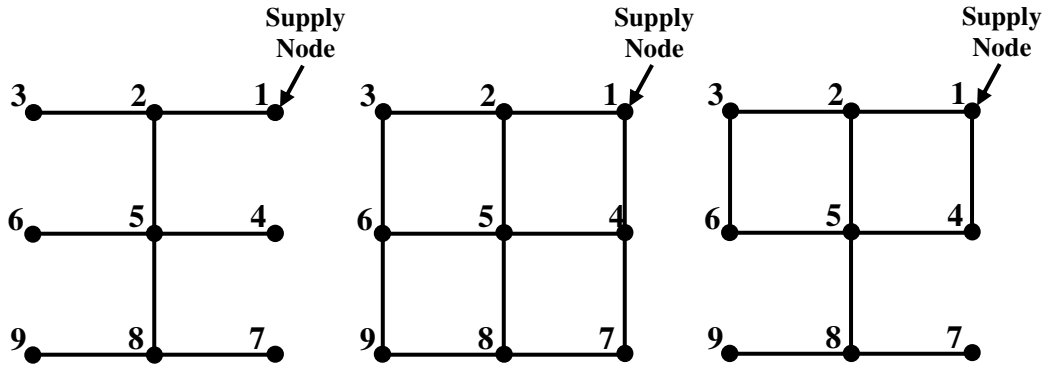

a) Branched topology (b) Fully looped topology (c) Partially looped topology

Figure 3-6: Illustration of branched, fully looped and partially looped topologies

In addition to cost consideration, reliability becomes an important parameter involved in determining the optimal planning of the WDS. The difficulties associated with operating the WDS in a long-term basis is the main reason behind considering reliability in the planning and design of the WDS. The effects of aging of system components and the unpredictable increase in future demands on the long-term performance of the WDS are some of aspects hard to determine during the planning and design phase. However, adding reliability to the process of determining the optimal system planning has made the establishment of the WDS extremely hard to achieve. This is attributed to two main reasons. First, there is still some doubt about the definition of the term 'reliability' of the WDS. Second, the great increase in the complexity of WDS design resulted from considering reliability as an essential design factor.

Given that planning of the WDS components under cost consideration plays a crucial role in saving a great amount of capital, several approaches were developed to address the coupling effect between topology and sizing of system components on determining the least-cost design of the WDS. Nevertheless, this joint effect has been

yet fully addressed. To improve the long-term performance of the WDS, several approaches were also developed to incorporate reliability in the design of the WDS. The vast majority of these methods did not include layout optimization. Even those attempted to include reliability did not fully address the effect of topology on both design and reliability of the WDS. In general, the approaches developed to handle the coupling effect of components layout on design and reliability of the WDS can be categorized into two groups: 1) coupled layout and design approaches; and 2) coupled layout, design and reliability approaches.

3.5.1 Approaches that do not consider reliability

The coupled problem of topology and pipe size optimization aims to determine the cheapest set of pipe sizes that make up a feasible design of the WDS. Practically, it yields a single feasible design that is supposed to have the cheapest set of pipe sizes and belongs to the optimal topology. This indicates that the computational solution of this problem involves three main objectives: 1) minimizing cost; 2) minimizing violation of hydraulic constraints; and 3) minimizing violation of topologic constraints. Nevertheless, all previous studies attempted to address the problem of joint effect between topology and design computationally solved this problem as a single-objective optimization problem. The penalizing strategy was employed to handle the violations with both hydraulic constraints and topologic constraints.

The coupling between topology and design of the WDS was first handled as two separate processes. The first process or stage optimizes topology followed by the second stage for pipe sizing (Rowel and Barnes 1982; Morgan and Goulter 1982; Kessler et al. 1990; Cembrowicz 1992). Rowel and Barnes (1982) developed a two-stage model that determined a least-cost branched layout first. Then, pipes are introduced to interconnect the branches of the network in the second stage. Morgan and Goulter (1982) developed an approach that is composed of two linear programs.

The first one determines the optimum topology, while the other is used for sizing pipes. However, the method used to add pipes to branches does not guarantee that the designs generated would be fully looped. In other words, the criterion used simply requires connecting each node using two pipes without investigating whether these pipes provide independent paths or not. Kessler et al. (1990) and Cembrowicz (1992) tackled the problem by choosing links for either addition or removal from a predefined base graph. The base graph is the network consisting of the full set of feasible links.

However, all the aforementioned approaches assume that the problem of coupled topology and design could be divided into two separate optimization problems in which layout optimization is followed by pipe size optimization. This assumption neglects the strong interdependence between topology and design where sequential procedures as described above can be expected to yield suboptimal results. For example, given that the cost is not involved in the first stage, these methods do not guarantee that the optimal topology has been passed on to the second stage. As a result, there is no doubt that such methods only addressed the strong coupling between topology and components design of the WDS to some varying degrees. The two-stage optimization approach could be attributed to the highly complex optimization problem resulting from combining the large solution spaces of both topology and pipe size design.

The introduction of evolutionary algorithms as optimization techniques able to simultaneously handle multiple objectives was extensively exploited to develop approaches for handling this complex problem (Davidson and Goulter 1995; Walters and Smith 1995; Geem *et al.* 2000, Afshar 2007). Evolutionary algorithms often generate infeasible solutions when solving problems that involve constraints. The penalizing strategy that involves designing a penalty-based cost function was mostly used to handle constraints. In Kougias and Theodossiou (2013) and Dridi *et al.* (2008), case-specific constraint violation penalties that require special calibration procedures were frequently introduced to address this issue.

More recently evolutionary optimization approaches have been attempted (Walters and Lohbeck, 1993). For example, Davidson and Goulter (1995) proposed a method to optimize the layout of rectilinear branched networks. As no guarantee could be given for the feasibility of the designs obtained using genetic algorithm (GA) operators, two additional steps called recombination and perturbation were applied. Walters and Smith (1995) employed graph theory in an evolutionary algorithm for designing branched networks. Graph theory was combined with the conventional crossover and mutation operators to avoid the creation of infeasible designs in the reproduction process. Geem *et al.* (2000) employed a heuristic method called harmony search to optimise the design of branched networks. To avoid infeasible designs in the search process, a tree-growing algorithm starting from the base graph was used.

Also, Afshar *et al.* (2005a) developed iterative two-stage approach such that, in the first stage, the optimal diameters for a predefined layout are determined using non-linear programming method. In the second stage, an iterative pipe removal search process is carried out to reduce the cost without undermining the node connectivity constraint. Any infeasible solutions generated in the early stages due to the randomness in creating the initial population of solutions by the GA are gradually discarded using constraint violation penalties. To ensure the feasibility of branched solutions, at least one independent path from the source nodes to each of the demand nodes is required. Afshar (2007a,b; 2005b) also proposed several approaches that basically restricted the evolutionary algorithms used to feasible solutions. These included a genetic algorithm using three modified roulette wheel selection schemes (Afshar, 2007a), the conventional roulette wheel (Afshar, 2007b) and a max-min ant algorithm (Afshar, 2005b).

The above review shows that all approaches proposed in literature did not fully address the problem of coupled topology and design in four main optimization aspects. First, dividing the entire solution space of topology and design into two

separate and independent solution spaces in two-stage models undermines the concept of the strong coupling between topology and design. Screening out topologies in the first stage does not guarantee that the optimal topology has been passed on to the second stage. Second, severely restricting the coupling between topology and design to the feasible part of the entire solution space in one-stage models does not guarantee that the optimal topology would always belong to the part of feasible solutions particularly in problems of which infeasible solutions comprise a reasonable part of the entire solution space.

From the viewpoint of practicality, searching into the feasible part of the solution space requires designing problem specific procedures for discarding infeasible solutions on an ad hoc basis. Finally, limiting the coupling between topology and design to the violation of hydraulic constraints during normal operating conditions puts serious limitations on the performance of the obtained solutions during failure or abnormal operating conditions. Associating reliability assessment in simultaneous process with relaxing the search procedure into the entire solution space (i.e. feasible and infeasible) of topology and design is the key towards addressing the aforementioned optimization issues of the WDS.

3.5.2 Approaches that consider reliability

The incorporation of reliability as a trade-off factor in the coupled topology and design problem resulted in a dramatic change in the definition of optimal design of the WDS. Instead of determining the optimal topology, a set of optimal topologies are determined in the coupled topology, design and reliability problem. As such, the computational solution yields a set of optimal solutions rather than a single optimal solution. Besides violating hydraulic constraints and topologic constraints, the complexity of the problem has been greatly increased by the objective of maximizing reliability, which is in a conflict with minimizing cost. The necessity of adding

reliability to the problem of coupled topology and design has greatly increased complexity of the WDS optimization problem. In effect, very few approaches have been proposed to address this extremely complex problem.

In general, the vast majority optimization studies that included reliability did not optimize the topology. Awumah *et al.* (1989) developed a two-stage model for optimizing the pipe sizes and topology of a WDS. In the first stage, a topology model determines whether a link is to be included in the topology or not using a zero-one integer program. The topology is then passed on to the second stage to adjust pipe diameters in the final design.

Awumah and Goulter (1992) also proposed an alternative approach using informational entropy theory. The design optimization model was run repeatedly with a different maximum limit for the initial construction cost imposed each time as a means to generate different topologies. Tanyimboh and Sheahan (2002) also used informational entropy to investigate the combined effects of topology, pipe size design and reliability in an approach in which the topology, pipe sizing, reliability and redundancy were considered in successive stages. Even though the study did not fully address the joint effects between topology, pipe sizing and reliability because of dividing the design process into multiple stages, it was the only remarkable study attempted to address the coupling effect between topology, pipe sizing and reliability of the WDS.

Evidently, the aforementioned studies did not fully address the joint problem of topology, design and reliability optimization in an integrated fashion. Simply because dividing the whole strongly coupled optimization process into a sequence of stages contradicts with the concept of the strong coupling between topology, design and reliability. The topology optimization stage does not guarantee that the optimal topologies have been retained for the design stage. Consequently, the design optimization stage does not guarantee that optimal designs have been retained for the reliability screening stage.

3.6 CONCLUSIONS

The design and operation of the WDS are highly complex multi-objective problems that essentially require employing effective optimization techniques to be solved. This chapter has conducted a comprehensive review of the main optimization methods used to solve the optimization problem of the WDS. The two optimization techniques, namely conventional and evolutionary algorithms, applied to handle these multi-criteria problems have been reviewed. A special focus on genetic algorithms has been provided. Apart from being efficient, the application of conventional methods was recognized to place serious limitations to solving the highly constrained non-linear problems having discrete solution spaces. Due to being point-to-point approaches, conventional methods are not able to effectively solve multi-objective optimization problems. The point-to-point approaches face by the danger of potentially falling into the trap of local optima.

In contrast, the GA technique is a population-to-population approach capable to simultaneously search in multiple directions into the entire solution space. This important feature makes the GA techniques suitable for handling highly complex combinatorial problems having discrete solution spaces. A description of the main procedures required to implement the simple GA have been provided in sufficient detail. The different strategies proposed for improving the GA performance in handling constraints along with pointing up their limitations have been also reviewed. A special focus on the advancements in methods developed to implement the multi-objective GA has been presented.

The last section of this chapter has been devoted to the two groups of approaches proposed to address the joint effect between topology, design and reliability optimization of the WDS. The first group is categorized under the concept of coupling topology to the design optimization of the WDS. Two types of models

classified under this group, namely two-stage and single-stage models, has been reviewed. The limitations of these models have been highlighted and discussed. The two-stage models dealt with topology and design optimization as a sequence of two separated stages, which ignore the concept that topology and design are strongly coupled. Single-stage models had the limitation of severely restricting the search to the feasible region of the solution space.

The second group is classified under the concept of joining topology and reliability to the design optimization of the WDS. All models falling into this group did not fully address this joint issue by dividing the optimization into a sequence of separated stages. An integrated approach for handling the joint problem of topology, design and reliability optimization of the WDS has been recognized to be in high demand.

CHAPTER FOUR

NEW PENALTY-FREE MULTI-OBJECTIVE EVOLUTIONARY APPROACH TO COUPLED TOPOLOGY AND PIPE SIZE OPTIMIZATION OF WATER DISTRIBUTION SYSTEMS

4.1 INTRODUCTION

Water distribution systems (WDSs) represent a vital part of the infrastructure in developed societies. The establishment of WDSs mainly includes topology design, which is planning of the system components, and sizing of such components to evaluate the hydraulic performance of the system. However, WDSs deteriorate with time and require periodic maintenance to maintain the system capacity at the required levels. This increases considerably the overall cost of the system. Even though the capital cost is made up of the costs of system components such as pipes, valves, tanks and pumps, the capital cost is mainly due to pipeline provision and construction (Djebedjian *et al*., 2008). The operation cost is mainly due to energy and water treatment costs. Constructing and putting WDSs into operation is very expensive and it follows that good planning of the layout of the network of pipes can lead to a substantial reduction in the capital cost in addition to the long-term maintenance and operation costs.

The topology of WDSs can be categorized as: branched or tree-like, fully looped, and partially looped. Branched systems are suitable for small and low-density rural areas, while fully or partially looped systems are proper for urban areas (Swamee and Sharma, 2008). Branched configurations are similar to a tree and branch structure

(Figure 4.1a) in which the tree trunk represents the supply main while branches stand for pipes connecting consumption points or demand nodes to the supply main. Branched systems have only one supply path from the source to any demand point. This has the disadvantage of cutting off the water supply to the consumers downstream of any section of pipe that is not in service, e.g. due to a mains break. The main advantages of branched systems are that the capital cost is relatively low; they are easy to operate; and are suitable for sparsely populated areas (Swamee and Sharma, 2008). To reduce the effect of such situations, looped systems that have multiple supply paths from the source to the demand points are preferred. The reliability and cost of looped systems is highly dependent on the number of loops (Tanyimboh and Sheahan, 2002; Tanyimboh and Setiadi, 2008).

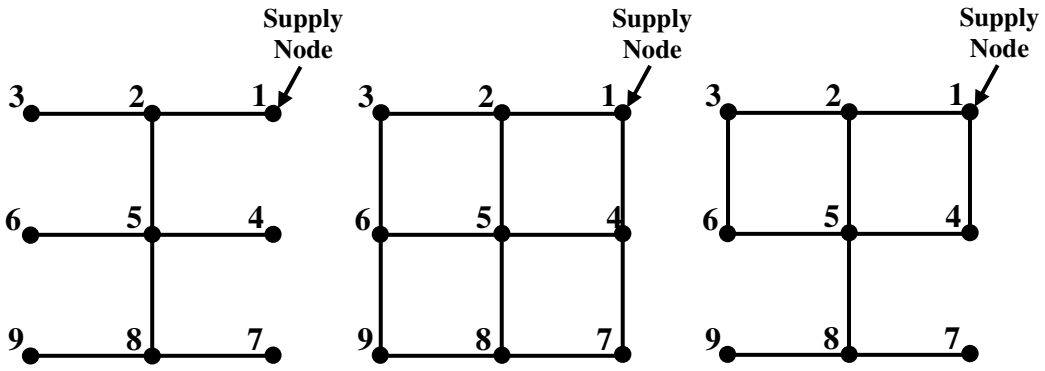

a) Branched topology (b) Fully looped topology (c) Partially looped topology

Figure 4-1: Illustration of branched, fully looped and partially looped topologies

In fully looped systems, pipes are structured in such a way that each demand node can be supplied from the source(s) through at least two independent paths as shown in Figure 4.1b. Two supply paths are said to be independent if they do not have a pipe in common. From the viewpoint of system reliability, this looping condition has the advantage of providing an alternative flow path in case the other paths are out of service. Partially looped systems lie between branched and fully looped configurations where each demand node has at least two flow paths but not all of them are independent. For example, nodes 1 to 6 in Figure 4.1c satisfy looping

condition, while nodes 7 to 9 do not because they are supplied through pipe 5-8 only. Cutting off the water supply in pipe 5-8 has the effect of putting nodes 7 to 9 out of service.

Most previous studies on WDS optimization have assumed that the topology is known *a priori*. In reality, this is not always the case due to the high complexity of determining the optimal layout from the large set of 2^{np} feasible and infeasible layouts where *np* is the number of candidate pipes. The complexity arises from the fact that the layout alone is not sufficient to evaluate the system cost or hydraulic performance, for example, without sizing system components. This makes the coupling between layout and design so strong that they should be determined simultaneously if the optimal solution is desired. A detailed review of the previous studies attempted to address this joint effect has been presented in section 5 of chapter 3.

In this chapter, a new penalty-free multi-objective evolutionary approach to the simultaneous topology and pipe size optimization of WDSs is presented. The penalty-free strategy enabled the approach to fully exploit the entire solution space that consists of both feasible and infeasible solutions. This means that pressure-deficient and *topologically* infeasible solutions were fully incorporated in the genetic algorithm without recourse to constraint violation penalties or tournaments. In other words, infeasible solutions are not targeted and removed arbitrarily purely by virtue of their infeasibility or by the use of extraneous penalties. A new procedure for handling *topologically* infeasible solutions has been proposed. The effectiveness of the approach is demonstrated by solving three benchmark problems. Better solutions than the best solutions in the literature were found for all the above-mentioned benchmark problems. By optimizing the topology and pipe sizes simultaneously and assessing infeasible solutions rationally, new least cost designs and/or new optimal topologies were found. In addition, a hitherto branched design optimization problem in the literature was solved as a looped design.

4.2 PROBLEM FORMULATION

A discrete combinatorial optimization problem with two objectives namely the capital cost and infeasibility both of which are minimized was developed. A novel unified feasibility measure that accounts for both nodal pressures and network topology is developed. The optimization is considered under the following assumptions. (1) The network configuration including all of the feasible links is known. This network is termed the fully connected or full topology network herein. (2) The pipe diameters and the links to be included or excluded are the decision variables of the problem. The aim is to find and size the optimal subset of links. (3) Node demands are known with certainty. Although nodal demands may be uncertain in practice, demands and other WDS aspects that can lead to uncertainty are not addressed herein. (4) The required pressure head at each demand node is given.

The optimization approach is basically composed of two main minimization objectives. The overall formulation of the developed approach can be summarized as follows:

Minimize initial construction cost: $f_1 = \sum_{ij \in N_p} f\left(L_{ij}, D_{ij}\right)$ (4.1)

Eq. 4.1 represents the objective of minimizing the initial construction cost, which is typically a function of pipe length L_{ij} and diameter D_{ij}. The WDS should satisfy both the conservation of mass and energy represented by Eq. 2.1 and Eq. 2.2. These constraints are met externally herein by employing the hydraulic solver EPANET 2 (Rossman, 2000) in the optimization process.

Any designs proposed should be both hydraulically and topologically satisfactory. This was addressed by ensuring there is a sufficient number of supply paths and sufficient pressure at all demand nodes. These two requirements were combined to formulate the second objective as follows:

Minimize infeasibility: $f_2 = LIM + HIM$ (4.2)

where

$$LIM = \sum_{i \in N} \max(0, R_i^{req} - R_i) \quad (4.3)$$

$$HIM = \sum_{i \in N} \max(0, H_i^{req} - H_i) \quad (4.4)$$

The first term (*LIM*) in Eq. 4.2 represents the objective of minimizing total topological infeasibility measure. The topological infeasibility at node *i* is quantified in terms of the shortfall in the available number of independent supply paths R_i with respect to the required number R_i^{req}; $R_i^{req} = 1$ for branched configurations and $R_i^{req} = 2$ for fully looped configurations. If $R_i \geq R_i^{req}$ at all nodes, then the topology is feasible and consequently $LIM = 0$. Otherwise, the topology is infeasible and *LIM* takes a positive value. For a branched topology, a node not satisfying the required level of node reachability of $R_i^{req} = 1$ is isolated and takes a value of 1. For a fully looped topology, the topological infeasibility at a node can be either 1 or 2. It is 1 if the node is reachable by only one independent flow path and 2 if the node is isolated.

The second term *HIM* in Eq. 4.2 represents the residual-head infeasibility measure that addresses any shortfall in the nodal available head H_i with respect to the required head H_i^{req}. If $H_i \geq H_i^{req}$ for all nodes, then the design is hydraulically feasible and therefore $HIM = 0$. Otherwise, the solution is infeasible and *HIM* takes a positive value.

Two key features can be highlighted from the introduced definition of infeasibility. First, the formulated problem practically represents a single-objective problem. This is because each feasible solution will have zero infeasibility according to Eq. 4.2.

This solution has the properties that it is topologically and hydraulically feasible (i.e. $LIM = 0$; $HIM = 0$). In other words, all topologically and hydraulically feasible solutions are mutually equal in terms of infeasibility. Even though there could be more than one feasible solution in each generation of the GA, the survival of such solutions will be dependent only on cost in the feasibility region. Accordingly, only the cheapest feasible solution will be retained in each optimization process.

Secondly, it is anticipated that Eq. 4.2 will reduce the large range of infeasibility values associated with using DDA hydraulic models. During the hydraulic simulation, such models always consider nodal demands are satisfied in full and irrespective of the available heads. This has the effect of producing large negative values of nodal heads in order to satisfy this requirement for extremely infeasible solutions. However, the most infeasible solution that can not be dominated by any other infeasible solution in the coupled topology and pipe size optimization is the one having zero cost. Since all nodes making up this solution are isolated, it will be assigned a total amount of infeasibility equal to $N \times R_i^{req} + (N\text{-}NS) \times H_i^{req}$ (i.e. $LIM = N \times R_i^{req}$; $HIM = (N\text{-}NS) \times H_i^{req}$) in which N and NS respectively denote the number of demand nodes and source nodes in the network. Bearing in mind that $R_i^{req} \leq 2$ and H_i^{req} is normally small, i.e. 15 m (OFWAT, 2004), the maximum value of infeasibility in each generation of the GA will be relatively small.

To optimize the layout and pipe sizes simultaneously, a pipe diameter of zero was introduced to enable different layouts to be generated by removing any link from the fully connected network or the network with full topology (Afshar, 2007a). A diameter of zero in Eq. 4.1 yields zero cost, which reflects the real situation for a non-existent link. However, this results in an undefined value of the headloss in Eq. 2.3. Therefore, to resolve this problem, the link removal case was modelled as a closed pipe when simulating the WDS.

Most importantly, a penalty-free strategy that enables infeasible solutions to participate fully in the optimization process has been adopted herein. In other words, no penalty terms designed to artificially increase cost of infeasible solutions was incorporated in Eq. 4.1. The reason for incorporating infeasible solutions is that in the latter stages some essential genes in the optimal solution may no longer be present in the current population of feasible solutions if, arbitrarily, some solutions are discarded purely because they are infeasible. This strategy also has the advantage of approaching the optimal design from both the feasible and infeasible regions of the solution space. In this way, the optimum design can be found by either lowering the cost of a near-optimal feasible design or converting a near-optimal infeasible design to a feasible design. The motivation is that optimal solutions for WDSs often occur at the boundary of the feasible region of the solution space.

4.2.1 Topology Confirmation

There is no guarantee that the operations of crossover and mutation will always create feasible topologies. A topology confirmation module coded in C to address this issue was developed. The module uses the EPANET 2 hydraulic analysis results to identify any isolated nodes; such nodes cannot be reached from any source. The module also establishes whether all demand nodes have at least two independent paths or not, in the case of fully looped designs. Using the results from EPANET 2, the total number of paths supplying each demand node, from all sources collectively, was determined based on the flow directions. The path enumeration algorithm for multi-source multi-demand networks that Yassin-Kassab *et al.* (1999) developed was used.

The topology confirmation starts once the total number of paths NP for each node is available. If $NP = 0$, the node cannot be supplied. If $NP = 1$, the node can be supplied. If $NP \geq 2$ at all nodes, a path inter-dependency investigation is carried out

to confirm the status of the network as partially or fully looped. A simple and practical procedure that does not involve an exhaustive enumeration of all the paths supplying each node was adopted. For a pair of independent supply paths, removing a pipe from one path does not affect the other path. The procedure simply entails removing all the pipes one at a time and observing the reachability of all nodes in each case. If all nodes are reachable from one or more sources after the removal of all pipes one by one with replacement, then the system is fully looped and partially looped otherwise.

It is worth observing that EPANET 2 sets default values of node pressures and pipe flows within parts of a network that are not connected to a source. For example, isolated nodes are assigned large negative pressures. This was resolved by assigning zero flows to pipes and zero pressures to nodes that are not connected to a source, as illustrated in Appendix A. Addressing the topology, pipe flow rates and nodal pressures in this way enabled a consistent and bias-free fitness assessment of both feasible and infeasible solutions that obviates constraint violation penalties or tournaments.

4.2.2 Constraint Handling

Dridi *et al*. (2008) stressed the inherent difficulties associated with constraint violation penalties that are commonly used to incorporate constraints in EAs. These include time-consuming pre-optimization trial runs and parameter calibration. The proposed joint topology design, pipe sizing, initial construction cost optimization employs a penalty-free evolutionary search method in which infeasible solutions do not incur additional constraint-violation penalties. In terms of practicality, Siew and Tanyimboh (2012) highlighted the advantages of penalty-free methods. Penalty-free methods eliminate the necessity of designing penalty functions. They are relatively straightforward to implement without sacrificing the efficiency of the GA (Siew and

Tanyimboh, 2012). Penalty-free methods can maintain infeasible solutions that may have useful genetic material that may not be common in feasible solutions. For example, cheaper solutions made up of small pipe sizes can be maintained throughout the whole optimization. If selected for crossover, this would increase the chances of trying small pipe diameters in more solutions.

Other constraint handling methods have been proposed e.g. the constraint violation-based ranking tournament (Deb *et al.* 2002). Ray *et al.* (2001) proposed three stages of nondomination ranking using the objective and constraint functions in the following priority order: (a) objective functions only; (b) constraint functions only; and (c) all objective and constraint functions collectively. The results in Deb *et al.* (2002) suggest that the constraint violation-based nondomination ranking tournament outperforms the Ray *et al.* (2001) three-stage nondomination ranking approach. The advantages of the constraint violation-based nondomination ranking tournament over the method proposed by Fonseca and Fleming (1998a-b) can be found in Deb *et al.* (2002). Constraint handling in NSGA II (Deb *et al.* 2002) uses a binary tournament in which feasible solutions automatically dominate infeasible solutions. The approach here is different in that it seeks a measure of the utility value of all feasible and infeasible solutions and ranks the solutions accordingly. The aim is to approach the active constraint boundaries quickly from both the feasible and infeasible regions by avoiding any arbitrary removal of infeasible solutions. In other words, the search strategy seeks to retain and exploit the beneficial properties of all efficient solutions as it is thought that efficient solutions that are just feasible or just infeasible will be found on both their respective sides of the active constraint boundaries.

4.3 COMPUTATIONAL SOLUTION

The fast robust elitist genetic algorithm NSGA II (Deb *et al.* 2002) was used to solve the optimization problem. NSGA II has been used extensively and its merits have

been reported elsewhere (see e.g. Deb *et al.* 2002, Dridi *et al.* 2008). The optimization problem was posed as in Eq. 4.5.

$$\text{Minimize } \mathbf{f} = (f_1, f_2)^{\mathrm{T}} \tag{4.5}$$

The decision variables are the pipe diameters D_{ij} to be selected within the domain of the available discrete pipe sizes and the zero-diameter that identifies pipes subject to removal. To make the two objectives in Eq. 4.5 roughly similar in magnitude, each f_i^m the value of objective m for solution i, was normalized as in Eq. 4.6

$$fn_i^m = \left(f_i^m - f_{\min}^m\right) / \left(f_{\max}^m - f_{\min}^m\right); \qquad \forall i, \forall m \tag{4.6}$$

in which, in the generation in question, $f_{\min}^m$ = minimum value of objective m; $f_{\max}^m$ = maximum value of objective m; and fn_i^m = normalized value of objective m for solution i. Accordingly, the application of elitism herein will be modified to become based on normalized objectives as per Eq. 4.6. Originally, NSGA II uses normalized objectives to evaluate diversity of solutions only.

NSGA II can be briefly described as follows (Figure 4.2). First, an initial population is randomly created. Using this population, the operators of tournament selection, crossover and mutation are used to produce an offspring population. To apply elitism, the parent and offspring populations are combined into a single population that is then sorted into various levels of non-domination. Each non-domination level or front has solutions of equal merit with respect to the objectives or criteria involved. To determine the best solutions among the current merged population of parents and offspring in order to create the next generation, solutions with the best rank are selected first followed by solutions with the next best rank and so on. The process continues until a front is reached that has more solutions than required to achieve the population size. If this situation arises, then, to obtain the required population size, the solutions having the largest crowding distances are chosen. The

crowding distance is a parameter that represents the spatial density of the solutions nearest to a particular solution; crowding distance increases as sparseness increases.

The calculation of the crowding distance starts by sorting the merged populations of parents and offspring in ascending order according to each objective function value. To maintain the boundary solutions for each objective function, i.e. solutions with smallest and largest objective values, they are assigned an infinite distance value. Now, each objective function is normalized before calculating the crowding distance of non-boundary solutions. The non-boundary solutions are allocated a distance value equal to the absolute normalized difference in the function values according to each objective. The overall crowding distance value is calculated by adding up all individual distance values that correspond to each objective. The crowding distance is very important in guiding the selection process at the various stages of NSGA II towards a uniformly distributed POF. This is because, for two solutions belonging to the same front, the crowding distance operator prefers the solution that is located in a lesser crowded region (i.e. the solution with the larger crowding distance).

NSGA II uses a fast non-dominated sorting approach that requires $O(mn^2)$ computations. First, two entities are calculated for each solution: 1) domination count n_s, which is the number of solutions that dominate the solution s; and 2) S_s, a set of solutions that the solution s dominates. Accordingly, all solutions of the first non-dominated front will have a domination count of zero. Now, for each solution with $n_s = 0$, the domination count of all its members is reduced by one. After doing this, for any member of which the domination count becomes zero, it will belong to the second non-dominated front. Now, the above procedure is continued with each member of the second non-dominated front. This procedure continues until identifying all fronts. Now, for each solution not belonging to the first non-dominated front, the non-domination count it can take is at most (n-1). Therefore, each of these solutions will be visited at most (n-1) times before its domination count becomes zero. At this point, the solution is allocated a non-domination level and will never be visited again. Given that are at most (n-1) of such solutions, the total

complexity is $O(n^2)$ and the overall complexity of the conducted procedure is $O(mn^2)$.

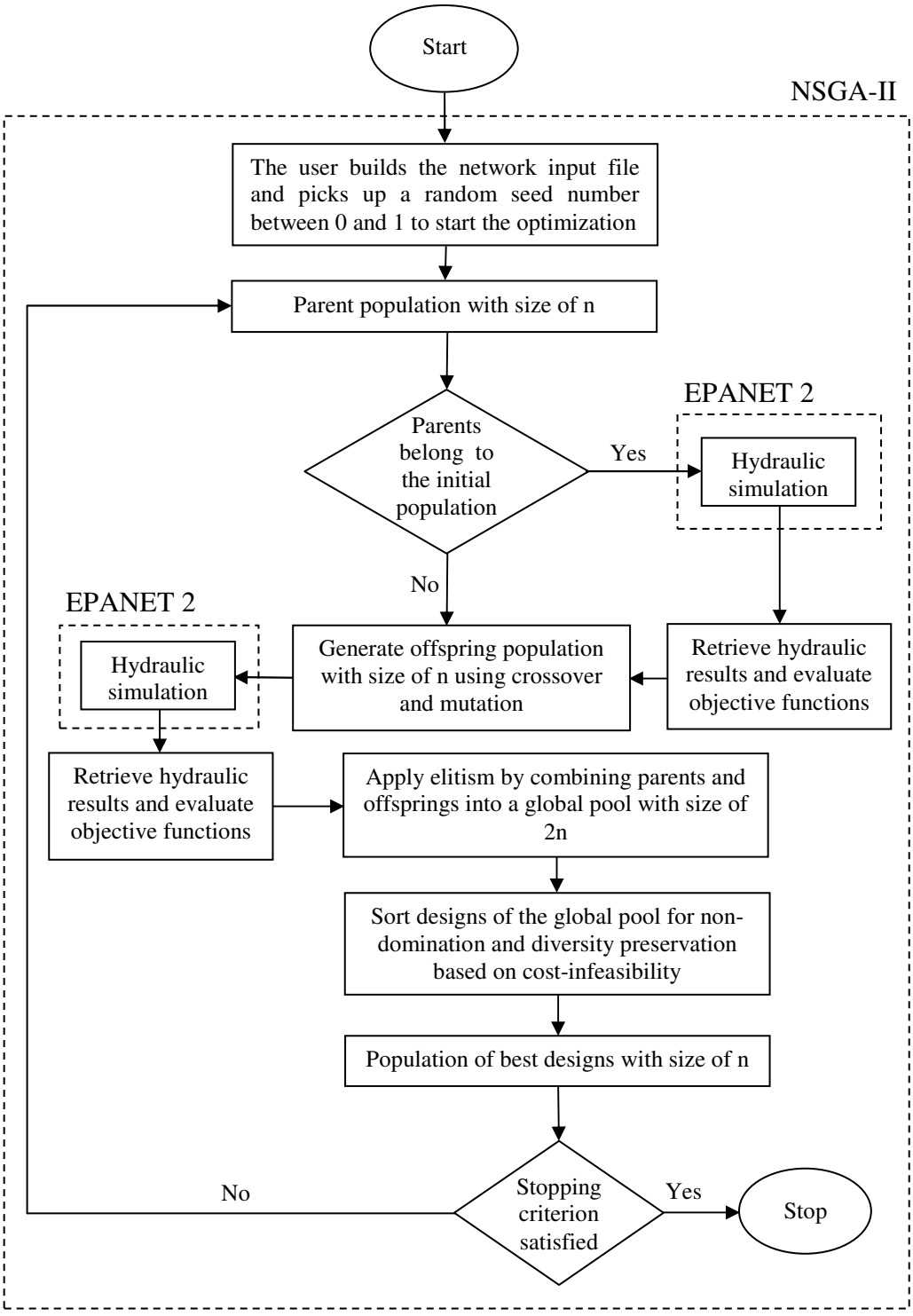

Figure 4-2: Flow chart of the proposed approach

4.4 APPLICATION OF THE PENALTY-FREE MULTI-OBJECTIVE EVOLUTIONARY APPROACH TO COUPLED TOPOLOGY AND PIPE SIZE OPTIMIZATION OF WATER DISTRIBUTION SYSTEMS

The proposed approach was applied to two benchmark optimization problems: a hypothetical single-source network and a multiple source real system. Both branched and fully-looped designs were considered for each of the two networks. Even though these networks do not describe in full the actual situation of real-world WDSs, they have been extensively analyzed by previous studies and so providing good grounds to compare the performance of the proposed approach. An Intel Core 2 Duo CPU 2.99 GHz, 3.21 GB RAM personal computer was used in this study. Since different computer specifications would have been used previously, assessing the efficiency of the present approach with design evaluations along with CPU time would provide a fair comparison of results.

With respect to the GA parameters required to optimize the two networks, a typical population size of 100 was used. The single-point crossover operator was used to generate two offsprings from two parents using crossover probability p_c of 1.0. By default, this is the optimal crossover probability value for NSGA II and arises from the fact that global elitism is enforced by merging the offspring and parent populations in each generation. The crossover probability determines the number of offspring to be produced from parents, i.e. in each generation, 50 crossover operations are conducted on the parent population to produce an offspring population with size of n = 100. The operator of tournament selection was used to select two parents to be subject for crossover. To potentially make weak solutions, i.e. extremely infeasible solutions, survive when selected through the tournament, a tournament size of 2 was used.

Once the offspring population is created, the operator of random mutation goes over the whole bits making the offspring population. To identify whether the selected bit is to be changed to its binary complement from 0 to 1 or 1 to 0, the mutation operator

uses a random number between 0 and 1. If the generated random number is less than or equal to the mutation probability, p_m, then the selected bit is mutated. To identify the best mutation rate, bit-mutation probabilities in the range [0.001, 0.3] for the two network examples were investigated. A bit-mutation (absolute) probability of $p_m \approx 1/n_g$ where p_m = mutation rate and n_g = chromosome length as determined by the number of genes was adopted.

4.4.1 Example 1

The network of Example 1 is a single source network made up of 9 nodes and 12 pipes as shown in Figure 4.3. The source located at node 9 has an elevation of 50 m. All of the other nodes are demand nodes with an elevation of zero. The minimum desired head at all of the demand nodes is 30 m. All of the pipes have a length of 100 m and Hazen-Williams coefficient of 130. The decision variables are a set of 13 discrete pipe sizes plus the link removal option of diameter zero (Afshar, 2007a). As such, the solution space for this network comprises $14^{12} = 5.67\times10^{13}$ feasible and infeasible solutions. A 4-bit binary substring was used to code the fourteen pipe diameters (Appendix B). This gave 2^4 or 16 substrings of which two were redundant. The redundant substrings were mapped to the link removal option to increase the chances of creating new layouts. Full details of the binary representation of pipe diameters and the corresponding cost per metre are shown in Appendix B. Since the network is composed of 12 pipes, each design is represented by a chromosome that has a 48-bit binary string. Within each optimization process, 100 offsprings were produced from 100 parents. Each selected bit from the offspring population is subject to mutation using a mutation probability of $1/n_g = 1/48$, i.e. a 2.1% chance that any single bit would mutate.

To evaluate the convergence properties of GA, the optimization process were initiated a number of times from different starting points. In each run, the GA was

allowed to proceed until reaching a maximum number of Function Evaluations (FE) of 200,000 using a maximum number of generations of 2,000 (Appendix C). FE is a product of population size by maximum number of generations. As a result, the search space investigated herein represents a fraction of 1 / (2.8×10^8) of the design space of this network. Due to the uniqueness of flow directions in branched networks along with the small size of this network, 10 random runs each started with a random seed different from other runs were carried out.

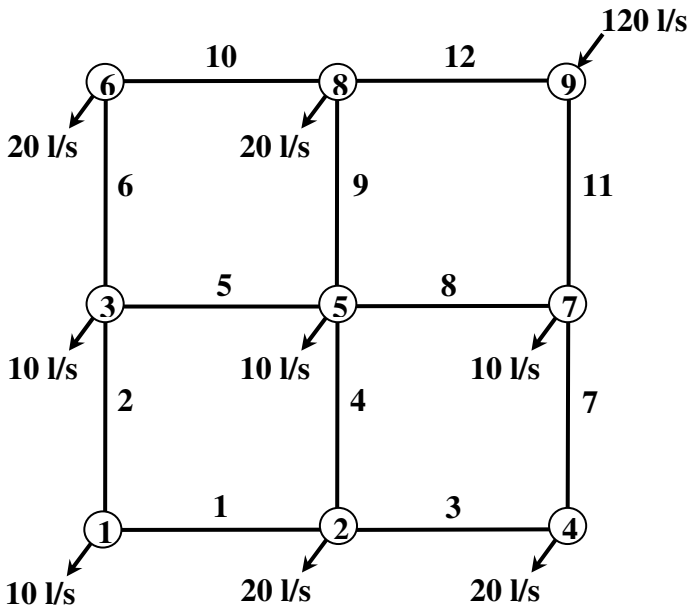

Figure 4-3: Full topology of Example 1

Table 4.1 and Figure 4.4 show results of the achieved least cost branched design of Example 1. In all of the previous approaches, the critical node was identified to be Node 1. It is Node 2 in the present optimal design (Figure 4.4). The small surplus head of 0.06 m at the critical node would appear to suggest that the achieved solution is at least a near-global optimum. Figure 4.5 shows the best achieved Pareto Optimal Front (POF) for Example 1. The best POF is the front produced by the random run in which the cheapest least-cost design is achieved among all conducted runs. With reference to Eq. 4.2, the maximum infeasibility value of f_2 = 249 (Figure 4.5) is the summation of the prescribed minimum nodal residual pressure head of 30 m and the

minimum required nodal connectivity of R_i^{req} = 1, for all the eight demand nodes, i.e. 30 × 8 = 240, and the minimum required nodal connectivity of R_i^{req} = 1 at all nodes, i.e. 9 × 1 = 9. With a cost of zero, this solution is always non-dominated. This zero cost solution has no pipes. Consequently, selecting the zero cost solution for crossover results in link removal in the offspring. This zero cost solution is very important as it safeguards the potential for creating new layouts in every generation.

Table 4-1: Present and previous cheapest branched designs for Example 1

Pipe	Diameter (mm)		Node	Pressure head (m)		Surplus pressure head(m)	
	Afshar (2007)	Present		Afshar (2007)	Present	Afshar (2007)	Present
2	100	100	1	**30.21**	30.21	**0.21**	0.21
4	120	100	2	30.94	**30.06**	0.94	**0.06**
6	120	120	3	32.12	32.12	0.12	0.12
7	100	100	4	32.89	32.90	0.89	0.90
8	120	140	5	33.78	36.94	0.78	0.94
10	140	140	6	34.95	34.95	0.95	0.95
11	140	140	7	39.78	39.77	0.78	0.77
12	140	140	8	39.78	39.77	0.78	0.77

The critical nodes are shown in bold

Additionally, the zero-cost solution has added another important feature to the optimization. It dramatically reduced the large negative pressures produced by DDA hydraulic models. For example, the maximum infeasibility herein was early reduced to a fixed value of 249 m (Appendix C). In the initial stages of the GA, solutions with small diameters were randomly generated. These solutions will have some cost accompanied with large pressure deficits when modelled by EPANET 2 (Appendix C). For example, the maximum infeasibility before generating the zero-cost solution was found to be about 4,477 (Appendix C). On average, each demand node within this solution would have an infeasibility of about 560. When such small diameters were replaced with zero diameter, smaller nodal pressure deficits of 30 were

allocated herein while reducing cost to zero. Reducing the maximum infeasibility has the advantage of making infeasible solutions closer to the feasibility boundary and thus converting an infeasible solution to a feasible one could be faster.

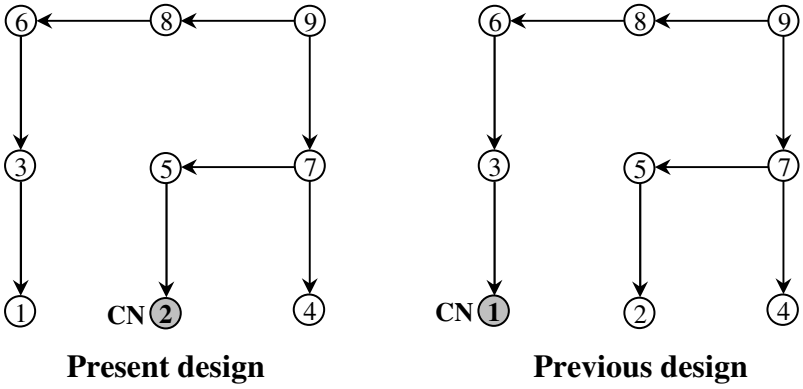

Figure 4-4: Optimal branched layout for Example 1 (CN denotes critical node)

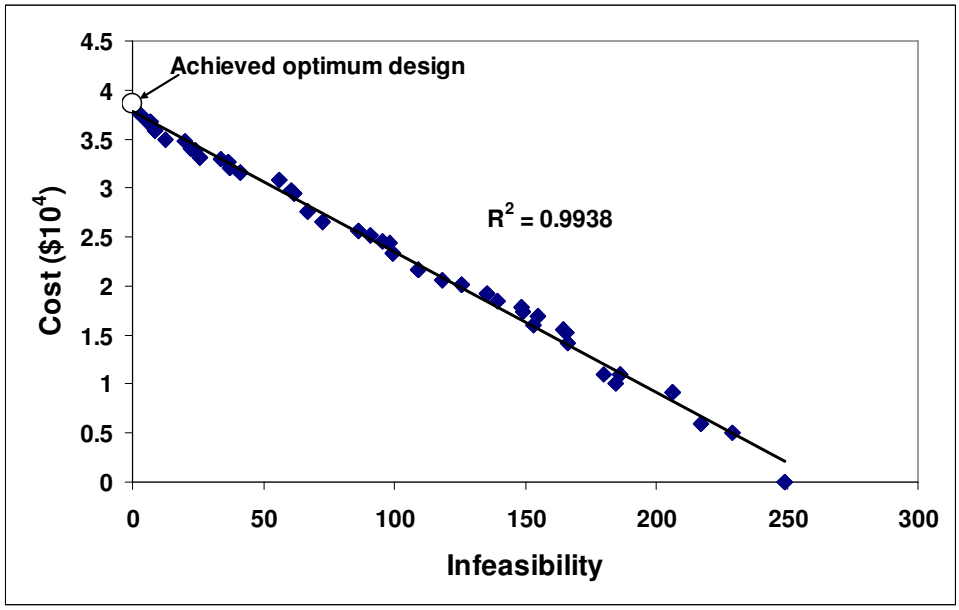

Figure 4-5: Best achieved POF for the branched design of Example 1

Table 4.2 summaries the results to date and demonstrates clearly the effectiveness of the proposed approach. The best design generated costs $38,600 and is actually the cheapest solution to date. Out of 10 random runs, the optimum design having a cost of $38,600 was identified in 8 different runs. The best run took a CPU time of about 10 seconds after 10,400 function evaluations. The two remaining runs both found a

feasible solution that costs \$39,800. The average, median and maximum optimum cost for the 10 GA runs were \$38,840, \$38,600 and \$39,800 respectively. The standard deviation (*SD*), coefficient of variation (*CV*) and SD/f_1^* were \$505.96, 0.0130 and 0.0131, respectively. f_1^* = \$38,600 is the cost of the optimal solution. It can be seen that the values of *CV* and SD/f_1^* are small and similar. *CV* is indicative of the consistency of the results whereas SD/f_1^* is indicative of the quality of the results; self-evidently the smaller the values and the more the similarity, the better. Several near-optimal solutions were also found by the 10 GA runs as shown in Table 4.3.

Table 4-2: Summary of the cheapest branched design for example 1

Author	**Approach description**	**Cost (\$)**	**No of evaluations**
Geem *et al* (2000)	Layout optimization followed by pipe size using harmony search	39,800	N/A[a]
Afshar (2005b)	Simultaneous layout and pipe size using max-min ant system	39,800	7,900
Afshar (2007a)	Simultaneous layout and pipe size using GA with four crossover selection schemes	39,400	7,500
Afshar (2007b)	Simultaneous layout and pipe size using GA with three crossover selection schemes	39,400	7,500
Proposed approach	Multi-objective penalty-free GA with unified measure for hydraulic and topological infeasibility	39,800	9,500
		39,700	9,900
		39,600	21,100
		39,400	28,200
		38,600[b]	**10,400**

[a]A direct comparison is not possible as a hybrid approach involving a tree growing algorithm and harmony search was used. [b] New best least cost feasible solution

The robustness of the proposed approach is evident from providing very similar POFs (Figure 4.6) and demonstrating a stable convergence within the 10 GA runs (Appendix C). Within all the conducted runs, the zero-cost solution was maintained until the end of the optimization. Furthermore, the optimum solution was detected at different locations of the optimizations due to starting each optimization process from different locations.

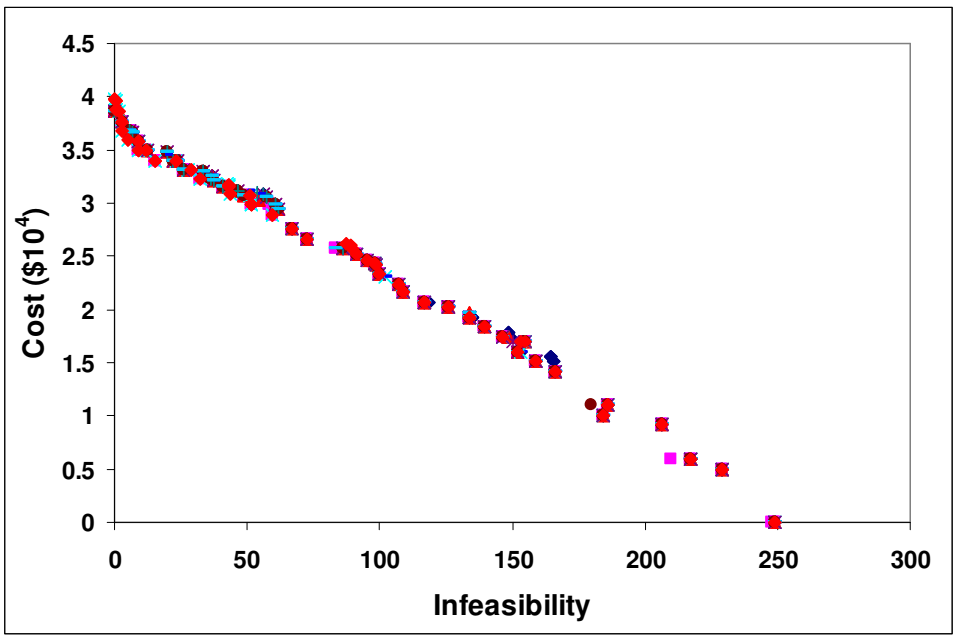

Figure 4-6: Individual POFs for the 10 GA runs of branched Example 1

Example 1 was also optimized as a looped network. Two different optimal layouts each with an associated optimal design (Designs 1 and 2) were created (Figure 4.7, Table 4.3 and 4.4). Figure 4.8 shows the best POF achieved. As all hydraulically and topologically feasible designs have an infeasibility value of zero the non-domination sorting procedure ensures that only the cheapest feasible design can survive at the feasibility boundary as the least cost looped design. There are a few hydraulically feasible branched designs next to the least cost looped design (Figure 4.8).

The zero-cost solution was generated in the early stages of the optimization (Appendix C). Herein, the maximum infeasibility value of 258 is the sum of the nodal head deficit for all nodes with insufficient pressure and supply paths shortfall for all nodes with less than two independent supply paths. Since all of the 8 demand nodes in this design are not connected to the source node, the second term of Eq. 4.2 results in a residual head deficit *HIM* of $8 \times 30 = 240$ m. In addition, all 9 network nodes contribute a further layout infeasibility *LIM* value of $9 \times 2 = 18$ through the first term in Eq. 4.2. Inherently, infeasible solutions dominate the POF (Figure 4.8);

all feasible solutions except for the cheapest are dominated as explained above. In comparison with the branched design case herein, the maximum deficit was slightly increased by just 3.6%.

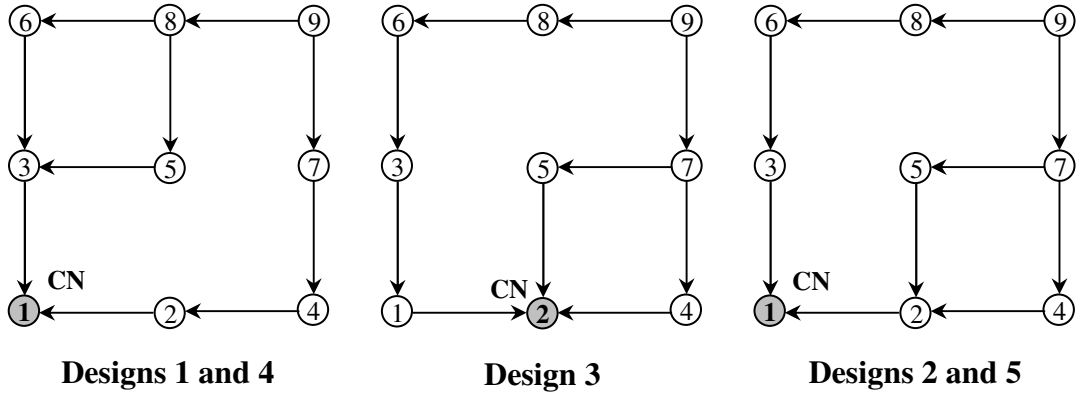

Figure 4-7: Optimal looped layouts for Example 1 (CN denotes critical node)

Due to the increased problem complexity and larger solution space of looped networks in comparison with branched networks, the number of random GA runs was increased to 20. The complexity arises from the existence of alternative feasible flow distributions for looped networks. A maximum of 200,000 function evaluations per GA run were allowed (Appendix C). Interestingly, two different optimum designs having a cost of f_1^* = \$41,400 were found (Designs 1 and 2 in Table 4.4). Designs 1 and 2 were achieved after 5,000 and 10,500 function evaluations respectively. The CPU time was about 4.8s and 10.1s for Designs 1 and 2 respectively. Designs 1, 2 and 3 in Tables 3.4 and 4.4 were identified 5, 3, and 10 times respectively by the 20 random GA runs.

Each of Designs 4 and 5 in Tables 4.3 and 4.4 was found once. The average, median and maximum values of the least cost solutions were \$41,885, \$42,200 and \$42,300 respectively. The *SD*, *CV* and SD/f_1^* values were \$406.88.96, 0.0097 and 0.0098, respectively. It is worth highlighting that the least cost branched design of this network having a cost of \$38,600 was identified 13 times by the 20 GA runs. This

result is significant in that it suggests it may be possible to combine and solve the branched and looped least cost network design problems together.

Table 4-3: Node pressures of the optimal looped designs for Example 1

Node	Node pressures of the achieved designs (m)				
	Design 1	Design 2	Design 3	Design 4	Design 5
1	30.04	30.13	30.07	30.07	30.03
2	31.26	30.66	30.06	30.67	31.00
3	30.37	31.18	32.02	31.41	32.33
4	33.72	35.00	30.76	35.08	33.69
5	32.25	33.70	34.99	33.67	36.17
6	30.72	36.40	34.88	32.82	36.96
7	40.44	38.88	39.81	41.18	38.52
8	39.08	40.63	39.73	38.27	40.95

Table 4-4: Pipe diameters of the optimal looped designs for Example 1

Pipe	Diameters of the achieved designs (mm)				
	Design 1	Design 2	Design 3	Design 4	Design 5
1	100	80	80	100	80
2	80	100	100	80	80
3	140	100	80	120	80
4	-	80	100	-	100
5	100	-	-	80	-
6	80	100	120	100	100
7	140	140	100	140	120
8	-	100	120	-	140
9	100	-	-	100	-
10	100	140	140	120	140
11	140	140	140	140	140
12	140	140	140	140	140
Cost($)	41,400	41,400	42,200	42,200	42,300

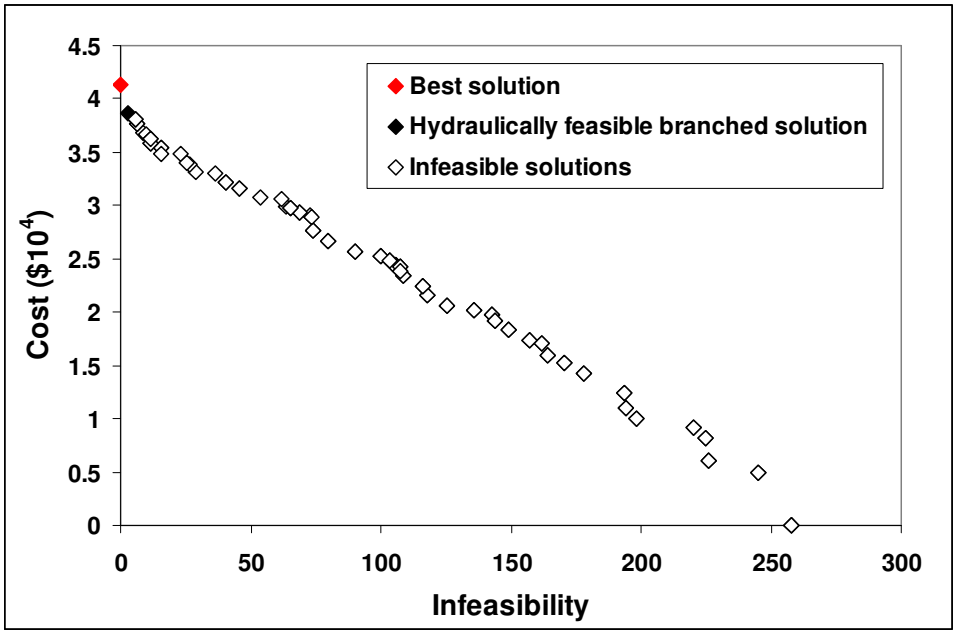

Figure 4-8: Best achieved POF for the looped design of example 1

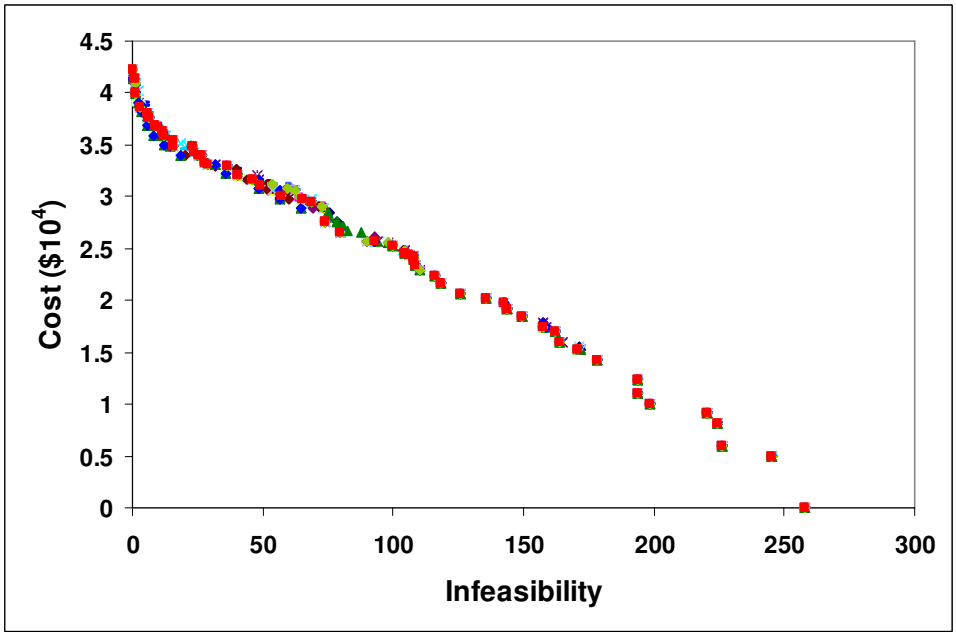

Figure 4-9: Individual POFs for the 20 GA runs of looped Example 1

4.4.2 Example 2

To demonstrate the performance and efficiency of the proposed approach in solving the complex optimization problem of coupled topology and pipe size of WDS, a larger example network (Figure 4.10) was solved using the approach. Example 2 represents part of a real system, the Winnipeg system (Morgan and Goulter, 1985). This network has 2 sources, 20 nodes and 37 pipes. The Hazen-Williams roughness coefficient for all pipes is 130. The full details of node demands, nodal required heads and pipe lengths are shown in Appendix B.

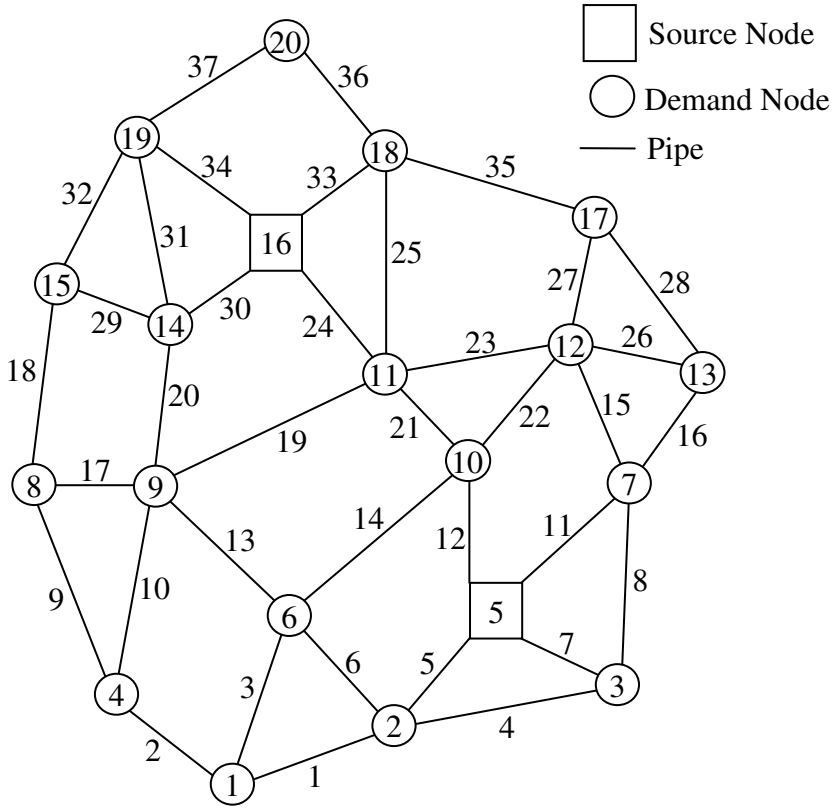

Figure 4-10: Full topology of Example 2

Using a 4-bit binary substring, since this network has 37 pipes, each solution was represented with a chromosome whose length is 148 genes. The resulting redundant codes from this representation were mapped to the link removal option. The binary representation of pipe diameters and the corresponding costs per metre used to

evaluate the construction cost for each proposed solution of this network as per Eq. 4.1 are shown in Appendix B. Within each reproduction process, 100 offsprings were produced from 100 parents using crossover probability of one. Each bit in the offspring population is subject to mutation using bit-wise mutation probability of $1/n_g = 1/148$.

Allowing for pipe removal, the solution space of this network comprises a combined total of $14^{37} = 2.55\times10^{42}$ hydraulically and/or topologically feasible and infeasible solutions. Due to the large size of this network in comparison with example 1, the maximum allowed number of function evaluations (FE) was increased to 500,000 using a maximum number of generations of 5,000 (Appendix C). As a result, the size of the search space investigated herein comprises just a fraction of $1 / (5.1\times10^{36})$ of the design space of this network.

Tables 4.5 and 4.6 along with Figure 4.11 show the results for the branched design of Example 2. The solution of \$1,684,228 (Design 1) is the cheapest design to date while the near-optimal solution of \$1,692,058 (Design 2) is also cheaper than the best solution in the literature. The layout of Design 1 has not been identified previously. Its creation here is, therefore, a remarkable achievement. Two single-source branched networks were created by removing 19 pipes (51%) out of 37 in each of Designs 1 and 2 (Appendix C). 20 GA runs were performed using different randomly created initial populations. The least cost of f_1^* = \$1,684,228 (Design 1) was identified two times out of 20 (Appendix C).

This achievement required a number of function evaluations of 154,500 FEs and a CPU time of about 2.12 minutes according to the best POF. Design 2 was identified once among the 20 runs (Appendix C). The average, median and maximum values of the least cost solutions were \$1,753,359, \$1,733,044 and \$1,889,386 respectively. The *SD*, *CV* and SD/f_1^* values were \$60,731.81, 0.0346 and 0.0361, respectively. Figure 4.12 shows the best achieved POF. A good distribution of solutions is evident.

This may be attributable to the larger solution space made up of a large number of branched layouts and pipe size combinations.

Table 4-5: Present and previous optimum branched designs for Example 2

Pipe	Diameter (mm)		
	Afshar (2005a)	Present approach	
		Design 1	Design 2
1	400	400	400
2	300	350	300
5	550	500	500
6	250	300	250
7	250	250	250
11	350	350	400
12	350	450	350
16	350	350	300
17	350	350	350
20	400	400	400
21	-	300	-
22	300	400	300
24	300	-	300
27	-	350	-
29	250	300	300
30	550	500	500
33	400	350	400
34	300	300	300
35	300	-	300
36	300	300	300
Cost ($)	1,693,393	**1,684,228**[a]	**1,692,058**[a]

[a]Two new best least cost feasible solutions

In comparison with Example 1, the detection of zero-cost of this larger network required larger number of function evaluations (Appendix C). The zero-cost solution herein has an infeasibility of 1,290, i.e. $LIM = 20 \times 1 = 20$, while *HIM* is summation

of minimum required pressures at all demand nodes, which is 1,270 m. Initially, the maximum infeasibility reached a very large negative value of about 279,374 (Appendix C). This large value would, on average, reflect creating a large infeasibility of about 15,520 at each demand node. Overall, the reduction in infeasibility was about 200 times.

Table 4-6: Present and previous optimum branched designs for Example 2

Node	Head (m)			Surplus head (m)		
	Afshar (2005a)	Present approach		Afshar (2005a)	Present approach	
		Design 1	Design 2		Design 1	Design 2
1	83.68	79.37	83.69	8.68	4.37	8.69
2	94.67	90.34	94.67	20.67	16.34	20.67
3	80.85	80.85	80.86	7.85	7.85	7.86
4	75.23	75.38	75.25	3.23	3.38	3.25
5	102.00	102.00	102.00	-	-	
6	74.85	82.20	74.86	1.85	9.20	1.86
7	72.28	72.31	86.50	5.28	5.31	19.5
8	76.04	73.03	73.03	4.04	1.03	1.03
9	80.36	77.35	77.35	10.36	7.35	7.35
10	82.37	80.27	82.38	13.37	11.27	13.38
11	82.42	74.26	82.43	11.42	3.26	11.43
12	72.85	71.56	72.87	2.85	1.56	2.87
13	65.51	65.53	72.15	1.51	1.53	8.15
14	90.88	87.85	87.85	17.88	14.85	14.85
15	74.32	81.05	81.05	1.32	8.05	8.05
16	96.00	96.00	96.00	-	-	
17	67.15	67.34	67.17	0.15	0.34	0.17
18	80.97	83.07	80.98	10.97	13.07	10.98
19	81.93	81.93	81.93	11.93	11.93	11.93
20	68.78	70.89	68.79	1.78	3.89	1.79

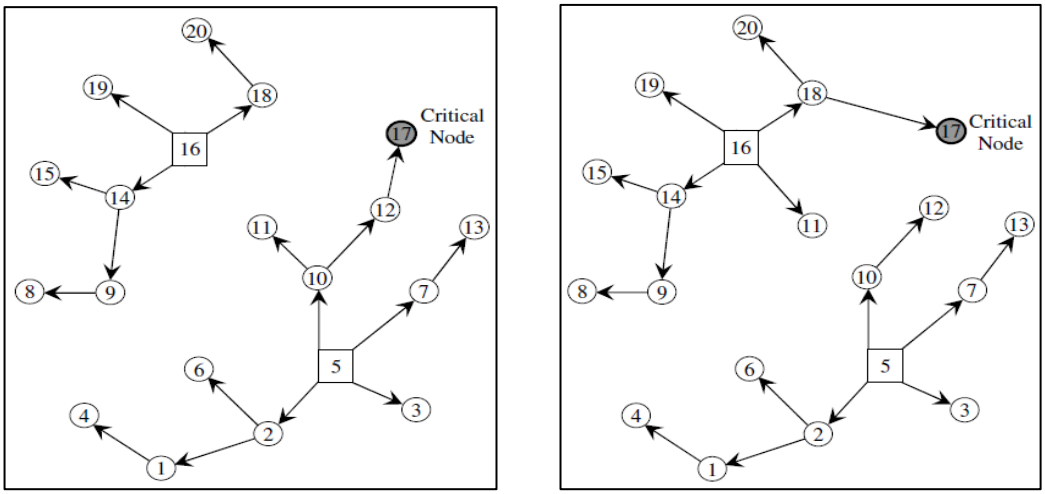

Design 1 **Design 2**

Figure 4-11: Optimal branched layouts for Example 2

Table 4-7: Summary of the present and previous branched designs for Example 2

Author	Approach description	Cost ($)	No of evaluations
Afshar (2007b)	Simultaneous layout and pipe size using GA with four crossover selection schemes	1,783,086	100,000
Afshar (2007a)	Simultaneous layout and pipe size using GA with three crossover selection schemes	1,783,086	100,000
Afshar (2005b)	Simultaneous layout and pipe size using max-min ant system	1,710,121	22,800
Afshar (2005a)	Application of iterative two-stage procedure to layout and pipe size optimization	1,693,393	NA
Proposed approach	Multi-objective penalty-free GA with unified measure for hydraulic and topological infeasibility	**1,692,058**[a]	**170,300**
		1,684,228[a]	**154,500**

[a]Two new best least cost feasible solutions

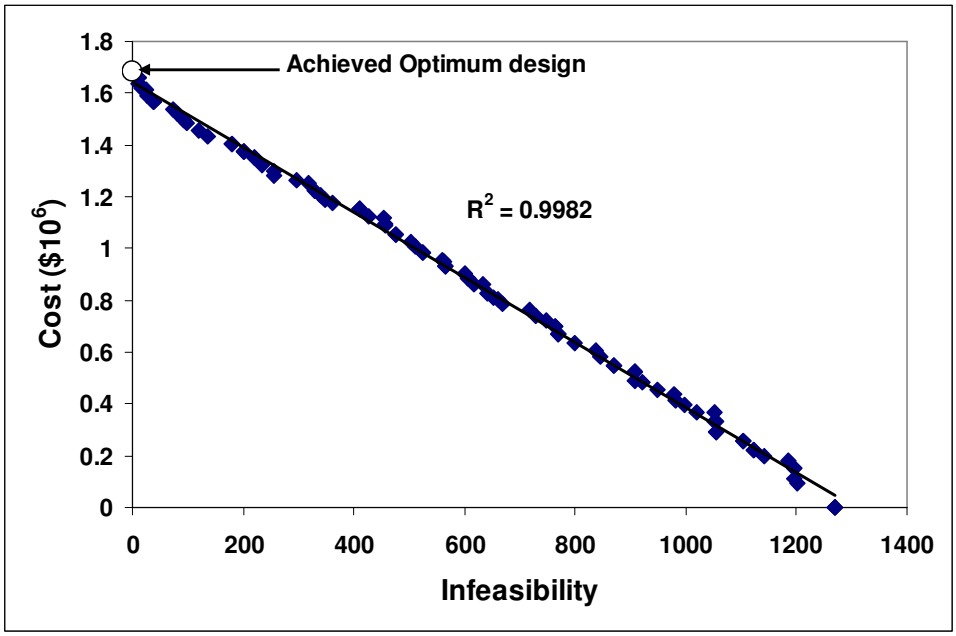

Figure 4-12: Best achieved POF for the branched design of example 2

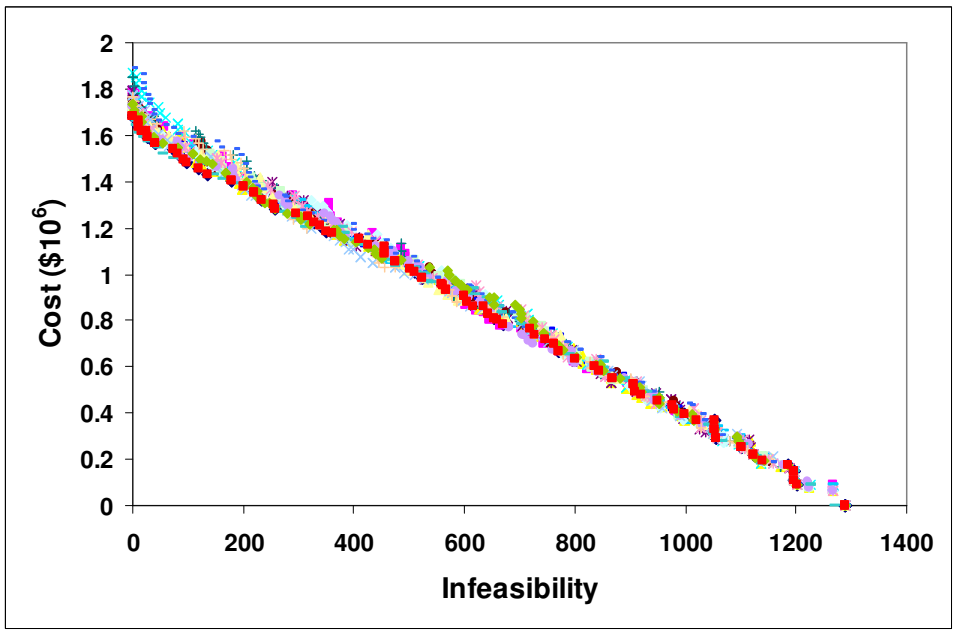

Figure 4-13: Individual POFs for the 20 GA runs of branched Example 2

Table 4.8 to 4.9 and Figure 4.14 show the results for the looped design of Example 2. Remarkably, three new feasible solutions that are cheaper than the previous best solution in the literature were created. A new layout was created also, as shown in Figure 4.14. The new layout is that of the new cheapest solution of f_1^* = \$1,972,559

(Design 3) that has only 25 pipes. The previous best solution has 26 pipes (Figure 4.14). Out of 20 random runs of the GA, the cheapest design of $1,972,559 was identified two times (Appendix C). This required 901,300 function evaluations and consumed a CPU time of about 12.41 minutes. Two of the 20 runs resulted in Near-optimal Designs 1 and 2 respectively. The termination criterion was 1,000,000 function evaluations (Appendix C).

The average, median and maximum values of the least cost solutions were $2,019,891, $1,998,076 and $2,095,167 respectively. The *SD*, *CV* and SD/f_1^* values were $43,683.82, 0.0216 and 0.0222. The robustness of the proposed approach is evident from consistency and stable convergence of the POFs achieved from the 20 conducted runs (Appendix C). All runs appear to be very similar in following a stable convergence at the optimal least cost solution in each run.

Table 4-8: Diameters of the present and previous optimum looped designs for Example 2

Pipe	Diameter (mm)			
	Afshar (2005a)	Present approach		
		Design 1[a]	Design 2[a]	Design 3[a]
1	400	400	400	400
2	350	300	300	300
5	500	500	500	500
6	250	250	250	250
7	250	250	250	250
8	125	200	125	125
9	125	125	125	125
11	350	350	350	400
12	350	400	350	350
13	125	125	125	-
14	-	-	-	150
16	300	300	300	300
17	350	400	350	350

18	-	-	-	-
20	400	400	400	400
21	150	250	150	-
22	300	300	300	250
23	-	-	-	200
24	250	150	250	300
27	125	150	125	-
28	125	150	150	125
29	350	250	250	250
30	500	500	150	500
32	150	125	125	125
33	450	400	450	400
34	250	300	300	300
35	300	300	300	300
36	300	300	250	300
37	125	150	200	125
Cost ($)	1,983,935	1,979,767	1,974,644	1,972,559

[a]Three new best least cost feasible solutions

Table 4-9: Nodal heads of the present and previous optimum looped designs of Example 2

Node	Head (m)				Surplus head (m)			
	Afshar (2005)	Present approach			Afshar (2005)	Present approach		
		Design 1	Design 2	Design 3		Design 1	Design 2	Design 3
1	79.07	80.14	80.27	80.30	4.07	5.14	5.27	5.30
2	90.44	90.79	90.88	91.08	16.44	16.79	16.88	17.08
3	78.56	77.25	78.95	82.69	5.56	4.25	5.95	9.69
4	74.80	72.20	72.38	72.16	2.80	0.20	0.38	**0.16**
5	102.00	102.00	102.00	102.00	-	-	-	-
6	73.02	73.23	73.97	76.34	**0.02**	0.23	0.97	3.34
7	74.65	76.34	76.12	85.51	7.65	9.34	9.12	18.51
8	72.52	73.99	74.50	72.85	0.52	1.99	2.50	0.85
9	76.58	76.37	79.10	77.32	6.58	6.37	9.10	7.32
10	79.46	81.44	79.33	84.42	10.46	12.44	10.33	15.42

11	72.72	72.19	72.68	76.10	1.72	1.19	1.68	5.10
12	70.40	70.38	70.15	70.65	0.40	0.38	**0.15**	0.65
13	68.37	64.00	64.34	70.40	4.37	**0.00**	0.34	6.40
14	87.29	87.76	90.69	88.02	14.29	14.76	17.69	15.02
15	78.57	73.23	74.96	73.57	5.57	0.23	1.96	0.57
16	96.00	96.00	96.00	96.00	-	-	-	-
17	71.15	67.83	70.53	68.96	4.15	0.83	3.53	1.96
18	86.90	81.84	87.98	81.94	16.90	11.84	17.98	11.94
19	70.79	78.01	75.83	78.73	0.79	8.01	5.83	8.73
20	73.77	71.78	69.14	71.22	6.77	4.78	2.14	4.22

Highlighted numbers are critical surplus

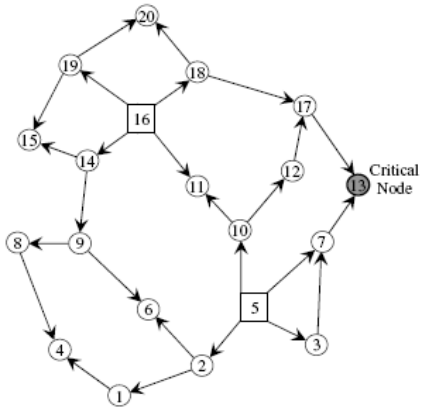

Present approach design 1

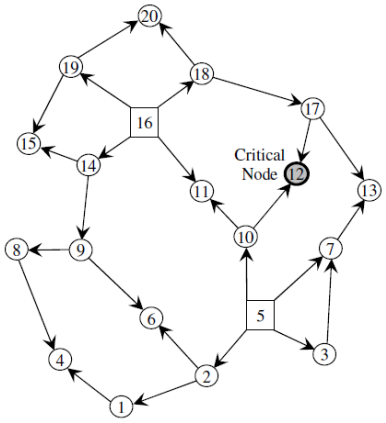

Present approach design 2

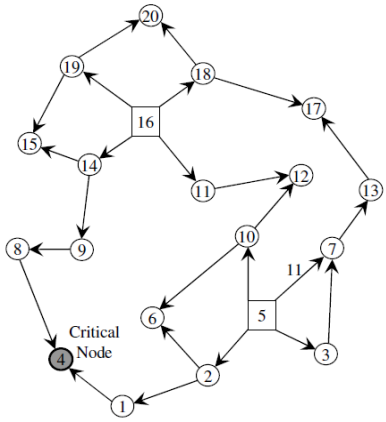

Present approach design 3

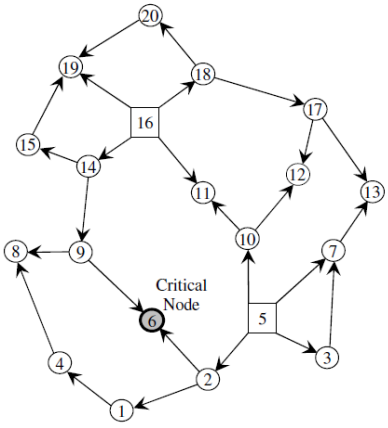

Afshar (2005a)

Figure 4-14: Optimal looped layouts for Example 2

Figure 4.15 shows the best POF achieved. For the topologically infeasible solutions the increase in cost is relatively gentle as the overall hydraulic performance improves while the infeasibility measure is decreasing. For the feasible branched solutions, the cost increases sharply as more pipes are added to create loops. A number of hydraulically feasible branched solutions lie near the cost axis, between the infeasible solutions and the least cost looped solution that has zero infeasibility. The cheapest feasible branched solution among the 20 conducted GA runs has a cost of \$1,694,966, which is slightly more expensive than the cheapest branched design of \$1,684,228 (Tables 4.5 and 4.7).

Due to the increase in node connectivity of looped designs, the infeasibility of zero-cost solution was increased to 1,310, i.e. i.e. $LIM = 20 \times 2 = 40$, while *HIM* is summation of minimum required pressures at all demand nodes, which is 1,270 m. In the initial stages of the GA, the maximum infeasibility reached a very large negative value of about 495,837 (Appendix C). This indicates that, on average, each demand node would have a very large infeasibility of about 27,546 at each demand node. Overall, the reduction in infeasibility was about 380 times.

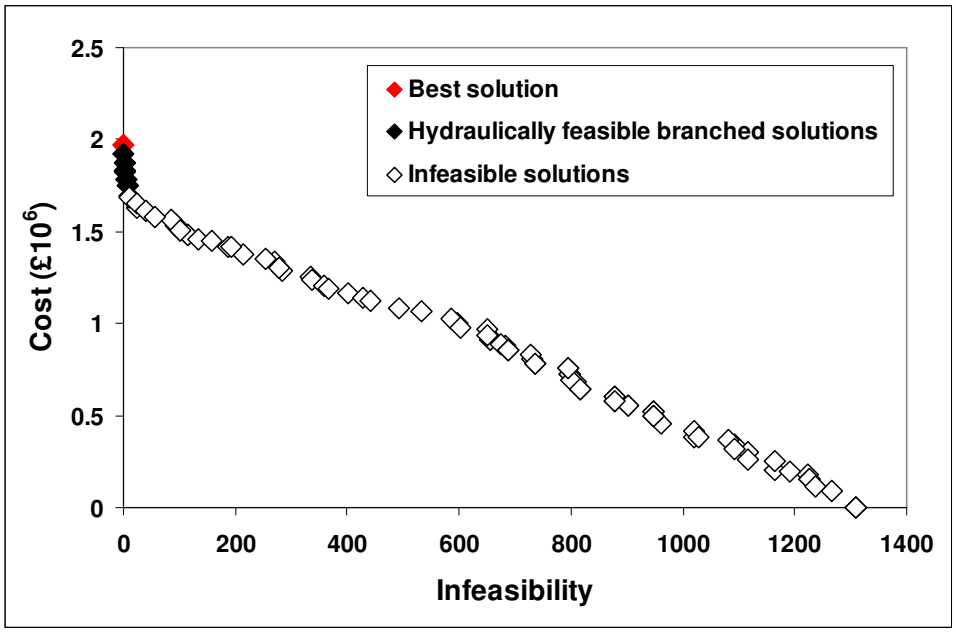

Figure 4-15: Best achieved POF for the looped design of Example 2

Figure 4-16 shows the POF of the 20 runs conducted for the looped design of example 2. Clearly, all fronts are very similar and consistently develop from the zero cost design until the corresponding least-cost design. Some of designs that appear to be dominated is because of the nature of this multi-objective problem. In other words, the problem is three-objective optimization problem though presented herein in two dimensions.

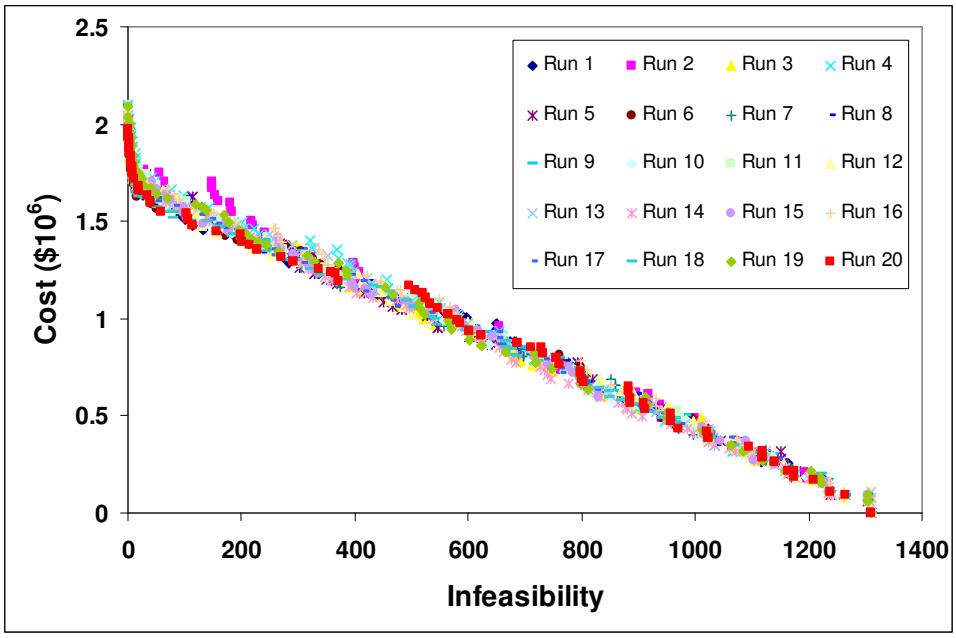

Figure 4-16: Individual POFs of the 20 GA runs for looped Example 2

4.5 CONCLUSIONS

A new penalty-free multi-objective evolutionary approach to coupled topology and pipes size optimization of water distribution systems has been presented. The proposed approach provides strong evidence to support the incorporation of infeasible solutions in the design optimization of water distribution networks. Arbitrarily penalizing or removing hydraulically or topologically infeasible solutions can lead to the loss of some essential features of the optimal solution from the gene

pool. By contrast, the penalty-free fully inclusive approach developed does not avoid infeasible solutions and retains the advantage of progressing towards the optimum solution from both the feasible and infeasible sections of the solution space. It is believed the performance of the algorithm is enhanced in this way by virtue of the presence of both feasible and infeasible non-dominated near-optimal solutions in successive generations. For problems involving layout optimization, a procedure for handling topologically infeasible solutions in a rational manner is a precondition if the entire solution space is to be exploited in full. This issue was successfully addressed in this chapter.

A new procedure for topology confirmation to tackle the handling of isolated parts from the network supplying source(s) has been developed. This development enabled the potential of quantifying infeasible topologies in an unbiased way. Each infeasible layout is assigned an amount of layout infeasibility proportional to the number of isolated nodes contained in the layout and the type of the topology to be optimized, branched or looped. A new definition of design infeasibility composed of two terms, which are layout infeasibility and hydraulic infeasibility, has been introduced. This definition is able to recognize whether a design is both topologically and hydraulically feasible or only hydraulically infeasible or hydraulically feasible but topologically infeasible or both topologically and hydraulically infeasible.

The benefits of solving the layout and pipe size optimization problems simultaneously rather than sequentially have been demonstrated. The results show that the present approach is efficient and yields good results consistently. Three benchmark problems in the literature were considered and in each case a new best solution was found. In all, six new feasible solutions that are cheaper than the best in the literature were found. The results also suggest further improvements may be achieved by combining and solving the branched and looped design optimization problems together. A weakness of the proposed formulation is that it yields only the least cost feasible solution. A possible remedy might include the introduction of criteria to differentiate between different feasible solutions in addition to the

construction cost. It is recognised also that the infeasibility measure adopted is dimensionally inconsistent. Further improvements are thus indicated.

CHAPTER FIVE

A NOVEL PENALTY-FREE MULTI-OBJECTIVE EVOLUTIONARY OPTIMIZATION APPROACH TO GLOBAL AND LOCAL MAXIMUM ENTROPY MINIMUM COST DESIGNS OF WATER DISTRIBUTION SYSTEMS

5.1 INTRODUCTION

The new methodology of coupled topology and pipe size optimization of WDS has been presented in the previous chapter. A penalty-free multi-objective evolutionary approach has been developed to handle this complex optimization problem. The penalty-free strategy enabled entirely exploiting the solution space composed of feasible and infeasible solutions. This exploitation has the advantage of proceeding towards the optimal solution from both the feasibility and infeasibility regions of the solution space. To account for both topologic and hydraulic infeasibility for each solution, a new definition of solution infeasibility has been introduced. The proposed methodology was applied to solve three benchmark problems in literature. In each case, the proposed approach outperformed all previous methods by efficiently and consistently yielding better results.

The only weakness of the proposed approach is that it yields a single least cost feasible solution. This is due to no incorporation of any criteria able to distinguish between feasible solution has been considered in the proposed formulation. Another important justification of adding such a criterion is that the least cost feasible solution

is marginally able to satisfy hydraulic requirements. This indicates that any failure in a system component can significantly affect the hydraulic performance of such solutions. It is anticipated that the incorporation of any criterion to distinguish between feasible solutions will retain a minimum amount of spare capacity at an extra amount of construction cost.

From the reliability viewpoint, conventional optimum designs of WDS, i.e. obtained from minimizing cost only, are able to supply consumers with sufficient amounts of water at the required pressures based on the assumption that all system components are in service. This has the restriction that such a design is conditioned on the uninterrupted availability of all the components making up the whole system. However, real systems are very likely to be subject to component failures and deterioration with time. For example, pipe breakage could happen due to suddenly increased pressures or pipe diameters could become smaller because of accumulated sediments on the internal walls of pipes. These circumstances significantly affect WDS capacity especially those having the cheapest set of pipe diameters. As a result, WDSs should be designed to have some spare capacity above the minimum that can be used to partially or fully compensate for any reduction in capacity during failure conditions.

The absence of an agreed definition of reliability for WDSs along with the computational complexity associated with its accurate evaluation (Wagner *et al.* 1988) led researchers to suggest various alternative reliability measures that are easy to evaluate within an optimization framework. These measures include statistical entropy (Tanyimboh and Templeman 1993), resilience index (Todini 2000), network resilience (Prasad and Park 2004), modified resilience index (Jayaram and Srinivasan 2008) and surplus power factor (Vaabel *et al.* 2006).

Among these measures, entropy has been shown to provide more accurate assessment of reliability than other measures (Reca *et al.* 2008, Raad *et al.* 2010, Banos *et al.* 2011, Tanyimboh *et al.* 2011, Wu *et al.* 2011, Saleh *et al.* 2012,

Czajkowska and Tanyimboh 2013). The evidence showed that, on average, as entropy increases reliability increases. Setiadi et al (2005) found that the overall correlation between hydraulic reliability and entropy is positive. Furthermore, Tanyimboh and Sheahan (2002) demonstrated that two different layouts having the same ME value tend to have similar hydraulic and mechanical properties such as hydraulic reliability. It may be noted also that, in comparison to the other alternative reliability measures, entropy is very easy and quick to calculate (Tanyimboh and Templeman 2000).

The introduction of statistical entropy as a surrogate measure of reliability of WDSs has shown that Maximum Entropy (ME) designs have built-in spare capacities above the minimum prescribed. The fact that entropy is highly dependent on the pipe flow directions makes it possible to achieve alternative designs delivering ME flows and having different levels of compromise between cost and reliability. Tanyimboh and Templeman (1993a,b) suggested three reasons for designing WDSs to deliver ME flows: they are more reliable; they are relatively inexpensive in comparison to traditional minimum-cost designs; and they are not computationally hard to achieve. The provision of feasible designs at local levels of ME is highly desirable objective for WDS to be optimized on a budget while maintaining a minimum level of reliability. If high levels of reliability are desired, feasible designs near global optimum can provide highly reliable solutions with different levels of ME at or near the GME. However, the very large number of feasible sets of flow directions made the early studies focus on maximizing entropy only locally by limiting the search space to predefined sets of flow directions.

The aim of the proposed approach is to combine the two objectives of achieving local and global levels of ME into one optimization process. This goal was achieved by combining both local and global components of maximizing entropy with hydraulic feasibility component into a unified minimization objective. Additionally, the purpose of combining objectives is to reduce objectives in this many-objective problem. This way, providing a set of solutions with small amounts of infeasibility

reflects the provision of hydraulically feasible high entropy solutions belonging to different ME groups.

The GMEMC optimization (global maximum entropy minimum cost) is a many-objective problem that associates a number of optimization issues with the application of Multi-Objective Evolutionary Algorithms (MOEAs). As stated in Saxena *et al.* (2013), three difficulties can be experienced: 1) High computational cost; 2) Poor scalability of most available MOEAs (e.g. most designs will have the same rank as number of objectives increases); and 3) Difficulty in visualizing a POF for problems with more than 4 objectives (e.g. difficulty in identifying the non-dominated solutions when visualizing a POF with objectives more than 4). The available approaches for handling many-objective problems can be classified into two categories: preference-ordering and objective reduction approaches. In the first group, all objectives are considered essential while a preference ordering is induced over the non-dominated solutions. This strategy makes such approaches lack diversity in POF along with increasing computational cost exponentially with number of objectives. The second group classifies objectives into redundant and essential. A redundant objective is the one whose elimination does not affect the identification of POF. Evidently, such an objective can not be guaranteed to be available in a many-objective problem.

In this chapter, motivated by the computational simplicity of the informational entropy function, a new penalty-free multi-directional search formulation that strikes a balance between the twin goals of maximizing the entropy both locally within any feasible set of flow directions and globally across all feasible sets of flow directions is presented. Unlike previous entropy-based approaches such as Tanyimboh and Sheahan (2002), the method does not specify the flow directions or candidate topologies in advance of the optimization. The penalty-free formulation proposed aims to exploit fully the entire solution space that consists of both feasible and infeasible solutions based on topology and/or nodal pressures.

Furthermore, a concept of objective reduction has been suggested to handle this many-objective problem. The solution method of the proposed approach is based on computationally converting this Many-Objective (MO) optimization problem into two-objective problem such that it always yields a set of alternative feasible solutions instead of a single feasible one. The four-objective problem was computationally reduced to two-objective problem by combining three objectives into a single one. This reduction was based on aggregating the objectives of minimizing hydraulic infeasibility and both local and global maximizations of entropy into a single objective named total infeasibility. To demonstrate the advantages of aggregating objectives over separating objectives in such an MO optimization problem, two formulations were thoroughly investigated. The performance and efficiency of the proposed approach are demonstrated by designing a benchmark network and a real network from literature. For both networks, the results obtained achieve an appropriate balance between feasible and infeasible solutions.

5.2 OPTIMIZATION MODEL

In this chapter, a multi-directional search strategy that aims at maximizing the entropy for all the different sets of flow directions was formulated. The approach is a multi-objective optimization that simultaneously minimizes both the cost and the design constraint violations while maximizing the entropy both locally within the feasible sets of flow directions and globally across all feasible sets of flow directions. As such, the proposed approach is a many-objective optimization problem that is composed of four objectives. Due to the encountered difficulties in solving MO problems as described in Section 1 of this chapter, two solution methods to deal with this MO optimization problem were formulated herein. The first one is based on reducing the complexity of the problem by aggregating the objective of minimizing hydraulic infeasibility with the objectives of local and global maximization of

entropy. The second formulation conventionally handled the problem by maintaining the four separate objectives.

5.2.1 Formulation 1: Aggregation of Objects

The purpose of this formulation is to develop a multi-directional search strategy efficiently able to achieve a Pareto optimal front (POF) with a better compromise between the cost and entropy while maintaining the objective of globally maximizing entropy. The fact that, due to the high dependence of entropy on pipe flow directions, there is a large number of *ME* designs for any WDS was the motivation behind the development of the new strategy. Thus, the concept of the multi-directional search strategy maximizes the entropy for all the different sets of pipe flow directions in the design space of the pipe size optimization problem. For each candidate solution or design in the GA's population, the actual entropy *S* value (based on the actual pipe flow rates) and corresponding maximum entropy *ME* value (i.e. the largest possible value with the same flow directions) are determined. The path starting from each *S* value towards the corresponding *ME* represents the *local* search direction for each generated design. Minimizing the distances of the *local* search between the pairs of (*S*, *ME*) is the key element that contributes to widening the range of *ME* designs achieved. To maintain a *global* search during the whole optimization process, the *local* search directions are linked to the *global* maximum entropy (GME) value. The GME is updated iteratively during the search, ultimately to reach the global maximum entropy minimum cost (GMEMC) design.

The overall problem formulation can be described by defining the four objectives driving the multi-directional search strategy proposed in the present approach. The first objective is the minimization of the construction cost, i.e.

$$minimize\ f_1 = \text{cost} = \sum_{ij \in N_p} f\left(L_{ij}, D_{ij}\right) \tag{5.1}$$

The WDS should satisfy both the conservation of mass and energy requirements. These constraints are met externally herein by employing the hydraulic solver EPANET 2 (Rossman, 2000) used in the optimization process. The rest of the objectives were combined in one minimization objective named infeasibility as follows:

$$\textit{minimize } f_2 = \text{infeasibility} = TD + (ME\text{-}S) + (GME\text{-}ME) \tag{5.2}$$

where

$$\text{TD} = \sum_{i \in N} \max(0, H_i^{req} - H_i) \tag{5.3}$$

where TD is the total deficit in the required head at the demand nodes. H_i and H_i^{req} are the available pressure and the required pressure at node i respectively while S is the actual network entropy calculated using Eq. 2.42. The required pressure is the pressure above which the nodal demand is satisfied in full. If the available pressure H_i is larger than or equal to the corresponding desired pressure H_i^{req} at all of the demand nodes, the design is considered hydraulically feasible and TD takes a value of zero. The second term represents the local entropy search component that has a value of zero when both the actual entropy S and the corresponding maximum entropy ME values are equal. The third term represents the global entropy search component that links each local ME to the current global maximum entropy GME value.

Clearly, Eq. 5.2 takes a value of zero if and only if all of the three search components are equal to zero. In other words, the current formulation has converted the MO problem into a two-objective problem in which there is only one single feasible solution having zero infeasibility. This dramatic conversion to the number of objectives involved in the search process has provided four main advantages to solve this MO problem.

First, the objective space has been reduced to two dimensions: cost and infeasibility. Therefore, the difficulty in visualizing the four dimension objective space has been overcome and so it will be easier to recognize designs belonging to the non-dominated solutions. Secondly, the problem complexity has been reduced to be solved in two dimensions instead of four and so improving the search efficiency of the proposed approach. Thirdly, the existence of one single feasible solution ensures maintaining a global search towards maximizing entropy. This is due to that the GMEMC design is the only solution that is hydraulically feasible and has local and global entropy search components of zero. Fourthly, the formulated two-objective problem still maintains the goal of multi-objective optimization problems by which a set of hydraulically feasible solutions are achieved. Clear inspection of the contribution of the second and third terms in Eq. 5.2 can explain this important feature.

For a typical node with, say, two incident pipes downstream, $S_i \leq \ln(3) \approx 1.1$, where S_i = nodal entropy value (Eq. 2.44). With reference to Eq. 2.42, given that $P_i = T_i / T \leq 1.0$, where P_i is the fraction of the total flow through the network that reaches node *i,* it can be expected that the network entropy value *S* in Eq. 2.42 will be relatively small for the typical WDS with one or several supply nodes (Eq. 2.43). Thus, it can be expected that the relative entropy measures of ME – S and GME – ME will be small. A well-known property of the Shannon (1948) entropy measure is that its maximum value of $\ln(n)$ corresponds to the uniform probability distribution $p(x_i) = 1/n, \forall i,$ where n = total number of possible outcomes. Accordingly, two (assumed) downstream incident pipes and the nodal demand lead to $S_i \leq \ln(3)$ in Eq. 2.44. In other words, the contributions of the second and third terms in Eq. 5.2 can be relatively insignificant if the amount of hydraulic infeasibility is large. This indicates that any solution having insignificant amount of infeasibility is most likely to be hydraulically feasible. For a well distributed POF, there will be a set of infeasible solutions located near the feasibility boundary. Herein, these solutions represent

hydraulically feasible solutions having an amount of infeasibility resulting from the *local* and *global* components of entropy maximization.

For hydraulically infeasible solutions, the infeasibility objective focuses on satisfying the hydraulic requirements because the contribution of the second and third terms in Eq. 5.2 is insignificant in this region. By contrast, this contribution becomes significant if a design is hydraulically feasible. Therefore, once a hydraulically infeasible design becomes hydraulically feasible by evolution through crossover and/or mutation, the optimization process focuses on reducing the local and global entropy search components of the design. This is the mechanism by which the multi-directional search strategy carries out both the local and global optimization simultaneously.

Finally, Eq. 5.2 shows that the present formulation of entropy maximization problem of WDS enables simultaneous search for local and global maximization of entropy through the introduced definition of infeasibility. Minimizing the infeasibility to zero or near zero reflects reaching global or near global ME, while minimizing the infeasibility to some amount reflects reaching a local or near local ME. Previously, network entropy was explicitly handled as a separated maximization objective that had the consequence of making the search process focus on global maximization of entropy while paying less attention to local maximization of entropy (Saleh and Tanyimboh, 2011). Further, the global search of maximizing entropy was enriched with another separated objective of maximizing the global component of entropy maximization (Saleh and Tanyimboh, 2012).

5.2.2 Formulation 2: Separation of Objectives

To demonstrate the advantages of aggregating objectives over separating objectives in this MO optimization problem, the MO problem is conventionally formulated to search explicitly into four dimensions as follows:

$$minimize\ f_1 = \text{cost} = \sum_{ij \in N_p} f\left(L_{ij}, D_{ij}\right) \tag{5.4}$$

$$minimize\ f_2 = \text{hydraulic infeasibility} = TD = \sum_{i \in N} \max(0, H_i^{req} - H_i) \tag{5.5}$$

$$minimize\ f_3 = \text{local entropy component} = (ME\text{-}S) \tag{5.6}$$

$$minimize\ f_4 = \text{global entropy component} = (GME\text{-}ME) \tag{5.7}$$

Eq. 5.6 is the objective of maximizing entropy (S) locally with respect to ME to which S belongs. Minimizing the term (ME-S) to or near zero indicates that the design entropy has reached its maximum or near maximum entropy value. Eq. 5.7 accounts for global maximization of ME with respect to the GME among generated designs. Accordingly, minimizing the term (GME-ME) to or near zero reflects that the ME value has reached the global or near global value with respect to the generated search space of ME values.

5.3 COMPUTATIONAL SOLUTION

The fast robust elitist GA NSGA II (Deb, 2002) was used to solve the MO optimization problem for the two formulations as follows:

$$\text{Formulation 1: Minimize } \mathbf{f} = (f_1, f_2)^T \tag{5.8}$$

$$\text{Formulation 2: Minimize } \mathbf{f} = (f_1, f_2, f_3, f_4)^T \tag{5.9}$$

in which the decision variables are the pipe diameters D_{ij} to be selected within the domain of the available discrete pipe sizes. In comparison with objective separation, it is anticipated that coupling the concept of objectives aggregation with NSGA II herein could add two underlying values to the overall efficiency and performance of objective aggregation formulation. First, the problem computational complexity has been significantly reduced. For example, sorting solutions for non-domination and

diversity preservation by NSGA II is carried out by comparing solutions with respect to two objectives (cost and infeasibility) instead of four (cost, TD, S, ME). Secondly, the operator of crowding distance is expected to enhance the performance of the multi-directional search process by maintaining good distribution of the search components of local and global entropy. For example, maintaining a good distribution of solutions near the hydraulic feasibility boundary could reflect well distributed hydraulically feasible solutions to local entropy components. Preserving a good distribution of local entropy components means distributing solutions to different set of ME values, which is the objective of multi-directional search strategy.

In each generation of the GA, each solution in the population is analysed using the hydraulic analysis model EPANET 2. The resulting pipe flow rates are used to calculate the entropy (Eq. 2.42). For this purpose, a prototype model coded in C for automatic detection of flow directions has been developed. The calculation of the maximum value of the WDS entropy (ME) in Eq. 2.42 generally requires numerical nonlinear optimization. However, much simpler path entropy methods that are quick, non-iterative and do not involve numerical optimization directly have been developed (Yassin-Kassab *et al.* 1999, Ang and Jowitt 2005, etc.). Two models were coded in C and integrated with NSGA II. The first one uses the simplified path entropy method (SPEM) that Ang and Jowitt (2005) developed to calculate ME for single-source networks. The second model employs the α-method developed by Yassin-Kassab *et al* (1999) to calculate ME for multiple source networks. The non-linear equations of αs were solved numerically by coding Bisection Method in C. The overall description of the approach is shown in Figure 6.1.

It is worth mentioning that calculating the number of paths from source node i to demand node j (NP_{ij}) for all sets of sources was carried out by first dividing the network into a number of sub-networks equal to NS. Then, applying the algorithms of *Global Node Numbering*, *Source Reachability*, *Demand Node Reachability*, *Local node Numbering* and *Node Weighting*, all of which developed by Yassin-Kassab *et al* (1999), to each sub-network one at a time to determine the number of paths supplied

from each source to each demand node.

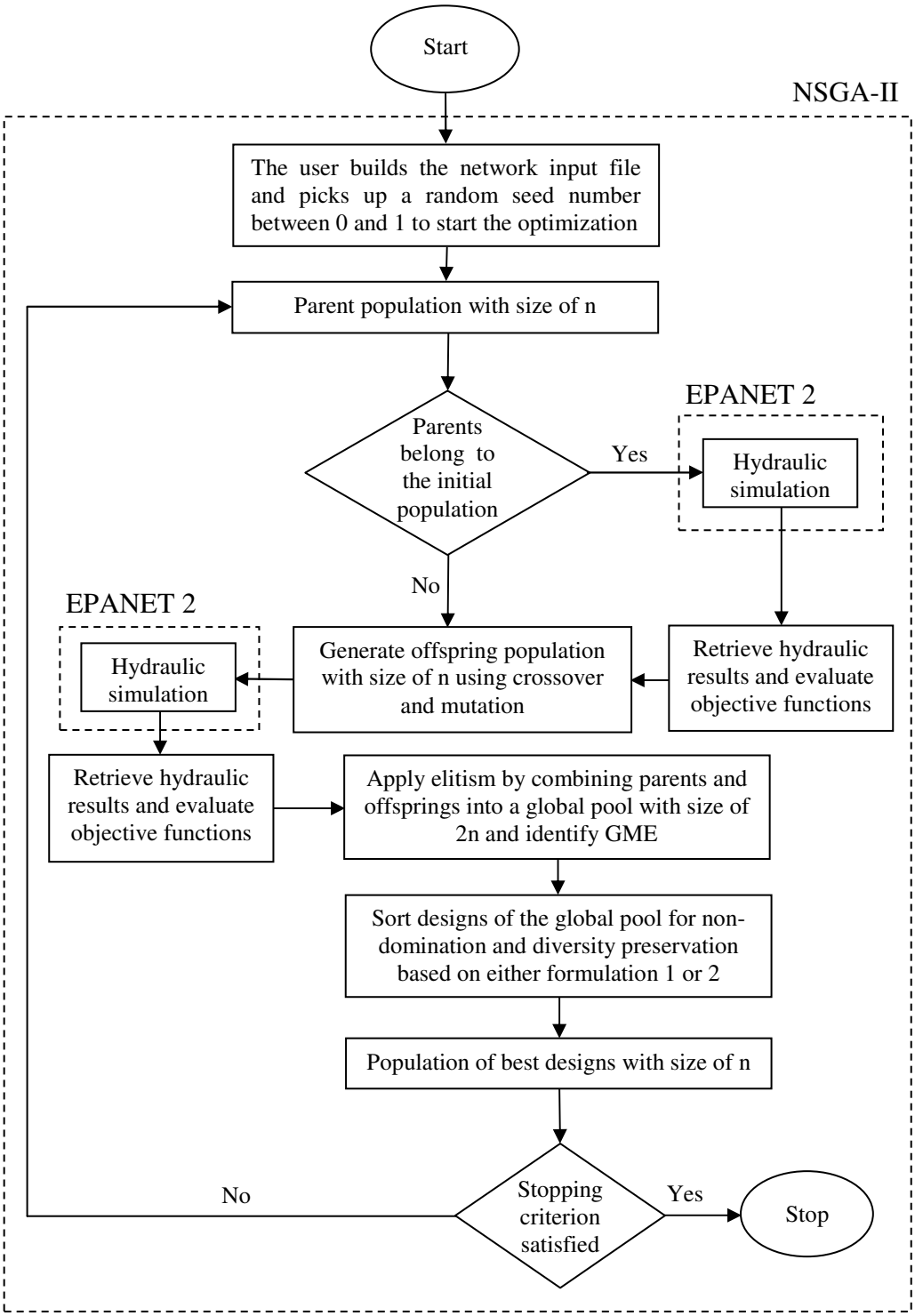

Figure 5-1: Schematic of the proposed Global and Local MEMC designs of WDS

The formulated multi-directional search strategy approach employs the penalty-free search method in which the cost of infeasible designs is not artificially increased by incorporating penalty terms into the cost objective function. In terms of practicality, Siew and Tanyimboh (2012) highlighted three advantages of penalty-free methods against penalty-based ones. The employment of penalty-free methods eliminates the necessity of designing penalty functions, adding parameters of search boundary, and special procedure to deal with problem constraints. Thus, the implementation of penalty-free methods is straightforward and not on an ad hoc basis.

From the viewpoint of efficiency, it was found that the application of penalty-free methods does not come at the expense of requiring large number of design evaluations to reach optimal or near optimal solution (Siew and Tanyimboh, 2012). The concept behind the development of penalty-free methods is to maintain infeasible solutions having useful values of decision variables that could not be available within feasible solutions. For example, the most infeasible solution made up of the cheapest decision variable can be maintained throughout the whole optimization. The incorporation of such a solution into each reproduction process increases the chances of trying the cheapest decision variable in different locations within each reproduction process.

5.4 APPLICATION OF THE PENALTY-FREE MULTI-OBJECTIVE EVOLUTIONARY OPTIMIZATION APPROACH TO GLOBAL AND LOCAL MAXIMUM ENTROPY DESIGNS OF WATER DISTRIBUTION SYSTEMS

The proposed approach was applied to two benchmark optimization problems: a hypothetical single-source network and a multiple source real system. The first network has been extensively analysed by previous maximum entropy approaches and so it provides good grounds to compare the performance of the proposed approach. As a result, the first network was optimized using the two formulations of the approach, while the second network was optimized using the objectives

aggregation formulation. An Intel Core 2 Duo CPU 2.99 GHz, 3.21 GB RAM personal computer was used in this study. Since different computer specifications would have been used previously, assessing the efficiency of the present approach with design evaluations along with CPU time would provide a fair comparison of results.

With respect to the GA parameters required to optimize the two networks, a typical population size of 100 was used. The single-point crossover operator was used to generate two offsprings from two parents. To increase the chances of trying out new solutions in each generation, the crossover probability p_c was set at p_c = 1.0, i.e. in each generation, 50 crossover operations are conducted on the parent population to produce an offspring population with size of n = 100. The operator of tournament selection of size of 2 was used to select two parents to be subject for crossover. The operator of random mutation was used to identify the selected bits among the offspring population to be subject to a mutation. A fixed bit-mutation (absolute) probability of $p_m \approx 1/n_g$ where p_m = mutation rate and n_g = chromosome length as determined by the number of genes used.

To evaluate the consistency of GA convergence, 20 random GA runs were carried out for each network example. To ensure reaching a stable convergence for each run, the GA was allowed to proceed until reaching a maximum number of function evaluations of 1,000,000 using a maximum number of generations of 10,000. The convergence point was identified at the point beyond which no improvement to the cost of the highest entropy feasible solution takes place. It is worth mentioning that, for each of the two formulations of the proposed approach, 20 random runs of the GA were conducted to design network example 1.

5.4.1 Example 1

Example 1 is a benchmark hypothetical grid network in the literature (Figure 5.2). This network was used previously in various studies concerned with entropy

(Awumah and Bhatt 1990, Tanyimboh and Sheahan 2002, Setiadi et al. 2005, Tanyimboh and Setiadi 2008, Saleh and Tanyimboh 2011). The network has a single source and is made up of 12 nodes and 17 pipes. The source has an inflow and total head of 445 l/s and 100 m respectively. All the demand nodes are located at an elevation of zero and all of the demands must be supplied at a minimum total head of 30 m. All of the pipes have a length of 1000 m and a Hazen-Williams roughness coefficient of 130. There are 12 commercially available alternative pipe diameters for each of the 17 pipes making up the whole network as shown in Figure 5.2. The set of diameters, in mm, are 100, 125, 150, 200, 250, 300, 350, 400, 450, 500, 550 and 600. The cost of pipe diameters in GBP per metre for this specific network is equal to $800D^{1.5}$.

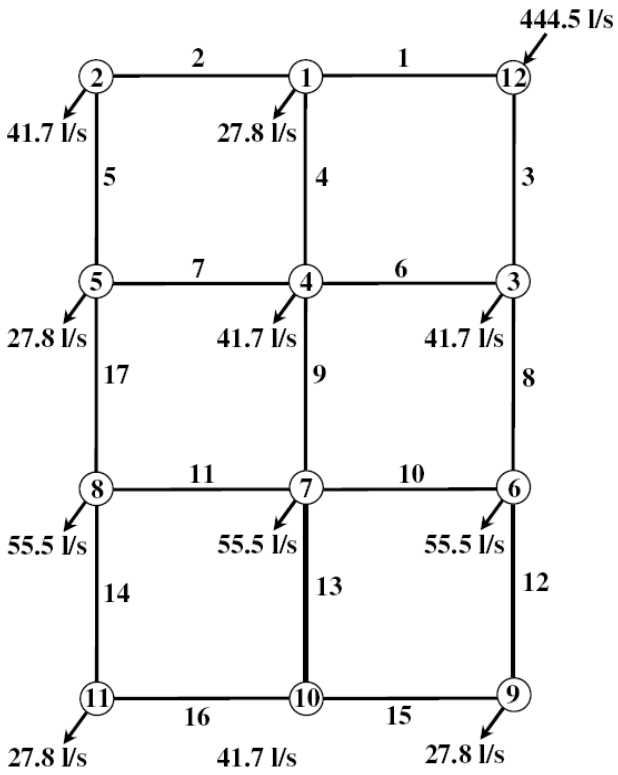

Figure 5-2: Network configuration of example 1 (with node demands in l/s)

A binary string having a length of 4 bits was used to represent all of the decision variables. This means that each decision variable was represented with 4 genes in the

genotype space. The size of the solution space is therefore $12^{17} = 2.22\times10^{18}$. To decode a binary string into the allocated pipe diameter, an index is assigned to each binary string. Since a 4-bit string produces 16 binary configurations, with 12 possible options for each pipe, there are four codes (out of 16) that are redundant. To make genetic operators avoid generating illegal solutions, the redundant codes were arbitrarily allocated to the largest pipe diameter (Appendix D). Each solution to the problem was to be created by selecting a value for each decision variable of which there are 17, each solution in the genotype space was represented with a chromosome of 68 genes in length. Accordingly, a mutation rate of 1.5% was used. The binary representation and cost of pipe diameters in GBP per metre length were taken as $£800D^{1.5}$ where D is the pipe diameter in metres (Appendix D).

Tables 5.1 and 5.2 show the convergence and consistency statistics of the two formulations based on 20 GA runs each. For all optimization aspects considered, it is evident that the concept of aggregating objectives outperformed the idea of handling objectives as being separated. First, for local and global maximization of entropy, formulation 1 achieved far cheaper solutions than those obtained in formulation 2. This can be noticed from the results of minimizing the cost of GMEMC and MMEMC designs in each optimization process. This achievement is attributed to the simplicity of recognizing minimizing cost solutions by considering two objectives of cost and infeasibility minimization only. Furthermore, aggregating objectives appear not to affect the global maximization of entropy. For example, both formulations achieved identical entropy values of the GMEMC design.

Most importantly, the principle of aggregating objectives has improved the number of feasible solutions in the POF in comparison with those obtained based on separating objectives. On average, this improvement accounted for about 250%. Bearing in mind that the formulated approach is penalty-free, i.e. infeasible solutions can effectively compete with feasible ones because of being cheaper, the inclusion of such large number of feasible solutions is remarkably a big achievement. Finally, the effect of reducing number of objectives using objectives aggregation is evident

(Tables 5.1 and 5.2). The formulation of aggregating objectives has significantly improved the convergence efficiency in terms of both function evaluations and CPU time. In contrast, the concept of separating objectives even showed no convergence at all in some of the conducted GA runs.

Table 5-1: Convergence and consistency statistics of aggregated objectives approach based on 20 GA runs

Measure		Minimum	Mean	Median	Maximum	SD
GMEMC	entropy	3.546994	3.572314	3.561168	3.5925	0.017663
	cost (£10^6)	2.071852	2.777158	2.80947	4.009645	0.442991
MMEMC	entropy	2.562376	2.718013	2.731925	2.905255	0.112548
	cost (£10^6)	1.174796	1.243972	1.24908	1.372123	0.042435
Number of feasible solutions		36	43.85	44	49	3.198046
FEs for convergence		174,700	508,140	435,600	999,500	283,826
CPU time for convergence (min)		12.951	37.669	32.291	74.094	21.040

Table 5-2: Convergence and consistency statistics of separated objectives approach based on 20 GA runs

Measure		Minimum	Mean	Median	Maximum	SD
GMEMC	entropy	3.54393	3.581819	3.590623	3.5925	0.016495
	cost (£10^6)	2.929917	3.60671	3.470388	4.607337	0.475678
MMEMC	entropy	2.514125	2.595017	2.602118	2.677528	0.043589
	cost (£10^6)	1.427802	1.882145	1.879564	2.640965	0.334522
Number of feasible solutions		10	17.85	17	26	3.785168
FEs for convergence		317,500	755,020	791,100	1,000,000	219,306
CPU time for convergence (min)		23.537	55.970	58.645	74.131	16.257

To make a good approximation to the true POF of this example, the resulting POFs obtained from the 20 GA runs in each formulation were combined in a global pool of size 2,000. Then, the NSGA II criteria for non-domination and diversity preservation sorting were used to produce a merged POF of size of 100. Figures 5.3 and 5.4 show the merged POF for both formulations respectively.

The improvement in the number of feasible solutions achieved by aggregating objectives is evident from the continuity and good distribution of the feasible part of

the merged POF (Figure 5.3). In particular, 55% of the merged POF solutions obtained from the objectives aggregation runs were feasible, while only 17% of the merged POF solutions obtained from merging the runs of separating objectives were feasible. Furthermore, the merged POF obtained from aggregating objectives is so consistent that all solutions are non-dominated in total deficit and cost (Figure 5.3). This is attributed to the fact that the contribution of total deficit of significantly infeasible solutions is so large that they can not be compared to that of (*ME-S*) and (*GME-ME*). In other words, the effect of entropy components in sorting solutions based on cost and infeasibility is insignificant in the infeasibile region. When this contribution is significant, solutions are most likely hydraulically feasible and so will be located at or near the feasibility boundary.

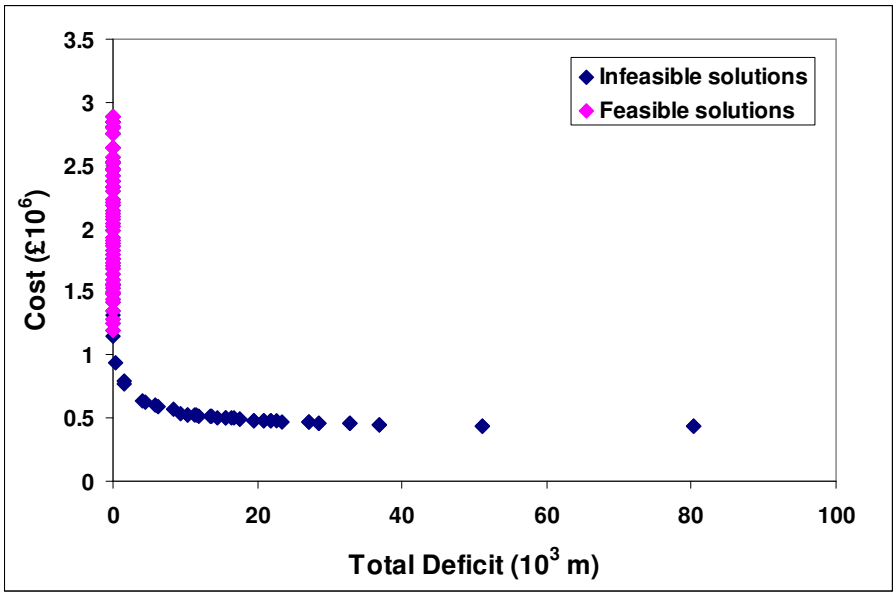

Figure 5-3: Total Deficit versus cost of merged POF of formulation 1

In contrast, most solutions obtained from separating objectives were dominated in total deficit and cost (Figure 5.4). When sorting solutions based on more than two objectives, any solution non-dominated in at least one objective other than the rest of objectives is overall considered non-dominated. So, the inclusion of such total deficit and cost dominated solutions was due to being non-dominated in the local and global components of maximizing entropy. The small number and the unequal distribution

of feasible solutions included in the merged POF are evident from Figure 5.4. The high costs of feasible solutions obtained herein are clear from shifting up the feasibility part of the merged POF in comparison with that of Figure 5.3.

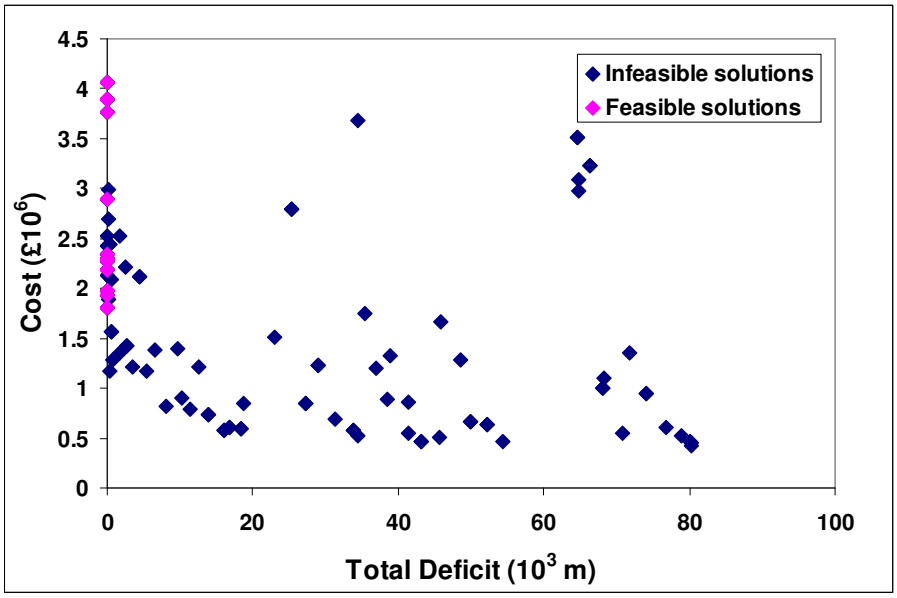

Figure 5-4: Total Deficit versus cost of merged POF of formulation 2

The consistency of the merged POF achieved from aggregating objectives is obvious from relating entropy to cost (Figure 5.5). Evidently, almost all feasible solutions are non-dominated herein. The near globality of maximizing entropy is apparent from the nearly vertical trend of the feasible part of the merged POF. The improvement in and the well distribution of the number of feasible solutions are also evident in Figure 5.5. In contrast, the merged POF obtained from separating objectives is not consistent. This can be noticed from that the vast majority of solutions obtained from separating objectives are dominated in cost and entropy (Figure 5.6). Moreover, the contribution of feasible solutions along with being not well distributed in the merged POF reflects the advantages of aggregating objectives over handling them as being separated (Figure 5.6). Additionally, it appears that the GMEMC solution has not been part of the merged POF. This is because that GMEMC solutions belonging to the GME were so expensive that they become dominated when sorted in the global pool of the 20 GA runs.

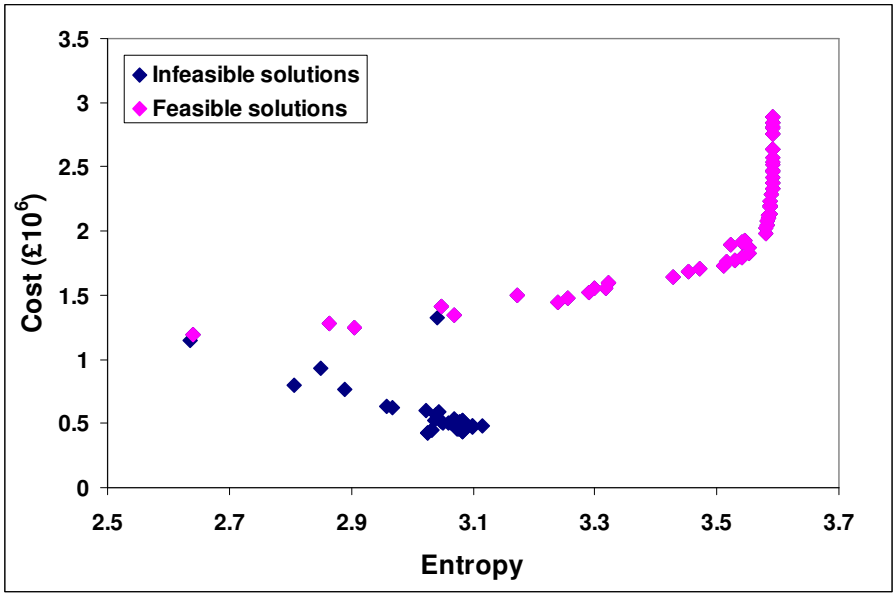

Figure 5-5: Entropy versus cost of merged POF of formulation 1

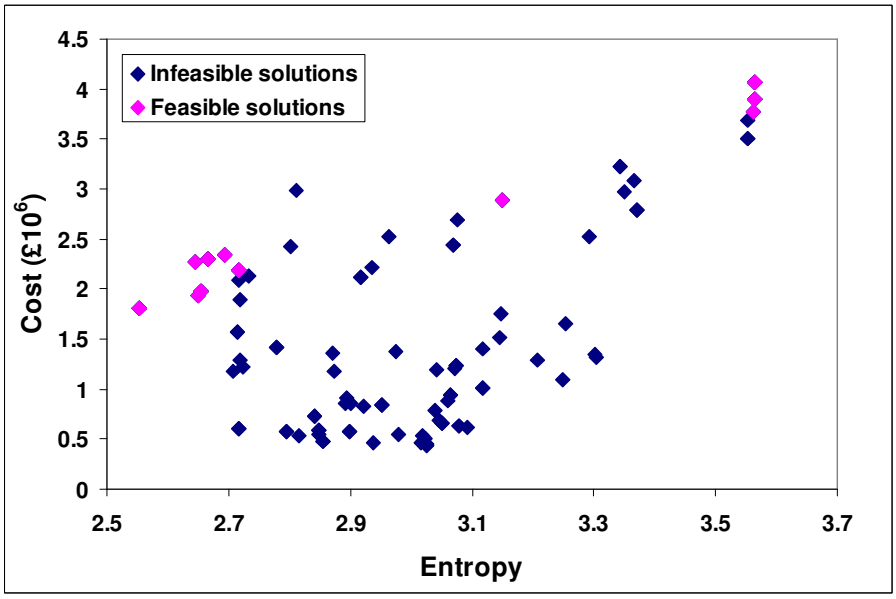

Figure 5-6: Entropy versus cost of merged POF of formulation 2

The performance of achieving a wide range of well distributed ME feasible solutions using the concept of aggregating objectives is evident from Figure 5.7. All feasible solutions were distributed across a span of entropy values ranged between 2.6415 and 3.5925. Herein, the trend of maximizing entropy appears to exploit all high entropy solutions. For example, all infeasible solutions were distributed nearly over

the first half of this span. This situation is totally different in case of separating objectives where a number of high entropy solutions were infeasible (Figure 5.8).

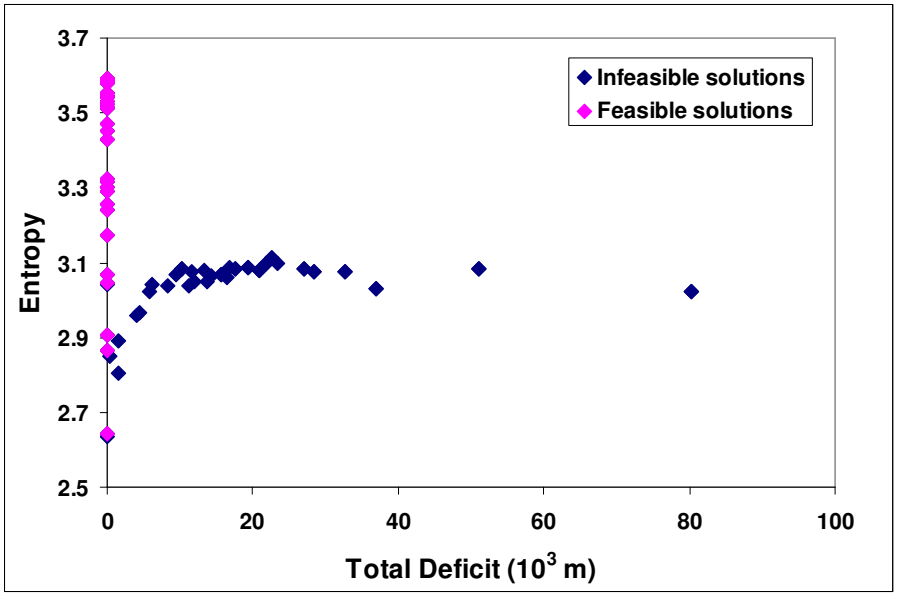

Figure 5-7: Total Deficit versus cost of merged POF of formulation 1

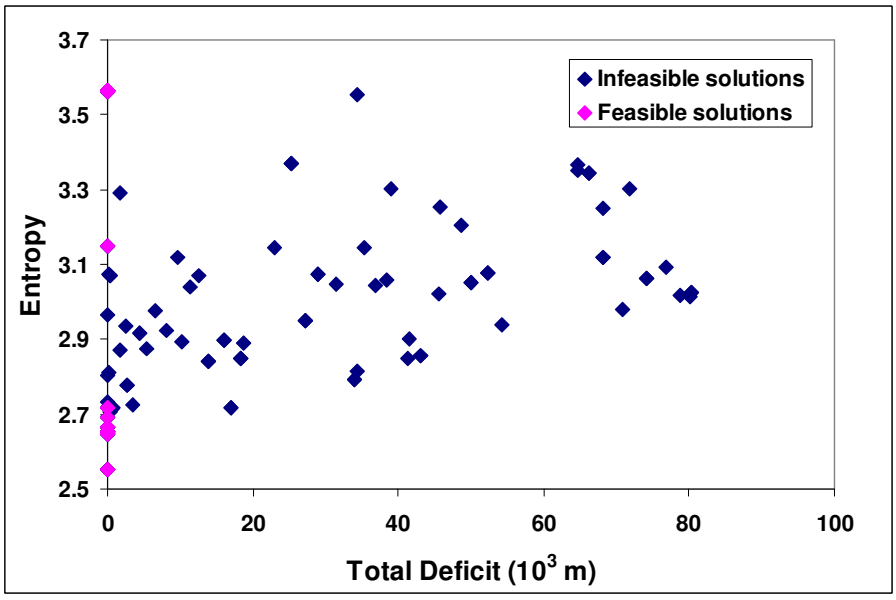

Figure 5-8: Total Deficit versus cost of merged POF of formulation 2

Obtaining high entropy but significantly infeasible solutions is not beneficial to the optimization. Since the aim of incorporating entropy maximization herein is to

obtain a wide range of high entropy feasible solutions, the concept of separating objectives appears not able to achieve this goal. The inconsistency of the merged POF and the unequal distribution of feasible solutions across almost the same range of entropy values are very clear herein. This inconsistency makes it difficult to interpret the trend of maximizing entropy in relation with minimizing total deficit.

In terms of searching into the solution space of ME groups, the concept of aggregating objectives shows the ability to reduce the search space of ME values that can be produced from a WDS (Figure 5.9). For example, all solutions making up the merged POF obtained using aggregated objectives formulation were found to belong to only 13 groups of ME. Out of 13 groups, the feasible solutions were distributed to 8 groups of ME. For each ME group, a number of solutions with different entropy values were obtained (Figure 5.9). In contrast, the merged POF obtained from separating objectives were found to contain 54 groups of ME (Figure 5.10). Out of 54 groups of ME, the feasible solutions were distributed to only 7 groups of ME. The relationship between entropy and ME obtained from separating objectives shows that this concept is not suitable for designing large networks whose ME design space is huge.

Overall, and based on the previous extensive investigation on the suitability of handling the objectives of optimizing cost, pipe size and both local and global maximization of entropy, it appears that the concept of aggregating objectives is more suitable for dealing with this complex problem than the idea of separating objectives. Therefore, from this point ahead, further analysis of the merged POF obtained from aggregating objectives is carried out.

Table 5.3 shows the feasible designs of the merged POF based on Formulation 1: aggregation of objectives. A new GMEMC design that has not been obtained previously using discrete pipe diameters was achieved, with the beneficial consequence that this helped to extend the range of feasible solutions found. An

average of 508,140 EPANET 2 hydraulic analyses was required for each GA run. This number of analyses consumed an average CPU time of 37.67 minutes.

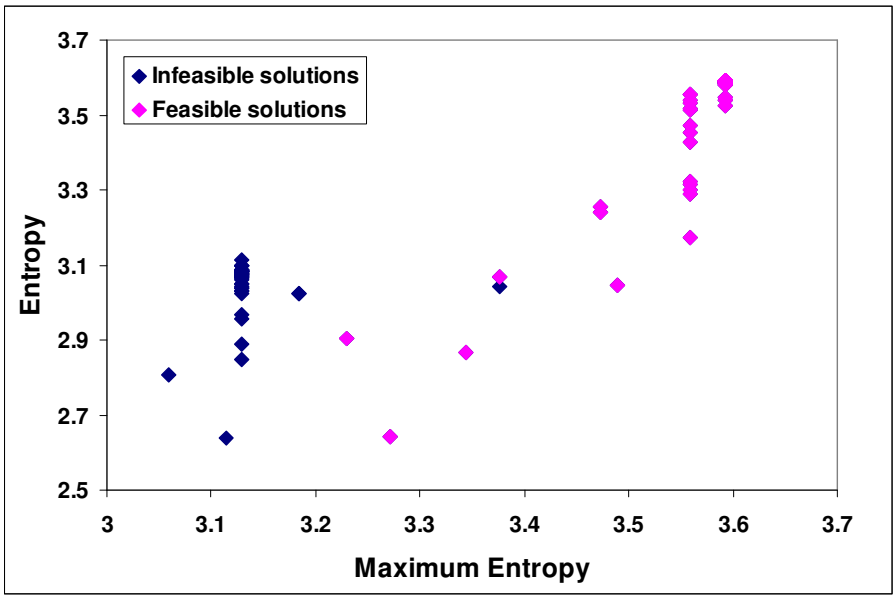

Figure 5-9: ME versus entropy of merged POF of formulation 1

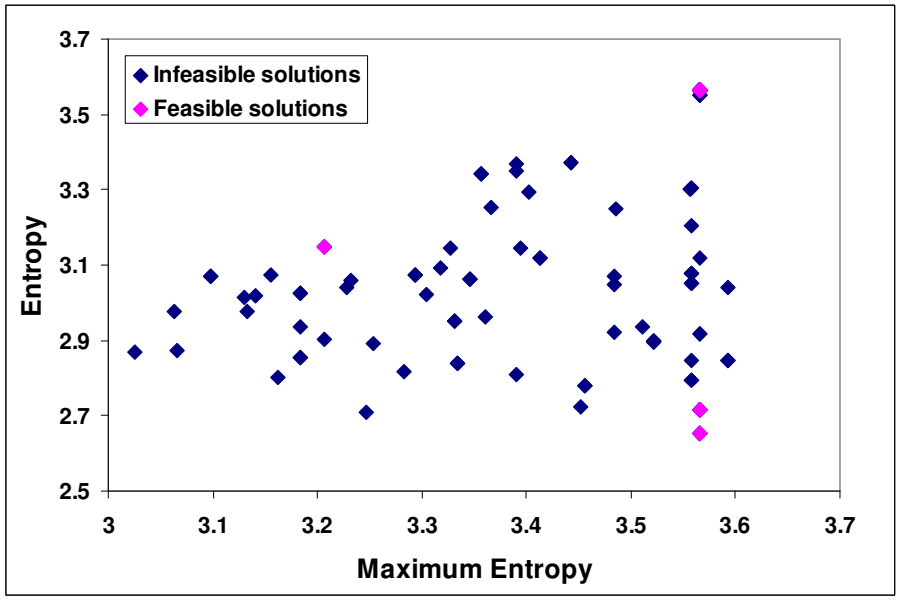

Figure 5-10: ME versus entropy of merged POF of formulation 2

Table 5-3: Achieved MEMC feasible designs for Example 1

Design	Cost (£10^6)	Critical Surplus (m)	Entropy	Design	Cost (£10^6)	Critical Surplus (m)	Entropy
1	1.687	0.384	3.4528	28	1.283	2.414	2.8648
2	1.522	0.564	3.2890	29	1.477	5.604	3.2556
3	1.553	0.114	3.3003	30	2.020	5.359	3.5806
4	1.350	0.618	3.0684	31	2.203	9.154	3.5875
5	1.413	1.414	3.0471	32	2.042	6.699	3.5823
6	1.594	1.397	3.3224	33	1.767	1.747	3.5303
7	1.558	0.859	3.3167	34	1.494	0.734	3.1729
8	2.373	14.404	3.5914	35	1.724	0.327	3.5122
9	2.187	7.818	3.5868	36	1.756	2.194	3.5151
10	1.887	1.667	3.5233	37	1.706	1.591	3.4721
11	2.291	12.354	3.5891	38	1.798	0.378	3.5410
12	2.419	15.446	3.5917	39	1.638	0.108	3.4276
13	2.330	12.648	3.5906	40	1.910	0.958	3.5410
14	2.137	3.377	3.5867	41	1.984	0.138	3.5800
15	2.095	0.282	3.5847	42	2.806	29.066	3.5925
16	2.226	6.178	3.5878	43	2.520	27.608	3.5923
17	2.458	15.879	3.5919	44	2.797	29.148	3.5924
18	1.252	3.481	2.9053	45	2.847	29.096	3.5925
19	1.924	0.926	3.5465	46	2.636	28.925	3.5924
20	2.119	0.335	3.5856	47	2.534	28.179	3.5924
21	2.378	14.544	3.5914	48	2.753	29.130	3.5924
22	2.335	12.775	3.5908	49	2.636	28.925	3.5924
23	2.076	7.531	3.5828	50	2.476	25.829	3.5920
24	1.866	1.267	3.5524	51	2.565	28.663	3.5924
25	1.829	0.241	3.5523	52	2.890	29.113	3.5925
26	1.195	2.009	2.6415	53	2.753	29.130	3.5924
27	1.443	1.191	3.2404	54	2.847	29.096	3.5925

Previously, the highest ME value obtained for this network was first found at 3.183 (Tanyimboh and Setiadi, 2008) using continuous pipe sizes. The first attempt to design this network for global maximization of entropy using discrete pipe sizes was by Saleh and Tanyimboh (2011) where the ME was increased to 3.5583 with a cost

of £3.010 millions. Recently, Saleh and Tanyimboh (2012) found that the GME belongs to a different set of flow directions having ME value of 3.5928 with a cost of £2.126 millions. However, the achieved GMEMC design was based on *continuous* pipe sizes.

The strong performance of the proposed approach for handling the twin goals of local and global maximization of entropy is evident from the achieved improvements in two aspects. First, the improvement in the global search capability of the approach is evidenced by a new GMEMC design using discrete pipe sizes. This design has not been achieved in previous studies to date aimed at globally maximizing the entropy of WDS using discrete pipe sizes. The present discrete diameter GMEMC design has an entropy value of 3.5925 while the previous discrete diameter GMEMC design had an entropy value of 3.5583. Also, the amount of surplus pressure at the critical node of the GMEMC design has been reduced here to 29.11 m from 38.78 m in Saleh and Tanyimboh (2011). The present GMEMC design is more expensive than the previous Saleh and Tanyimboh (2011) design by just 2.15%. The cheapest ME design was also improved here in terms of both cost and entropy. The cheapest ME design here has a cost and entropy value of £1.195 million and 2.6415 respectively. In contrast, the previous cheapest ME design has values of cost and entropy of £1.288 and 2.5605 respectively in Saleh and Tanyimboh (2011).

Secondly, the new formulation herein has the advantage that the majority of designs in the POF are feasible as shown in Figure 5.3. Clearly, there are a large number of feasible solutions where the POF extends along the feasibility boundary (where the total deficit is zero). The number of feasible designs was found to account for 54% of the achieved POF. This is significant when compared to previous studies in which the vast majority of designs in the POF were infeasible (Saleh and Tanyimboh, 2011). Also, it can be seen that the feasible solutions are well distributed in terms of cost (Figure 5.3) and entropy (Figures 5.5 and 5.7). The achieved feasible designs were found to range from £1,194,911 to £2,890,476 in cost and from 2.6415 to 3.5925 in entropy. It is worth highlighting that the inclusion of the GME as one of

the achieved ME groups shows that the concept of aggregating objectives did not achieve the multiple local MEs at the expense of the GME. This is due to the explicit recognition of both the local and global entropy maximization components in the formulation.

It should be additionally noted that, due to the combination of the discrete pipe sizes and the multi-objective formulation, each objective can have a range of small and large values in the solutions achieved. For example, the surplus heads at the critical nodes were found to range from 0.108 m to more than 29.113 m. Figure 5.7 shows the plot of the total deficit vs. entropy. Finally, the multi-directional search capability is evident from the different maximum entropy solution classes (or clusters) seen clearly in Figure 5.9. The feasible designs were found to belong to 8 ME groups. Five ME groups of infeasible designs can be seen also; all the infeasible ME groups except for one have only one design (Figure 5.9).

5.4.2 Example 2

The present approach was applied to a real network that represents the main WDS supplying the zone within the boundaries of the city of Ferrara-I as shown in Figure 5.11. The system is a multiple-source network that has 49 nodes, 76 pipes and 29 loops. It is supplied by two reservoirs at nodes 1 and 49. The two reservoirs supply a total demand of 367 l/s and have a total head of 30 m each. All demand nodes are located at an elevation of zero. The total length of the pipes is about 25.2 km. All pipes have a Manning roughness coefficient of 0.015. The data of pipe lengths and node demands are shown in Appendix D. The design requirements as indicated by the utility operator of this system (Creaco *et al*, 2010; Creaco *et al*, 2012) are that the minimum head at which nodal outflow occurs is 5 m, while the desired head at which nodal demands are satisfied in full is set at 28 m. All pipe diameters are part of the existing system of Ferrara-I. However, the cost of pipe diameter 450 mm was not available in the provided set and determined from the best fit of available pipe sizes.

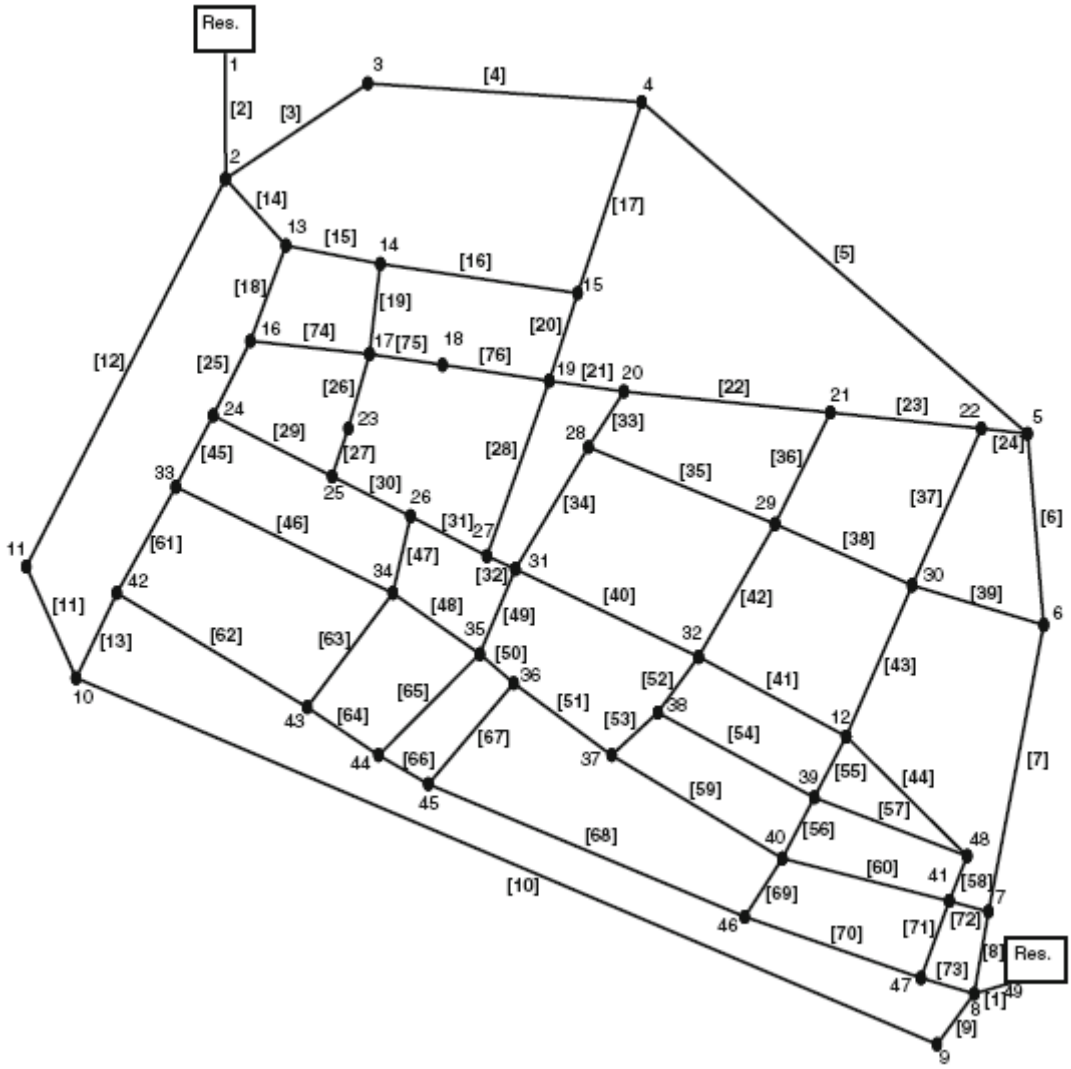

Figure 5-11: Layout of Example 2 (Pipe numbers are shown in square brackets)

A binary string of 3 bits in length was used to represent all of the decision variables. Since a 3-bit binary string produces 8 binary configurations, which is equal to the number of decision variables herein, there will be no redundant codes in the representation process. In other words, each pipe diameter has a unique binary string. The size of the solution space is therefore $8^{76} = 4.31\times10^{68}$, which is larger than the solution space of Example 1 by 1.94×10^{50} times. To complete the mapping between the binary codes and the corresponding allocated pipe diameter, an index was

assigned for each binary string (Appendix D). Each solution to the problem was to be created by selecting a value for each decision variable of which there are 76, each solution in the genotype space was represented with a chromosome of 228 genes in length. Accordingly, a mutation rate of 0.4% or 1/228 was used. The full binary representation and pipe diameters along with the corresponding cost for pipe purchase and laying as provided by the utility operator are shown in Appendix D.

Table 5.4 shows the feasible designs of the merged POF of Example 2. It is worth mentioning that the aim of applying the present approach to a real network is to demonstrate its practicality in providing a good trade-off between cost and reliability for a range of feasible designs in one integrated optimization process. Thus, the achieved GMEMC design herein is only optimal with respect to the generated search space that amounted to 20,000,000 design evaluations.

To assess the robustness of the present approach, a record of the global search towards maximizing entropy of the conducted runs is presented in Figure 5.12. The results show that the approach is robust where the overall progress of maximizing entropy appears to be consistently increasing throughout the whole optimization. It is worth highlighting that the trend of maximizing entropy could be changed to correct the search path of global maximization of entropy as shown in Figure 5.12. This situation occurs when a new higher ME than the one to which the highest entropy of previous reproduction process belongs is found. For example, if the highest entropy in the previous optimization process is found not to belong to the current GME, it is replaced with highest entropy belonging to the GME. This is the function performed by the global component of maximizing entropy.

The improvement in the amount of feasible designs contributing to the POF is evident from extending the front along the feasibility boundary as shown in Figure 5.13. The feasible designs were found to account for 27% of the achieved POF. This percentage appears to be relatively reduced with respect to the one achieved in the Example 1. The reduction could be specifically attributed to two main reasons: the

high desired pressure required at each demand node with respect to the total heads at the supplying sources; the existence of a number of infeasible designs located very close to the feasibility boundary as shown in Figure 5.14. For example, there are 5 marginally infeasible designs with a total pressure deficit less than 0.05 m.

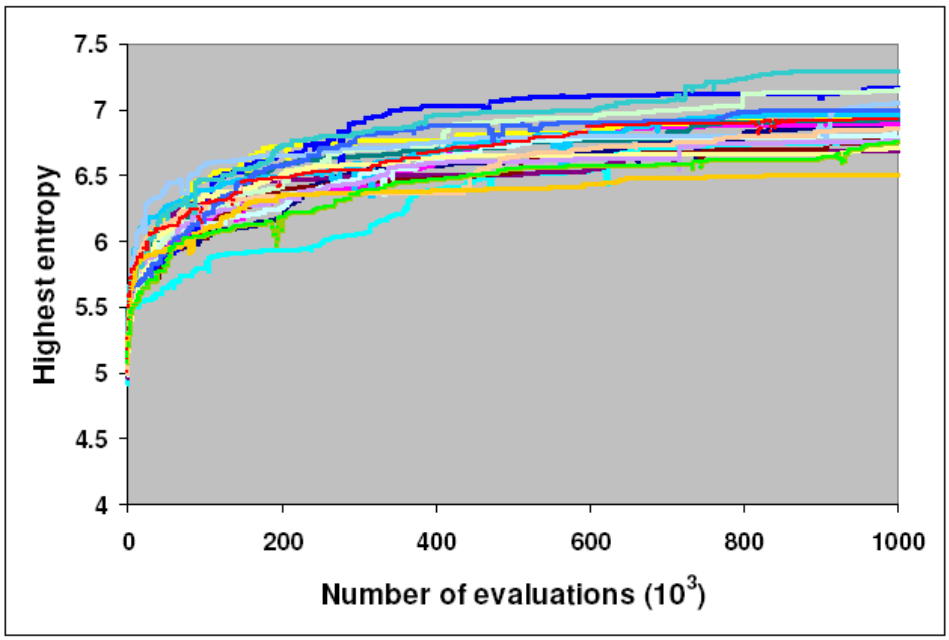

Figure 5-12: Record of GA progress for the conducted runs of Example 2

The achievement of high entropy feasible solutions is evident from locating most infeasible solutions in the region of low entropy values (Figure 5.15). Any high entropy solution with high entropy value is either feasible or marginally infeasible (Figure 5.16). This complies with the aim of the proposed approach to provide feasible solutions with high entropy values. In addition to these designs, other MEMC designs have been achieved. The good trade-off between cost and entropy is reflected by providing a range of feasible designs distributed to a span of €2.741 million in cost and 2.5021 in entropy as shown in Figure 5.17. The cheapest feasible design has cost and entropy values of €8.011 million and 4.7968 respectively, while the most expensive one has cost and entropy values of €10.285 and 7.2989 respectively.

Table 5-4: Achieved MEMC feasible designs for Example 2

Design	Cost (€10^6)	Critical Surplus (m)	Entropy	Design	Cost (€10^6)	Critical Surplus (m)	Entropy
1	10.285	0.050	7.2989	15	9.091	0.033	6.7056
2	10.263	0.047	7.2979	16	9.041	0.013	6.5965
3	10.194	0.010	7.2953	17	8.925	0.091	6.4448
4	10.123	0.075	7.2654	18	8.810	0.046	6.3697
5	9.986	0.046	7.2475	19	8.778	0.015	6.3347
6	9.919	0.009	7.2435	20	8.571	0.010	5.9393
7	9.831	0.040	7.1973	21	8.506	0.010	5.8109
8	9.654	0.019	7.1574	22	8.350	0.027	5.6531
9	9.499	0.021	7.0861	23	8.262	0.159	5.3858
10	9.418	0.037	6.9375	24	8.149	0.020	4.8264
11	9.381	0.008	6.9226	25	8.091	0.030	4.8262
12	9.284	0.004	6.8437	26	8.044	0.049	4.8046
13	9.251	0.007	6.8388	27	8.011	0.049	4.7968
14	9.196	0.024	6.7794				

Furthermore, marginally infeasible designs still offer practical solutions while saving a significant amount of cost as shown in Figure 5.16. For example, the marginally infeasible design located at a distance less than 0.01 m from feasibility boundary has a cost of €9.737 and entropy of 7.163. This design is marginally lower than the most expensive feasible design in terms of entropy but with the advantage of saving a considerable amount of cost of €547,847. Moreover, the good distribution of feasible designs to a wide range of ME values can be noticed in Figure 5.18. For example, the feasible designs were found to belong to 26 different ME groups and only two designs belonged to the same group. This is also applicable to infeasible designs belonging to another set of ME groups. The distribution of achieved designs to a variety of ME groups reflects the advantageous performance of the multi-directional search strategy.

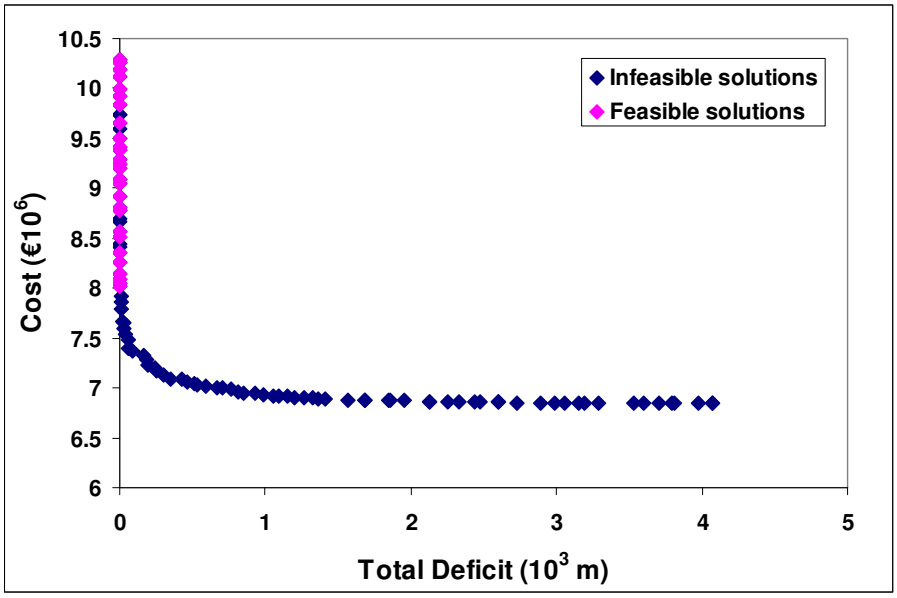

Figure 5-13: Total Deficit versus cost of merged POF of Example 2

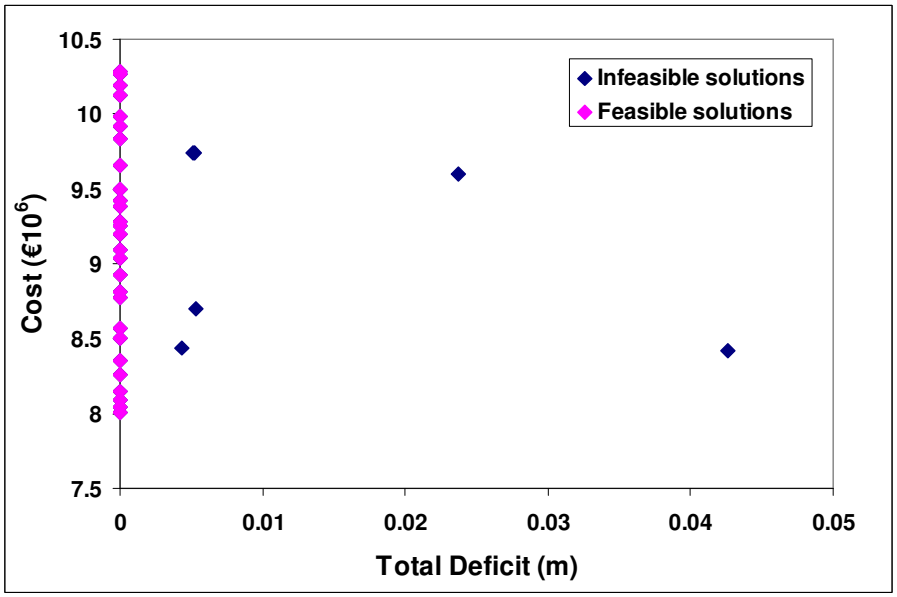

Figure 5-14: Close focus on deficit-cost of merged POF of Example 2

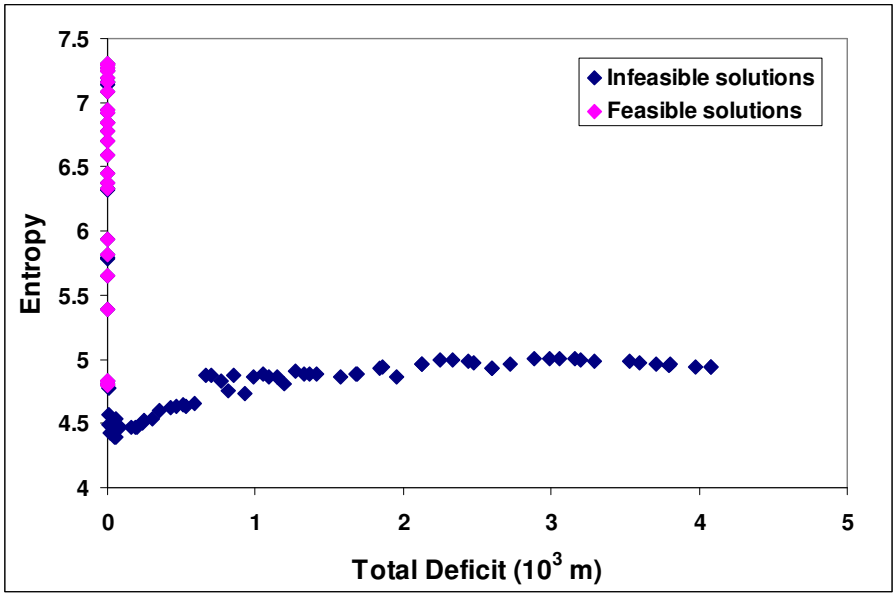

Figure 5-15: Total Deficit versus cost of merged POF of Example 2

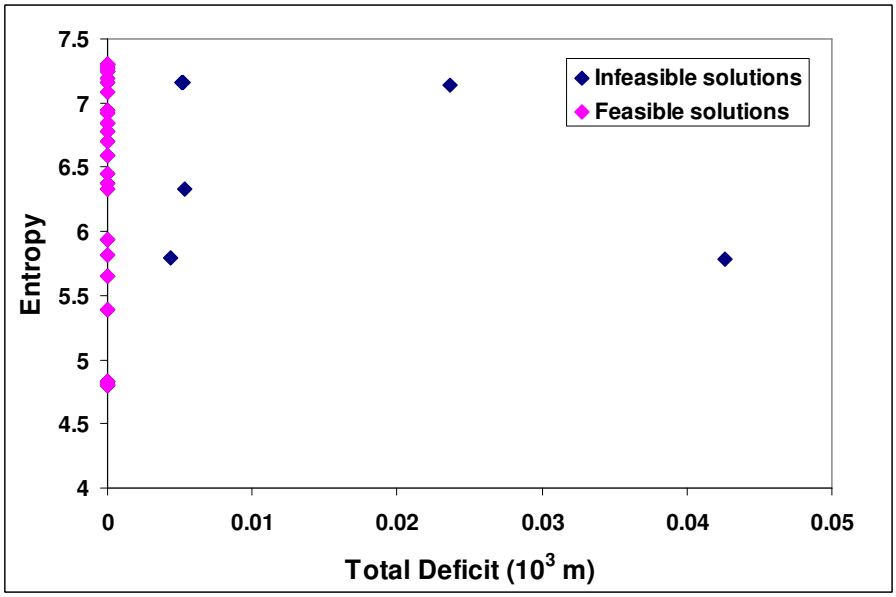

Figure 5-16: Close focus on deficit-entropy of merged POF of Example 2

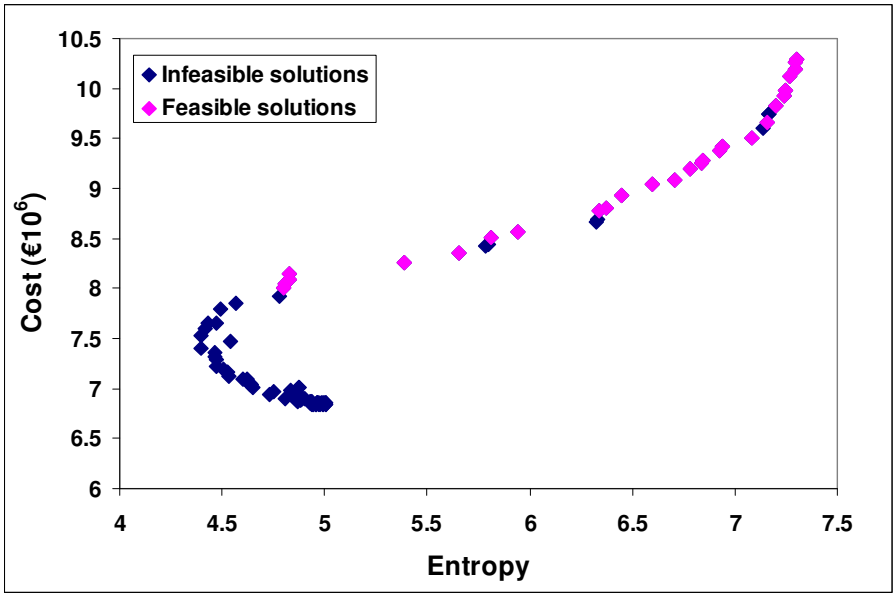

Figure 5-17: Entropy versus cost of merged POF of Example 2

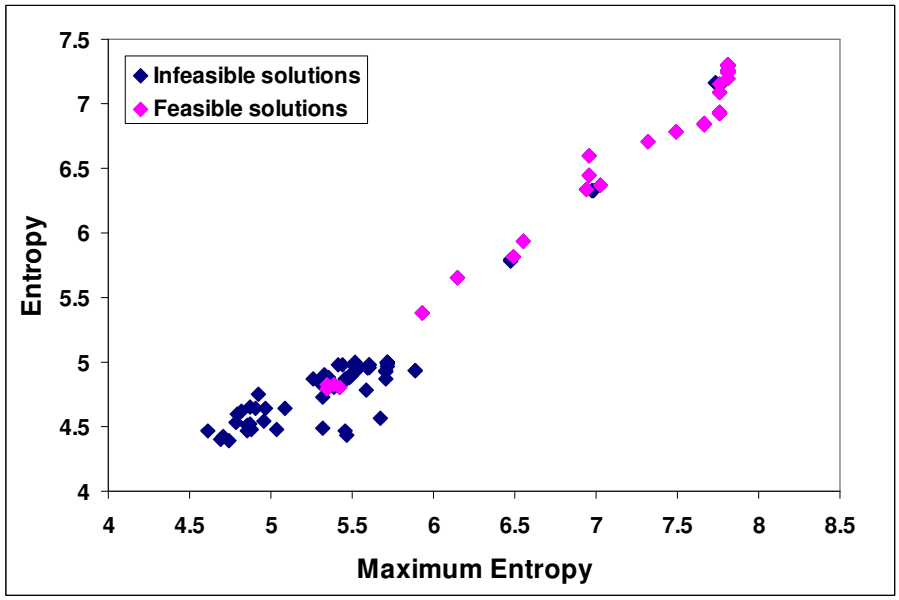

Figure 5-18: Maximum Entropy versus entropy of merged POF of Example 2

5.5 CONCLUSIONS

The results of the proposed penalty-free multi-objective evolutionary optimization approach to local and global maximum entropy minimum cost designs of WDS has been presented. Due to the nature of this many-objective optimization problem composed of four objectives, two formulations to handle this many-objective problem were proposed. The first one is based on aggregating the objectives of local and global components of maximizing entropy with minimizing total deficit to form one objective defined as infeasibility. The other one is to deal with the four objectives as they are separated. The two formulations were equally applied to design a benchmark problem in literature. The extensive investigation of the results showed that the concept of aggregating objectives is more suitable than to separate them to handle this many-objective problem in many optimization aspects: 1) Cheaper high entropy feasible designs were achieved using the aggregated objectives formulation approach; 2) Dramatic improvement in the number of feasible solutions; 3) the aggregated objectives formulation approach was computationally more efficient than the separated objectives approach; and 4) the obtained POFs were very consistent.

The proposed approach of aggregating objectives illustrates the effectiveness of maximizing the entropy values associated with different sets of flow directions while maintaining the objective of globally maximizing the entropy of the WDS and minimizing the cost. A good balance between feasible and infeasible solutions was achieved in the Pareto optimal front. A good distribution of entropy values was achieved for the feasible designs. Feasible designs belonging to different maximum entropy classes were produced. Furthermore, the proposed methodology has the advantage that it yields a range of alternative optimal solutions within the various maximum entropy classes. In other words, multiple alternative optimal solutions are generated for each competitive set of flow directions that the procedure provides. Further, the application of the proposed concept of handling many-objective

problems of WDS was successful. The approach was able to solve a real problem for global and local maximization of entropy while considering all involved objectives as essential. For further saving of cost, the achieved results encourage extending the proposed approach to include topology optimization of WDS.

CHAPTER SIX

A NOVEL APPROACH TO TOPOLOGY, PIPE SIZE AND ENTROPY-BASED OPTIMAL DESIGNS OF WATER DISTRIBUTION SYSTEMS

6.1 INTRODUCTION

The new methodology of penalty-free multi-objective evolutionary optimization of local and global MEMC designs has been presented in the previous chapter. The novelty of this approach stemmed from being the first in literature to address the complex issue of flow directions associated with calculating network entropy. To handle this MO optimization problem, two methods were extensively compared on a benchmark network: objectives aggregation and separation. The method of aggregating all involved objectives other than cost outperformed the method of dealing with all objectives as being separated. The developed methodology demonstrated performance by providing a good balance between cost and entropy for a benchmark network and a real system in literature. This work along with the study of coupled topology and pipe size optimization showed that the relationship between topology, pipe size and reliability is very strong, i.e. optimal design cost and reliability should be evaluated based on simultaneous determination of topology and pipe sizes. The success of this work along with the study of coupled topology and pipe size optimization have set a solid ground for the research to proceed towards the final phase, i.e. combining topology, pipe size and entropy-based optimization into

one integrated optimization process.

Previous optimization studies that included reliability did not optimize the topology. Awumah *et al.* (1989) developed a two-stage model for optimizing the pipe sizes and topology of a WDS. In the first stage, a topology model determines whether a link is to be included in the topology or not using a zero-one integer program. The topology is then passed on to the second stage to adjust pipe diameters in the final design. Awumah and Goulter (1992) also proposed an alternative approach using informational entropy theory. The design optimization model was run repeatedly with a different maximum limit for the initial construction cost imposed each time as a means to generate different topologies. Tanyimboh and Sheahan (2002) also used informational entropy to address the combined effects of topology, pipe size design and reliability in an approach in which the topology, pipe sizing, reliability and redundancy were considered in successive stages. The aforementioned studies did not fully address the joint problem of topology, pipe sizing and reliability optimization in an integrated fashion.

This chapter describes a novel penalty-free multi-objective evolutionary optimization approach to the simultaneous topology, pipe size and both local and global ME designs of WDS. The developed approach has been achieved by integrating the local and global ME optimization approach developed in the previous chapter with the coupled topology and pipe sizes optimization developed in chapter four. The maximization of entropy is tackled in an entirely novel way by considering both the local and global maximum entropy aspects. The local maximum entropy values arise from: (a) multiple topologically distinct design families and (b) the multiple feasible sets of flow directions for a fixed topology. For *each feasible topology*, there is a *local* maximum entropy value for *each feasible set of flow directions.* The *global* maximum entropy value is the largest among the local maxima.

The success of the concept of aggregating objectives has been exploited to extend the definition of infeasibility developed in previous chapter. This extension has

incorporated the measures of topological infeasibility, nodal residual head infeasibility and entropy-based performance into one definition. As a result, the number of objectives has been significantly reduced in this MO problem. Furthermore, a binary coded genetic algorithm (BCGA) was used to suggest a method for handling the issue of redundant codes in the BCGA in an efficient way that exploits natural selection. Using commercial discrete pipe sizes, the topology, pipe size and reliability design optimization herein is applied to two examples: 1) a well-known hypothetical benchmark problem; and 2) a benchmark real system; to obtain a set of optimal cost-effective and reliable designs in each case.

6.2 FORMULATION OF THE OPTIMIZATION APPROACH

A novel penalty-free multi-objective evolutionary approach to the simultaneous optimization of topology, pipe size design and entropy-based reliability for WDSs has been developed. The infeasibility of nodal connectivity (*LIM*), nodal residual-head infeasibility (*HIM*) and the levels of local reliability (*ME-S*) and global reliability (*GME-ME*) were combined together to form an augmented measure of design infeasibility. The overall multi-objective optimization problem was formulated as a three-objective problem. The decision variables are (a) the individual pipe diameters that are selected from commercially available discrete pipe sizes and (b) the zero-one integer variables for selecting the pipes that define the topology.

The optimization approach is basically composed of six objectives. As a procedure of reducing objectives of this MO problem, four objectives were aggregated to form one single objective. The overall formulation of the developed approach can be summarized as follows:

Minimize initial construction cost: $f_1 = \sum_{ij \in N_p} f\left(L_{ij}, D_{ij}\right)$ (6.1)

Minimize augmented infeasibility measure (*AIM*):

$$f_2 = LIM + HIM + (ME\text{-}S) + (GME\text{-}ME) = LIM + HIM + (GME\text{-}S) \tag{6.2}$$

Minimize network complexity measure (*NCM*): $f_3 = \sum_{ij \in N_p} NCM_{ij}$ (6.3)

where

$$LIM = \sum_{i \in N} \max(0, R_i^{req} - R_i) \tag{6.4}$$

$$HIM = \sum_{i \in N} \max(0, H_i^{req} - H_i) \tag{6.5}$$

Apart from terms in Eq. 6.3, all other terms were previously explained in full. Eq. 6.1 represents the objective of minimizing the initial construction cost, which is typically a function of pipe length L_{ij} and diameter D_{ij}. This equation is subject to satisfying both the conservation of mass and energy represented by Eqs. 2.1 and 2.2, which are met externally herein by employing the hydraulic solver EPANET 2 (Rossman, 2000) in the optimization process.

Eq. 6.2 is the objective of minimizing the augmented infeasibility measure (AIM), which is an extension of infeasibility formulated previously, that consists of four terms. All these terms were previously explained in detail. Clearly, the new infeasibility formulation here involves multiple objective functions. First, minimizing the local level of reliability reflects generating a range of near maximum-entropy solutions with $ME - S \approx 0$. Secondly, minimizing the distance between the *GME* (i.e. the greatest entropy value among the current solutions) and each ME ensures maintaining a global search towards maximizing entropy. This has the advantage of maintaining the topology and flow directions of the GMEMC (global maximum-entropy minimum-cost) solution throughout the optimization. In addition, given that $ME - S = 0$ for any maximum entropy solution, the $GME - ME$ term encourages the generation and retention of a range of non-dominated maximum

entropy solutions. Research elsewhere including the examples cited in Section 1 of Chapter 5 has demonstrated that on average the hydraulic capacity reliability and/or redundancy of a WDS improve as the statistical entropy increases. For any feasible WDS topology, there are multiple feasible sets of flow directions; each feasible set of flow directions has a maximum entropy value.

Close inspection of Eq. 6.2 shows that it has a unique solution having zero augmented infeasibility measure in each generation of the GA. This solution has the properties that it is topologically and hydraulically feasible (i.e. $LIM = 0$; $HIM = 0$) with $S = ME = GME$ (i.e. $ME - S = 0$ and $GME - ME = 0$). This uniqueness ensures a global search of maximizing entropy throughout the duration of the optimization. The other solutions will have some positive value of the augmented infeasibility measure *AIM*. An infeasible solution having a significant *AIM* value is likely hydraulically infeasible because the contribution of the residual head infeasibility *HIM* in Eq. 6.2 is so large that it dominates any contributions from the topology and entropy measures. The results in Section 5 of this Chapter clarify this issue further. Solutions having a relatively small augmented infeasibility measure *AIM* are likely hydraulically feasible or marginally infeasible because of the relatively small contributions of the topology and entropy measures. This can be explained by inspecting the range of values each term Eq. 6.2 can take.

For each demand node, the required residual head is typically not less than a minimum of about H_i^{req} = 7m (OFWAT, 2008), while the looping and/or node reachability criterion will rarely exceed $R_i^{req} = 2$ for each demand or supply node. In the previous chapter, it has been shown that, for a typical node with, say, two incident pipes downstream, $S_i \le \ln(3) \approx 1.1$. As a result, it can be expected that the relative entropy measures of *ME* – *S* and *GME* – *ME* will be small.

The location of the residual-head feasibility boundary $(HIM = 0)$ with respect to the augmented feasibility boundary $(AIM = 0)$ depends on the ranges between the

lowest and the highest values of both *S* and *ME*. The larger these ranges are, the larger the distance between the residual-head feasibility boundary and the augmented feasibility boundary. A small value of augmented infeasibility may also reflect how far a hydraulically feasible solution is from the local and/or global maximum entropy solution. The processes of converting hydraulically infeasible solutions into feasible solutions plus the local and global maximization of entropy are the key mechanisms by which the proposed approach performs this multi-objective optimization.

Finally, to incorporate explicitly the topology into the optimization model, a measure of topological complexity was introduced. As a first attempt, this measure simply counts the number of links or pipes (Eq. 6.3); NCM_{ij} = 1 if pipe *ij* is included in the topology and NCM_{ij} = 0 otherwise. The rationale for this measure is that, other things being equal, a network with more pipes is more complex than one with fewer pipes. This objective aims to generate and retain a range of topologically distinct solutions. More sophisticated measures of complexity (see e.g. Yazdani *et al.* 2011) could be investigated in future. Different levels of network complexity may have varying degrees of advantages and/or disadvantages that may include, for example, ongoing maintenance costs and practical operational issues such as network segmentation. Higher-level decisions involving these and other issues not discussed here such as water quality etc. may be easier if the Pareto-optimal front contains a range of solutions that are qualitatively diverse.

6.3 NATURAL SELECTION PROCEDURE FOR REDUNDANT BCGA CODES

The binary coding system in which each discrete decision variable value is represented with *n*-bit string of fixed length of *n* was used. To represent all the decision variable values in the genotype space, the number of discrete values should be less than or equal to 2^n, which is the number of *n*-bit arrangements that can be

produced from an *n*-bit binary string. Each code or *n*-bit binary string should represent a value in the genotype space. However, if the number of discrete decision variable values represented is not a power of 2, some codes may be redundant. Options for dealing with redundant codes include: (a) discarding redundant codes; (b) assigning a low fitness value to solutions with redundant codes; and (c) allocating the redundant codes in a fixed, random or probabilistic way to the values in the domain of the parameter in question (Herrera *et al.* 1998). Options (a) and (b) may result in the loss of useful genes. Option (c) has the disadvantages that it may introduce bias if the redundant codes are not allocated uniformly to the discrete parameter values while a random allocation may degrade the genetic information that is transferred from parents to offspring. Also, any scheme that associates redundant codes to valid codes as in Option (c) has a potential to mislead the GA search.

Herein, redundant codes were assumed to represent closed pipes; consequently these pipes have a flow-carrying capacity of zero. The closed pipes are assigned fictitious pipe diameters that do not belong to the set of diameters that may be used to solve the problem under consideration. However, a solution that contains a fictitious diameter does not represent a real solution. Fictitious diameters are different from real diameters in that they have no utility value. Thus it is anticipated that they will be recognized as useless and eliminated quickly by natural selection.

6.4 COMPUTATIONAL SOLUTION

The optimization problem addressed here is a many-objective problem having 6 essential objectives. The concept of aggregating objectives was employed to reduce number of objectives by half. This has the advantage of significantly reducing the computational complexity from $O(mn^4)$ to $O(mn^2)$ comparisons (Deb *et al.* 2002), where m = number of objectives and n = population size. The aim of reducing objectives is to overcome the difficulties associated with such optimization problems

listed by Saxena *et al.* (2013), i.e. high computational cost, poor scalability of most available multi-objective evolutionary algorithms as the number of objectives increases, and difficulty in visualizing the Pareto-optimal fronts (POFs) of problems with more than four objectives. The fast robust elitist genetic algorithm NSGA II (Deb *et al.* 2002) was used to solve the optimization problem. The overall approach is described in Figure 6.1. The optimization problem was posed as in Eq. 6.6.

$$\text{Minimize } \mathbf{f} = (f_1, f_2, f_3)^{\mathrm{T}} \tag{6.6}$$

Most importantly, the present method of reducing objectives considers all objectives as essentials, i.e. the estimation of POF is dependent on all objectives. Herein, no objective has been classified as being essential or redundant, i.e. an objective has no effect on reaching POF (Saxena *et al.*, 2013). Additionally, no preference of an objective has been made over another objective, i.e. preference-ordering approach (Saxena *et al.*, 2013).

The decision variables are the pipe diameters D_{ij} to be selected within the domain of the available discrete pipe sizes and the zero-one pipe link-selection or topology-definition variables NCM_{ij} for all pipes ij under consideration. To make all three objectives in Eq. 6.1 roughly similar in magnitude, each f_i^m the value of objective m for solution i, was normalized as in Eq. 6.7.

$$fn_i^m = \left(f_i^m - f_{\min}^m\right) / \left(f_{\max}^m - f_{\min}^m\right); \qquad \forall i, \forall m \tag{6.7}$$

in which, in the generation in question, $f_{\min}^m$ = minimum value of objective m; $f_{\max}^m$ = maximum value of objective m; and fn_i^m = normalized value of objective m for solution i.

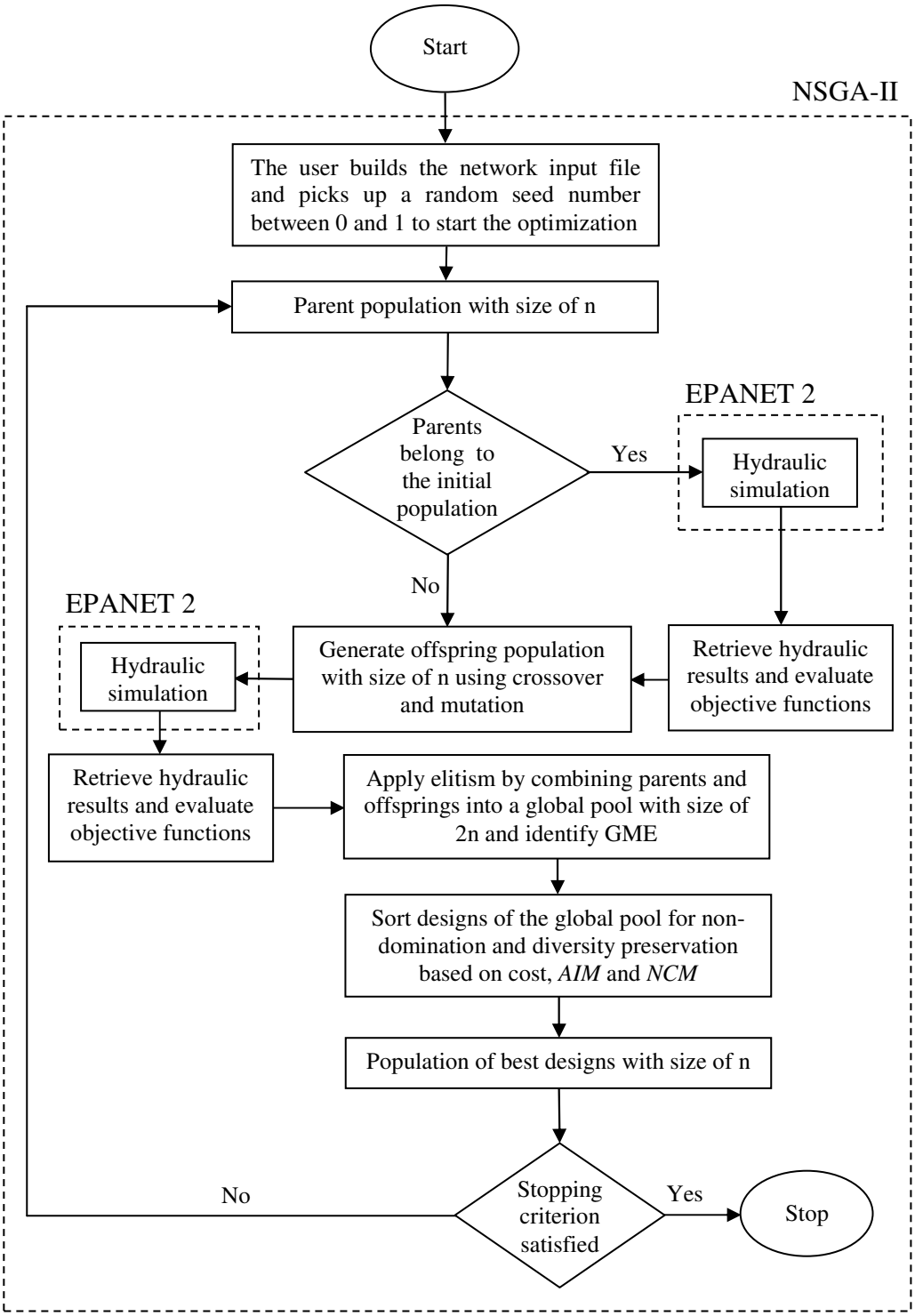

Figure 6-1: Flow chart of the proposed approach

6.5 APPLICATION OF THE TOPOLOGY, PIPE SIZE AND ENTROPY-BASED OPTIMIZATION APPROACH

The developed approach is applied to two benchmark optimization problems: a hypothetical single-source network and a multiple source real system. Even though these networks do not describe in full the actual situation of real-world WDSs, they have been extensively analyzed by previous studies and so providing good grounds to compare the performance of the proposed approach. An Intel Core 2 Duo CPU 2.99 GHz, 3.21 GB RAM personal computer was used in this study. Since different computer specifications would have been used previously, assessing the efficiency of the present approach with design evaluations along with CPU time would provide a fair comparison of results.

6.5.1 Example 1

The proposed approach was applied to a well known benchmark network in the literature. The general topology of this 6-loop hypothetical grid network is shown in Section 6 of the previous Chapter. This network was considered in previous studies on entropy and topology optimization based on continuous pipe sizes (Awumah *et al*. 1990, 1991; Tanyimboh and Sheahan 2002). The same input data of minimum and required heads of H_j^{min} = 0 and H_j^{req} = 30 m respectively has been used. The minimum head H_j^{min} is the (assumed) head below which the outflow at a demand node ceases. H_j^{req} = 30m here may be somewhat high. However, its adoption aims to maintain consistency with previous results in the literature. The decision variables are the 17 zero-one pipe link-selection or topology-definition variables NCM_{ij} and the 17 pipe diameters D_{ij} to be selected from the available discrete pipe sizes. R_i^{req} = 2 in this problem specifies a fully looped topology. This network is relatively small. However, it was chosen for several reasons including (a) previous related research; (b) the problem complexity; and (c) the novelty of the proposed solution approach. It

is possible that new insights can be obtained from this example that would be much harder using a large network.

The decision variables are 12 commercially available discrete pipe diameters of 100, 125, 150, 200, 250, 300, 350, 400, 450, 500, 550 and 600 mm, i.e. the same range as in the above-mentioned previous studies. Each pipe can have one of the 12 available pipe diameters, or it may not be included in the topology. There are therefore 13 options for each pipe. The size of the solution space is therefore $13^{17} = 8.65\times10^{18}$. A 4-bit binary coding system was used. There are 17 pipes in the network and each solution was represented by a 68-bit chromosome. A 4-bit string produces 16 binary configurations. With 13 possible options for each pipe, there are three codes (out of 16) that are redundant. Three fictitious pipe diameters of 650, 700 and 750 mm were respectively allocated to the three redundant codes (Appendix E). The pipe costs in GBP per metre length were taken as $£800D^{1.5}$ where D is the pipe diameter in metres (Appendix E).

An initial random population of size 100 and a stopping criterion of a maximum of 10,000 generations were used. This corresponds to a maximum limit of 10^6 function evolutions (FEs) or a sampling rate of (10^6 FEs)/(8.65×10^{18} solutions) = 1 FE per 8.65×10^{12} solutions. Selection for crossover was carried out using a binary tournament. Single-point crossover was used to produce two offspring from two parents. The crossover probability p_c was set at $p_c = 1.0$, i.e. in each generation, 50 crossover operations are conducted on the parent population to produce an offspring population with size of n = 100. Once the offspring population is created, the mutation operator changes selected bits from 0 to 1 or 1 to 0. The adopted best mutation rate of $1 / n_g$ was used, i.e. $p_m = 1/68 \approx 0.015$. For the population as a whole, this corresponds to a mutation rate of one bit per chromosome on average.

To evaluate the GA, 30 randomly initiated runs were carried out. Table 6.1 summarizes the general characteristics of the GA from this example. The feasible solution having the highest entropy within each generation was used to gauge the

progress of each GA run. Within the maximum number of function evaluations (FEs) allowed here of 10^6, the convergence point was taken as the point after which there was no improvement in both the entropy and cost of the feasible solution with the highest entropy value. A feasible solution in this context is a solution that satisfies the nodal demands and residual heads in full and has no fictitious pipe sizes. Among the conducted GA runs, the minimum, mean, median and maximum costs of GMEMC (global maximum entropy minimum cost) solution were £2,177,413; £2,787,246; £2,730,261 and £3,552,885 respectively. The standard deviation was £349,057. The minimum, mean, median and maximum values of entropy for the GMEMC solution were 3.380570, 3.560733, 3.561684 and 3.592495. The standard deviation was 0.041524.

Table 6-1: Convergence and consistency statistics of 30 GA runs for example 1

Measure	Minimum	Mean	Median	Maximum	Standard deviation
GMEMC entropy	3.380570	3.560733	3.561684	3.592495	0.041524
MMEMC entropy	2.401622	2.489328	2.476941	2.660135	0.059723
GMEMC cost (£10^6)	2.177413	2.787246	2.730261	3.552885	0.349057
MMEMC cost (£10^6)	1.181715	1.293399	1.292801	1.496615	0.074389
Number of fully looped feasible solutions (out of 100)	36	48.533	50	57	5.778
Number of partially looped and branched feasible solutions per 100	0	6.2	5	13	3.219
Smallest surplus residual head for feasible solutions (m)	0.007	0.629	0.464	2.691	0.654
Function evaluations (FEs) for convergence	314700	733413	806050	979200	208529
Extinction of all fictitious pipes (FEs)	1500	4600	3850	17300	3725
Extinction of 750mm pipes (FEs)	500	2050	1650	8500	1594
Extinction of 700mm pipes	900	2583	1950	5700	1406

(FEs)					
Extinction of 650mm pipes (FEs)	900	4003	2600	17300	3885
Hypervolume[a]	0.653	0.661	0.660	0.682	0.004
CPU time for convergence (minutes)	27.35	63.75	70.06	85.11	18.13

[a] The hypervolume for the merged POF of 100 nondominated solutions is 0.676.

Among the conducted 30 GA runs herein, the GME was found to have a value of 3.5928 belonging to the base graph or the full topology of the network. This value corresponds to the GME achieved in a previous study aimed to globally maximize entropy of water distribution systems with fixed topologies (Saleh and Tanyimboh, 2012). This achievement indicates that the incorporation of topology optimization with pipe size and entropy maximization has not affected the global search of the proposed approach. Out of 30 runs, the GME was found in 10 GA runs at various stages of the optimization. The minimum and maximum numbers of function evaluations required to identify the GME were 237,700 and 748,700 respectively. The GMEMC solution reported here was achieved in 4 GA runs out of 30. Generating the GME at an early stage in the optimization is a key element towards reaching the GMEMC solution. The earlier the GME is found the faster a near-GMEMC solution is achieved.

It is worth mentioning that very similar ME values to the GME have been found within the GA runs in which GME has not been reached. For example, a ME value of 3.581115 has been detected in 12 GA runs out of 30 runs. This value classified as ME group of 4 (Table 6.2a) was found to belong to a new layout generated by removing one pipe from the base graph of the original network as shown in Figure 6.3a. The recognition of such an important layout reflects the benefits of incorporating layout optimization as an essential optimization aspect towards achieving high entropy WDS designs.

Since the aim of this study is to include a wide range of other maximum entropy minimum cost (MEMC) solutions in addition to the GMEMC, the *Minimum* Maximum Entropy Minimum Cost (MMEMC) solution is indicative of the range of maximum entropy groups found by the GA in each run. The minimum, mean, median and maximum costs of the MMEMC solution were £1,181,715; £1,293,399; £1,292,801 and £1,496,615. The standard deviation was £74,389. The corresponding minimum, mean, median and maximum values of entropy were 2.401622, 2.489328, 2.476941 and 2.660135. The standard deviation was 0.059723. Also, the design with the smallest surplus head at the critical node was recorded in each GA run to investigate the GA's ability to locate (near-) maximum entropy solutions close to the residual-head feasibility boundary, as a possible indicative measure of the optimality of the solutions. The minimum, mean, median and maximum smallest-surplus-heads at the critical nodes were 0.007, 0.629, 0.464 and 2.691 m, respectively. The standard deviation was 0.654 m.

Figure 6.2 shows 3-dimensional plots of cost, combined residual-head and topological infeasibility, and entropy, of the individual Pareto-optimal fronts (POFs) from the 30 GA runs. The solutions in the POFs increase steadily in entropy and cost as they become more feasible as the residual-head feasibility boundary is approached from right to left in Figure 6.2. The solutions at the feasibility boundary meet the topological and residual-head requirements in full. They include the cheapest feasible maximum entropy solution which was obtained by removing the maximum number of pipes (i.e. five) from the base graph that does not undermine the looping condition ($R_i \geq R_i^{req} = 2$). Other feasible solutions with higher maximum entropy values that correspond to different layouts (as shown in Figure 6.3) are also present at the feasibility boundary.

The most infeasible solution in Figure 6.4 is the design that results from the removal of all the 17 candidate pipes from the base graph or fully connected network. This solution has zero cost, zero entropy, maximum topological infeasibility of 24 (i.e. 2 independent paths per node × 12 nodes) and maximum residual-head infeasibility of

330 m (i.e. 11 demand nodes × 30 m residual head per demand node). Any crossover between this solution and another solution is guaranteed to create two layouts. Retention of this infeasible and self-evidently non-dominated solution throughout the entire evolution of the optimization is possible because of the penalty-free strategy applied here.

The POFs from the 30 GA runs in Figure 6.2 appear to show great similarity. The hypervolume indicator was calculated for each POF after normalizing the objectives according to Eq. 6.7. The hypervolume is a measure of the fraction of the objective space that the achieved POF dominates. The hypervolume increases as the achieved POF approaches the true POF. It increases also as the range and/or evenness of solutions in the POF increase. Larger hypervolume values are thus preferred (see e.g. Knowles 2005). The minimum, mean, median and maximum hypervolume values of the POFs were 0.653, 0.661, 0.660 and 0.682 respectively, with a standard deviation of 0.004.

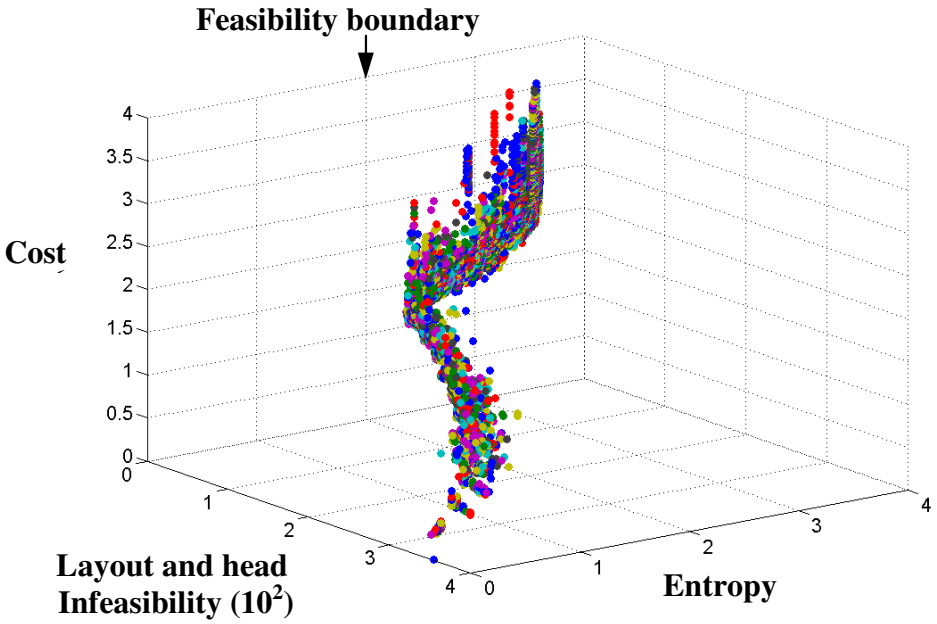

Figure 6-2: Individual Pareto-optimal fronts for the 30 randomly initiated GA runs

The 100 solutions in each of the 30 POFs were then merged and sorted considering non-domination and diversity based on the crowding distance as in NSGA II. The

hypervolume value of the final merged POF of 100 non-dominated solutions was 0.676. Overall, with reference to Figure 6.2 and considering the nature of the normalization of the objective function values in Eq. 6.7 that is not absolute, the hypervolume results for the individual and merged POFs seem reasonably consistent and encouraging.

The merged POF has 23 hydraulically feasible nondominated fully looped solutions based on cost, augmented infeasibility measure *(AIM)* and number of pipes (as summarised in Table 6.2a) of which there are 14 different maximum entropy groups and 11 different fully looped topologies (as shown in Figure 6.3a). All topologically and/or hydraulically infeasible solutions of the merged POF were found to be topologically infeasible ($R_i < R_i^{req} = 2$), of which only three were hydraulically feasible ($H_i \geq H_i^{req}$ = 30 m; Eq. 4) as shown in Table 6.2b and Figure 6.3b.

A topologically infeasible solution that is hydraulically feasible does not have the stipulated number of supply paths but all its nodes are reachable and have sufficient flow and pressure. This relatively small number of topologically infeasible solutions that has sufficient flow and pressure at all demand nodes would appear to suggest the residual head criterion (*HIM*) has priority over the topology criterion (*LIM*) in Eq. 6.2 (*AIM*). This may be due to the dominance of the residual head in Eq. 6.2. These results seem to suggest that, concomitant with partial topological feasibility or node reachability, i.e. $0 < R_i < R_i^{req}$, the GA prioritises residual-head feasibility over full topological feasibility, i.e. $R_i \geq R_i^{req}$. Also, the critical nodes highlighted in Figure 6.3 and Table 6.2 show that it is hard to predict the location of the critical node without solving the design optimization problem.

It is worth highlighting that the achievement of ME group 14 (Figure 6.3a) reflects the ability of the introduced measure of layout infeasibility *LIM* ($R_i \geq R_i^{req}$ = 2) to recognize the minimum number of pipes required to satisfy the looping condition herein. For example, this layout was generated by removing 5 pipes, which account

for about 30% of the total pipes of the full topology, from the base graph without undermining the looping condition. Additionally, the cheapest fully looped feasible design (solution 14 in Table 6.2a) was achieved by removing 4 pipes from the base graph.

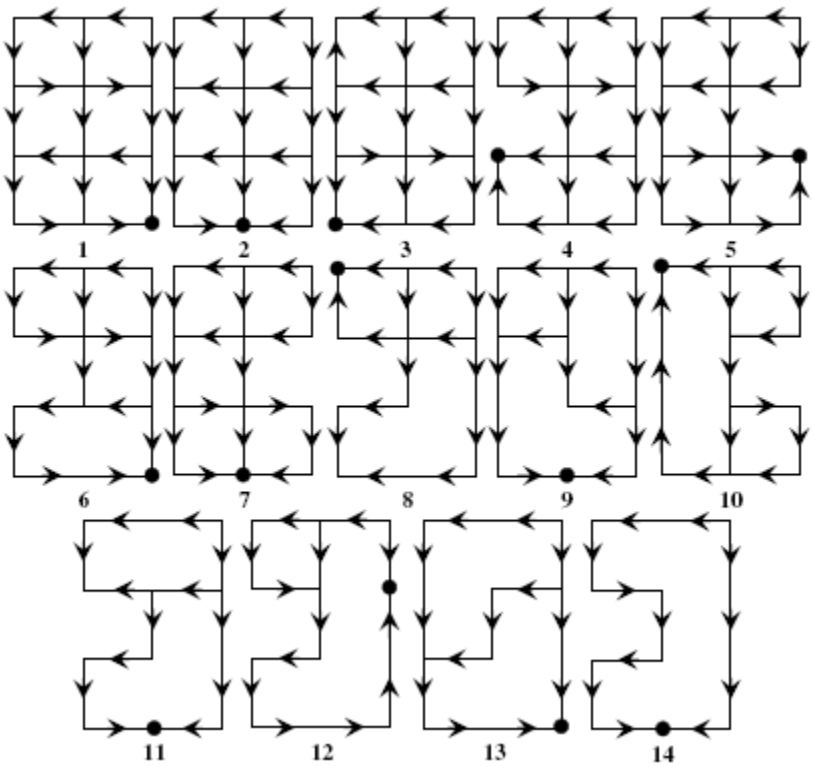

Figure 6-3a: Topologies and flow directions of the fully looped hydraulically feasible maximum entropy groups. The solid circles represent the nodes with the smallest residual heads.

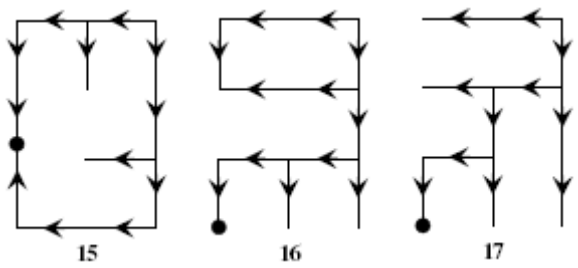

Figure 6.3b: Topologies and flow directions of the branched and partially looped hydraulically feasible maximum entropy groups. The solid circles represent the nodes with the smallest residual heads.

Accordingly, it is anticipated that increasing the size of base graphs could bring further saving of cost due to the effect of pipe removal on cost minimization. Real world systems represent a good example of such situation in which the full topology of the network is made up of large number of pipes.

Table 6-2a: Fully looped hydraulically feasible solutions in the merged POF

Solution number	Cost (£10^6)	Surplus head [a] (m)	Critical node	Actual entropy *(S)*	Maximum entropy (ME)	*ME-S*	*GME-ME*	ME group
1	2.52235	19.734	9	3.592494	**3.592800**[b]	0.000306	0.000000	1
2	1.592572	9.817	10	3.257305	3.330590	0.073285	0.262210	2
3	1.823409	2.083	11	3.439667	3.489588	0.049921	0.103213	3
4	2.756591	21.594	8	3.581014	3.581115	0.000101	0.011685	4
5	1.977641	11.642	6	3.545526	3.546760	0.001234	0.046041	5
6	3.138684	38.903	9	3.449581	3.449665	0.000084	0.143135	6
7	3.067751	38.729	9	3.449580	3.449665	0.000085	0.143135	6
8	2.930185	36.096	9	3.449268	3.449665	0.000397	0.143135	6
9	2.235305	8.626	9	3.448149	3.449665	0.001517	0.143135	6
10	1.871266	5.864	10	3.395190	3.398060	0.002870	0.194740	7
11	1.292923	1.350	2	2.850790	2.891747	0.040958	0.701053	8
12	1.271386	3.443	10	2.647933	2.723657	0.075724	0.869144	9
13	2.969728	33.350	2	3.265855	3.269803	0.003947	0.322998	10
14	1.173127	1.910	10	2.367236	2.469176	0.101940	1.123624	11
15	2.849506	35.237	3	2.940251	2.940255	0.000004	0.652545	12
16	2.839981	34.462	3	2.940250	2.940255	0.000005	0.652545	12
17	2.769049	34.041	3	2.940247	2.940255	0.000008	0.652545	12
18	2.729939	32.628	3	2.940223	2.940255	0.000033	0.652545	12
19	2.683465	32.394	3	2.940159	2.940255	0.000097	0.652545	12
20	2.605798	30.773	3	2.940102	2.940255	0.000154	0.652545	12
21	2.535235	23.781	3	2.939597	2.940255	0.000659	0.652545	12
22	1.529674	9.394	9	2.614232	2.624432	0.010200	0.968369	13
23	1.721305	6.330	10	2.419348	2.425825	0.006477	1.166975	14

[a] This refers to the surplus residual head at the critical node. The critical node is the node with the smallest surplus head in each solution. [b] The largest entropy value found.

Table 6-2b: Hydraulically feasible branched and partially looped solutions of the merged POF

Solution number	Cost (£10^6)	Surplus head (m)	Critical node	Actual entropy *(S)*	Maximum entropy (ME)	*ME-S*	*GME-ME*	ME group
24	1.508359	18.840	8	2.447343	2.447345	0.000002	1.145456	15
25	1.075510	0.842	11	2.387568	2.404150	0.016582	1.188651	16
26	1.050212	0.503	11	2.360799	2.360799	0.000000	1.232002	17

Another important feature achieved by the proposed approach is in the provision of three branched and partially looped feasible solutions in the merged POF. This result indicates that the approach is capable of achieving the three types of network configurations in one go. Even though branched and partially looped solutions are not desirable due to lack of providing independent flow paths at demand nodes, they provide further saving of cost in comparison with fully looped solutions. It is worth mentioning that fully looped configurations could not provide a practical solution to some real world systems. For example, the right-of-way in some streets can make the accessibility between two consumption points unachievable.

Figure 6.4 shows the merged POF in terms of the infeasibility and cost of each solution. Surprisingly, the merged POF is so consistent that approximately all solutions appear to be non-dominated in both cost and infeasibility and irrespective of the other objectives (*S* and *ME*). This consistency is attributed to the introduction of *AIM* objective in which the objectives of *LIM* and *HIM* measures dominate *ME-S* and *GME-ME* objectives in the infeasibility region. Additionally, the cost of infeasible solutions starts to increase from zero (solution generated by removing all pipes from base graph) to the cheapest feasible solution and in proportion with decrease in infeasibility. The contribution of feasible solutions in the merged POF is evident from extending the range of feasible solutions along the feasibility boundary (*LIM* = 0; *HIM* = 0). All solutions making up the merged POF belong to a variety of 14 topologies (Figure 6.5). The effect of including layout optimization on pipe size and entropy optimization is evident from extending the POF in such a way that it

intersects infeasibility axis.

Figure 6.5 demonstrates the merged POF in terms of infeasibility and entropy. The reduction in the feasible part of the merged POF herein is attributed to the small range of values resulted from the entropy function of WDS. The effect of including layout optimization on pipe size and entropy optimization is evident from extending the POF in such a way that it intersects infeasibility axis. It can be noted that the range of entropy among infeasible solutions is larger than that of feasible solutions. This is due to that the vast majority of infeasible solutions are topologically infeasible. Topologically infeasible solutions are characterized with having a number of zero-entropy nodes. For example, the absolute infeasible solution has zero entropy due to being made up of zero-entropy nodes. Reducing topological infeasibility by adding pipes will result in reducing number of zero-entropy nodes and so increasing *S*. This changes increase until no node with zero entropy is achieved.

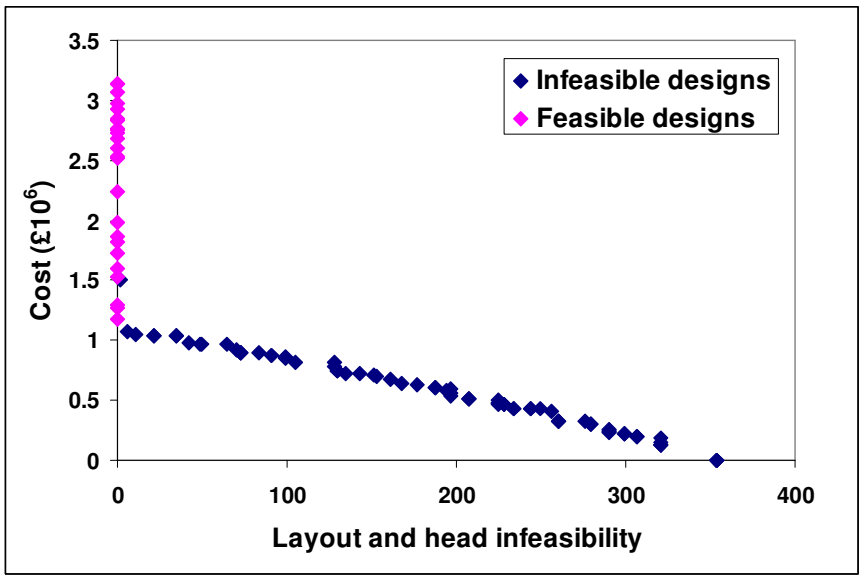

Figure 6-4: Infeasibility versus cost of merged POF

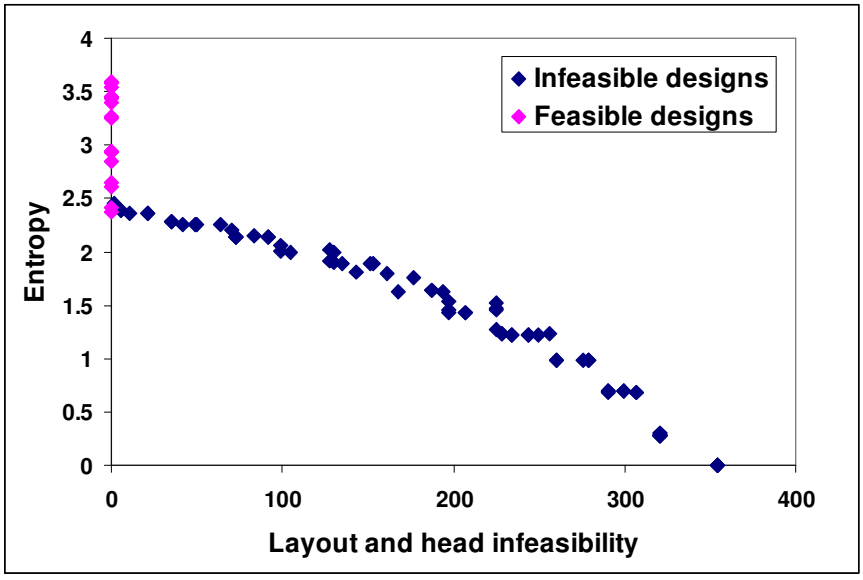

Figure 6-5: Infeasibility versus entropy of merged POF

The relationship between cost and entropy of the merged POF is shown in Figure 6.6. Clearly, some feasible solutions appear to be dominated in cost and entropy. The inclusion of such designs is attributed to being non-dominated in the other objective, which is number of pipes. The effect of number of pipes on cost, infeasibility and entropy is shown in Figures 6.7 to 6.9. For each set of pipes, there are number of designs with different costs. This is due to the fact that such designs have different topologies and entropy values.

Figure 6.8 shows that the minimum number of pipes required to achieve a topologically feasible solution is 12, which is about 70% of the total pipes making up the base graph. The effect of topology on infeasibility can be noticed in providing a number of designs with different infeasibilities for each set of pipes. The difference between the range of entropy for infeasible solutions and feasible ones is obvious in Figure 6.9. Herein, the existence of a number of solutions with different entropy values for each set of pipes is attributed to the effect of topology and flow directions on entropy.

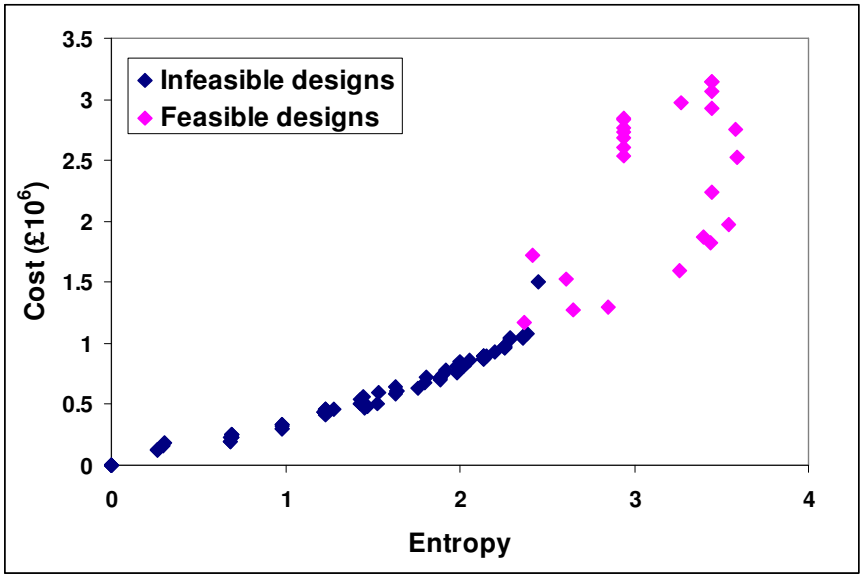

Figure 6-6: Entropy versus cost of merged POF

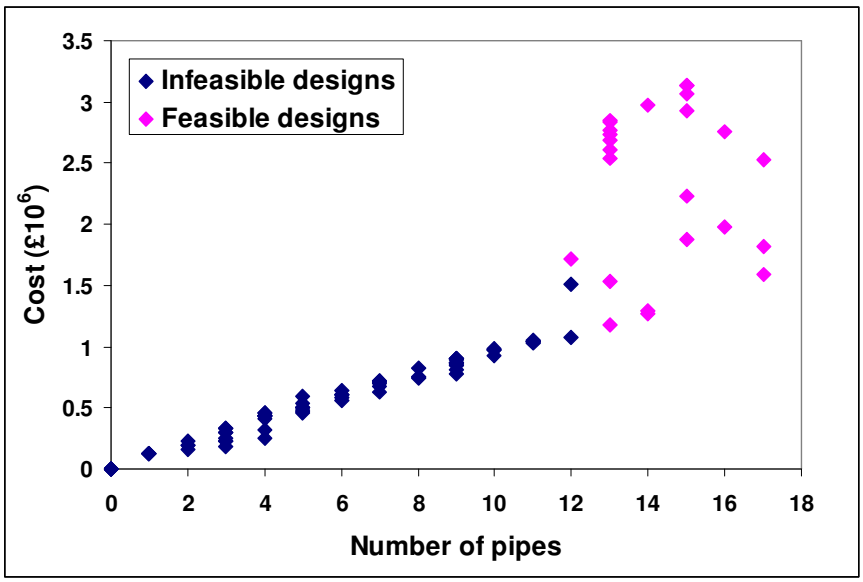

Figure 6-7: Number of pipes versus cost of merged POF

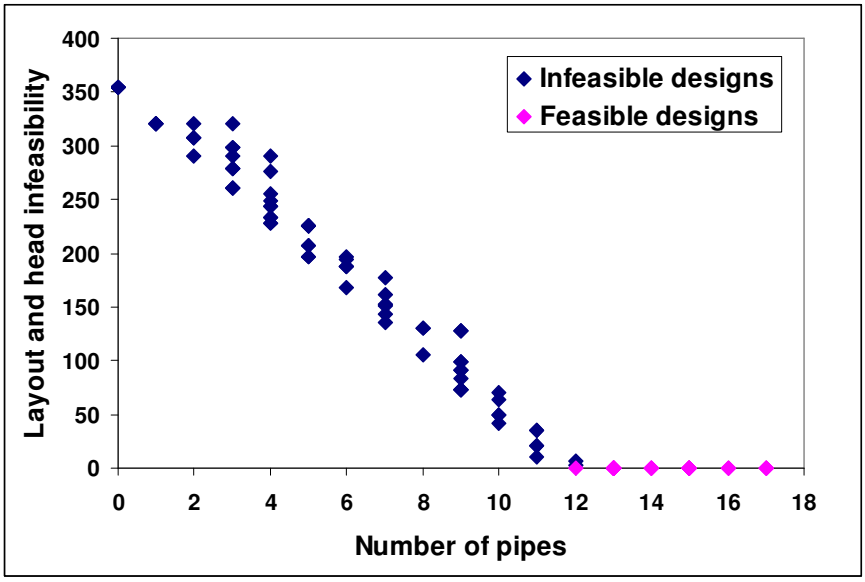

Figure 6-8: Number of pipes versus infeasibility of merged POF

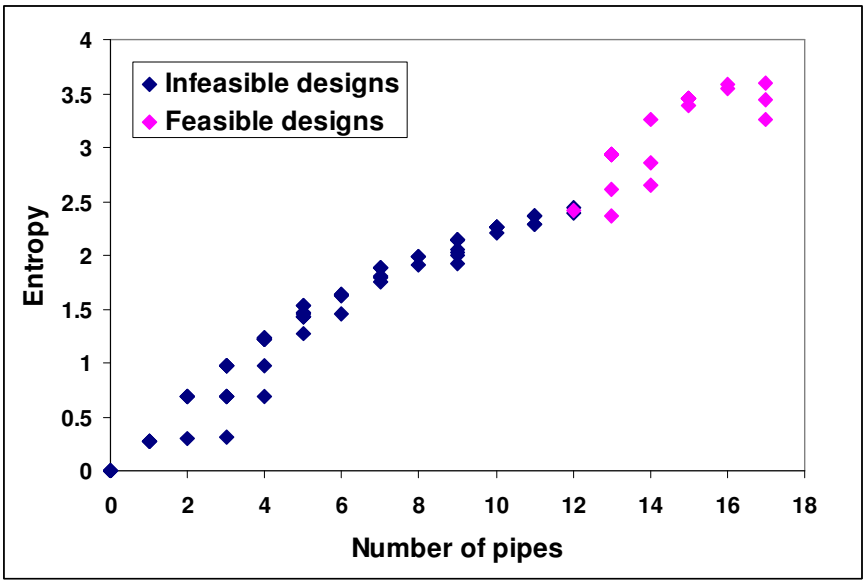

Figure 6-9: Number of pipes versus entropy of merged POF

The variety in the topologies, maximum entropy groups and flow directions along with the differences in the individual hydraulically feasible solutions achieved can be seen in Table 6.2 and Appendix F, while Figures 6.4 to 6.9 provide evidence of the multifaceted nature of the optimization. Within the individual maximum entropy groups in Table 6.2, there is a range of $ME - S$ values. Also, the effectiveness of the local maximization of entropy is evident in that all the 26 feasible solutions in Table

6.2 have small deviations (i.e. $ME - S$) of entropy S from the corresponding maximum entropy ME values. This shows that in general the solutions are (near-) maximum entropy solutions. The graph showing the entropy values achieved vs. the respective maximum entropy values for all solutions in the merged POF in Figure 6.10 has a strong positive correlation of R^2 = 0.976 and provides further confirmation. In the many-objective problem addressed here this high level of similarity is noteworthy.

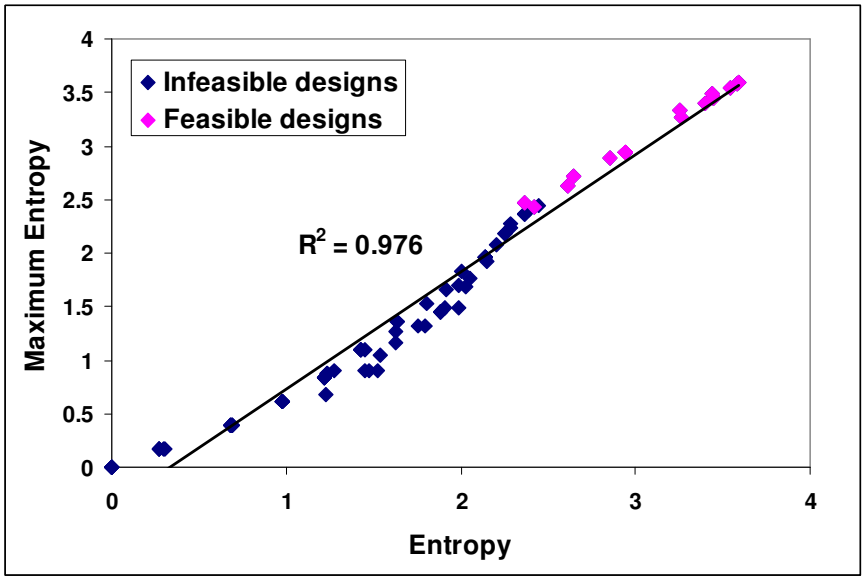

Figure 6-10: Similarity between the actual and potential entropy values of the solutions in the merged Pareto-optimal front

The fully looped feasible solutions achieved range in cost from £1,173,127 to £3,138,684. The branched and partially looped feasible solutions range in cost from £1,050,212 to £1,508,359. The $GME - ME$ values in Tables 6.2a and 6.2b respectively reveal that, as a group, the branched and partially looped solutions collectively appear to be the furthest away from the GME solutions. It is worth mentioning that the existence of significant surpluses in the heads at the critical nodes (Table 6.2) in most of the achieved solutions is likely due to the three-objective formulation and entropy maximization in particular in a discrete solution space. Furthermore, the $ME - S$ term in Eq. 6.2 that is for local maximization of

entropy favours least-cost maximum-entropy solutions over other least-cost solutions that may have smaller surpluses in the residual heads at the critical nodes.

The achieved solutions are distributed among 11 different fully looped topologies as shown in Figure 6.3a. The optimization of topology played an important role in achieving a good compromise between maximizing entropy and minimizing cost. For example, the cheapest achieved ME solution having an entropy value of 2.367236 and cost of £1,173,127 belongs to a topology generated by removing 4 pipes from the base graph. At the same time, the GMEMC solution having an entropy value of 3.592494 and cost of £2,522,350 was achieved without removing any pipe from the base graph. To appreciate further the benefits of topology optimization, consider ME Groups 4 and 5 belonging to two different topologies made up of the same number of pipes of 16, for example. However, ME Group 5 has produced a solution with cost of £1,977,641 and entropy of 3.545526, which is further cheaper than a very similar solution belonging to ME Group 4 having cost of £2,756,591 and entropy of 3.581014. This shows that topology optimization can increase the range and cost effectiveness of the optimal solutions.

Another important result obtained from topology optimization was the identification of the pipes that are relatively unimportant. For example, removing pipe 5-8 from the base graph resulted in a very high ME group with a maximum entropy value of 3.581115 (ME Group 4), which is the second highest achieved here and only marginally lower than the GME of 3.5928 (Table 6.2a). Also, it can be seen that ME Groups 4, 6, 8, 11, 12 and 14 do not include pipe 5-8 (Figure 6.3a). It may be noted also that ME Groups 5, 7 and 10 do not include pipe 7-10. It is worth observing that the various topologies in Tanyimboh and Sheahan (2002) do not include any topologies such as those in Figure 6.3a that do not have pipes 5-8 and 7-10 (see Saleh *et al.* 2012 for more such examples).

Even for a small network such as the present example, this illustrates clearly the benefits of integrating topology in the optimization of WDSs. The beneficial effects

of topology optimization are also evident in Figures 6.4 to 6.9. Overall, there is strong positive correlation between the number of pipes and (i) cost; (ii) entropy; and (iii) overall feasibility. For any given number of pipes the cost of the cheapest solution appears to increase with the number of pipes (Figure 6.7). It can be seen that the proposed GA provides feasible solutions with significant differences in cost and/or entropy for the same numbers of pipes. Figure 6.7 also reveals remarkable differences in cost from 12 to 17 pipes.

The convergence characteristics of the GA for the conducted runs in detail are demonstrated in terms of tracking the GMEMC design that is characterized with having minimum *AIM* (Figure 6.11) and highest entropy (Figure 6.12) among all solutions in each generation. The minimum, mean, median and maximum number of function evaluations (FEs) within which convergence took place was 314,700; 733,413; 806,050 and 979,200 respectively. The standard deviation was 208,529. The minimum, mean, median and maximum CPU times in minutes were 27.35, 63.75, 70.06 and 85.11. The standard deviation was 18.13 minutes. In all 30 GA runs the fictitious pipe sizes were eliminated in the early stages. Figure 6.13 shows that fictitious pipe sizes are eliminated at different stages of the optimization. The minimum, median, mean and maximum numbers of function evaluations (FEs) within which fictitious pipe diameters ceased to exist in total were 1500, 4600, 3850 and 17300 respectively. The standard deviation was 3725 FEs. It was found that the rates of elimination were different for the three different sizes. The elimination rate seems faster for the larger and more expensive fictitious pipes (Table 6.1 and Figure 6.14). These results suggest the procedure for handling redundant binary strings is stable and efficient.

It is worth mentioning that, prior to their complete elimination, fictitious pipe diameters were included in both feasible and infeasible solutions. Combining the objectives of minimizing topological infeasibility, minimizing residual-head infeasibility and maximization of entropy into one objective appears to be a key factor in the efficient solution of this extremely complex discrete nonlinear multi-

objective combinatorial optimization problem. Tracking the various components in Figures 6.11 to 6.19 suggest progress towards near-optimum solutions is very quick. Figures 6.11 to 6.19 also show that the active search space expands quickly from the random initial population, and infeasible solutions participate in the optimization from an early stage until the end.

Figures 6.11 to 6.19 would appear to reveal a very slight gentle rise in the mean cost and mean number of pipes after the initial rapid reduction that could be due to the effect of maximizing the entropy. Figure 6.15 and Figure 6.16 show that the cost and number of pipes increase as the entropy increases. Table 6.1 also summarises the GA's characteristics. As mentioned earlier, less than 1 in every 8.65×10^{12} solutions were sampled in each GA run. Therefore, it may be concluded that the similarities between the respective means and medians together with the relatively small standard deviation values in Table 6.1 would appear to suggest the GA's performance is satisfactory.

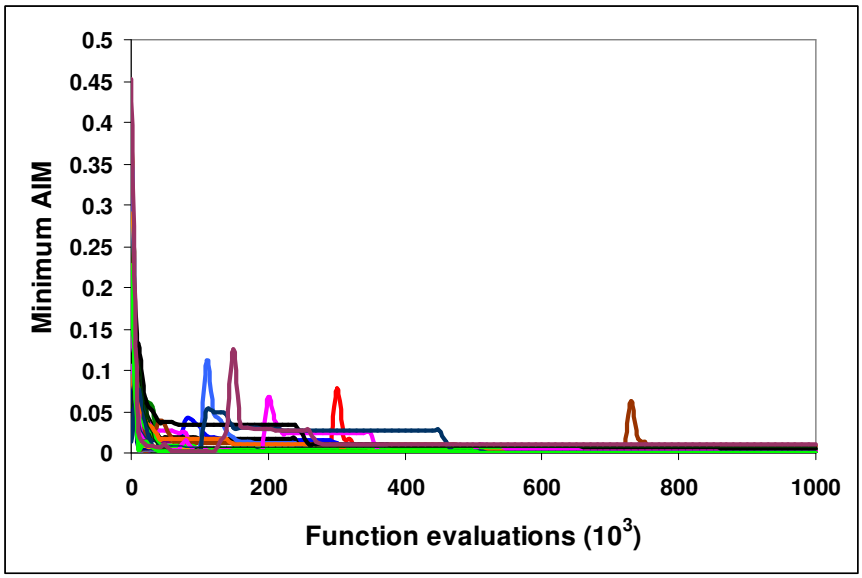

Figure 6-11: Evolution and convergence characteristics for minimum augmented infeasibility in the population of 100 solutions in each GA run

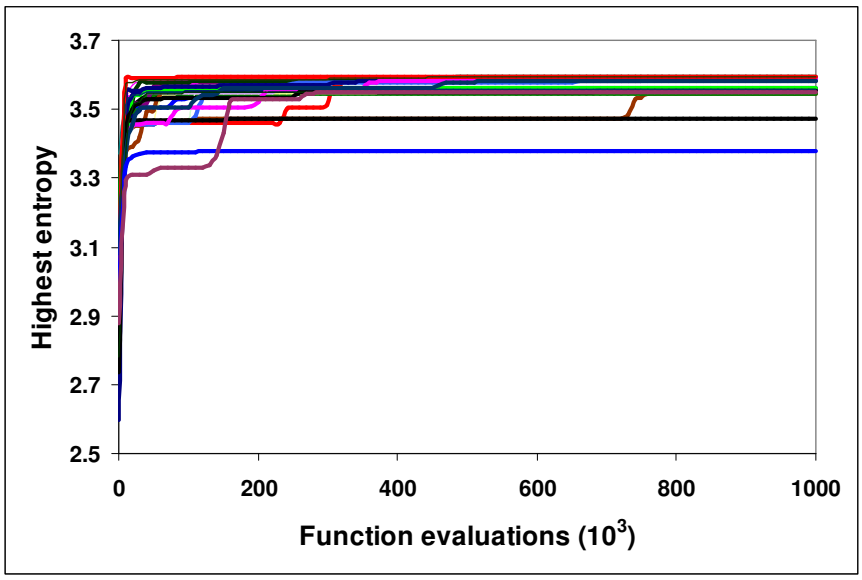

Figure 6-12: Evolution and convergence characteristics for highest entropy among feasible solutions in the population of 100 solutions in each GA run

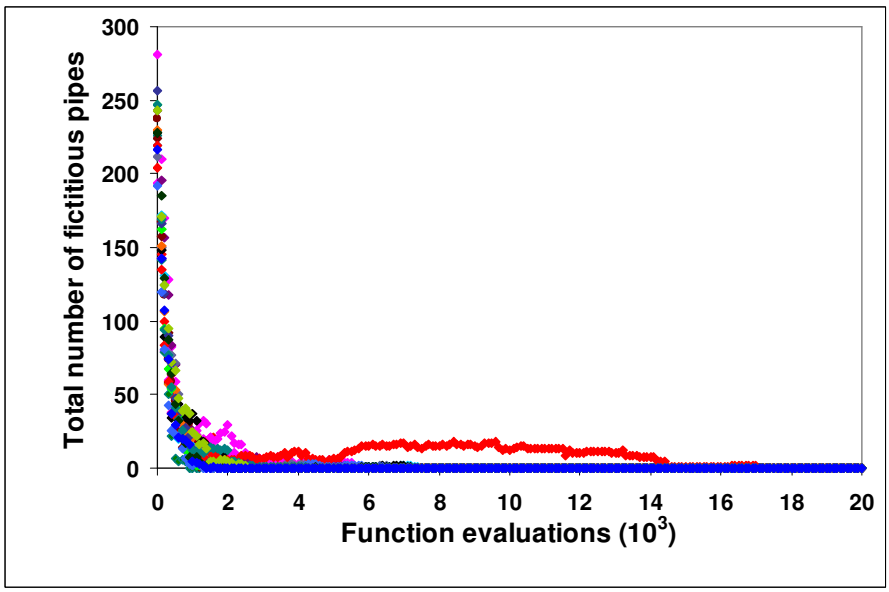

Figure 6-13: Evolution and convergence characteristics for total number of fictions pipes in each GA run

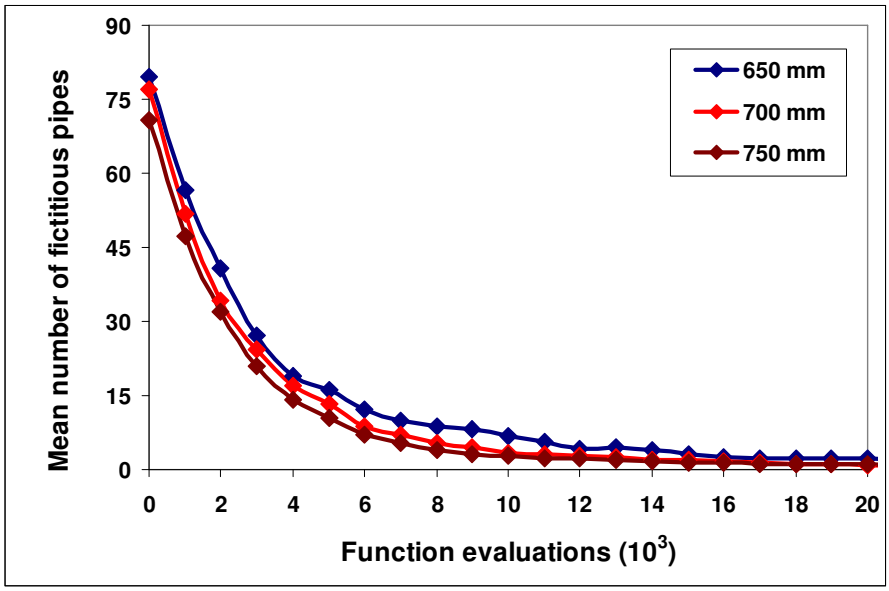

Figure 6-14: Evolution and convergence characteristics for mean number of fictitious pipes based on 30 GA runs

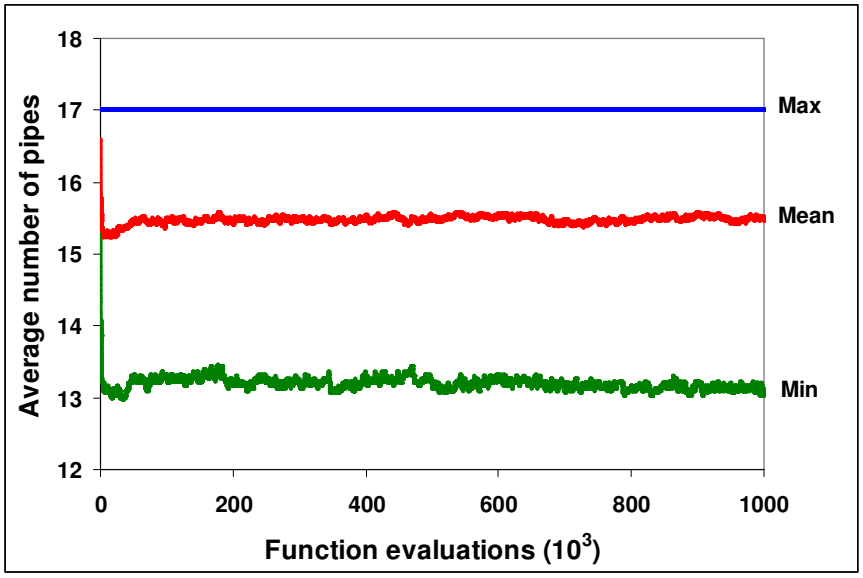

Figure 6-15: Evolution and convergence characteristics for mean number of pipes in fully looped feasible solutions based on 30 GA runs

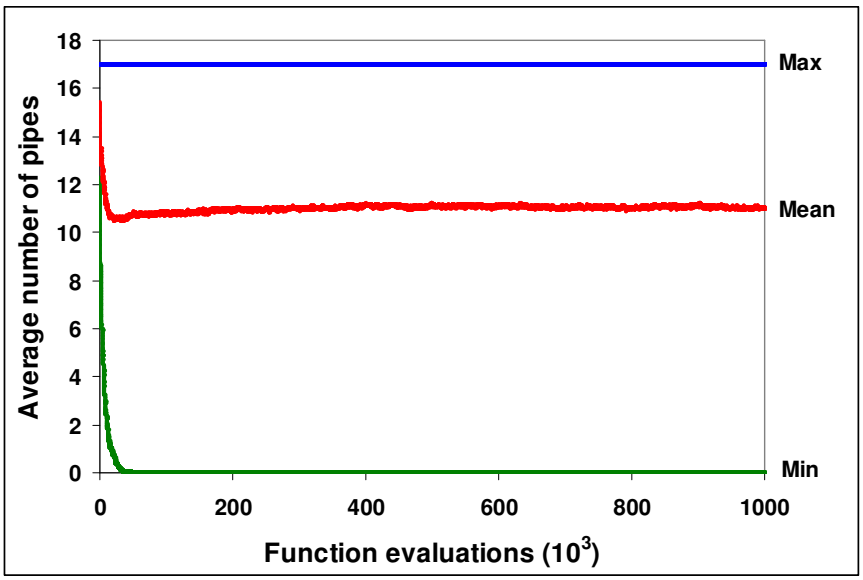

Figure 6-16: Evolution and convergence characteristics for mean number of pipes in all feasible and infeasible solutions based on 30 GA runs

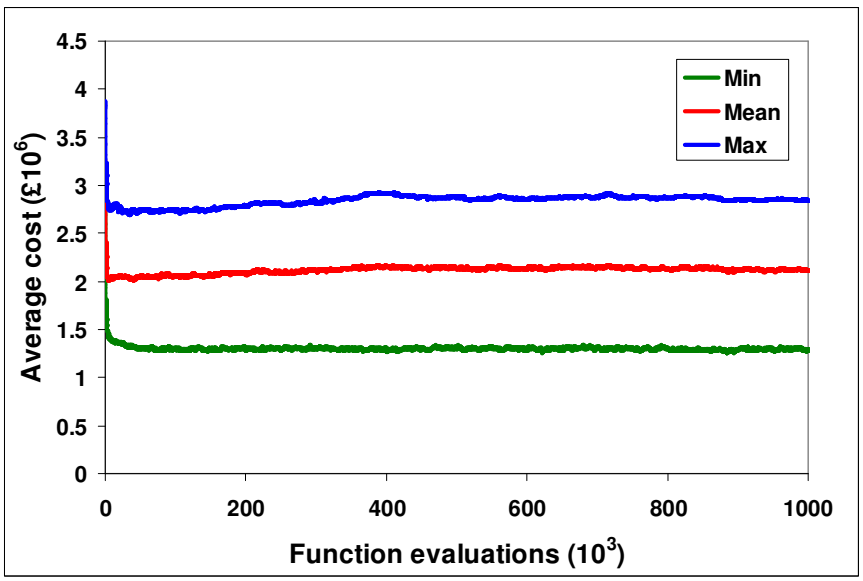

Figure 6-17: Evolution and convergence characteristics for mean cost of fully looped feasible solutions based on 30 GA runs

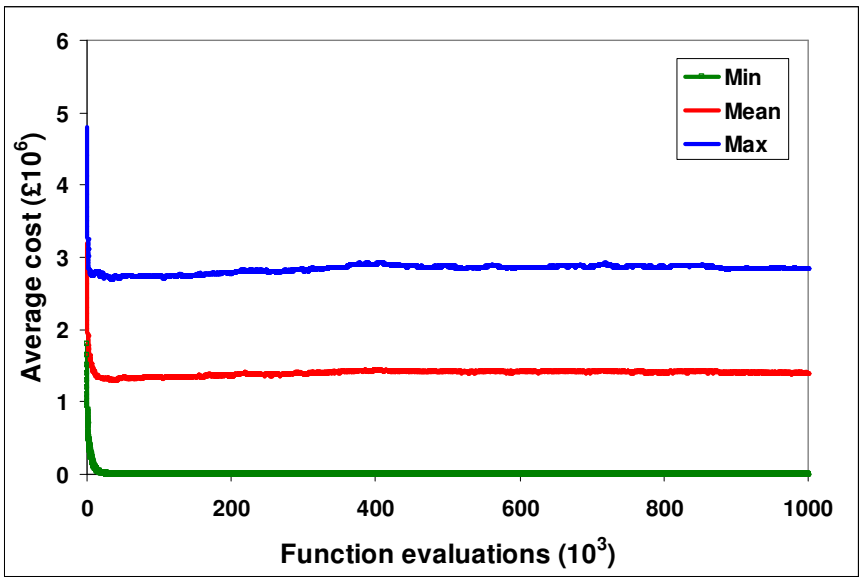

Figure 6-18: Evolution and convergence characteristics for mean cost of all feasible and infeasible solutions based on 30 GA runs

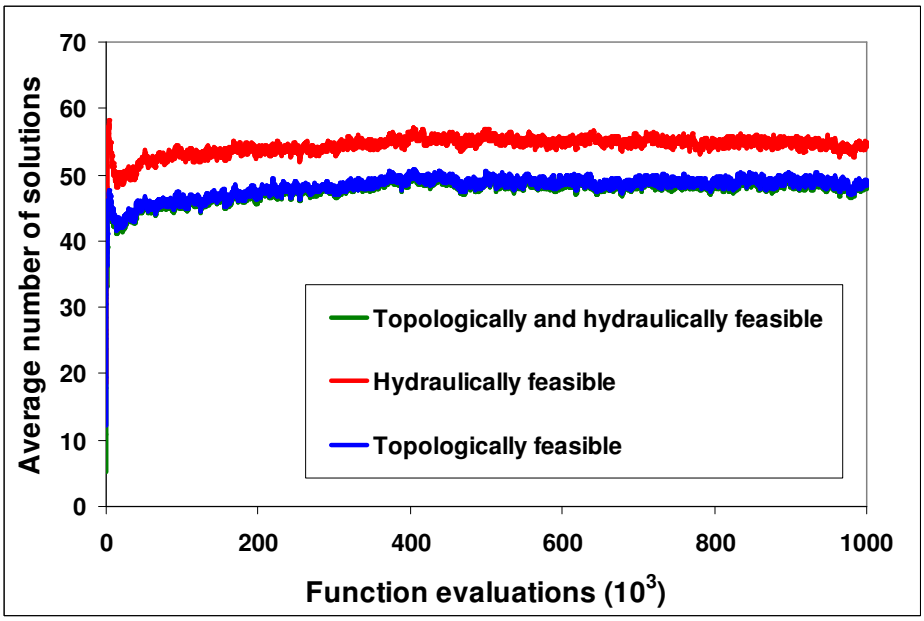

Figure 6-19: Evolution and convergence characteristics for mean number of solutions that are topologically and hydraulically feasible, hydraulically feasible, and topologically feasible based on 30 GA runs

The details of selected solutions from the merged POF that may be of interest including the hydraulically infeasible solution with the smallest residual-head constraint violation from the 30 GA runs were provided (Appendix F). In general, a solution on the right is preferable to and more expensive than a solution on the left. It can be seen that, with the exception of two designs only, the *AIM*, *HIM* and *LIM* measures reflect this in full as all three measures decrease monotonically from left to right. The entropy values increase from left to right except for a small decrease from Solution 26 that is partly looped to Solution 25 that is fully looped and from solution 9 to 2 that are both fully looped. The $ME - S$ values are small and indicate the solutions are (near-) maximum entropy solutions as desired. The $GME - ME$ values decrease monotonically from left to right as desired. The numbers of pipes (and numbers of loops) increase monotonically from left to right. Except for a small reduction in cost from Solution 9 that has four loops (15 pipes) to Solution 2 that has six loops (16 pipes), the costs increase from left to right. Solution 9 has a higher entropy value than Solution 12. Thus it seems the properties of Solutions 9 and 12 further exemplify the benefits of integrating the topology in the design optimization. It is interesting to note, however, that the surplus heads at the critical nodes seem not to follow any trend. This seems to illustrate the complex properties of the water distribution system and the many-objective optimization problem formulated and solved here. Overall, the results in Appendix F seem very satisfactory.

6.5.2 Example 2

The proposed approach is applied to a larger benchmark network in literature. This network is part of the Winnipeg system (Morgan and Goulter, 1985). This network has been designed for coupled topology and pipe size optimization in chapter 4. Allowing for pipe removal, the solution space of this network comprises a combined total of $14^{37} = 2.55\times10^{42}$ hydraulically and/or topologically feasible and infeasible solutions. Using a 4-bit binary substring, since this network has 37 pipes, each solution was represented with a chromosome whose length is 148 genes. Since a 4-bit string produces 16 binary configurations, there are two codes (out of 16) that are

redundant. Two fictitious pipe diameters of 750 and 800 mm, respectively, were allocated to the two redundant codes as explained in Section 3 of this Chapter. The pipe costs in units per metre length for the fictitious pipe diameters were taken from the cost graph shown in Figure 6.20.

An initial random population of size 100 and a stopping criterion of a maximum of 10,000 generations were used. This corresponds to a maximum limit of 10^6 function evolutions (FEs) or a sampling rate of (10^6 FEs)/(2.55×10^{42} solutions) = 1 FE per 2.55×10^{36} solutions. Selection for crossover was carried out using a binary tournament with size of 2. Single-point crossover was used to produce two offspring from two parents. The crossover probability p_c was set at p_c = 1.0, i.e. in each generation, 50 crossover operations are conducted on the parent population to produce an offspring population with size of n = 100. Once the offspring population is created, the mutation operator changes selected bits from 0 to 1 or 1 to 0 using a mutation rate of p_m = 1/148 ≈ 0.00675. This very low mutation rate reflects, on average, mutating one bit per chromosome for the whole population.

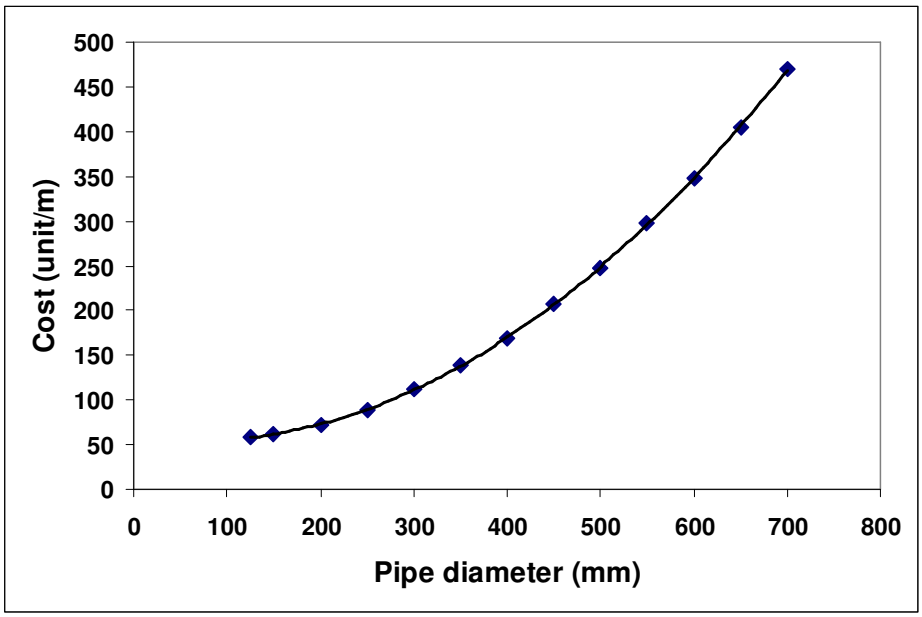

Figure 6-20: Relationship between pipe diameter and cost for network example 2

To evaluate the robustness of the GA on this larger network, 30 randomly initiated

runs were conducted using a population size of 100. It is worth mentioning that the aim of designing such a relatively large network is to demonstrate the applicability of the proposed approach to solve real world systems. To identify the optimal population size for this network, a sensitivity analysis using different population sizes is required. Within each random run, the maximum number of function evaluations (FEs) allowed here of 10^6. Among the conducted GA runs, the minimum, mean, median and maximum costs of GMEMC solution were £5,626,414; £6,814,409; £6,843,641 and £7,738,914 respectively. The standard deviation was £561,343. The minimum, mean, median and maximum values of entropy for the GMEMC solution were 4.476402; 4.872415; 4.895875 and 5.190007 respectively. The standard deviation was 0.185378.

Among the conducted 30 GA runs herein, the GME was found to have a value of 5.541571 belonging to the base graph or the full topology of the network. The inclusion of the full topology as one of the optimal layouts indicates that the incorporation of topology optimization with pipe size and entropy maximization has not affected the global search of the proposed approach. Out of 30 runs, the GME and the GMEMC design were found in one GA run. This result could be attributed to the relatively small population size and/or the complexity of the problem used to optimize this network. Increasing population size and maximum number of FEs may improve the results.

To evaluate the search performance towards including a wide range of other maximum entropy minimum cost (MEMC) solutions than the GMEMC, the *Minimum* Maximum Entropy Minimum Cost (MMEMC) solution is indicative of the range of maximum entropy groups found by the GA in each run. The minimum, mean, median and maximum costs of the MMEMC solution were £2,253,554; £2,549,198; £2,502,468and £2,925,169. The standard deviation was £179,179. The corresponding minimum, mean, median and maximum values of entropy were 2.981072, 3.140691, 3.136344 and 3.306349. The standard deviation was 0.089291. Also, the design with the smallest surplus head at the critical node was recorded in

each GA run to investigate the GA's ability to locate (near-) maximum entropy solutions close to the residual-head feasibility boundary, as a possible indicative measure of the optimality of the solutions. The minimum, mean, median and maximum smallest-surplus-heads at the critical nodes were 0.002, 0.082, 0.058 and 0.335 m, respectively. The standard deviation was 0.083 m. Table 6.3 summarizes the general characteristics of the GA from this example.

The overall consistency of the POFs achieved from the conducted runs was assessed with the hypervolume indicator after normalizing the objectives according to Eq. 6.7. The minimum, mean, median and maximum hypervolume values of the POFs were 0.642, 0.645, 0.645 and 0.648 respectively, with a standard deviation of 0.002. After merging the 100 solutions in each of the 30 POFs under the criteria of non-domination and diversity based on the crowding distance as in NSGA II, the hypervolume value of the final merged POF of 100 non-dominated solutions was 0.661. The very similar values of hypervolume indicator among the conducted runs are indicative of the robustness of the search performance of the proposed approach.

The performance of the procedure suggested for handling redundant codes appears to be encouraging. All fictitious pipe sizes are eliminated at different stages of the optimization. The minimum, median, mean and maximum numbers of function evaluations (FEs) within which fictitious pipe diameters ceased to exist in total were 13400, 39314, 41100 and 80600 respectively. The standard deviation was 14452 FEs. As anticipated, the rates of elimination were different for the two different sizes. The elimination rate seems faster for the larger and more expensive fictitious pipes (Table 6.3). These results suggest the procedure for handling redundant binary strings is stable and efficient. It is worth mentioning that, prior to their complete elimination, fictitious pipe diameters were included in both feasible and infeasible solutions.

The merged POF produced 31 fully looped maximum entropy feasible solutions and found to belong to 26 fully looped layouts (Figure 6.21a) each belongs to a unique

ME group. The achieved fully looped layouts were generated by removing a number of pipes ranged from 1 (Layout 2) to a maximum of 14 pipes (layout 26). Herein, the maximum number of removed pipes accounted for about 38% of the total number of pipes making up the base graph. The benefit of layout optimization on cost saving can be seen in the range of design costs achieved herein. For example, the cheapest fully looped feasible solution belonging to layout 24 and having a cost of 2,374,070 units was achieved by removing 12 pipes from the base graph, while the most expensive fully looped feasible solution belonging to layout 2 and with cost of 7,738,914 was generated by removing one pipe.

Table 6-3: Convergence and consistency statistics for network 2 based on 30 GA

Measure	Minimum	Mean	Median	Maximum	Standard deviation
GMEMC entropy	4.476402	4.872415	4.895875	5.190007	0.185378
MMEMC entropy	2.981072	3.140691	3.136344	3.306349	0.089291
GMEMC cost (£10^6)	5.626414	6.814409	6.843641	7.738914	0.561343
MMEMC cost (£10^6)	2.253554	2.549198	2.502468	2.925169	0.179179
Number of fully looped feasible solutions (out of 100)	37	46.207	46	52	2.631
Number of partially looped and branched feasible solutions per 100	2	8.586	9	14	3.275
Smallest surplus residual head for feasible solutions (m)	0.002	0.082	0.058	0.335	0.083
Function evaluations (FEs) for convergence	552000	905224	949800	997500	106861
Extinction of all fictitious pipes (FEs)	13400	39314	41100	80600	14452
Extinction of 800mm pipes (FEs)	5400	25914	24600	78200	16222
Extinction of 750mm pipes (FEs)	11800	39028	41100	80600	14800
Hypervolume[a]	0.642	0.645	0.645	0.648	0.002
CPU time for convergence (minutes)	69.10	113.32	118.90	124.87	13.38

[a] The hypervolume for the merged POF of 100 nondominated solutions is 0.661.

The achieved layouts demonstrate also the ability of the proposed approach to recognize important pipes to be subject for removal. For example, the vast majority of layouts were obtained by removing pipe number 35. Another important result is that some of the achieved fully looped layouts generated by dividing the base graph into two fully looped sub-networks (layouts 19-21). The number of loops in each layout ranged from 6 to 18 loops. The effect of number of loops on maximizing entropy can be seen in Table 6.4a.

In addition to the fully looped feasible solutions, seven branched and partially looped maximum entropy feasible solutions were achieved (Table 6.4b). Herein, one branched maximum entropy feasible solution with cost of 1,808,731 units and *ME-S* of zero was achieved by removing a maximum number of pipes 18 (Layout 33). This solution can be compared to the cheapest least cost solution (not maximum entropy solution) in literature having cost of 1,693,393 units (Afshar, 2005). The difference in cost of these two branched solutions is attributed to the constraint of maximizing entropy, which has not been included at all in any previous study.

Figure 6.22 shows the relationship between infeasibility and cost of the merged POF. The feasible part of the POF has been extended due to the large design space of network 2 in comparison with that of network 1. Herein, the most infeasible solution was generated by removing all the 37 candidate pipes from the base graph or fully connected network. This solution has zero cost, zero entropy, maximum topological infeasibility of 40 (i.e. 2 independent paths per node × 20 nodes) and maximum residual-head infeasibility of 1,270 m (i.e. sum of product of demand node by corresponding residual head). As stated previously, the inclusion of such design is very important from the view point of layout optimization. This is because any operation of crossover between this solution and another solution is guaranteed to create two layouts. Retention of this infeasible and self-evidently non-dominated solution throughout the entire evolution of the optimization is possible because of the penalty-free strategy applied here.

Even though this network is large, the produced range of entropy values is still narrow due to the properties of Eq. 2.42 (Figure 6.23). All feasible solutions are characterized by having high entropy values, which reflects the aim of the proposed approach to achieve high entropy feasible solutions. The effect of maximizing entropy on cost is evident from Figure 6.24. The POF herein appears to be consistent in terms of continuation between the infeasible and feasible parts.

Table 6-4a: Fully looped feasible solutions in merged POF of example 2

Solution number	Cost (units)	Surplus head[a] (m)	Critical node	Actual entropy *(S)*	Maximum entropy (ME)	*ME-S*	*GME-ME*	Layout
1	7,209,000	0.306	15	5.171049	**5.557610**[b]	0.386561	0.000000	1
2	6,563,651	0.267	19	5.109483	5.277704	0.168221	0.279906	1
3	6,392,398	0.643	19	5.051366	5.281130	0.229764	0.276480	1
4	7,738,914	0.470	15	5.190007	5.541571	0.351563	0.016039	2
5	6,756,341	0.175	19	5.137941	5.280588	0.142647	0.277022	2
6	6,672,388	0.669	19	5.075552	5.284013	0.208461	0.273597	2
7	7,601,494	0.148	15	5.181323	5.536762	0.355439	0.020848	3
8	7,399,096	0.082	15	5.130746	5.422957	0.292211	0.134653	4
9	6,376,680	0.411	15	5.022152	5.232052	0.209900	0.325558	5
10	6,894,839	0.024	15	5.061369	5.437145	0.375776	0.120465	6
11	4,916,521	0.293	15	4.594931	4.709163	0.114232	0.848447	7
12	5,307,348	0.628	8	4.672370	5.062133	0.389763	0.495477	8
13	4,957,599	0.853	15	4.641112	4.786899	0.145787	0.770711	9
14	4,774,924	1.594	15	4.498214	4.604216	0.106002	0.953394	10
15	4,698,694	0.701	15	4.498006	4.604195	0.106189	0.953415	10
16	5,552,754	1.241	15	4.655285	5.039450	0.384165	0.518160	11
17	5,025,859	3.256	13	4.556314	4.818961	0.262647	0.738649	12
18	4,394,286	0.515	17	4.320600	4.434738	0.114138	1.122872	13
19	4,235,979	3.219	20	4.177757	4.350449	0.172692	1.207161	14
20	3,372,806	2.753	7	3.836534	3.997189	0.160655	1.560421	15
21	3,230,154	1.063	1	3.802677	3.851815	0.049138	1.705795	16
22	3,960,139	0.866	7	3.956164	4.051982	0.095818	1.505628	17
23	3,538,884	0.162	7	3.800675	3.955395	0.154720	1.602215	18

24	4,433,439	6.644	7	3.976741	4.238134	0.261393	1.319476	19
25	3,426,289	3.712	7	3.693540	3.974741	0.281202	1.582869	20
26	4,039,451	1.481	17	3.795224	3.891766	0.096542	1.665844	21
27	3,107,144	1.568	13	3.503619	3.723526	0.219906	1.834085	22
28	2,454,604	0.435	20	3.287140	3.317104	0.029964	2.240506	23
29	2,374,070	0.066	19	3.203094	3.359538	0.156445	2.198072	24
30	2,561,895	1.473	19	3.179116	3.291627	0.112511	2.265983	25
31	2,460,335	1.141	8	3.130207	3.137692	0.007485	2.419918	26

[a] This refers to the surplus residual head at the critical node. The critical node is the node with the smallest surplus head in each solution. [b] The largest entropy value found.

Table 6-4b: Hydraulically feasible branched and partially looped solutions of the merged POF of example 2

Solution number	Cost (units)	Surplus head (m)	Critical node	Actual entropy *(S)*	Maximum Entropy (ME)	*ME-S*	*GME-ME*	Layout
32	2,197,697	1.550	4	3.079714	3.120364	0.040650	2.437246	27
33	1,922,166	1.045	20	2.980528	2.992726	0.012198	2.564884	28
34	2,027,732	0.040	17	2.968468	2.990397	0.021929	2.567213	29
35	1,991,802	0.045	17	2.957860	2.983705	0.025845	2.573905	30
36	3,052,542	1.358	1	2.954783	2.963028	0.008244	2.594582	31
37	3,042,543	0.371	4	2.942952	2.963028	0.020076	2.594582	32
38	1,808,731	0.371	4	2.915428	2.915428	0.000000	2.642182	33

The effect of number of pipes required to satisfy node connectivity requirement on solution cost can be noticed in Figure 6.25. Overall, as number of pipes increases cost increases. Similarly, entropy increases in line with number of pipes (Figure 6.26). This is attributed to the increase of number of loops along with number of pipes. Figure 6.27 depicts the minimum number of pipes required to construct a fully looped topology from the base graph, which are 23 pipes herein. Overall, the strong positive correlation between the number of pipes and (i) cost; (ii) entropy; and (iii) overall feasibility are evident from Figures 6.25 to 6.27. It can be seen that the proposed GA provides feasible solutions with significant differences in cost and/or

entropy for the same numbers of pipes. Figure 6.25 also reveals remarkable differences in cost from 23 to 37 pipes.

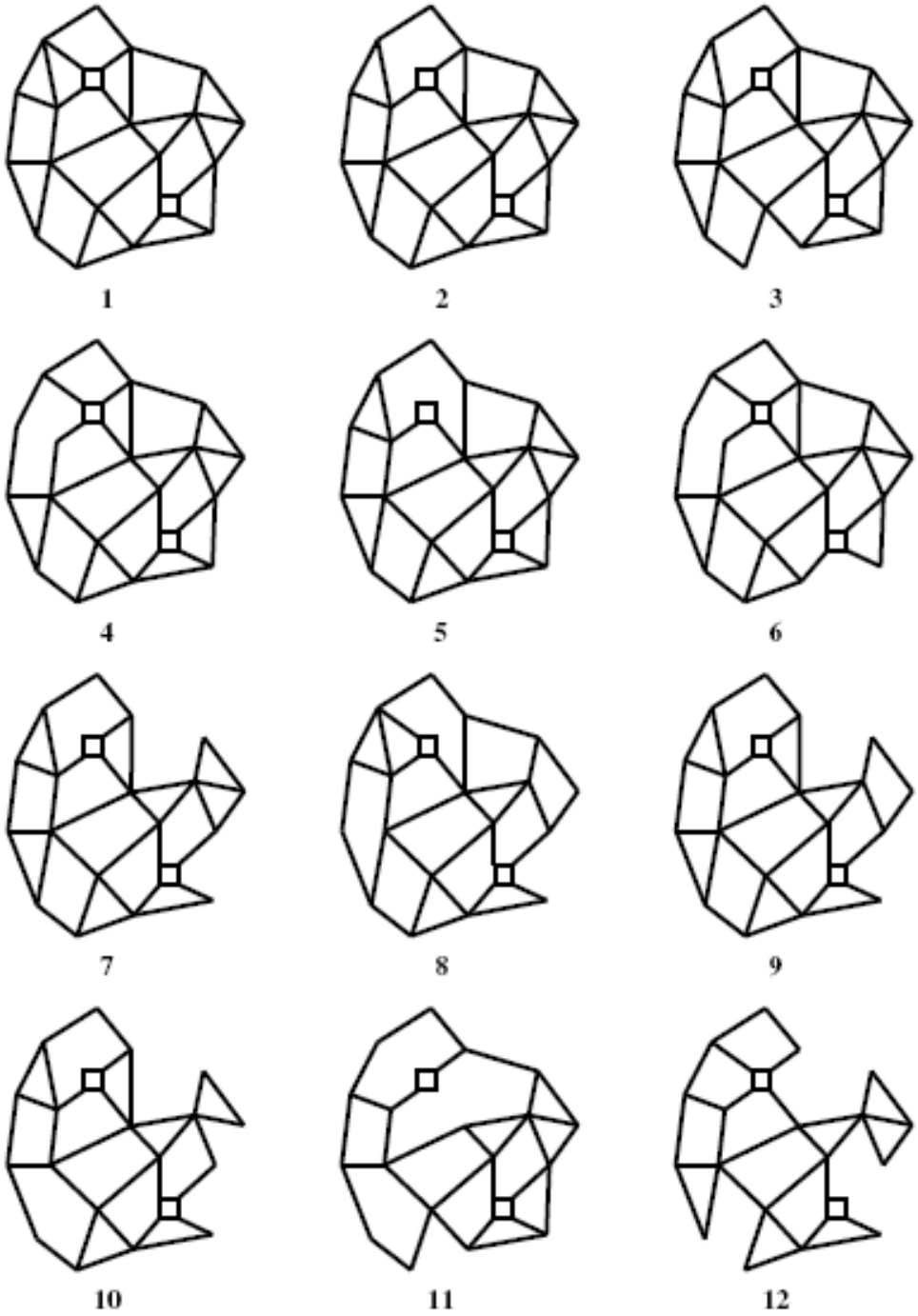

Figure 6-21a: Topologies of the fully looped hydraulically feasible maximum entropy groups for network example 2

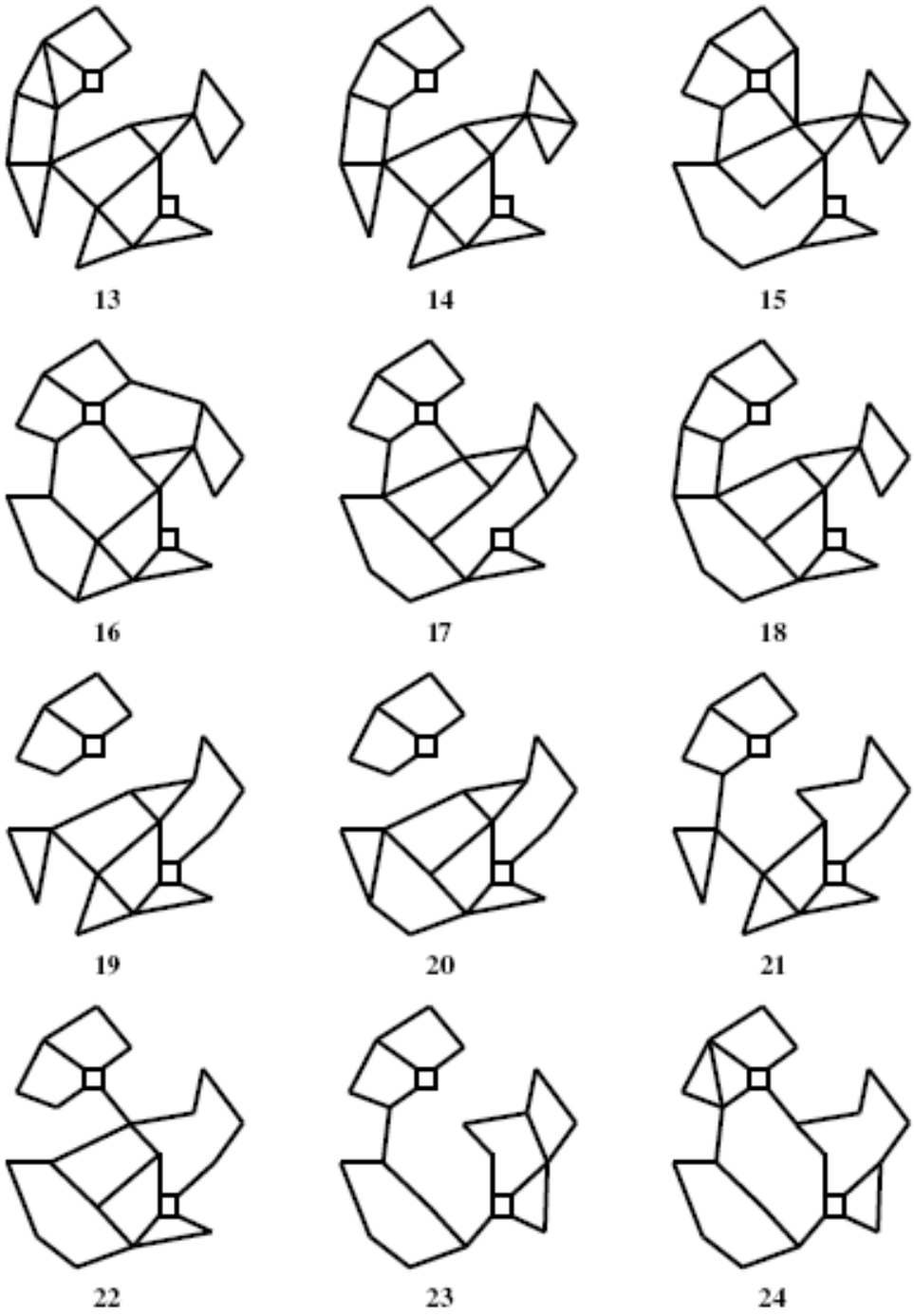

Figure 6.21a: *Continued*

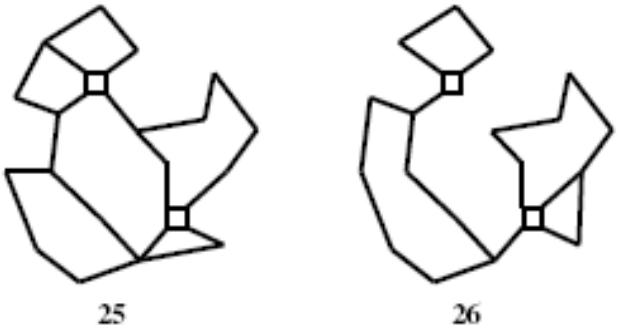

Figure 6.21a: *Continued*

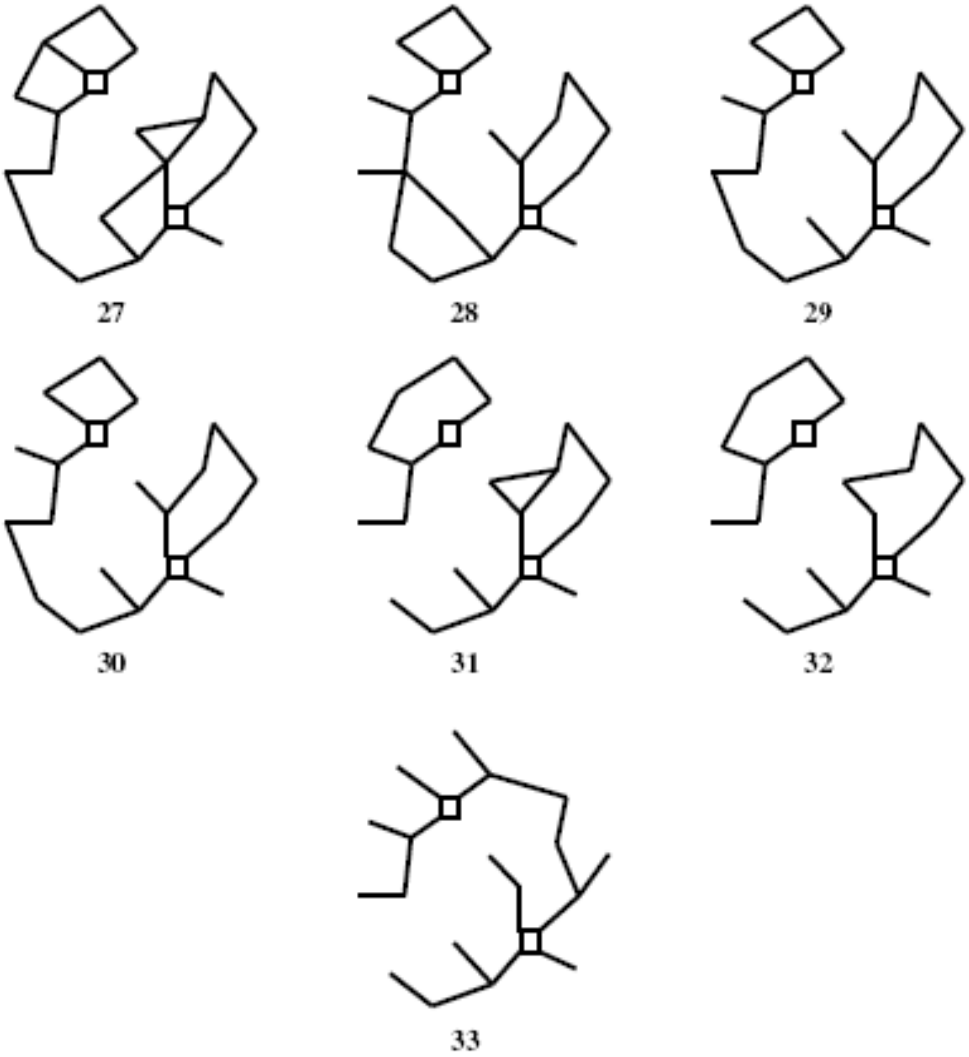

Figure 6-21b: Topologies of the branched and partially looped hydraulically feasible maximum entropy groups for network example 2.

Even though the proposed approach demonstrated giving priority to reducing topologic and hydraulic infeasibility over maximizing entropy within the topology and hydraulic infeasible region, it still associates this process with maximizing entropy. This is evident from the overall strong correlation between entropy and ME, which reflects that all solutions are near optimal with respect to ME (Figure 6.28). The result that even infeasible solutions have entropy values close to the corresponding ME shows that the proposed approach does accompany maximizing entropy with reducing topologic and hydraulic infeasibility. This could be attributed to the small amount of contribution both *ME–S* and *GME–ME* make in Eq. 6.2 in comparison with *LIM* and *HIM*. Achieving infeasible ME solutions is very beneficial to the optimization in terms of reducing the effort needed to convert an infeasible solution to a feasible one while maximizing entropy. In other words, creating a feasible solution from an infeasible one herein implies achieving a ME feasible solution. Additionally, marginally infeasible cheap solutions that are comparable to feasible solutions in terms of entropy could provide practical solutions.

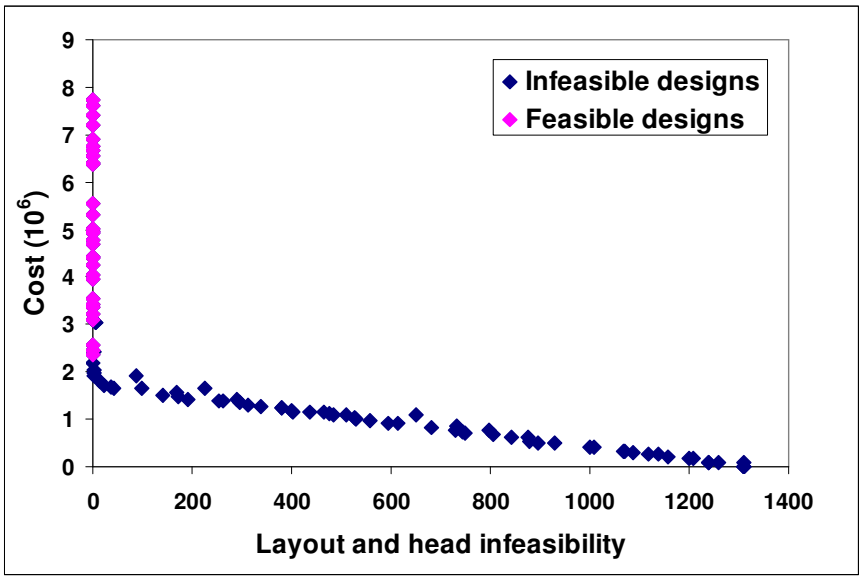

Figure 6-22: Infeasibility versus cost of merged POF for network 2

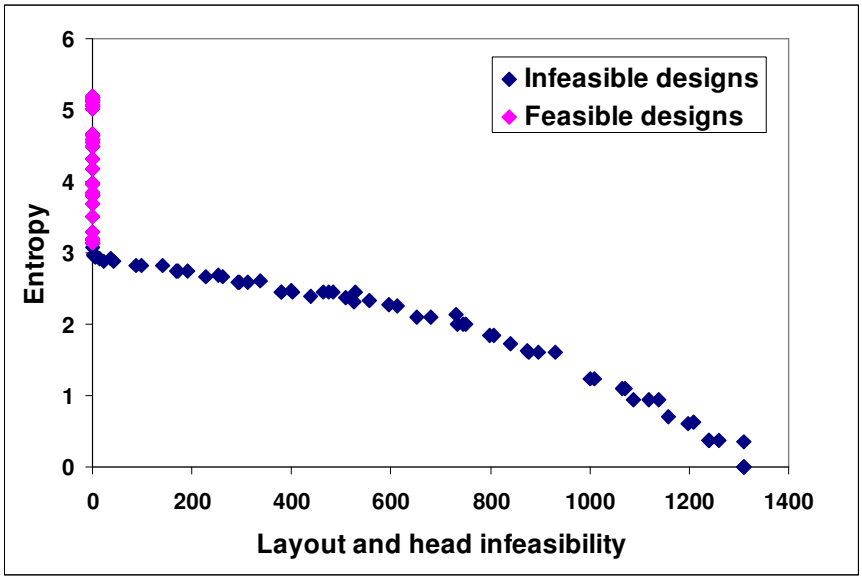

Figure 6-23: Infeasibility versus entropy of merged POF for network 2

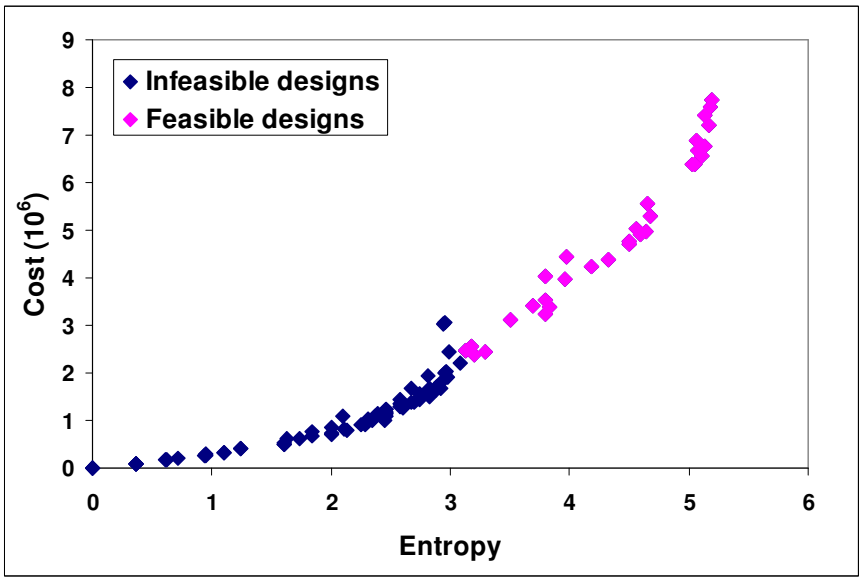

Figure 6-24: Entropy versus cost of merged POF for network 2

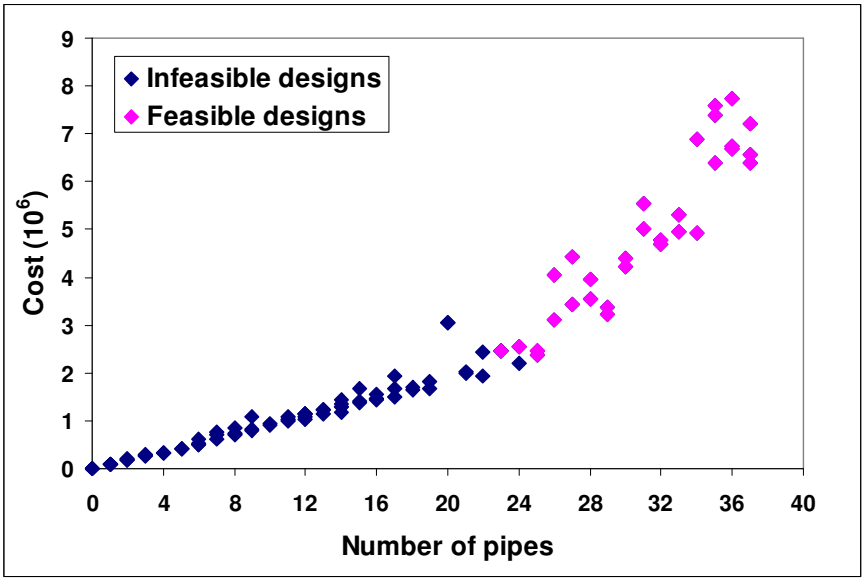

Figure 6-25: Number of pipes versus cost of merged POF for network 2

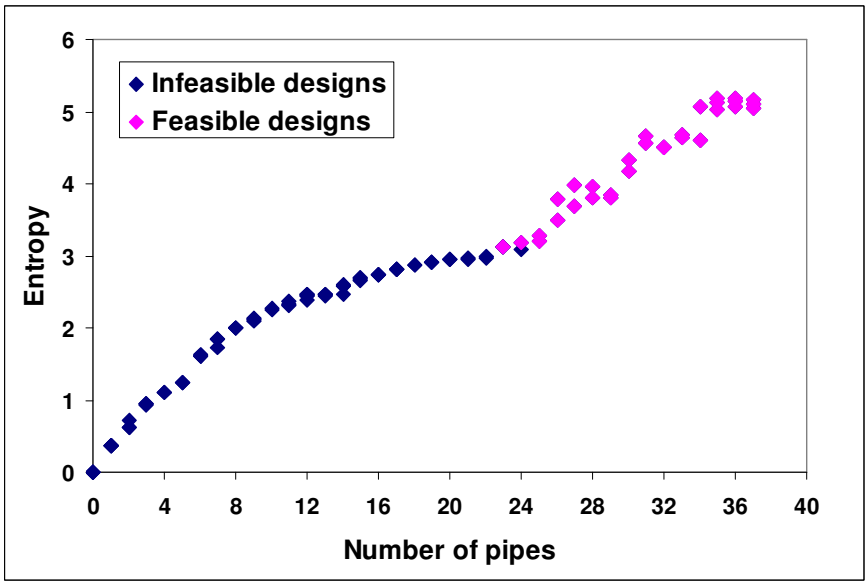

Figure 6-26: Number of pipes versus infeasibility of merged POF for network 2

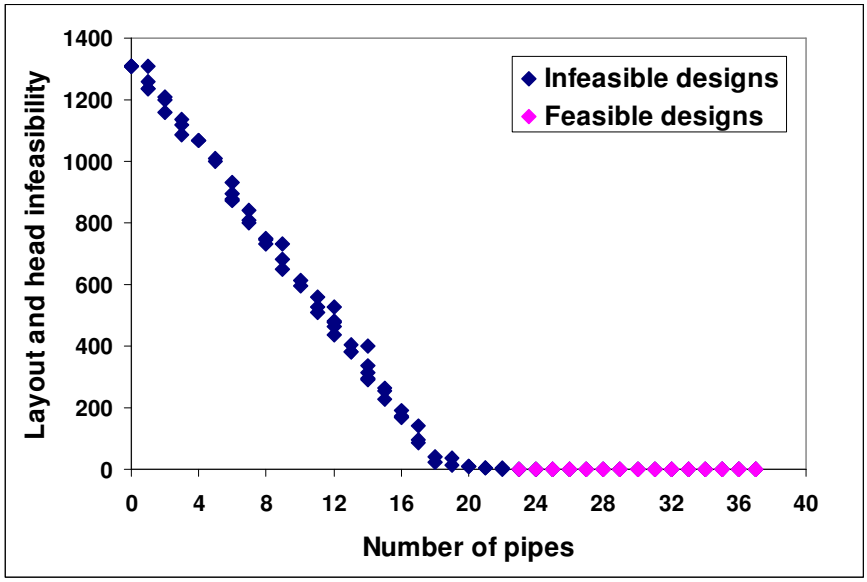

Figure 6-27: Number of pipes versus entropy of merged POF for network 2

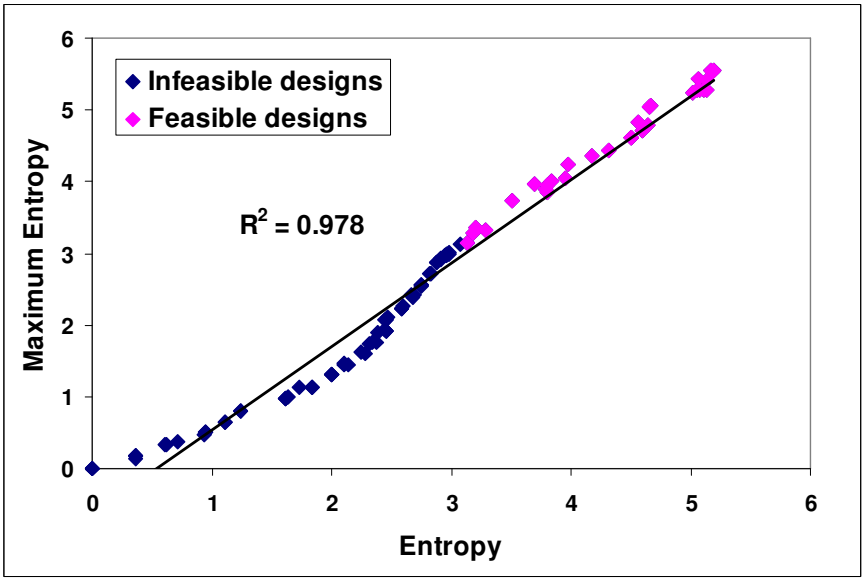

Figure 6-28: Similarity between the actual and potential entropy values of the solutions in the merged Pareto-optimal front for network 2

6.6 CONCLUSIONS

An innovative approach to the simultaneous topology, pipe size and entropy-based reliability optimization of water distribution systems has been proposed and demonstrated. The provision of many cost effective candidate solutions distributed among a diverse range of optimal topologies was the main goal. Information-theoretic entropy was used as a computationally efficient surrogate measure of the hydraulic reliability and redundancy. Reducing the computational complexity of the many-objective constrained nonlinear combinatorial optimization problem addressed here by introducing an augmented infeasibility measure that combines the residual-head infeasibility, topological infeasibility and entropy maximization without employing extraneous weighting coefficients that require additional case-specific calibration. To achieve this goal, a topological status detection procedure that enhanced the EPANET 2 hydraulic simulations was developed. A compelling feature of the formulation is that constraint-violation tournaments or penalties are not required. Accordingly, the penalty-free GA proposed allows full exploitation of all feasible and infeasible solutions generated during the evolution to guide the search. Furthermore, any redundant codes in the binary-coded GA are optimized out in a bias-free way through natural selection.

The approach produced very similar Pareto-optimal fronts from 30 different randomly generated initial GA populations for two test cases in the literature. The first one is a hypothetical network, while the other is part of a real system. The optimization model seems promising also in terms of the computational effort required to approach the Pareto-optimal front and the quality of the solutions generated. The achieved results suggest carrying out further investigations into the potential of extending the method to more complex problems with more scope for savings in cost.

CHAPTER SEVEN

CONCLUSION

7.1 INTRODUCTION

Establishing a new water distribution system capable to satisfy water demands on a long-term basis involves optimally designing the system under considerations of components topology, design cost and reliability of the system. These three optimization aspects are recognized to be highly interdependent that considering one aspect alone is not sufficient to obtain the optimal design of the WDS. As a result, the determination of the optimal topology and optimal sizing of system components along with optimally assessing reliability should be carried out in a simultaneous process if achieving the optimal design is desired. However, the simultaneous incorporation of these multiple conflicting objectives into the decision making process makes the determination of an optimal design that is superior in all objectives unachievable. Furthermore, it is highly complex to identify the best designs within a huge solution space composed of the full solution spaces of topology, design and reliability. With the massive increase in the solution space associated with real-world problems, the requirement of employing effective optimization techniques capable to handle this highly complex multiple criteria combinatorial problem is inevitable.

Given the complexity of combining topology, pipe sizing and reliability optimization of the WDS into one integrated simultaneous process, several researchers solely focused on coupling topology to pipe size optimization. The coupling of topology

with pipe size optimization is commonly carried out as a sequence of two stages where a set of optimal topologies are identified in the first stage with the aid of geometric methods such as graph theory. In the second stage, the obtained set of optimal topologies is sized to identify the optimal design under the constraint of cost while satisfying some functional requirements. In such approaches, the optimal design obtained in the second stage highly depends on the optimality of topologies obtained from the first stage. Since cost constraint is often not involved in the first stage, two-stage approaches of this type do not guarantee that the optimal topology to which the optimal design belongs is not screened out in the first stage.

Evolutionary algorithms (EA) have been widely recognized to be able to simultaneously handle multiple objectives optimization problems. Genetic algorithms (GA) classified under the high class of EA have attracted many researchers as an efficient and robust optimization technique suitable for simultaneously solving mutli-objective problems. As a result, GA based methods able to combine topology and design optimization in a simultaneous way were developed. These approaches are based on generating topology and sizing components in one optimization process. To force the search process into the feasible region, the penalizing strategy was commonly used to add extra cost to solutions violating hydraulic constraints. Even such approaches were capable to simultaneously handle the optimization processes of topology and design in one process, the optimality of solutions was severely affected by the application of penalizing strategy in two different ways. First, there is no guarantee that the penalty parameters obtained by a trial and error procedure are optimal for the system under consideration. Second, severely restricting the search procedure to the region of feasible solutions does not guarantee that the optimal topology is always located into the feasibility region.

Only few researchers have attempted to incorporate reliability into the problem of coupled topology and design optimization of the WDS. These studies were based on coupling topology and design optimization as either a two-stage or a single-stage

process, while assessing reliability of solutions obtained from the coupled topology and design optimization process(s) in a further separated stage. Since accurately assessing reliability is computationally prohibitive in practice, alternative measures of hydraulic reliability of the WDS were used. However, the relationship between topology, design and reliability is so strong that they should all be integrated in the optimization in a simultaneous way. Up to date, no approach simultaneously addressing the joint effect of topology, design and reliability has been developed in literature.

The goal of this research was to develop a robust and efficient approach able to integrate the optimization of topology, design and hydraulic reliability for a WDS in a seamless way. This development mainly coped with the issue of simultaneously searching into the huge solution space of topology, design and reliability. The research carefully solved this issue and developed a robust and practical approach able to exploit the solution space in full. As such, the search procedure takes place in both the feasible and infeasible regions of the solution space. The development was formulated in such a way that no time consuming calibrations are required to apply the approach to a WDS.

The developed approach for simultaneous optimization of topology, design and reliability of the WDS has been achieved by developing and incorporating a variety of new models coupled with employing two models available in literature. First, a new model for topology confirmation able to handle any topologic configuration of the WDS has been developed and incorporated. This model features in rectifying the unrealistic results of isolated nodes and pipes provided by the hydraulic simulator. Second, a new model for automatic detection of pipe flow directions capable to deal with any set of flow directions has been developed and incorporated. The model features in interpreting individual pipe flow directions obtained from the hydraulic simulation as a full set of flow directions. Third, a new concept for handling the many-objective WDS optimization problem has been developed and implemented. The main feature of this concept is the ability to reduce number of objectives

involved in the computational process while considering all problem objectives as being essential. Finally, a new concept for handling redundant codes associated with implementing binary coded genetic algorithms has been developed and implemented. To enhance the optimality of search procedure, the approach employs the penalty-free strategy that enables searching through the regions of feasible and infeasible solutions. Accordingly, any proposed solution whether it is hydraulically or topologically infeasible could potentially survive throughout the whole optimization process.

Two models borrowed from literature have been modified and incorporated. The EPANET 2 hydraulic model is used to determine nodal heads and pipe flows. EPANET 2 has been modified to provide realistic results when some parts of the WDS are isolated from the source. The fast non-dominated sorting and elitist NSGA II optimization model is employed to handle the multi-objective optimization problem. NSGA II has been modified in such a way that both ranking and diversity preservation are carried out within a unified search space. The approach has been successfully applied to optimize problems involving topology and design as detailed in Chapter four, design and reliability as detailed in Chapter five, and topology, design and reliability as detailed in Chapter six. This chapter provides an overall summary and general conclusions of the conducted research along with a number of recommendations suggested for future work.

7.2 SUMMARY AND CONCLUSIONS

7.2.1 Coupled topology and design optimization of WDS

The coupled topology and design optimization approach has been developed to obtain the least-cost design of the WDS as detailed in Chapter four. The approach mainly combines three models: a new algorithm developed for topology confirmation, the EPANET 2 hydraulic simulator and the fast non-dominated sorting

elitist multi-objective NSGA II optimization algorithm. The approach incorporates three main objectives that were computationally reduced to two objectives. The first objective is to minimize design cost typically taken as being function of pipe length and diameter. The second objective is to minimize topologic infeasibility to ensure that the inter-connectivity of all demand nodes is fully satisfied. This is carried out by developing and incorporating a new model for topology confirmation capable to detect and quantify the infeasibility of any generated topology. The third objective is to minimize hydraulic infeasibility to ensure that all nodal demands are satisfied in full. This is done by minimizing the deficit in nodal pressures among all demand nodes making up the proposed design.

The new model for topology confirmation has been developed to deal with any generated topology that could contain parts isolated from the supplying source(s). Both the second and third objectives were aggregated into a single objective known as infeasibility. As such, the infeasibility implements two objectives at a time. The infeasibility objective is able to recognize whether a design is both topologically and hydraulically feasible or only hydraulically infeasible or hydraulically feasible but topologically infeasible or both topologically and hydraulically infeasible. Furthermore, the infeasibility objective has provided great advantage to reducing computational complexity of the coupled topology and design problem. The penalty-free strategy proposed for handling constraints in genetic algorithms is used to enhance the convergence procedure of the approach by the potential of approaching the optimal solution through the regions of feasible and infeasible solutions. Most importantly, the penalty-free strategy has the advantage of alleviating the ad-hoc procedure encountered in applying the penalizing strategy.

The approach has been applied to three benchmark networks taken as case studies: a branched single-source hypothetical network; a branched multi-source real network; and an 18-loop multi-source real network. For the three cases, the approach has achieved new designs that are cheaper than those in literature while just exploring an extremely small part of the whole solution space. The application of the penalty-free

strategy has enabled the approach to maintain the zero-cost design generated by removing all pipes from the topology composed of the full set of pipes. This important design is advantageous to topology optimization by ensuring the action of pipe removal when selecting such a design in the reproduction process. The approach has demonstrated robustness and consistency in converging at the optimal solution when initiated from different starting points. In all case studies, the optimal solution has been identified more than once. Even in runs where the optimal solution has not been reached, the approach identified good solutions that are cheaper or marginally more expensive than those previously obtained in literature.

7.2.2 Maximum entropy design optimization of WDS

The global and local maximum entropy design optimization approach has been formulated to couple reliability with the design optimization of the WDS as detailed in Chapter 5. The reliability is measured in terms of statistical entropy previously proven to increase in line with hydraulic reliability. The approach maximizes entropy of actual pipe flows in two different ways. First, it is locally maximized with respect to the maximum entropy group to which the design belongs. Second, it is globally maximized in reference with the global maximum entropy group (GME) being the highest among all proposed designs. The approach has effectively addressed the issue of flow directions associated with calculating entropy of the WDS. A new model for automatic detection of flow directions able to handle any set of flow directions has been developed and incorporated. To calculate actual entropy and maximum entropy for each proposed design, the model assembles individual pipe flow directions obtained from the hydraulic simulation into a full set of flow directions. The formulation has also included a proposed method for handling many-objective problems. The approach mainly combines three models: a new algorithm developed for automatic detection of flow directions, the EPANET 2 hydraulic simulator and the fast non-dominated sorting elitist multi-objective NSGA II optimization algorithm.

The approach is a penalty-free many-objective problem that involves four main objectives. The first objective is to minimize design cost typically dependent on pipe length and diameter. The second objective is to minimize the total deficit in pressure among all demand nodes in order to ensure full satisfaction of nodal demands. The third objective is to locally maximize actual entropy with respect to the maximum entropy group to which the design belongs. The fourth objective is to globally maximize entropy with respect to the maximum entropy group that is the highest among all proposed designs. As such, four entities are evaluated for each proposed design: cost, hydraulic infeasibility, actual entropy and maximum entropy. The goal of maximizing entropy both locally and globally while minimizing cost and hydraulic infeasibility is to achieve a set of feasible designs well distributed between the minimum maximum entropy minimum cost design (MMEMC) and global maximum entropy minimum cost design (GMEMC).

The approach has been applied to two benchmark networks taken as case studies from literature: 6-loop single-source hypothetical network and 29-loop multi-source real system. In the first case, a new GME that is the highest in literature has been achieved. Given the approach is a many-objective problem of which the solution method experiences severe difficulties, a new method that aggregates three objectives and deals with them as being essential in the solution procedure has been proposed. An extensive analysis of the effect of aggregating objectives as opposed to separating objectives on the overall performance of the approach has been carried out. The concept of aggregating objectives outperformed that of separating objectives in terms of efficiency, robustness, performance and consistency of achieved results. Even though the approach uses penalty-free strategy, aggregating objectives was very advantageous to increasing number of feasible solutions consistently distributed between the MMEMC design and the GMEMC design. The formulation of aggregating objectives was applied to design the second case. The results showed that the approach is consistently robust and efficient in providing a significant number of optimal maximum entropy designs.

7.2.3 Joint topology, design and reliability optimization of WDS

The joint topology, design and reliability optimization approach has been developed to tackle the extremely complex design problems associated with establishing a new water distribution system while taking into consideration improving the long-term hydraulic performance of the system. The approach is the first in literature capable to identify the optimal designs based on determining topology, design and reliability of the WDS simultaneously. The approach alleviates the necessity of dividing the topology, design and reliability optimization into a sequence of separated stages as detailed in Chapter 6. The formulation couples the developed approach of coupled topology and design detailed in chapter 4 with the developed approach of design and reliability along with incorporating all involved models. As such, the merged approaches yield an extremely complex many-objective problem that involves six main objectives that form a huge objective space.

The main objectives involved include: minimizing design cost; minimizing topologic infeasibility; minimizing hydraulic infeasibility; local maximization of entropy; global maximization of entropy; and minimizing topologic complexity in the form of number of pipes making up the topology. The latter objective has been principally introduced to quantify topologic structures. Accordingly, the approach evaluates each proposed design based on determining six entities: it generates topology and accordingly quantifies topology infeasibility, sizes components making up the topology and evaluates cost, evaluates hydraulic infeasibility of the resulting design, calculates both actual and maximum entropy values and evaluates local and global maximum entropy components, and counts number of pipes. All these entities are involved in a simultaneous way and equally dealt with in the search procedure.

Due to the success of aggregating objectives concept proposed in the present research to handle the many-objective problem of the WDS, it has been applied in the present approach to tackle the increased number of involved objectives. The objectives of minimizing topologic infeasibility and minimizing hydraulic

infeasibility have been aggregated with the objectives of local and global maximization of entropy to form a single minimization objective. Accordingly, the number of objectives involved in the computational solution of the approach has been dramatically reduced by half whilst considering all aggregated objectives as being essential. In other words, no objective is considered redundant and all objectives contribute in determining the optimal solutions of the optimization process.

Motivated by the concept of generating topologies, a new rational method for handling redundant codes associated with implementing binary coded genetic algorithms has been proposed and incorporated. The concept adds a set of fictitious pipe sizes to the actual pipe sizes in order to overcome the problem of redundancy in binary coding representation.

The approach has been applied to two benchmark networks taken as case studies: 6-loop single-source hypothetical network and 18-loop multi-source real system. In both cases, the approach demonstrated the ability to identify the effect of topology optimization on saving cost and increasing reliability. The topology composed of the minimum number of pipes satisfying topologic constraint has been indentified to produce the MMEMC design, which is the cheapest feasible maximum entropy design. The topology composed of the full set of pipes has been maintained to yield the GMEMC design, which is the most reliable design in terms of maximum entropy. In between these two designs, a variety of maximum entropy minimum cost designs with different compromise between cost and entropy have been obtained.

The approach even has demonstrated ability to maintain hydraulically feasible designs not satisfying topologic constraints. Further cheaper hydraulically feasible maximum entropy designs belonging to branched and partially looped topologies have been obtained. Thanks to the penalty-free strategy that enabled maintaining the zero-cost design that enhances generating new topologies in each optimization process. The results obtained from the concept of fictitious pipe sizes have been

encouraging. All fictitious pipe sizes have been selected naturally in the early generations of the search process. Then, they were gradually removed one by one starting with the largest fictitious pipe size.

7.3 SUGGESTIONS FOR FUTURE WORK

The present research has addressed a great scope of the WDS design optimization problem. However, there are still some gaps need to be filled by carrying out further investigation in order to improve and complete the present study to cover a wider scope of the WDS optimization problem. The main issues suggested herein are presented and discussed below.

The difficulty associated with searching into the huge search space of topology, design and reliability of the WDS has been demonstrated to be extremely large for real-world systems. The developed approach for joint topology, design and reliability optimization of the WDS has been shown to be efficient and robust when applied to small networks. This completely clears the way for extending the scope of the present research to cover aspects that can enhance the search procedure of the GA. One suggestion towards that is to apply the concept of search space reduction in order to improve the convergence properties of the GA. This can be done in line with conducting further sensitivity analyses on optimality of GA parameters that suit a particular problem such as the effect of population size on convergence properties of the GA.

The success of the developed topology, design and reliability optimization approach in obtaining optimal designs for networks analysed under steady-state condition strongly suggests extending the present study to cover longer periods of time using extended period simulation analysis. This will widen the scope of the optimal maximum entropy minimum cost designs to include the operation of pumps, storage tanks and valves. As such, further operating conditions other than focusing on the

peak periods considered in steady-state analysis need to be incorporated in the suggested the extended scope.

The suggestion of coupling the present research with rehabilitation of the WDS is also worth investigating. The action of removing a pipe taken in the topology optimization could provide better decision than the action of lining or adding a parallel pipe taken in the rehabilitation process.

One important aspect suggested for widening the scope of the present research is to investigate the effect of the developed approach on water quality. The developed approach integrates the EPANET hydraulic model and the multi-objective NSGA II. EPANET 2 is able to evaluate different parameters for measuring water quality such as water age that can be handled as a minimization objective by NSGA II. The incorporation of water quality into the present research appears to be highly feasible and can be easily implemented.

The development of a new method proposed for handling redundant codes in binary coded genetic algorithms suggests that the time is ripe to assess and carry out further investigations on the performance of the proposed method in comparison with other methods proposed in GA literature. One aspect need to be investigated is the effect of the method of handling redundant codes on the convergence properties of the GA.

Another important aspect suggested for extending the present research scope is to employ more realistic hydraulic analysis model. The present research employs the demand-dependent analysis model (DDA) to evaluate nodal heads and pipe flows that satisfy hydraulic constraints. The DDA model experiences serious limitations when there is no sufficient pressure within a network. It yields misleading and unrealistic nodal pressures because of the assumption that all nodal demands are always fully satisfied irrespective of available nodal heads. The pressure dependent analysis models (PDA) are more realistic in depicting the behaviour of the WDS. They consider nodal demands as being dependent on nodal heads. Replacing the

DDA model with a PDA model such as EPANET-PDX (Seiw and Tanyimboh, 2011) is therefore worth doing. Accurately evaluating the hydraulic performance in the region of infeasible solutions could effectively enhance guiding the search procedures towards optimal solutions especially when large proportions of infeasible solutions are generated.

The present research implements the fast non-dominated sorting elitist NSGA II optimization model using the basic operators of single-point crossover and single bit-wise random mutation operator. Using more advanced operators to implement the operations of crossover and mutation could enhance the search process by further exploration and exploitation of the search space. Some suggested operators could include multi-point or uniform crossover, direction-based crossover, arithmetic crossover, directional mutation, inversion mutation and insertion mutation.

REFERENCES

Afshar, M.H., Akbari, M., and Marino, M.A., 2005a. Simultaneous layout and size optimization of water distribution networks: engineering approach. *Journal of Infrastructure Systems,* 11(4), 221-230.

Afshar, M.H., 2005b. Application of max-min ant system for joint layout and size optimization of pipe networks. *9th International Water Technology Conference*, IWTC9, 17-20 March, Sharm El-Sheikh, Egypt, 593-608.

Afshar, M.H. and Jabbari, Ibrahim. 2007a. Simultaneous layout and size optimization of pipe networks using genetic algorithms. *The Arabian Journal for Science and Engineering,* 33(2B), 391-409.

Afshar, M.H., 2007b. Evaluation of selection algorithms for Simultaneous layout and size optimization of water distribution networks. *Scientia Iranica,* 14(1), 23-32.

Alperovits, E., and Shamir, U., 1977. Design of optimal water distribution systems. *Water Resource Research*, 13(6), 885-900.

Ang, W. K., and Jowitt, P. W., 2005a. Some new insights on informational entropy for water distribution networks. *Engineering Optimization*, 37(3), 277-289.

Ang, W. K., and Jowitt, P. W., 2005b. Path entropy method for multiple-source water distribution networks. *Engineering Optimization*, 37(7), 705-715.

Awumah, K., Bhatt, S.K., and Goulter, I.C., 1989. An integer programming model for layout design of water distribution networks. *Engineering Optimization*, 15(1), 57-70.

Awumah, K., Goulter, I.C., and Bhatt, S.K., 1990. Assessment of reliability in water distribution networks using entropy-based measures. *Stochastic Hydrology and Hydraulics*, 4(4), 325-336.

Awumah, K., Goulter, I., and Bhatt, S. K., 1991. Entropy-based redundancy measures in water distribution network design. *Journal of Hydraulic Engineering*, 117(5), 595-614.

Awumah, K., and Goulter, I., 1992. Maximizing entropy-defined reliability of water distribution networks. *Engineering Optimization*, 20(1), 57-80.

Back, T., Fogel, D. B., and Michalewicz, Z., 1997. *Handbook of Evolutionary Computation*. New York: Taylor & Francis Group.

Baños, R., Reca, J., Martínez, J., Gil, C., and Márquez, A., 2011. Resilience indexes for water distribution network design: a performance analysis under demand uncertainty. *Water Resources Management*, 25(10), 2351–2366.

Bhave, R.P., and Gupta, R., 2006. *Analysis of Water Distribution Networks*. UK: Alpha Science International Ltd.

Bolc, L., and Cytowski, J., 1992. *Search Methods for Artificial Intelligence*. London: Academic Press.

Cembrowicz, R.G., 1992. Water Supply Systems Optimization for Developing Countries. *In*: B. Coulbeck and E. Evans, eds. *Pipeline Systems (Fluid Mechanics and its Applications)*. London: Kluwer Academic, 59-76.

Chandapillai, J., 1991. Realistic simulation of water distribution systems. *Journal of Transportation Engineering*, 117 (2), 258-263.

Creaco, E., Franchini, M., and Alvisi, S., 2010. Optimal Placement of Isolation Valves in Water Distribution Systems Based on Valve Cost and Weighted Average Demand Shortfall. *Water Resources Management*, 24(15), 4317-4338.

Creaco, E., Franchini, M., and Alvisi, S., 2012. Evaluating Water Demand Shortfalls in Segment Analysis. *Water Resources Management*, 26(8), 2301-2321.

Cullinane, M.J., Lansey, K.E., and Mays, L.W., 1992. Optimization-availability-based design of water distribution networks. *Journal of Hydraulic Engineering*, 118(13), 420-441.

Cunha, M. C., and Sousa, J., 2001. Hydraulic infrastructures design using simulated annealing. *Journal of Infrastructure Systems*, *7*(1), 32–39.

Cunha, M. C., and Ribeiro, L., 2004. Tabu search algorithms for water network optimization. *European Journal of Operational Research*, 157, 746-758.

Czajkowska, A., and Tanyimboh, T.T., 2013. Water distribution network optimization using maximum entropy under multiple loading patterns. *Water Science and Technology*, Water Supply, in press.

Dandy, G. C., Simpson, A. R., and Murphy, L. J., 1996. An improved genetic algorithm for pipe network optimization. *Water Resources Research*, 32(2), 449–458.

Davidson, J.W., and Goulter, I.C., 1995. Evolution Program for Design of Rectilinear Branched Networks. *Journal of Computing in Civil Engineering*, 9(2), 112-121.

Deb, K., Pratap, A., Agarwal, S., and Meyarivan, T., 2002. A fast and elitist multiobjective genetic algorithm: NSGA-II. *IEEE Transactions on Evolutionary Computation,* 6(2), 182-197.

Djebedjian, B., Yaseen, A. and Ezzeldin. R., 2008. Reliability-Based Optimization of Layout and Sizing of Water Distribution Systems. *12th International Water Technology Conference*, IWTC12, 27-30 March Alexandria, Egypt, 759-779.

Dnan, N., Mays, L. W., and Lansey, K. E., 1990. Optimal reliability-based design of pumping and distribution systems. *Journal of Hydraulic Engineering*, 116(2), 249-268.

Dorigo, M., 1992. *Optimization, Learning and Natural Algorithms*. Thesis (PhD). Politecnico di Milano, Italy.

Dridi, L., Parizeau, M., Maihot, A., and Villeneuve, J-P, 2008. Using evolutionary optimization techniques for scheduling water pipe renewal considering a short planning horizon. *Computer-Aided Civil and Infrastructure Engineering*, 23(8), 625-635.

Eshelman, L., and Shaffer, J., 1993. Real-coded genetic algorithms and interval-schemata, *In*: Whitley, L., ed. *Foundations of Genetic Algorithms*, San Francisco: Morgan Kaufmann Publishers, volume 2, 187-202.

Eusuff, M. M., and K. E. Lansey, 2003. Optimisation of water distribution network design using shuffled frog leaping algorithm. *Journal Water Resources Planning and Management*, *129*(3), 210–225.

Fogel, L., Owens, A., and Walsh, M., 1966. *Artificial Intelligence through Simulated Evolution*. New York: John Wiley and Sons.

Fonseca, C., and Fleming, P., 1993. Genetic Algorithms for Multiobjective Optimization: Formulation, Discussion and Generalization. *5th International Conference on Genetic Algorithms*, July 1993 San Francisco. USA: Morgan Khaufmann, 416-423.

Fonseca C.M., and Fleming P.J., 1998a. Multi-objective optimization and multiple constraint handling with evolutionary algorithms – Part I: A unified formulation. *IEEE Transactions on Systems*, *Man*, *and Cybernetics*, *Part A*, 28, 26-37.

Fonseca, C.M., and Fleming, P.J., 1998b. Multi-objective optimization and multiple constraint handling with evolutionary algorithms – Part II: Application example. *IEEE Transactions on Systems*, *Man*, *and Cybernetics*, *Part A*, 28, 38-47.

Fujiwara, O., and Ganesharajah, T., 1993. Reliability assessment of water supply systems with storage and distribution networks. *Water Resources Research*, 29(8), 2917-2924.

Geem, Z.W., Kim, J.H., and Yoon, Y.N., 2000. Optimal Layout of Pipe Networks Using Harmony Search. *4th International Conference on Hydro-Science and Engineering*. 26-29 September, Seoul, South Korea.

Geem, Z. W., Kim, J. H., and Loganathan, G. V., 2002. Harmony search optimization: Application to pipe network design. *International Journal of Modelling and Simulation*, *22*(2), 125–133.

Gen, M., and Cheng, R., 1997. *Genetic Algorithms and Engineering Design*. New York: John Wiley and Sons.

Gen, M., and Cheng, R., 2000. *Genetic Algorithms and Engineering Optimization*. New York: John Wiley and Sons.

Gen, M., Cheng, R., and Lin, L., 2008. *Network Models and Optimization*. London: Springer-Verlag.

Germanopoulos, G., 1985. A technical note on the inclusion of pressure dependent demand and leakage terms in water supply network models. *Civil Engineering Systems*, 2, 171-179.

Gessler, J., 1985. Pipe network optimization by enumeration. *In*: Harry C. Torno, ed. *Speciality Conference*: *Computer Applications in Water Resources*, 10-12 July 1985 New York. Washington: ASCE, 572-581.

Glover, F., and Greenberg, H., 1989. New approaches for heuristic search: a bilateral linkage with artificial intelligence. *European Journal of Operational Research*, 39, 19-130.

Gupta, R., and Bhave, P. R., 1996. Comparison of methods for predicting deficient network performance. *Journal of Water Resource Planning and Management*, 122(3), 214-217.

Goldberg, D. E., 1989. *Genetic algorithms in search, optimization and machine learning*. 1st ed. USA: Addison-Wesley Longman Publishing Co.

Goldberg, D. E., Korb, B., and Deb, K., 1989. Messy genetic algorithms: motivation, analysis, and first results. *Complex Systems*, 3, 493–530.

Goldberg, D. E., and Deb, K., 1991. A comparative Analysis of Selection Schemes Used in Genetic Algorithm. *Foundations of Genetic Algorithms*, 69-93.

Halhal, D., Walters, G. A., Ouazar, D., and Savic, D. A., 1997. Water network rehabilitation with structured messy genetic algorithm. *Journal Water Resources Planning and Management*, 123(3), 137146.

Herrera, F., Lozano M., and Verdegay J.L., 1998. Tackling real-coded genetic algorithms: Operators and tools for behavioural analysis. *Artificial Intelligence Review*, 12, 265–319.

Holland J., 1975. *Adaptation in Natural and Artificial Systems*. Michigan: University of Michigan Press.

Holland, J. H., 1976. Adaptation. *In*: Rosen, R., and Snell, F. M., (eds). *Progress in Theoretical Biology*, volume 4. New York: Academic Press, 263-293.

Ishibuchi, H., and Murata, T., 1998. A multiobjective genetic local search algorithm and its application to flowshop scheduling. *IEEE Transactions on Systems*, *Man and Cybernetics-Part C: Applications and Reviews*, 28(3), 392-403.

Jayaram, N., and Srinivasan, K., 2008. Performance-based optimal design and rehabilitation of water distribution networks using life cycle costing. *Water Resources Research*, 44(1).

Kennedy, J., and Eberhart, R. C., 2001. *Swarm Intelligence*. USA: Morgan Kaufmann Publishers.

Kessler, A., Ormsbee, L., and Shamir, U., 1990. A Methodology for Least-Cost Design of Invulnerable Water Distribution Networks. *Civil Engineering Systems,* 7(1), 20-28.

Khinchin, A. I., 1953. The entropy concept in probability theory. *Uspekhi Mathematicheskikh Nauk*, 8(3), 3-20. Translation in Khinchin, A. I., 1957.

Knowles, J., 2005. A hybrid algorithm with on-line landscape approximation for expensive multiobjective optimization problems. *IEEE Transactions on Evolutionary*

Computations, 10(1), 50-66.

Kougias, I.P., and Theodossiou, N.P., 2013. Multi-objective pump scheduling optimization using harmony search algorithm and polyphonic HSA. *Water Resources Management*, 27(5), 1249-1261.

Koza, J. R., 1992. *Genetic Programming*. Cambridge: MIT Press.

Lansey, K. E., Duan, N., Mays, L. W., and Tung, Y. K., 1989. Water distribution system under uncertainties. *Journal Water Resources Planning and Management*, 115(5), 630-644.

Lansey, K. E., and Mays, L. W., 1989. Optimization model for water distribution systems design. *Journal of Hydraulic Engineering*, 115(10), 1401-1418.

Loubser, B. F., and Gessler, J., 1990. Computer-aided optimization of water distribution networks. *The Civil Engineering*, 413-422.

Maier, H. R., Simpson, A. R., Zecchin, A. C., Foong, W. F., Phang, K. Y., Seah, H. Y., and Tan, C. L., 2003. Ant colony optimization for the design of water distribution systems. *Journal Water Resources Planning and Management*, *129*(3), 200–209.

Martin, D. W., and Peters, G., 1963. The application of Newton's method to network analysis by digital computer. *Journal of the Institute of Water Engineers*, 17, 115-129.

Mays, L.W., 2002. *Urban water supply*. USA: McGraw Hill.

McCormick, W. T., Scheitzer, P. J., and White, T. W., 1972. Problem decomposition and data reorganization by a cluster technique. *Operations Research*, 20(5), 993-1009.

Michalewicz, Z., 1994. *Genetic Algorithm + Data Structure = Evolution Programs*. New York: Springer-Verlag.

Michalewicz, Z., 1995. A survey of constraint handling techniques in evolutionary computation methods. *In*: McDonnell et al. eds. *Evolutionary Programming IV*, Massachusetts: MIT Press, 135-158.

Montesinos, P., Garcia-Guzman, A., and Ayuso, J. L., 1999. Water distribution network optimization using modified genetic algorithm. *Water Resources Research*, *35*(11), 3467–3473.

Morgan, D.R., and Goulter, I.C., 1982. Least cost layout and design of looped water distribution systems. *9th International Symposium on Urban Hydrology, Hydraulics and Sediment control*, University of Kentucky, Lexington, KY, USA, 27-30.

Morgan, D.R. and Goulter, I.C., 1985. Optimal Urban Water Distribution Design. *Water Resources Research,* 21(5), 642-652.

Murphy, L. J., and Simpson, A. R., 1992. Pipe optimization using genetic algorithms. *Research Report No. R93*, Department of Civil Engineering, University of Adelaide, Australia.

Murphy, L. J., Simpson, A. R., and Dandy, G. C., 1993. Pipe network optimization using an improved genetic algorithm. *Research Report No. R109*, Department of Civil Engineering, University of Adelaide, Australia.

OFWAT, 2004. Levels of Service for the Water Industry in England and Wales: 2002-2003 Report. Ofwat Centre, 7 Hill Street, Birmingham B5 4UA, UK.

OFWAT, 2008. *Guaranteed Standard Schemes* [online]. Ofwat. Available from: http://www.ofwat.gov.uk/consumerissues/rightsresponsibilities/waterpressure [Accessed 29 January 2012].

Prasad, T.D., and Park, N.S., 2004. Multi-objective genetic algorithms for design of water distribution networks. *Journal of Water Resources Planning and Management*, 130(1), 73-82.

Raad, D.N., Sinske, A.N., and van Vuuren, J.H., 2010. Comparison of four reliability surrogate measures for water distribution systems design. *Water Resources Research*, 46(5), W05524.

Ray, T., Tai K., and Seow, C., 2001. An evolutionary algorithm for multiobjective optimization. *Engineering Optimization*, 33(3), 399-424.

Reca, J., Martinez J., Banos R., and Gil, C., 2008. Optimal design of gravity-fed looped water distribution networks considering the resilience index. *Journal of Water Resources Planning and Management*, 134(3), 234-238.

Rechenberg, I., 1973. *Optimieriung technischer Systeme nach Prinzipien der biologischen*. Stuttgart: Frommann-Holzboog.

Rowel, W.F. and Barnes, J.W., 1982. Obtaining the Layout of Water Distribution Systems. *Journal of the Hydraulics Division*, 108(1), 137-148.

Rossman, L.A., 2000. *EPANET 2: Users Manual*. Cincinnati, USA: U.S. Environmental Protection Agency.

Saleh, Salah H.A., and Tanyimboh, T.T., 2011. Global maximum entropy minimum cost design of water distribution systems. *13th International Water Distribution Systems Analysis Symposium,* 22-26 May 2011, Palm Springs, California. USA: ASCE, 206-213.

Saleh, Salah H.A., and Tanyimboh, T.T., 2012. Joint Pipe Size and Reliability Design Optimization of Water Distribution Systems. *10th International Conference on Hydroinformatics,* 14-18 July, 2012 Hamburg.

Saleh, S., Barlow, E., and Tanyimboh, T.T., 2012. Unbiased and accurate assessment of surrogate measures of hydraulic reliability of water distribution systems. *14th Water Distribution Systems Analysis Conference*, 24-27 September 2012 Adelaide, Australia: 148-157.

Savic, D., and Banyard, J., 2011. *Water Distribution Systems*. UK: ICE Publishing.

Saxena, K. S., Duro, J. A., Tiwari, A., and Deb, K., 2013. Objective reduction in many-objective optimization: Linear and non-linear algorithms. *IEEE Transactions on Evolutionary Computation*, 17(1), 77-99.

Setiadi, Y., Tanyimboh, T.T., and Templeman, A.B., 2005. Modelling errors, entropy and the reliability of water distribution systems. *Advances in Engineering Software*, 36(11-12), 780-788.

Shannon, C., 1948. A mathematical theory of communication. *Bell Systems Technical Journal*, 27(3), 379-428.

Siew, C., and Tanyimboh, T.T., 2011. The computational efficiency of EPANETPDX. *13th International Water Distribution Systems Analysis Symposium,* 22-26 May 2011, Palm Springs, California. USA: ASCE, 206-213.

Siew, C., and Tanyimboh, T.T., 2012. Penalty-Free Feasibility Boundary Convergent Multi-Objective Evolutionary Algorithm for the Optimization of Water Distribution Systems. *Water Resources Management*, 26(15), 4485-4507.

Swamee, Prabhata K. and Sharma, Ashock K., 2008. *Design of Water Supply Pipe Networks*. New Jersey: John Wiley & Sons.

Tanyimboh, T.T., 1993. *An Entropy-based Approach to the Optimum Design of Reliable Water Distribution Networks*. Thesis (PhD), University of Liverpool.

Tanyimboh, T.T., and Sheahan, C., 2002. A maximum entropy based approach to the layout optimization of water distribution systems. *Civil Engineering and Environmental Systems,* 19(3), 223-253.

Tanyimboh, T.T. and Setiadi, Y., 2008. Joint layout, pipe size and hydraulic reliability optimization of water distribution systems. *Engineering Optimization,* 40(8), 729-747.

Tanyimboh, T.T., 1993. *An Entropy-based Approach to the Optimum Design of Reliable Water Distribution Networks*. Thesis (PhD), University of Liverpool.

Tanyimboh, T.T., and Templeman, A.B., 1993a. Maximum entropy flows for single-source networks. *Engineering Optimization*, 22(1), 49-63.

Tanyimboh, T.T., and Templeman, A.B., 1993b. Calculating maximum entropy flows in networks. *Journal of Operational Research Society*, 44(4), 383-396.

Tanyimboh, T.T., and Templeman, A.B., 1993c. Optimum design of flexible water distribution networks. *Civil Engineering Systems*, 10(3), 243-258.

Tanyimboh, T. T., and Templeman, A. B., 1998. Calculating the reliability of single source networks by source head method. *Advances in Engineering Software*, 29(7-9), 449-505.

Tanyimboh, T.T., and Templeman, A.B., 2000. A quantified assessment of the relationship between the reliability and entropy of water distribution systems. *Engineering Optimization*, 33(2), 179-199.

Tanyimboh, T. T., and Templeman, A. B., 2004. A new nodal outflow function for water distribution networks. *In*: BHV Topping and CA Mota Soares (Eds.). *4th International Conference on Engineering Computational Technology,* 7-9 September 2004 Lisbon. UK: Civil- Comp Press., Paper 64.

Tanyimboh, T.T., and Templeman, A.B., 2010. Seamless pressure-deficient water distribution system model. *Water Management,* 163(8), 389-396.

Tanyimboh, T.T., Tietavainen, M.T. and Saleh, S., 2011. Reliability assessment of water distribution systems with statistical entropy and other surrogate measures. *Water Science and Technology*, *Water Supply*, 11(4), 437-443.

Todini, E., 2000. Looped water distribution networks design using a resilience index based approach. *Urban Water*, 2(2), 115-122.

Todini, E., and Pilati, S., 1988. A gradient algorithm for the analysis of pipe networks. In: Coulbeck, B. and Orr, C-H (eds.). *Computer Applications in Water Supply*, Volume 1, England: Research Studies Press Ltd, 1-20.

Vaabel, J., Ainola, L., and Koppel, T., 2006. Hydraulic power analysis for determination of characteristics of a water distribution system. *8th Annual Water Distribution Systems Analysis Symposium*, Cincinnati, Ohio, USA, 1-9.

Vasan, A., and Simonovic, S. P., 2010. Optimization of water distribution network design using differential evolution. *Journal Water Resources Planning and Management*, *136*(2), 279–287.

Vining, G., and Kowalski, S.M., 2006. *Statistical Methods for Engineers*. Boston: Cengage Learning.

Wagner, J. M., Shamir, U., and Marks, D. H., 1988. Water distribution reliability: simulation methods. *Journal of Water Resources Planning and Management*, 114(3), 276-294.

Wagner, J.M., Shamir, U., and Marks, D. H. 1988. Water distribution reliability: analytical methods, *Journal of Water Resources Planning and Management*, 114(3), 253-275.

Walters, G.A. and Lohbeck, T.K., 1993. Optimal Layout of Tree Networks Using Genetic Algorithms. *Engineering Optimization,* 22(1), 27-48.

Walters, G.A., and Smith, D.K., 1995. Evolutionary Design Algorithm for Optimal Layout of Tree Networks. *Engineering Optimization,* 24(4), 261-281.

Wood, D., and Charles, C., 1972. Hydraulic network analysis using linear theory. *Journal of Hydraulics Division*, volume 98, No. HY7, 1157-1170.

Wu, W., Maier, H., and Simpson, A., 2011. Surplus power factor as a resilience measure for assessing hydraulic reliability in water transmission system optimization. *Journal of Water Resources Planning and Management*, 137(6), 542-546.

Wu, Z. Y., Boulos, P. F., Orr, C. H., and Ro, J. J., 2000. An efficient genetic algorithm approach to an intelligent decision support system for water distribution networks. *The Hydroinformatics*, 26-29 July 2000 Iowa.

Wu, Z. Y., and Simpson, A. R., 1996. Messy genetic algorithms for optimization of water distribution systems. *Research Report No. R140*, Department of Civil Engineering, University of Adelaide, Australia.

Wu, Z. Y., and Simpson, A. R., 1997. An efficient genetic algorithm paradigm for discrete optimization of pipeline networks. *International Congress on Modeling and Simulation*, 8-11 December 1997 Hobart, Tasmania, Australia.

Yassin-Kassab, A., Templeman, A.B., and Tanyimboh, T.T., 1999. Calculating maximum entropy flows in multi-source, multi-demand networks. *Engineering Optimization*, 31(6), 695-729.

Yazdani, A., Otoo, R.A., and Jeffrey, P., 2011. Resilience enhancing expansion strategies for water distribution systems: a network theory approach. *Environmental Modelling and Software*, 26(12), 1574-1582.

APPENDIX A

TOPOLOGICAL STATUS DETECTION PROCEDURE

This brief appendix provides an outline description of the topological status detection procedure in Steps 1-4 below (i.e. Figs. A1a-d) using the network of Example 1 from EPANET 2. Pipes 111, 112 and 113 are closed. Table A1 shows the nodal heads and pipe flow rates from EPANET 2 before and after correction following detection of the status of the topology.

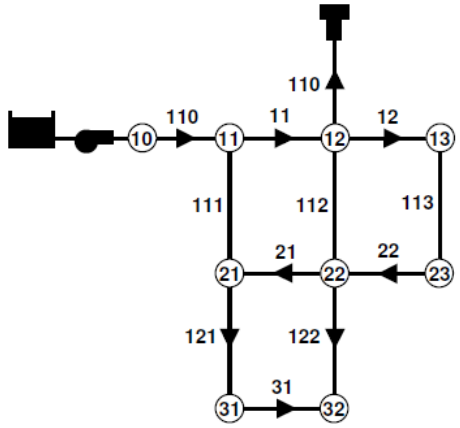

(a) Step 1: Illustration of pipe flows from status of EPANET 2 with pipes 111-113 closed.

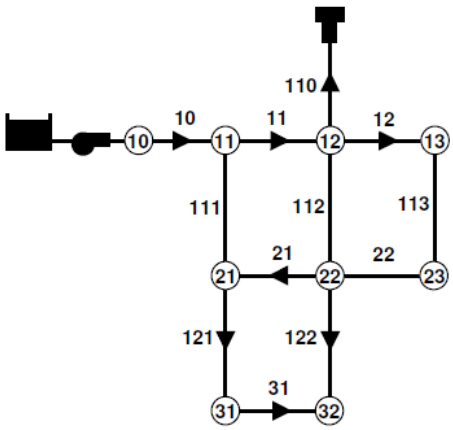

(b) Step 2: Detection of zero-flow pipe 22.

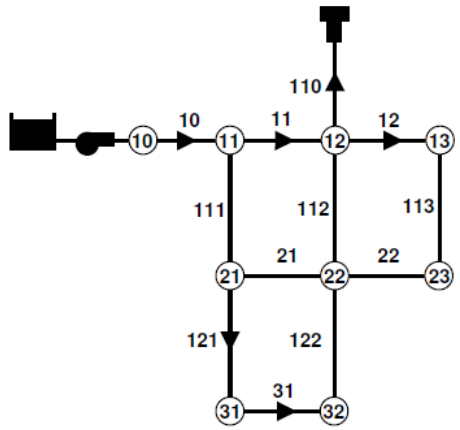

(c) Step 3: Detection of zero-flow status pipes 21 and 122.

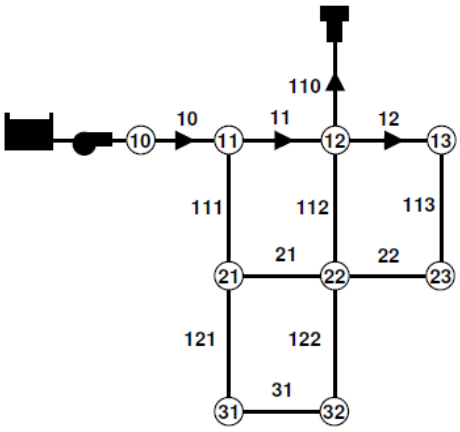

(d) Step 4: Detection of zero-flow of status of pipes 31 and 121.

Figure A1: Illustration of the topology status-detection procedure

Table A1: EPANET 2 results before and after topology status detection

	Flow rates (*l*/s)			Heads (m)	
Pipes	Before detection	After detection	Nodes	Before detection	After detection
10	115.61	115.61	10	296.20	296.20
11	91.43	91.43	11	85.44	85.44
12	21.03	21.03	12	82.27	82.27
21	-2.92	0.00	13	81.69	81.69
22	-5.26	0.00	21	-1.58×10^{7}	0.00
31	1.87	0.00	22	-1.58×10^{7}	0.00
110	-46.22	-46.22	23	-1.58×10^{7}	0.00
111	0.00	0.00	31	-1.58×10^{7}	0.00
112	0.00	0.00	32	-1.58×10^{7}	0.00
113	0.00	0.00			
121	8.18	0.00			
122	4.44	0.00			

APPENDIX B

INPUT DATA FOR EXAMPLES IN CHAPTER FOUR

Table B-1: Binary representation and unit costs for pipes of Example 1

Index	Pipe diameter (mm)	Cost ($/m)	Pipe status	Coding
0[a]	Not applicable	0	Closed	0000
1	Not applicable	0	Closed	1000
2	Not applicable	0	Closed	0100
3	80	23	Open	1100
4	100	32	Open	0010
5	120	50	Open	1010
6	140	60	Open	0110
7	160	90	Open	1110
8	180	130	Open	0001
9	200	170	Open	1001
10	220	300	Open	0101
11	240	340	Open	1101
12	260	390	Open	0011
13	280	430	Open	1011
14	300	470	Open	0111
15	320	500	Open	1111

[a] Represents any candidate pipe that is not included in a topology

Table B-2: Pipe and node details of example 2

Pipe	Start node	End node	Length (m)	Node	Demand (L/s)	Required Head (m)
1	1	2	760	1	165	75
2	1	4	520	2	220	74
3	1	6	890	3	145	73

4	2	3	1120	4	165	72
5	2	5	610	5[a]	-	-
6	2	6	680	6	140	73
7	3	5	680	7	175	67
8	3	7	870	8	180	72
9	4	8	860	9	140	70
10	4	9	980	10	160	69
11	5	7	890	11	170	71
12	5	10	750	12	160	70
13	6	9	620	13	190	64
14	6	10	800	14	200	73
15	7	12	730	15	150	73
16	7	13	680	16[a]	-	-
17	8	9	480	17	165	67
18	8	15	860	18	140	70
19	9	11	800	19	185	70
20	9	14	770	20	165	67
21	10	11	350			
22	10	12	620			
23	11	12	670			
24	11	16	790			
25	11	18	1150			
26	12	13	750			
27	12	17	550			
28	13	17	700			
29	14	15	500			
30	14	16	450			
31	14	19	750			
32	15	19	720			
33	16	18	540			
34	16	19	700			

35	17	18	850
36	18	20	750
37	19	20	970

[a]Source node

Table B-3: Binary representation and unit costs for pipes of Example 2

Index	Pipe diameter (mm)	Cost (units/m)	Pipe status	Coding
0[a]	Not applicable	0	Closed	0000
1	Not applicable	0	Closed	1000
2	Not applicable	0	Closed	0100
3	125	58	Open	1100
4	150	62	Open	0010
5	200	71.7	Open	1010
6	250	88.9	Open	0110
7	300	112.3	Open	1110
8	350	138.7	Open	0001
9	400	169	Open	1001
10	450	207	Open	0101
11	500	248	Open	1101
12	550	297	Open	0011
13	600	347	Open	1011
14	650	405	Open	0111
15	700	470	Open	1111

APPENDIX C

RECORDS OF GA PROGRESS FOR EXAMPLES IN CHAPTER FOUR

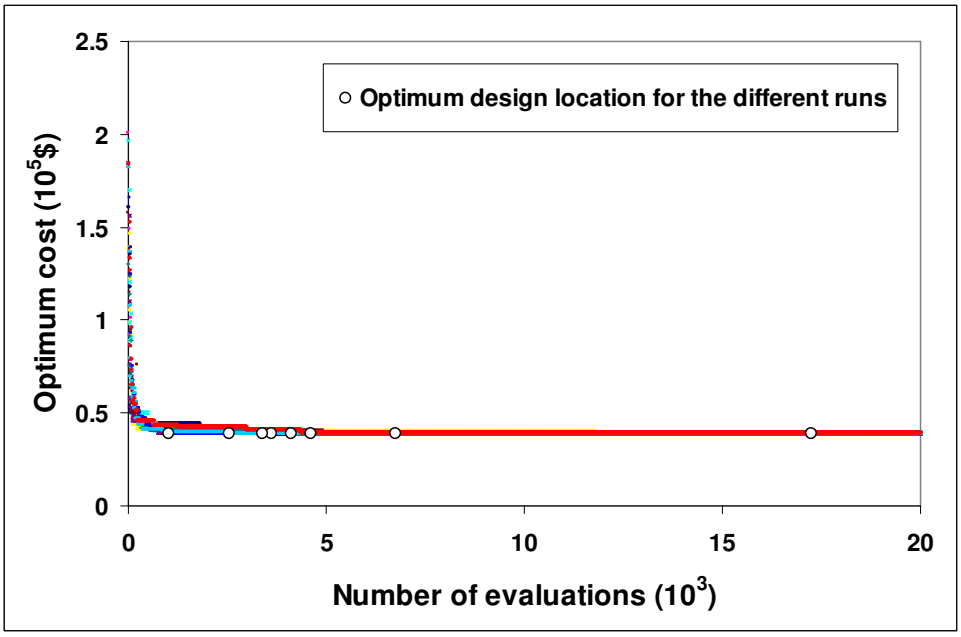

Figure C-1: Progress of 10 GA runs for branched design of Example 1

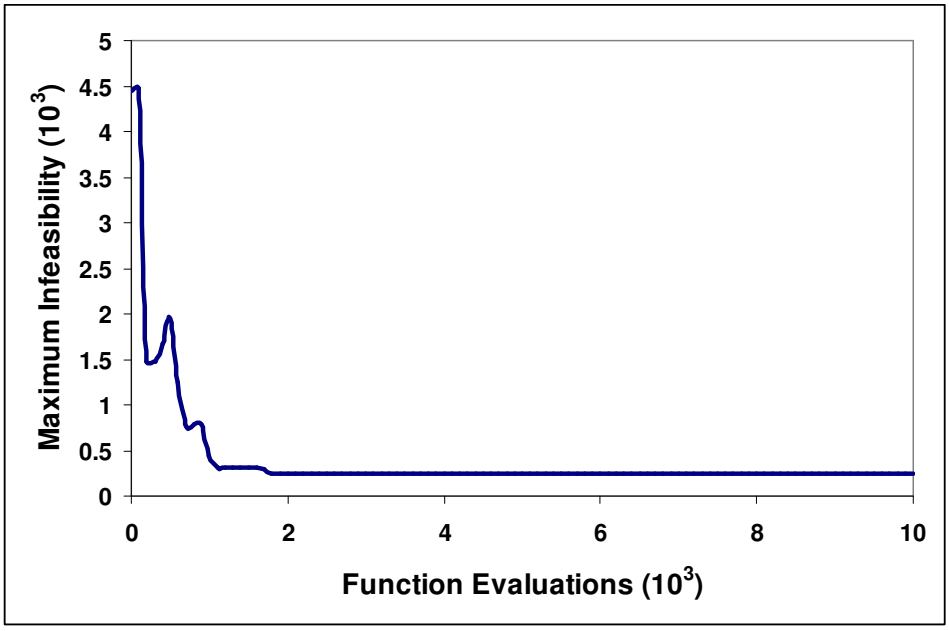

Figure C-2: Detection of zero-cost solution within one GA run of branched design of Example 1

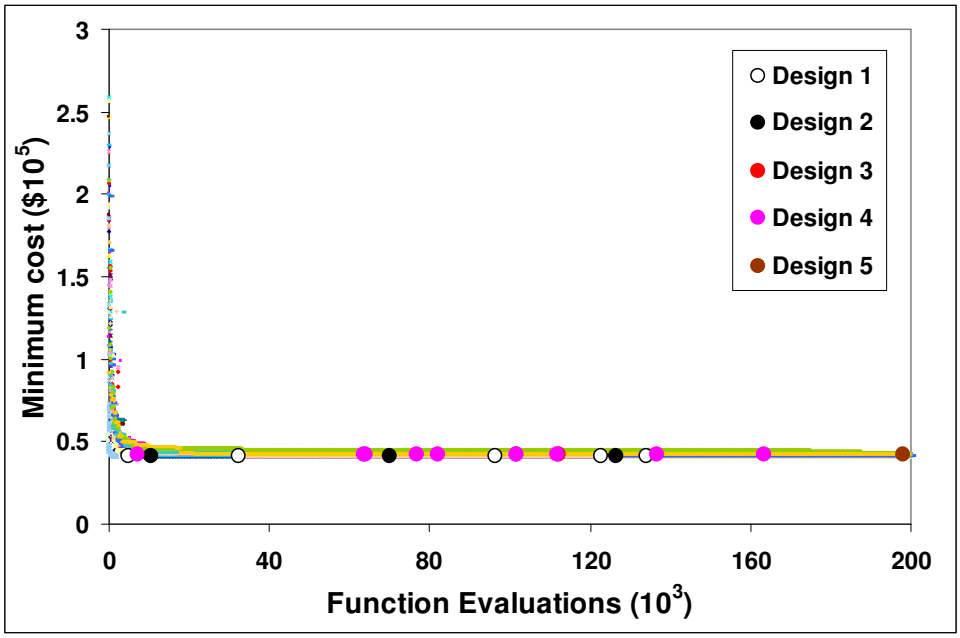

Figure C-3: Progress of 20 GA runs for looped design of Example 1

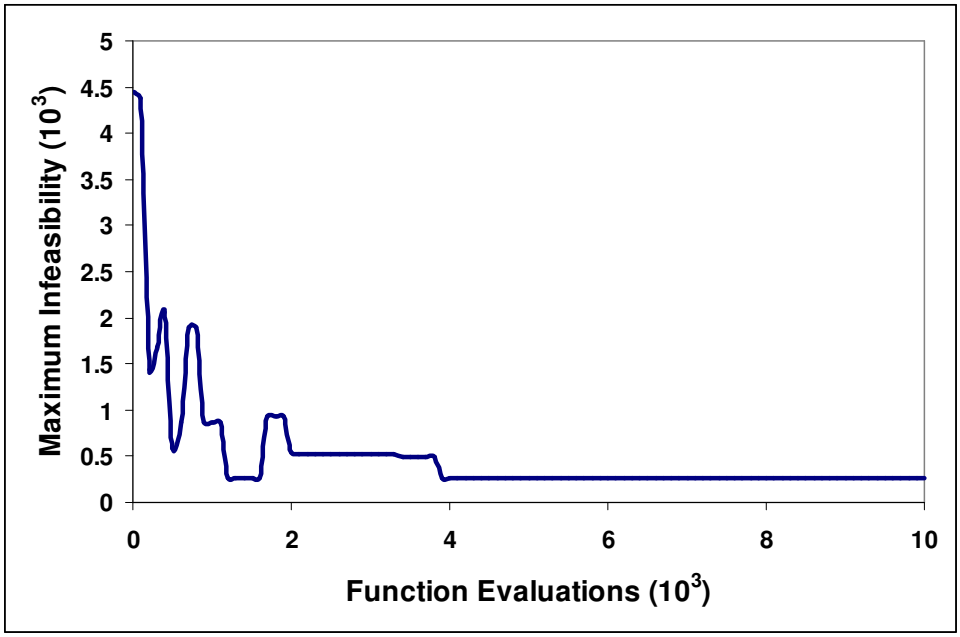

Figure C-4: Detection of zero-cost solution within one GA run of looped design of Example 1

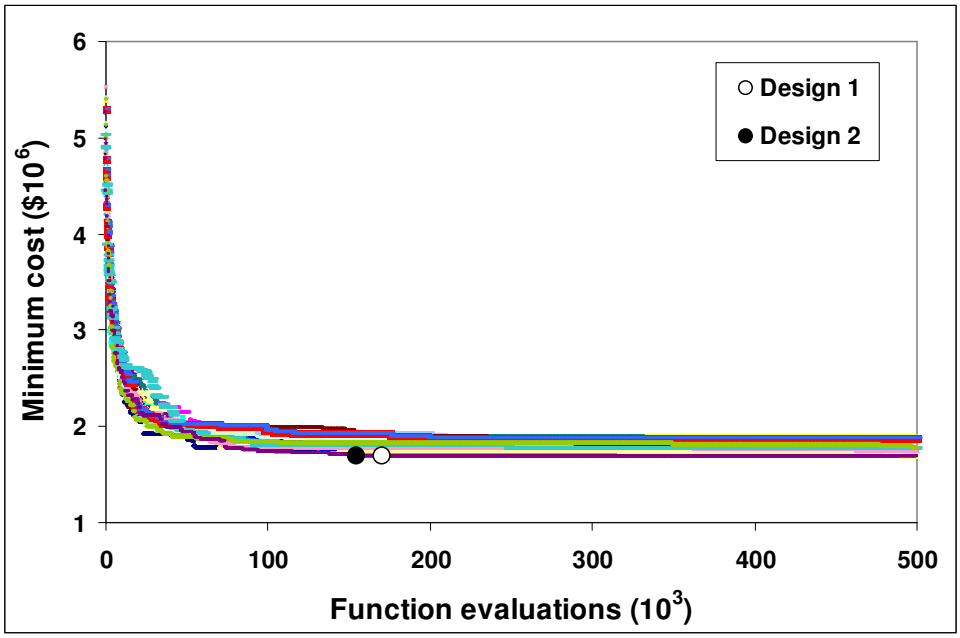

Figure C-5: Progress of 20 GA runs for branched design of Example 2

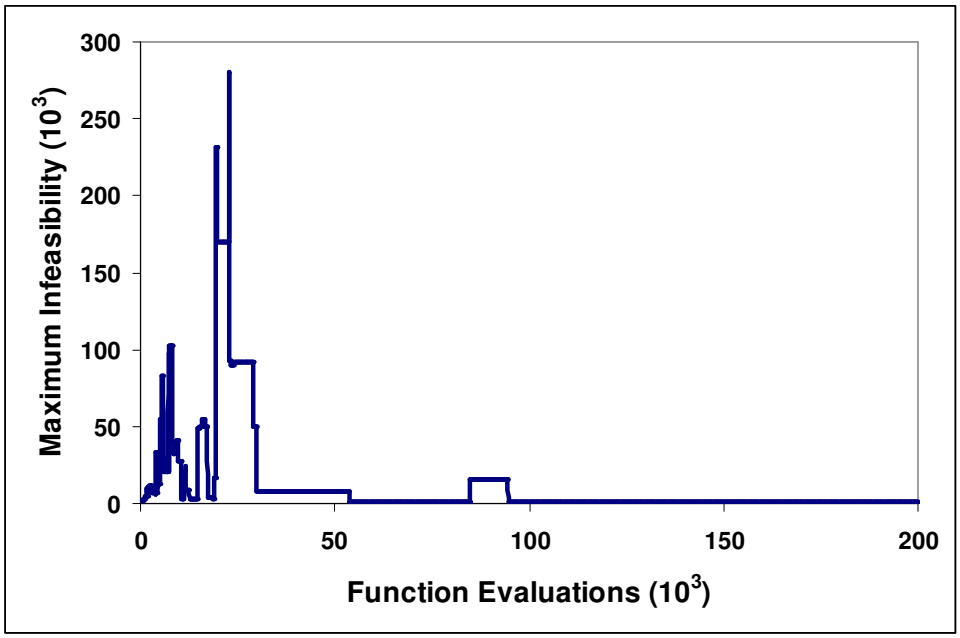

Figure C-6: Detection of zero-cost solution within one GA run of branched design of Example 2

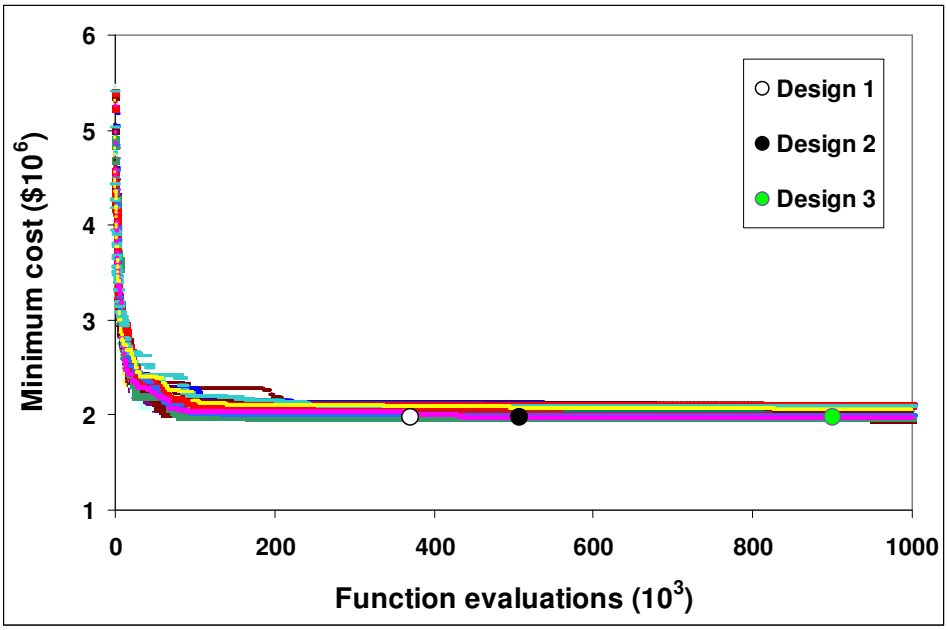

Figure C-7: Progress of 20 GA runs for looped design of Example 2

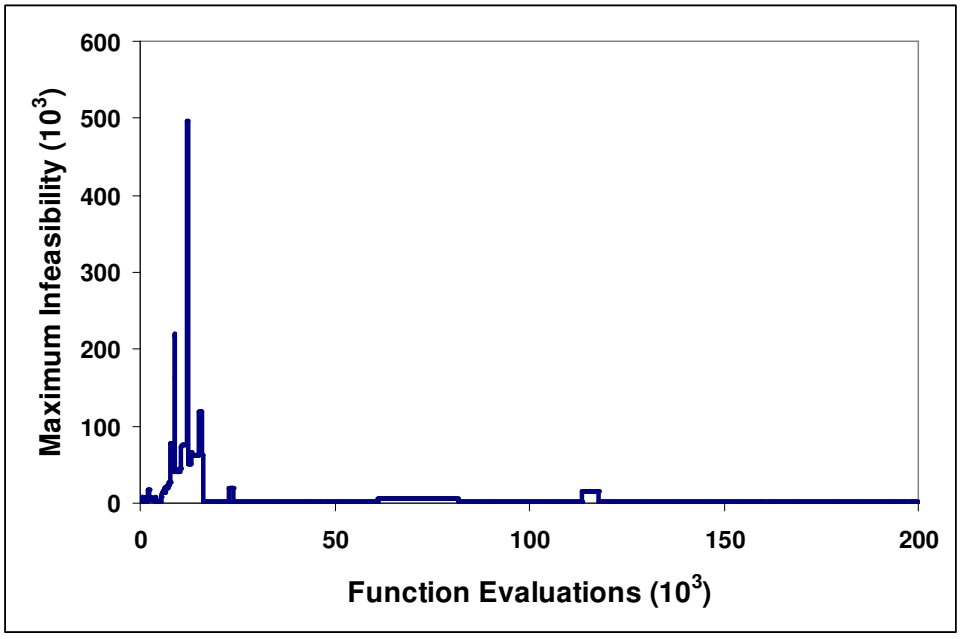

Figure C-8: Detection of zero-cost solution within one GA run of looped design of Example 2

APPENDIX D

INPUT DATA FOR EXAMPLES IN CHAPTER FIVE

Table D-1: Binary representation and unit costs for pipes of Example 1

Index	Pipe diameter (mm)	Cost (£/m)	Coding
0	100	25.3	0000
1	125	35.4	1000
2	150	46.5	0100
3	200	71.6	1100
4	250	100.0	0010
5	300	131.5	1010
6	350	165.7	0110
7	400	202.4	1110
8	450	241.5	0001
9	500	282.8	1001
10	550	326.3	0101
11	600	371.8	1101
12	600	371.8	0011
13	600	371.8	1011
14	600	371.8	0111
15	600	371.8	1111

Table D-2: Details of node demands and pipe lengths of Example 2

Node	Demand (l/s)	Pipe	Length (m)	Pipe	Length (m)
2	5	1	1	48	257.55
3	3	2	1	49	277.95

4	6.5	3	260	50	48.1
5	10.5	4	600	51	309.11
6	9.5	5	1200	52	150.25
7	6.5	6	600	53	174.42
8	8.5	7	800	54	396.55
9	9.5	8	200	55	169.47
10	10	9	500	56	178.62
11	4.5	10	2100	57	339.77
12	5.5	11	500	58	98.51
13	3.5	12	1000	59	458.41
14	4	13	304.16	60	386.4
15	5	14	341.16	61	135.01
16	4	15	210.5	62	559.91
17	8	16	422.28	63	319.1
18	6.5	17	529.66	64	193.48
19	7.5	18	254	65	393.04
20	6	19	252.9	66	60
21	8	20	230.65	67	243.45
22	8.5	21	159.46	68	646.8
23	2.5	22	456.91	69	236.22
24	4.5	23	313.99	70	422.08
25	4.5	24	73.8	71	244.93
26	7.5	25	192.73	72	5
27	6	26	176.53	73	31.84
28	6	27	124.94	74	258.71
29	8	28	478.71	75	154.7
30	7.125	29	282.03	76	229.87
31	9	30	262.9		
32	8.625	31	202.43		
33	5	32	52.91		
34	11.5	33	154.54		

35	16	34	352.16
36	16	35	165.08
37	13	36	325.05
38	10	37	377.94
39	6.625	38	275.39
40	8.5	39	239.08
41	6	40	404.28
42	6.5	41	367.51
43	10	42	391.18
44	16.5	43	229.78
45	18.5	44	404.76
46	9	45	215.2
47	5.5	46	575.37
48	4.625	47	210.89

Table D-3: Binary representation and unit costs for pipes of Example 2

Index	Pipe diameter (mm)	Cost (€/m)	Coding
0	150	271.94	000
1	200	299.43	001
2	250	328.01	010
3	300	359.54	011
4	350	399.03	100
5	400	438.63	101
6	450	461.34	110
7	500	502.78	111

APPENDIX E

INPUT DATA FOR EXAMPLES IN CHAPTER SIX

Table E-1: Pipe size representation and unit costs for network 1

Pipe size	Pipe diameter (mm)	Cost (£/m)	Pipe status	Coding
0[a]	Not applicable	0	Closed	0000
1	100	25.3	Open	1000
2	125	35.4	Open	0100
3	150	46.5	Open	1100
4	200	71.6	Open	0010
5	250	100.0	Open	1010
6	300	131.5	Open	0110
7	350	165.7	Open	1110
8	400	202.4	Open	0001
9	450	241.5	Open	1001
10	500	282.8	Open	0101
11	550	326.3	Open	1101
12	600	371.8	Open	0011
13	650	419.2	Closed	1011
14	700	468.5	Closed	0111
15	750	519.6	Closed	1111

[a] Represents any candidate pipe that is not included in a topology; i.e. $NCM_{ij} = 0$.

Table E-2: Pipe size representation and unit costs for network 2

Pipe size	Pipe diameter (mm)	Cost (units/m)	Pipe status	Coding
0[a]	Not applicable	0	Closed	0000
1	125	58	Open	1000
2	150	62	Open	0100
3	200	71.7	Open	1100
4	250	88.9	Open	0010
5	300	112.3	Open	1010
6	350	138.7	Open	0110
7	400	169	Open	1110
8	450	207	Open	0001
9	500	248	Open	1001
10	550	297	Open	0101
11	600	347	Open	1101
12	650	405	Open	0011
13	700	470	Open	1011
14	750	520.9	Closed	0111
15	800	591.7	Closed	1111

[a] Represents any candidate pipe that is not included in a topology; i.e. $NCM_{ij} = 0$.

APPENDIX F

DETAILS OF SELECTED SOLUTIONS IN CHAPTER SIX

Table F-1: Selected low ME solutions from the merged POF of Example 1

Pipes	Pipe diameters (mm)			
	Best infeasible solution	Least cost solution indicated		
		Branched	Partly looped	Fully looped
1-12	250	200	200	200
1-2	150	150	200	150
1-4	200	-	-	-
2-5	-	-	200	150
3-12	350	400	400	400
3-4	-	350	150	300
3-6	350	200	350	250
4-5	150	150	100	150
4-7	-	300	-	300
6-7	300	-	300	-
6-9	200	200	150	200
7-8	250	250	250	250
7-10	200	200	200	-
8-11	200	200	200	250
9-10	-	-	-	250
10-11	-	-	-	100
Cost (£10^6)	1.042	1.050	1.076	1.173
Critical node	11	11	11	10
Surplus head at critical node (m)	-6.92	+0.50	+0.84	+1.91
Number of pipes	11	11	12	13
Number of loops	0	0	1	2
Entropy	2.361	2.361	2.389	2.367
ME-S	0.000	0.000	0.017	0.102
GME-ME	1.232	1.232	1.189	1.124
ME group	17	17	16	11
AIM	22.376	12.232	7.205	1.226

LIM	11	11	6	0
HIM (m)	10.144	0	0	0
Solution number in Table 6.2	Not applicable	26	25	14

Table F-2: Selected high ME solutions from the merged POF of Example 1

Pipes	Pipe diameters (mm)[a] Least cost solution indicated				
	3-loop	4-loop	5-loop	6-loop	GME
1-12	350	450	350	350	450
1-2	300	550	250	125	400
1-4	300	300	300	300	300
2-5	200	350	300	125	450
3-12	300	200	300	350	200
3-4	-	300	300	350	350
3-6	300	400	-	200	300
4-5	200	400	300	300	550
4-7	100	200	200	350	200
5-8	250	-	350	150	125
6-7	200	300	400	200	400
6-9	200	100	250	200	100
7-8	-	350	350	200	450
7-10	-	-	-	100	200
8-11	200	300	200	200	300
9-10	200	200	200	125	250
10-11	100	350	250	300	300
Cost (£10^6)	1.272	2.235	1.871	1.593	2.522
Critical node	10	9	10	10	9
[c]Surplus head at critical node (m)	+3.44	+8.63	+5.86	+9.82	+19.73
Number of pipes	14	15	16	17	17
Number of loops	3	4	5	6	6
Entropy	2.648	3.448	3.395	3.257	3.593
ME-S	0.076	0.002	0.003	0.073	0.000
GME-ME	0.869	0.143	0.195	0.262	0.000
ME group	9	6	7	2	1

AIM	0.945	0.145	0.198	0.335	0.000
LIM	0	0	0	0	0
HIM (m)	0	0	0	0	0
Solution number in Table 6.2	12	9	10	2	1

LIST OF PUBLICATIONS

JOURNAL PAPERS

Saleh, S. H. A., and Tanyimboh, T.T., 2013. Coupled Topology and Pipe Size Optimization of Water Distribution Systems. *Water Resources Management*, 27(14), 4795-4814.

Tanyimboh, T.T., Tietavainen, M.T. and Saleh, S.H.A, 2011. Reliability assessment of water distribution systems with statistical entropy and other surrogate measures. *Water Science and Technology*, *Water Supply*, 11(4), 437-443.

CONFERENCE PAPERS

Saleh, S.H.A, Barlow, E., and Tanyimboh, T.T., 2012. Unbiased and accurate assessment of surrogate measures of hydraulic reliability of water distribution systems. *14th Water Distribution Systems Analysis Conference*, 24-27 September 2012 Adelaide, Australia: 148-157.

Saleh, S.H.A., and Tanyimboh, T.T., 2011. Global maximum entropy minimum cost design of water distribution systems. *13th International Water Distribution Systems Analysis Symposium,* 22-26 May 2011, Palm Springs, California. USA: ASCE, 206-213.

Saleh, S.H.A., and Tanyimboh, T.T., 2012. Joint Pipe Size and Reliability Design Optimization of Water Distribution Systems. *10th International Conference on Hydroinformatics,* 14-18 July, 2012 Hamburg.